Individual Differences in Cortical Constraints of Visual Abilities

Emily Cook

Thesis submitted in fulfilment of the degree of

Doctor of Philosophy

Department of Psychology

Royal Holloway, University of London

March, 2016

Declaration of Authorship

I, Emily Cook, hereby declare that this work was carried out in accordance with the Regulations of the University of London. I declare that this submission is my own work, and does not represent the work of others, published or unpublished, except where duly acknowledged in the text. No part of this thesis has been submitted for a higher degree at another university or institution.

Signed 

Date 01/03/16

Abstract

This thesis investigates how various cortical parameters constrain individual differences in low and intermediate level visual abilities by combining psychological and neuroscientific methodologies.

The first 3 experiments consider individual difference in cortical magnification. Firstly, inter- and intra-individual differences of retinotopic maps were investigated. It was documented that there is both high inter- and intra- individual variability in multiple cortical parameters. Whilst some clustering between early visual areas was identified, generally visual areas are uncorrelated with one another. Secondly, visual abilities measured psychophysically were compared to cortical magnification in maps thought to underlie these abilities. In contrast with previous literature (Duncan & Boynton, 2003), cortical magnification was a weak predictor of performance in both low level and intermediate level abilities.

Experiments 4, 5 and 6 demonstrate that pRF surround size in V1 correlates with individual differences in first and second order surround suppression. This suggests that the 2 processes may not be as different as suggested in the psychophysical literature (Morgan, Mason, & Baldassi, 2000). The more complex phenomenon of crowding also showed an association with pRF parameters, questioning the proposal (Whitney & Levi, 2011) that it is a separate and distinct phenomena to surround suppression.

The final experimental section of this thesis expands the link between visual abilities and cortical parameters to a more complex cognitive task. This section offers insight into the cortical processes underpinning the previously documented link between low level visual abilities and measures of IQ (Melnick, Harrison, Park, Bennetto, & Tadin, 2013). These experiments demonstrate that the links between surround suppression and visual reasoning abilities are mediated by levels of gamma-aminobutyric acid (GABA) in the early visual cortex.

Acknowledgements

I would first and foremost like to thank my supervisor, Jonas Larsson, for his support throughout. Additionally, Andy Smith provided invaluable guidance and advice. I would also like to thank Francesca Pizzorni Ferrarese for her assistance with pRF analyses and Steve Hammett for his help with GABA measurement. Financial support was provided by a Royal Holloway College Scholarship and by the University of London Postgraduate Research Study Grant Fund. I would like to thank my parents for their encouragement. Finally, I am grateful to Alessio for his support and advice.

Table of Contents

Table of Tables

Table of Figures

1 Introduction

1.1 Subdivision of the Visual Cortex

The cortical structures underlying vision have been known for many decades (Munk, 1881/1960). Since the identification of the occipital cortex as a visual centre (Munk, 1881/1960) and the first delineation of neurological maps (Inouye, 1909) understanding of the human visual system has rapidly increased. The close similarities between the human visual system and those of other mammals, particularly some primate species, has allowed a detailed exploration of the structure and function of these brain regions. Human lesion data has complemented this work (Fishman, 1997). Additionally, more recent investigations utilising MRI have, to a large extent, shown converging findings with those of the previous literature (Sereno et al., 1995).

Despite the wealth of knowledge regarding the processing underlying human vision, significant gaps in understanding exist. The precise role of various structures remains under debate. Furthermore, recent advances in MRI technology have highlighted minor discrepancies between the visual systems of humans and those of closely related primates (Brewer, Press, Logothetis, & Wandell, 2002; Tootell et al., 1997; Van Essen, 2004) particularly structures above MT (Larsson & Heeger, 2006). For example, V3A and V3 are now thought to have non-identical roles in the human and macaque brain, the human V3A is closely linked to motion perception whilst the macaque V3A is not (Galletti, Battaglini, & Fattori, 1990; Tootell et al., 1997). These contradictions cast doubt on the assumption that previous animal based data can be simply extrapolated to humans. They highlight the importance of utilising in vivo imaging of the human brain and remind us that although investigation of the visual system may seem advanced in comparison to other fields of cognitive neuroscience, there is still much to be learnt. It is vital to delineate the borders of visual areas and understand the role of each region. Furthering knowledge in this field is useful in five ways; understanding the extent of specialization, linking function to a particular structure, analysing pathologies, making inter- species comparisons and comparing results across participant samples (Wandell, Dumoulin, & Brewer, 2007).

1.1.1 Overview of Retinotopic Maps

The primary stage of visual processing is the reception of light by photoreceptors located on the retina. The retina translates light into nerve impulses, delivered to the brain via the optic nerve (Hubel, Wensveen, & Wick, 1995). The visual sensory processing centre is found in the posterior portion of the brain and directly above the cerebellum (Engel, Glover, & Wandell, 1997). After the retina but prior to reaching the visual cortex, axons decussate via the optic chiasma. In this way, the visual cortex in each hemisphere receives input from the contralateral half of the visual field (Nicholls et al., 2001).

The visual cortex can be divided into multiple discrete areas that are located in the occipital, temporal and parietal cortices (Bruce, Green, & Georgeson, 2003). These regions are determined by the pattern of visual space representation (Wandell & Winawer, 2011), functional properties (Kaas, 1997), connectivity profiles (Kaas, 1997) and characteristic anatomical landmarks (Andrews, Halpern, & Purves, 1997). These visual areas are organized in a hierarchical fashion, with early visual areas underlying simpler forms of visual perception (Maunsell & Newsome, 1987).

The visual cortex can be subdivided in terms of retinotopic organisation. This will be the primary method of area definition used throughout this thesis. Retinotopy is a form of topography, an organisational principle seen in many brain areas underlying sensory processing in which the sensory surface (e.g. skin or retina) is projected in an orderly fashion to a part of the central nervous system. In the visual system, adjacent points in the visual field are represented by adjacent points on the cortex. In this way, the map of the visual field in preserved. The retinotopic map is first represented in the primary visual cortex, with each side of the visual field represented in the V1 of the contralateral hemisphere. As the visual field progresses the map is repeated multiple times. At each repetition the map is reversed, appearing as a mirror image of itself in the subsequent presentation. Delineating these mirrored boundaries is used to subdivide the cortex.

In order to be accepted as a retinotopic map, the cortical area must fulfil several criteria (Wandell et al., 2007). Firstly, each map must contain only one representation for each

point in the visual field. Multiple representations of the same section of a visual field within one visual area is an indication that the initially defined single map may in fact contain multiple maps that require further delineation. Secondly, a substantial portion of the visual field must be represented. It should be noted that this criterion does not demand a full representation. Thirdly, the representation or the visual field must have a level of order, i.e. the projection of both eccentricity and polar angle onto the cortex should be continuous. This criterion is of particular importance as discontinuities in these representations are used to define borders between areas. Finally, and of most relevance to this thesis, the basic features of these maps must be consistent across individuals.

Since the advent of modern neuroimaging technology, retinal mapping has become a commonly used method of subdividing the human visual system. Over the last 25 years multiple maps have been identified; V1,V2,V3, LO1, LO2, hMT+, hV4, VO1, VO2, V3A, V3B, IPS0, IPS1, IPS2, IPS3 and IPS4, and it seems likely that additional maps will soon become apparent (Wandell et al., 2007). Retinotopic mapping is quick to collect, often taking less than an hour to obtain a participant's map (Wandell & Winawer, 2011), although it is limited by a poor understanding of individual differences. A brief overview of the key retinotopic maps relevant to this thesis will be provided.

1.1.1.1 Medial Occipital Maps

The visual areas located earliest in the processing hierarchy are found in the medial occipital cortex. These maps are well understood and consistently identifiable (Henriksson, Karvonen, Salminen-Vaparanta, Railo, & Vanni, 2012). V1, V2 and V3 represent visual space in similar ways. The central portion of visual space is represented near the occipital pole (Wandell et al., 2007). Moving in the caudal-rostral direction along the cortex, the visual space represented moves from the fovea to the periphery. The peripheral parts of visual space are represented on cortex closer to the collateral sulcus (Arcaro, McMains, Singer, & Kastner, 2009). This pattern is referred to as the eccentricity map (Engel et al., 1997). The medial occipital maps share a foveal representation (Schira, Tyler, Breakspear, & Spehar, 2009).

V1 is the earliest visual region and receives input directly from the retinogeniculate pathway. V1 has multiple connections with later visual areas (Maunsell & Newsome, 1987; Van Essen, Felleman, DeYoe, & Knierim, 1991) as well as subcortical structures

(Felleman & Van Essen, 1991). It can be identified anatomically, it is found within and surrounding the calcarine sulculs in the medial occipital cortex (Engel et al., 1997). V1 has a full representation of the contralateral visual field that is highly organised and continuous (Adams & Horton, 2003b). Moving from the lower to the upper lip of the calcarine sulcus, the representation of visual space shifts continuously from the lower vertical meridian to the upper vertical meridian (Engel et al., 1997). This pattern is referred to as the polar angle map.

V2 shares a border with V1. Unlike the earlier V1 map, V2 is split into a dorsal and ventral portion. The dorsal portion (V2d) shares a representation of the lower vertical meridian with V1. It extends away from the upper lip of the calcarine sulcus, displaying a polar representation of a quarter of the visual field. V2d represents the lower half of the contralateral visual field. Conversely, the ventral portion of V2 (V2v) shares the upper vertical meridian representation with V1 and extends away from the lower lip of the calcarine sulcus. The upper portion of the contralateral visual field is represented in this map. A notable difference between V2d and V2v is that V2v is generally wider (Van Essen, 2004). The eccentricity map in V2d and V2v are similar to that of V1, with more peripheral locations in visual space represented rostrally of the cortex.

The final visual area located in the medial occipital cortex is V3. Like V2, V3 is divided into a dorsal (V3d) and ventral (V3v) portion (Zeki, 1969). V3d borders V2d, sharing a horizontal meridian. The polar angle representation of the upper quarter of the contralateral visual field extends to the vertical meridian moving towards the parietal cortex. The boundary of V3d has a distinctive Y shape (Larsson & Heeger, 2006). Midway along the V3d vertical meridian border, the boundary splits into 2 branches. One branch progresses dorsally and caudally and the other extends rostrally. V3v borders V2v, sharing a horizontal meridian. Mirroring V3d, V3v extends ventrally and represents the lower quarter of the visual field. The boundary of V3v does not show the same Y shape as V3d (Larsson & Heeger, 2006). The eccentricity representation in V3 follows the pattern seen in V1 and V2.

1.1.1.2 Ventral Maps

In contrast to the medial occipital maps, the visual areas located ventrally and are less easily identifiable (Henriksson et al., 2012). Current retinotopical mapping methodologies

fail to locate VO1 in some subjects (Larsson & Heeger, 2006). In the past it has been argued that there was little retinotopic organization in this region (Arcaro et al., 2009). Advances in methodology revealed that this region in fact shows an orderly representation of eccentricity (Malach, Levy, & Hasson, 2002) and polar angle (Brewer, Liu, Wade, & Wandell, 2005). V4, VO1 and VO2 are located in this region. These maps are thought to underlie semi-complex visual processing, they are considered intermediate visual areas. Generally, they seem particularly important for object, colour and face processing (Arcaro et al., 2009). V4, VO1 and VO2 over represent the fovea to a greater extent than V1. The majority of the surface are of ventral maps is dedicated to the central 3° of visual space (Brewer et al., 2005).

V4 is located rostrally with respect to V3v and shares a representation of the upper vertical meridian with V3v. The polar angle representation of V4 includes the full contralateral visual field (Arcaro et al., 2009). This distinguishes it from the macaque single quadrant representation (Gattass, Sousa, & Gross, 1988). The human V4 polar map progresses rostrally until it reaches the border with VO1, identified as the lower vertical meridian (Arcaro et al., 2009). The eccentricity representation of V4 is similar to the medial occipital maps. V4 shares a foveal confluence with these early areas and displays an eccentricity representation that progresses towards the collateral sulcus in parallel with V1, V2v and V3v.

VO1 and VO2 are located rostrally to V4, in the ventral occipital cortex (Brewer et al., 2005). They are positioned along the posterior medial fusiform gyrus and within the posterior portion of the collateral sulcus (Arcaro et al., 2009). Unlike V4, VO1 and VO2 share a foveal representation separate to the medial occipital maps. The confluence is located on the border shared by VO1 and VO2. The extent to which the foveal representation is evenly split between the 2 areas differs between individuals, in some cases it is approximately equal but in others it is located mostly in VO2 (Arcaro et al., 2009). The eccentricity map for both areas extends posteriorly, the representation of peripheral space borders the peripheral representation of V3v (Brewer et al., 2005).

Both VO1 and VO2 contain a polar representation of the contralateral visual field. VO1 shares a representation of the lower vertical meridian with V4 and a representation of the upper vertical meridian with VO2 (Brewer et al., 2005). This boundary is not consistent

across individuals. In some cases, the VO1- VO2 border is better described as a midpoint between the horizontal meridian and the upper vertical meridian (Arcaro et al., 2009). VO2 is rostral with respect to VO1 (Kolster, Peeters, & Orban, 2010). The polar angle representation of VO2 progresses from the shared upper vertical meridian to the lower vertical meridian moving along the caudal-rostral direction.

1.1.1.3 Lateral Occipito-temporal maps

LO1 and LO2 were first mapped relatively recently and are not believed to have a homologous counterpart in the macaque (Larsson & Heeger, 2006). Both maps in the lateral occipital cluster represent the full contralateral visual field (Larsson & Heeger, 2006). LO1 and LO2 are located between V3d and MT. Anatomically, LO1 and LO2 are found in the fundus of the lateral occipital sulcus, although high individual variability exists (Larsson & Heeger, 2006). LO1 and LO2 are of a similar size to one another and relatively small in comparison to medial occipital maps (Larsson & Heeger, 2006). The surface area of LO1 and LO2 is approximately 30% of V1, 50% of V3 and 75% of V4 (Larsson & Heeger, 2006).

These regions are thought to play a role in shape processing due to their position in the object-selective lateral occipital complex (Grill-Spector et al., 1998; Malach et al., 1995). Silson and colleagues report that LO1 and LO2 have specialized and independent functional roles. TMS administered to LO1 disrupted orientation perception but shape perception remained intact. Conversely, TMS of LO2 had no effect on orientation discrimination but impaired shape perception (Silson et al., 2013).

In terms of polar representation, LO1 shares a lower vertical meridian with V3d. LO1 progresses from the boundary of V3d towards MT. As noted above, the V3d boundary has 2 branches (Larsson & Heeger, 2006). LO1 shares the branch located posteriorly and dorsally. The LO1-LO2 boundary is marked by the upper vertical meridian. There is individual variability in this boundary, in some participants the boundary is closer to the horizontal meridian. For example, in 23 hemispheres with clearly defined maps, 14 demonstrated an LO1-LO2 boundary at the upper vertical meridian and 9 at the horizontal meridian (Larsson & Heeger, 2006). The LO2 polar representation progresses from the boundary with LO1 to the anterolateral boundary of LO2, defined by the lower vertical meridian (Larsson & Heeger, 2006).

LO1 and LO2 share a foveal representation with the medial occipital maps. The eccentricity maps for both areas extend rostrally and dorsally (Larsson & Heeger, 2006). The eccentricity representation of LO1 is more continuous than that of LO2. The foveal representation of LO2 is immediately adjacent to the peripheral representation, with intermediate eccentricities excluded. Again, variability in this pattern was present across participants, approximately 50% of hemispheres demonstrate discontinuity of the eccentricity map (Larsson & Heeger, 2006).

The medial temporal area (MT) receives direct input from V1 (Orban, 1997) and feeds forward to multiple satellite components of the MT+ complex (V4 transitional zone, ventral MST, FST, peripheral MT, dorsal MST, middle superior temporal polysensory area and lower superior temporal area; Kolster et al., 2010). MT is homologous to V5 in monkeys (Shipp & Zeki, 1989). Retinotopic (Kolster et al., 2010) and anatomical measures (Tootell & Taylor, 1995) indicate that MT is approximately the same size as VOI and has a surface area 23% of V1 (Kolster et al., 2010). In contrast with other components of the MT+ cluster, MT has a left-right asymmetry. Left MT was found to be significantly smaller than right MT across 10 participants (Kolster et al., 2010).

MT contains a full representation of the polar map for the contralateral visual field. The lower vertical meridian is positioned caudally. In some cases MT abuts LO2 directly, but in others it is separated by a short distance (Larsson & Heeger, 2006). The polar map progresses rostrally, moving away from LO2 until the upper vertical meridian representation marks the second boundary (Kolster et al., 2010). MT has a foveal representation that is separate and discrete from both the medial occipital maps and the dorsal-occipito-parietal maps. This foveal representation is located near the lateral occipital sulcus (Kolster et al., 2010).

MT is thought to play a key role in motion perception (Kolster et al., 2010). Functional MRI data indicates that human MT responds selectively to moving random dot stimuli, in comparison to stationary random dot stimuli (Tootell et al., 1997). Motion perception capabilities can also be investigated though response to micro-stimulation in macaques. For example, micro-stimulation of MT can bias motion perception (Salzman, Britten, & Newsome, 1990). In macaques, clusters of directional sensitive MT neurons were

stimulated during a psychophysical judgement of the direction of random dots. The behavioural responses of the macaques was biased by the direction preference of the stimulated MT neurons.

1.1.1.4 Dorsal- Occipital maps

V3A occupies an intermediate role in the processing hierarchy, located between the medial occipital map cluster and the occipital cortex and closely connected to both the parietal and temporal cortex. V3A shares a boundary with V3d, extending from the rostral branch of the boundary towards the intraparietal sulcus (Swisher, Halko, Merabet, McMains, & Somers, 2007). The polar map of V3A shares a representation of the lower vertical meridian with V3d (Larsson & Heeger, 2006). Unlike other maps in the superior occipital cortex, V3A contains a full representation of both the upper and lower visual field (Tootell et al., 1997). The polar representation of V3A progresses until the representation of the upper vertical meridian is reached at the dorsal/rostral boundary with V7 (Larsson & Heeger, 2006).

V3A has a foveal representation distinct from both the medial occipital maps and the ventral occipital cluster (Larsson & Heeger, 2006). This representation of the central visual field is located in the intraparietal sulcus (Wandell et al.,2007). The eccentricity map of V3A expands in a direction that is medial relative to the fovea representation.

A key functional characteristic of V3A is a differential response to coherent global motion. Unlike V1, V3A shows a differentiation between random and coherent movement (Braddick et al., 2001; Koyama et al., 2005). A higher BOLD response is seen in human V3A while viewing of coherent motion compared to noise. This pattern was also seen for MT, but not V1 (Braddick et al., 2001).

V3B shares a boundary with V3A and also contains a full representation of the contralateral visual field (Wandell et al., 2007). V3B is dorsal and rostral to the Y-shaped boundary that characterises the division between V3d and V3A (Larsson & Heeger, 2006). V3B shares the foveal representation of V3A. From this foveal representation, the V3B eccentricity map expands laterally relative to the foveal representation and V3A. The eccentricity map of V3B is a mirror image of the map in V3A. The polar representation of visual space in V3B is in a similar direction to V3A, such that the upper

vertical meridian is located at the boundary with V7 and the lower vertical meridian is proximate to LO1. V3B is difficult to identify and define in multiple subjects (Larsson & Heeger, 2006).

1.2 Individual Differences in Size and Retinotopy of Visual Areas

The cortical areas underlying vision have been seen to vary greatly between individuals. This variability in terms of size measurements is well established within the literature. Andrews et al. (1997) report a high level of inter- individual variability in the size of both pre-cortical structures and the primary visual cortex measured in 15 healthy human brains during autopsy. The optic tract cross-sectional area, volumes of magnocellular and parvocellular layers of the LGN, the surface area of V1 and the volume of V1 varied by up to 3-fold across individuals. This finding of high V1 variability is consistent across the literature (Klekamp, Riedel, Harper, & Kretschmann, 1991; Leuba & Kraftsik, 1994; Murphy, 1985; Stensaas, Eddington, & Dobelle, 1974)

The variability between participants in cortical areas is also present in later components of the visual system (Dougherty et al., 2003). The size of retinotopically defined V1, V2 and V3 was measured in vivo. In broad agreement with Andrews et al. (1997), the sizes of these maps varied by approximately 2.5 times across participants (Dougherty et al., 2003).

In addition to size measurements, the organization of retinotopic maps also shows a high level of individual variability. Whilst the early medial occipital maps follow a generally consistent pattern across participants (Henriksson et al., 2012) and between species (Van Essen, 2004), later maps are often highly variable. Larsson and Heeger (2006) were unable to identify V3B and VO1 in a minority of hemispheres. Of the visual areas that were successfully identified, many showed inconsistent patterns across participants. For example, the continuity of the LO2 eccentricity map showed inter-individual differences (Larsson & Heeger, 2006). Similarly, variability in both the eccentricity and polar representation has been reported for VO1 and VO2 (Arcaro et al., 2009).

A commonly used measure in the study of retinotopic variability is cortical magnification. Cortical magnification is a form of local anisotropy, it describes the phenomena whereby some points in the visual cortex have larger areas of cortex devoted to their processing. Cortical magnification describes the relative amount of cortex devoted to processing an area of the visual field. The functional result of this unequal distribution of cortical space is that acuity is heightened at certain points in the visual field. Visual points close to the fovea have greater cortical representation (Van Essen, Newsome, & Maunsell, 1984) and also heightened acuity as measured through behavioural tasks (Johnston & Wright, 1985).

Theoretically, high levels of cortical magnification may by associated with either a high number of neurons or larger neurons. The retinotopic methods of this chapter cannot address this question directly as the spatial resolution of fMRI is insufficient to measure single cells. Early primate research (Dow, Snyder, Vautin & Bauer, 1981) indicates that high levels of cortical magnification reflect a greater number of neurons, rather than larger neurons. Human research addressing the correlation between cortex surface area and neuron characteristics supports this view. Individuals with large cortical surface size do not have proportionally large neurons (Kaas, 2000). Instead, individuals with a large visual cortex have a high number of neurons in this region (Leuba & Garey, 1987; Leuba & Kraftsik, 1994).

1.3 Individual Differences in Visual Abilities

Mirroring the differences between participants in retinotopic organisation (Larsson & Heeger, 2006), inter-individual variability in a variety of visual abilities has been well documented. These differences can be seen in low level visual tasks. Individual differences have been demonstrated in binocular perception of motion in depth (Nefs, O'Hare, & Harris, 2010). This form of perception can be achieved either by monitoring how binocular disparity changes with time or by comparing the velocity of motion in the left eye to the motion velocity in the right eye. Participants performed a series of psychophysical tasks using random dot stereograms designed to simulate motion-in-depths. Tasks relied of one of the two proposed mechanisms. Generally, participants relied more heavily on the binocular disparity mechanism and used the velocity

difference mechanism to a lesser extent. Although, a substantial number of participants (24%) did not show this pattern, instead favouring the velocity difference mechanism.

Individual differences are also present in more complex abilities, such as reading. Data has been presented (Shaywitz, Escobar, Shaywitz, Fletcher, & Makuch, 1992) indicating that there is a normal distribution of reading abilities in the general population. A longitudinal study of children from age 6 to age 12 measured reading ability at biennial intervals. The data supports the argument that dyslexia occurs in degrees, reflecting a high level of variability along a reading ability continuum.

As individual differences are present both in cortical measures (Arcaro et al., 2009; Larsson & Heeger, 2006) and visual abilities (Nefs et al., 2010; Shaywitz et al., 1992) it is possible that correlations exist between individual variability in the visual system and the forms of perception reliant upon them. The examination of individual differences for this purpose is seen particularly in research into the perception of illusion-inducing visual stimuli. Subjective perceptual experience is known to differ across individuals. Given the difficulties in self-report measures of conscious experience, understanding of individual differences in visual illusions has benefited from the introduction of measures of brain structure and functioning.

Behavioural differences in paradigms utilising the Necker cube have been consistently documented (Miller et al., 2010; Pettigrew & Miller, 1998). In Necker cube tasks, an individual's conscious perception alters whilst stimulation remains unchanged (Sterzer & Kleinschmidt, 2007). The rate at which the conscious perception switches between the two conflicting perceptions differs between participants (Pettigrew & Miller, 1998). Kanai and colleagues found that individuals with a relatively fast switch rate also showed larger superior parietal lobes and the underlying white matter had a higher integrity (Kanai, Bahrami, & Rees, 2010). It was also demonstrated that individuals with lower switch rates had an increased volume of grey matter in the anterior intraparietal sulcus (Kanai, Carmel, Bahrami, & Rees, 2011). Individual difference in cortical parameters correlated with individual differences in ability. Together these studies suggest a switching mechanism underlying opposing systems, relying on these structures, a hypothesis further strengthened by fMRI activity in these areas during switching (Kleinschmidt, Büchel, Zeki, & Frackowiak, 1998; Lumer, Friston, & Rees, 1998; Rees,

Kreiman, & Koch, 2002; Sterzer & Kleinschmidt, 2007) and disruption of the illusion following TMS (Kanai et al., 2010; Kanai, Carmel, et al., 2011).

Subjective conscious perception of visual stimuli can also be explored through individual variability in sensory awareness of perceptual illusions such as the Ponzo illusion (Ponzo, 1911) and Ebbinghaus illusion (Ebbinghaus, 1902). In these tasks, physically identical stimuli look different dependent upon the surrounding items. Strength of these illusions is correlated negatively with the surface area of V1 (Schwarzkopf, Song, & Rees, 2011), but not V2 and V3. It is thought that this correlation indicates that the scaling properties of brain size favour a smaller V1 due to non-proportional arborisation of dendrites in a larger V1 (Kaas, 2000). The finding that purely anatomical measures of the peri-calcarine surface area do not correlate with illusion strength (Schwarzkopf et al., 2011) indicates the importance of utilising fMRI data and segregating the visual cortex using retinotopic methods rather than solely anatomically (Kanai & Rees, 2011).

Maps may only be defined as such if there is consistency across individuals (Wandell et al., 2007). Therefore, a key obstacle in the acceptance of this method is the inconsistencies in mappings across healthy participants. Understanding the reasons for these differences at a behavioural level will remedy this challenge. It has been demonstrated throughout the literature that psychological functioning in basic vision varies across individuals. It is possible that this variability may be related to the differences in the retinotopic mappings. As demonstrated by Schwarzkopf et al. (2011), anatomical measurements do not correlate strongly with individual differences in ability. Retinotopic differences may have a closer relationship to visual abilities.

1.4 Cortical Magnification as a Limiting Factor

Cortical magnification may act as a key limiting factor to visual abilities. The availability of additional cortex to process a stimulus is likely to provide advantages to perception. Duncan and Boynton (2003) found individual variability in cortical magnification across V1 to be correlated with performance on a Vernier visual acuity task. Additionally, the size of V1 was also correlated negatively with Vernier acuity thresholds. It has been

found previously (Popovic & Sjöstrand, 2001) that M, the linear extent of visual cortex in mm/degree of visual angle (Daniel & Whitteridge, 1961), is related to acuity. Independent estimates of acuity thresholds, ganglion cell separation and M in humans indicated the presence of this relationship. However, conclusive evidence was not provided until Duncan and Boynton (2003) investigated co- variability in these measures within the same individuals.

Comparison of psychophysics and fMRI data in this way suggests that M in V1 may limit ability in visual acuity tasks because a different number of V1 neurons represent the minimally resolvable spatial distance across participants. A similar later study (Duncan & Boynton, 2007) suggests that this limiting function may be a characteristic of all early sensory streams. Tactile acuity thresholds were obtained for fingers D2, D3, D4 and D5 using a task that required participants to judge the location of a raised bump relative to 2 other bumps (Duncan & Boynton, 2007). Separately, cortical magnification in the primary somatosensory cortex was measured. Mirroring the work of Duncan and Boynton (2003) in the visual domain, a correlation was seen between cortical and psychophysical measures.

Duncan and Boynton (2003; 2007) indicate that cortical magnification is a limiting factor for early processing in multiple sensory domains. Perception is improved when more cortex is dedicated to processing the stimulus. Additionally, Leingärtner and colleagues have shown that the size of cortical areas is correlated with motor and tactile performance in mice (Leingärtner et al., 2007). This finding suggests that there might a general pattern of correlations between retinotopic parameters (such as map area) and behavioural abilities that extends outside of the cortical magnification-to-acuity pairing identified by Duncan and Boynton (2003; 2007) and is also seen in other species. To extend the findings of Duncan and Boynton (2003; 2007) it may be useful to consider correlations between more complex visual tasks and higher order retinotopic maps.

The presence of co-variability within individual participants (Duncan & Boynton, 2003) indicates a close interaction between cortical parameters and visual abilities of some kind. However, the specifics of this structure-function link have remained largely unknown until recently. Schwarzkopf, and colleagues (2012) found a correlation between the surface areas of V1 and V2, as defined by retinal mapping, and gamma band activity. The

peak frequency of oscillations in the gamma band (30-80Hz) was positively correlated with surface area of V1 and V2, 36% of inter-individual differences in gamma activity could be explained by V1 surface area (Schwarzkopf, Robertson, Song, Barnes, & Rees, 2012).

Gamma has been linked to sensory processing (Herrmann, Fründ, & Lenz, 2010). Increases in gamma activity are correlated with sensory stimulation in a variety of modalities (Chen & Herrmann, 2001; Eeckman & Freeman, 1990; Pantev, 1995). For example, Hoogenboom and colleagues found increases in gamma during a visual motion perception task (Hoogenboom, Schoffelen, Oostenveld, Parkes, & Fries, 2006). Gamma variability across participants may mediate the structure to sensory processing abilities relationship noted previously (Duncan & Boynton, 2003). Schwarzkopf et al. (2012) found no relationship between cortical thickness and gamma activity, suggesting that the individual difference reflect surface area rather than grey matter volume. This raises questions for past studies which have correlated behaviour with the structural parameter of grey matter volume (Van Gaal, Scholte, Lamme, Fahrenfort, & Ridderinkhof, 2011), these correlations may have been less direct than assumed and resulted from a close link between volume and surface area.

Whether or not gamma activity can be implicated as a mediating factor at later levels of visual processing remains unknown. Schwarzkopf et al. (2012) failed to find a correlation regarding V3 surface area and attribute the relationship identified between gamma activity and V2 surface area largely to the well documented link between V1 and V2 size (Dougherty et al., 2003). Also the model proposed by Schwarzkopf et al. (2012) in light of these findings is heavily reliant upon the specific microarchitecture of V1, how this functioning would be extrapolated to other areas is as yet unexplored. However despite these challenges, this study indicates the importance of considering underlying factors in the individual variability of structure-function correlates.

1.5 Inter- and Intra-Individual Forms of Variability

1.5.1 Inter-Individual Variability

A primary focus of variability has been the differences between participants. Both anatomically and retinotopically, multiple maps differ between participants. For example, V1 has been shown to differ by up to 3 times between participants (Andrews et al., 1997). Measures of cortical magnification differ between participants (Duncan & Boynton, 2003, 2007). This inter- individual variability in cortical magnification is reflected in differing levels of ability between participants. For example, acuity perception of luminance defined boundaries correlates with cortical magnification in V1 (Duncan & Boynton, 2003). Participants with more V1 cortex dedicated to processing visual space perform better than participants with less cortical magnification in V1 (Duncan & Boynton, 2003).

1.5.2 Intra-Individual Variability: Intra-Areal

Variability can also been seen within participants. The clearest form of variability is within a single map, intra-area variability. It is well established that the centre of the visual field is over-represented on the cortex (Popovic & Sjöstrand, 2001). At higher eccentricity, where the peripheral region of the visual field is represented, a lower level of cortical magnification is found. This effect is seen across multiple maps, but is more pronounced in some than others. For example, LO1 has a particularly high over-representation of the fovea (Larsson & Heeger, 2006).

This variability is reflected in the strong effect of eccentricity in many visual abilities. If visual abilities are linked to intra-area variability then a single participant should perform a single task to different levels of success depending of the position of the stimulus in visual space. Participants perform poorly when a stimulus is presented in the peripheral vision relative to central vision. This is seen for multiple visual tasks including speed perception (Tynan & Sekuler, 1982), acuity (Duncan & Boynton, 2003) and letter identification (Klein, Berry, Briand, D'Entremont, & Farmer, 1990).

It should be noted that the close pairing between cortical magnification and a perceptual eccentricity effect is not seen in all tasks. For example, flicker fusion thresholds (the frequency at which a flashing light appears to be constant) does not scale with cortical magnification (Rovamo & Raninen, 1984). Whilst temporal resolution decreases with movement away from the fovea, this decrease is much smaller than tasks reliant on spatial resolution (Aghdaee & Cavanagh, 2007). Additionally, in some tasks the peripheral deficit is reversed. Dykman and Antis (2015) explored the eccentricity effect of as stimuli consisting of dense random dots that move clockwise around a circular orbit. Viewed in the fovea, this stimuli appears as dynamic visual noise. In the periphery the circular motion is clearly visible.

1.5.3 Intra-Individual Variability: Inter-Areal

There is some debate regarding the extent of variability between visual maps. For example, does high levels of cortical magnification in one visual area lead to similarly high levels in other visual areas within the same participant? This question has been explored in terms of size measurements. Pre-cortical components of the visual system show a consistency in size within the same individuals (Andrews et al., 1997). Moving towards retinotopic maps at the earliest stages of the visual hierarchy (V1, V2 and V3) this consistency appears to break down to some extent. Whilst V1 and V2 correlate in size measures, V1 and V3 show little relationship (Dougherty et al., 2003).

As the size of retinotopic areas is closely linked to the level of cortical magnification (e.g. a larger cortical area would imply more cortex is devoted to the processing of each point in visual space), it would be expected that cortical magnification will also show high levels of inter-areal variability. If cortical magnification constrains perception, the consequence of inter-areal variability would be that participant performance differs across tasks. Participants who perform well in a luminance defined orientation discrimination task reliant on V1 (Duncan & Boynton, 2003) would not necessarily be expected to perform well on a second task reliant of later areas, for example motion perception (Tootell et al., 1997).

1.6 Receptive Field Properties as a Limiting Factor

It is possible that in addition to cortical magnification (Duncan & Boynton, 2003, 2007), other elements of retinotopy also constrain performance. A possible candidate for behavioural limitation is the characteristics of receptive fields. Each neuron in the visual cortex receives input from a specific location in the visual field, this is the receptive field. The classical receptive field is primarily excitatory, the neuron will fire upon stimulation (Cavanaugh, Bair, & Movshon, 2002). External to the classical receptive field is a suppressive surround. Activation of the suppressive surround will inhibit the firing of the neuron (DeAngelis, Freeman, & Ohzawa, 1994). The size of receptive fields increases with eccentricity (Dumoulin & Wandell, 2008), surround sizes are larger in the periphery than the fovea. Receptive field sizes also increase in size from V1 to V2 and from V2 to V3 (Dumoulin & Wandell, 2008).

Physiological surround suppression was first demonstrated in cats (Hubel & Wiesel, 1965). When cats are presented with stimuli that extends outside of the receptive field, neurons in areas 18 and 19 respond more weakly than when they are presented with optimally located stimuli. The majority of cell in the primate V1 are also susceptible to surround suppression, and neuronal responses in this area can be suppressed by up to 70% (Jones, Grieve, Wang, & Sillito, 2001).

The perceptual effects of surround suppression have been linked to the receptive field properties of the visual system. Surround suppression is a form of visual context modulation (Bair, Cavanaugh, & Movshon, 2003). The presence of a stimulus directly outside the classical receptive field inhibits a response to a stimulus located within the classical receptive field (Bair et al., 2003). For example, when a luminance defined grating is surrounded by a grating of higher contrast, the target grating will appear to be of a lower contrast than if it is displayed alone (Chubb, Sperling, & Solomon, 1989). Mirroring the pattern of receptive field size (Dumoulin & Wandell, 2008), perceptual surround suppression is strongest at higher eccentricities (Xing & Heeger, 2000).

1.6.1 Crowding

Crowding describes the deleterious influence exerted by adjacent stimuli during discrimination tasks. The surrounding stimuli have an inhibitory interaction with the target stimuli. For example, the presence of surrounding images may make a target image more difficult to identify. A letter presented in peripheral vision that is identifiable when alone may become difficult to decipher when placed within a clutter of other letters (Levi, 2008).

Crowding can be seen in a variety of tasks (Andriessen & Bouma, 1976) including face recognition (Louie, Bressler, & Whitney, 2007), orientation discrimination (Andriessen & Bouma, 1976) and Vernier acuity (Levi, Klein, & Aitsebaomo, 1985), but occurs only in vision (Levi, 2008). The effect of crowding can be quantified by obtaining a measurement of critical spacing. This refers to the distance between the target and surrounding images at which a deleterious influence occurs.

The cortical mechanisms underlying crowding are unknown (Levi, 2008). Multiple and diverse models have been proposed (Levi, 2008) and all share the claim that it is a failure of feature selection in some way. The neural location of the underlying cause of crowding is also debatable. Some have suggested that it may be attributed it to early visual areas (Levi, 2008). Crowding will occur if a target is presented to one eye and a distractor to the other (Flom, Weymouth, & Kahneman, 1963). This indicates that crowding occurs after binocular combination, possibly as early as V1. However, others argue that crowding must occur later than V1 (He, Cavanagh, & Intriligator, 1996). He and colleagues present data demonstrating that greater levels of crowding are seen for stimuli presented in the upper quadrants of the visual field than the lower quadrants. This asymmetry is not seen in cortical measures of
V1 (Horton & Hoyt, 1991b; Sereno, 1995).

V4 has been suggested as a likely candidate for the locus of crowding (Levi, 2008). Arman and colleagues argue for this later crowding locus (Arman, Chung, & Tjan, 2006). They investigated the neural correlates of crowding by measuring BOLD responses during a letter identification tasks. In the control condition the target was presented alone in peripheral vision, in the crowded condition the target was accompanied by additional

letters. BOLD responses in V1, V2 and V3 showed little difference across conditions, but V4 responses were suppressed in the crowded condition relative to the control. Evidence from a psychophysical study further strengthens the claim of a crowding locus later than V1 (Chung, Li, & Levi, 2007). First order distractor stimuli (luminance defined) could exert a deleterious influence on second order target stimuli (contrast defined), suggesting that crowding occurs at a location associated with the combination of first and second order stimuli.

The receptive field size and anisotropic properties of V4 (Pinon, Gattass, & Sousa, 1998) seem consistent with the influence exerted on the process of crowding by the size and orientation of stimuli (Toet & Levi, 1992). V4 shows cortical anisotropy (Pinon et al., 1998). This visual areas was defined using electrophysiological mapping and myeloarchietural criteria in Cebus monkeys. Cortical magnification in the isopolar dimension (parallel to the polar angle map) was 1.5-2 times larger than in the isoeccentric dimension (parallel to the eccentricity map). These properties of V4 are consistent with the anisotropy in the critical distance of crowding measured behaviourally (Toet & Levi, 1992).

The proposal of V4 as the locus of crowding is appealing but currently poorly supported. Additionally, non-retinotopic regions have been suggested to underlie crowding. For example, the pulvinar has also been proposed (Michael & Desmedt, 2004). Following a stoke in the pulvinar nucleus of the posterior thalamus patients demonstrated abnormal responses in crowding tasks, although there is some debate as the suitability of the task used as a measure of crowding (Levi, 2008).

1.6.2 Is Crowding a Form of Surround Suppression?

Crowding is a psychological phenomenon and has received attention primarily from this field (Petrov, Popple, & McKee, 2007). Surround suppression, has been studied in parallel but separately by neuroscientists. There is some indication that crowding and surround suppression are in fact a single phenomenon (Petrov et al., 2007). Surround suppression has been compared to crowding through psychophysical studies (Petrov, Carandini, & McKee, 2006; Petrov & McKee, 2006; Snowden & Hammett, 1998). At a

conceptual level, the two processes appear similar; activity of nearby stimuli/receptive fields inhibits the identification/activation of the target stimuli/neuron. Multiple similarities between the two phenomena have been identified (Petrov et al., 2007), strengthening the suggestion that crowding and surround suppression describe the same process occurring at a psychological and neurological level.

Both crowding and surround suppression have a peripheral locus. They occur only at high eccentricities and are not seen when stimuli are presented at the fovea (Bouma, 1970; Flom et al., 1963). Flom et al., (1963) presented stimuli peripherally and found participants were poorer at an identification task using Landolt C when black bars were placed tangentially to the target and within a certain distance of the target. The identification of the letter C was disrupted by the presence of non-letter flankers. Similarly, Bouma (1970) found that interference in peripheral vision was very extensive; in some cases the inference was as large as half the target eccentricity. Unlike Flom et al. (1963), both the target and surrounding stimuli used by Bouma (1970) were letters. This peripheral locus was also demonstrated in surround suppression by Snowden and Hammett (1998). Detection thresholds were highest in peripheral locations at all contrasts tested.

Radial-tangential anisotropy has also been shown to correlate with crowding and surround suppression. This form of anisotropy refers to a change in the strength of the phenomena dependent on the location in the visual field. In a radial position the stimulus' local pattern orientation is coincident with the angular meridian, in a tangential position it is not perpendicular (Mannion, McDonald, & Clifford, 2010). Tout and Levi (1992) presented participants with 3 T's. The 3 T's were randomly positioned either upwards or downwards. The task was to identify the orientation of the centre T. The stimuli were presented at eccentricities of 0 degrees, 2.5 degrees, 5 degrees and 10 degrees. Presentation was in the lower vertical meridian and on the nasal halves of the 45 degree diagonal field meridian and the horizontal meridian. The critical spacing value was higher at greater eccentricities, in the periphery the distance between the target and the flankers must be greater to avoid disruption of target identification (Toet & Levi, 1992). This is consistent with the findings of Flom et al. (1963) and Bouma (1970). Tout and Levi (1992) also report radial- tangential anisotropy, flankers were more disruptive to

orientation identification when they were aligned vertically than when alignment was horizontal.

Radial-tangential anisotropy was also demonstrated to occur in peripheral surround suppression (Petrov & McKee, 2006). Contrast detection thresholds were collected for a luminance defined vertical grating with a bow-tie surround. The surround consisted of 2 non-adjacent quadrants of the full annulus. The bow-tie surround was positioned radially or tangentially relative to the stimulus position in visual space. In the radial condition the stimulus was placed on the vertical meridian with the surround flanking the target vertically or the stimulus was placed on the horizontal meridian with the surround flanking the target horizontally, and vice versa for the tangential condition. The radial placement of the surround resulted in significantly higher level of suppression than the tangential.

Within the same comprehensive analysis of the spatial properties of surround suppression (Petrov & McKee, 2006) it was also found that the extent of suppression exerted on surrounding stimuli scales with eccentricity. The relationship between eccentricity and suppression extent can be explained in terms of the retinotopic properties of the visual cortex. Low cortical magnification in the periphery would be expected to underlie high surround suppression, because the limited cortical representation of visual space at high eccentricities results in a decrease in resolution (Duncan & Boynton, 2003). There was also some indication that surround suppression is unaffected by changes in stimulus size (Petrov & McKee, 2006).

Dependency on eccentricity and size invariance were also demonstrated for crowding (Toet & Levi, 1992; Tripathy & Cavanagh, 2002). Crowding extent increases at higher eccentricities (Toet & Levi, 1992) and the extent of crowding does not change with increases in target size (Tripathy & Cavanagh, 2002). Crowding and surround suppression also share sensitivity to the orientation (Andriessen & Bouma, 1976; Levi, Klein, & Hariharan, 2002a) and spatial tuning of stimuli (Chung, Levi, & Legge, 2001; Petrov, Carandini, & McKee, 2005).

Despite these similarities, others claim that crowding and surround suppression are in fact two distinct processes (Levi, 2008). Some have proposed inward-outward anisotropy as

an unambiguous differentiation of crowding and surround suppression (Levi, 2008). Inward-outward anisotropy can be illustrated by the increased difficulty experienced in identifying a word presented right of fixation in comparison to a word presented left of fixation (Bouma, 1973).

Preference is shown to a task that requires processing from low eccentricities to high eccentricities rather than from high eccentricities to low. Using a contrast detection paradigm and masks in various positions, it was demonstrated that this form of anisotropy occurs in crowding but not surround suppressions (Petrov et al., 2007). Unlike in previous discussions of the similarities between the two phenomena, a common stimulus was used in the comparison of the two processes. The authors suggest that lack of consistency in the investigation of crowding and surround suppression may have led to the false belief that they are different levels of the same process.

To fully delineate the relationship between surround suppression and crowding it is necessary to explore the retinotopic basis of both crowding and surround suppression. If these phenomenon are constrained by receptive field properties then it would indicate that they are in fact 2 levels of a single process. A close link between variability in these behavioural measures and receptive field properties would support this hypothesis. A shared cortical basis would indicate that within a single participant, levels of crowding and surround suppression are correlated. It would also suggest that receptive field properties function as a bottle-neck in perception, analogously to the role identified for cortical magnification by Duncan and Boynton (2003; 2007).

Recent advances in retinotopic mapping allow the collection of a detailed estimation of the receptive field size, the centre size and the surround/centre ratio (Zuiderbaan, Harvey, & Dumoulin, 2012). Using population receptive field mapping (pRF) receptive field parameters can be collected for multiple visual areas quickly and noninvasively. pRF modelling is an analysis technique that uses retinotopic data collected during MRI to estimate the size of receptive fields. Unlike standard retinotopic mapping which pairs a single voxel to a single point in space to which it responds most strongly, pRF modelling fits a Gaussian receptive field function to each voxel time series.

1.6.3 IQ

At the beginning of the 20th century, it was observed that children's performance ratings across a number of different school subjects were positively correlated (Spearman, 1904). Based on this observation Spearman suggested that these correlations reflected the influence of a modality-general mental ability that affected the performance on all kinds of tests, and he labelled this general ability factor as *g*. Since this discovery, the involvement of *g* in multiple perceptual domains has been documented (Deary, 1994; Li, Jordanova, & Lindenberger, 1998; Meyer, Hagmann-von Arx, Lemola, & Grob, 2010).

Recently, the link between IQ and perceptual abilities has been further developed (Melnick et al., 2013). Participants with high IQ levels were more susceptible to surround suppression, as measured in a separate psychophysical task. This relationship was identified with a broad range of intelligence subtypes, it was not confined to sensory measures of IQ. If, as is hypothesised and strongly supported by the literature (Jones et al., 2001), surround suppression is reliant on the receptive field properties of the early visual cortex, then IQ may also be determined by these properties. It therefore possible that, in addition to visual abilities, retinotopic properties may also predict complex cognitive abilities.

The links demonstrated to exist between IQ and surround suppression (Melnick et al., 2013) are conceptually similar to the associations between reading and crowding (Attkinson, 1991). In both cases, a complex cognitive ability is predicted from perceptual measures. The influence of crowding on reading is well documented and the reading deficits seen in dyslexia have been attributed to crowding (Attkinson, 1991). Crowding can occur in letter recognition tasks (Tout & Levi, 1992) as well as word recognition (Levi, 2008). The critical space for reading is the same as the critical space for crowding. Levi (2008) tested the effect of letter size and the effect of spacing on reading performance. Whilst size had no effect of reading performance, spacing influenced reading ability. Similarly, Pelli et al. (2007) found that crowding susceptibility was related to reading rate. The uncrowded span (the number of letters than can be acquired in one fixation) was proportional to the rate of reading. The link between crowding and reading is further supported by the study of amblyopic participants, a group

which shows poor reading ability. When presented with text consisting of largely spaced letters, amblyopic participants showed increased reading rate. This indicates that the reading deficit was in fact abnormal crowding (Levi, Song & Pelli, 2007).

The mechanisms underlying the potential links between IQ, perception and receptive field properties are currently poorly specified. IQ is a broad and complex construct. It is thought to represent a general and high level cognitive ability. The links between this measure and low level abilities, such as tactile discrimination (Li, Jordanova & Lindenberger, 1998) and pitch discrimination (Deary, 1994), are well established (Meyer et al., 2010). The work of Melnick et al. (2013) in the specification of this link and recent advances improving the ease and speed of receptive field measurement (Zuiderbaan et al., 2012) allow an opportunity to further characterise this relationship.

In addition to retinotopic properties of the visual maps, this link may also be mediated by neurotransmitters. One possible candidate underlying this link might be gamma-aminobutyric acid (GABA) concentrations in the nervous system. GABA is the main inhibitory neurotransmitter in the vertebrate central nervous system. Its main role consists of reducing neuronal excitability throughout the nervous system. GABA binds to specific transmembrane receptors at either pre- or postsynaptic levels. Ion channels opens in response to the binding and allow the flow of negatively charged ions into the neuron or positively charged ions out of the cell, causing hyperpolarization, hence the neuron will be less likely to fire an action potential. Given its documented role in perceptual surround suppression (Yoon et al., 2009) and hypothesised involvement in cortical surround suppression (Harvey et al., 2013), GABA may show involvement in the underlying mechanism linking intelligence to perceptual abilities (Melnick et al., 2013).

1.7 Summary

Variability between participants is seen both in retinotopic maps (Arcaro et al., 2009) and visual abilities (Nefs et al., 2010). Recent work has indicated a correlational relationship between cortical magnification and low level sensory abilities (Duncan & Boynton, 2003, 2007). The literature supports the hypothesis that retinotopic organisation may also constrain higher level visual abilities.

Part I: Does Cortical Magnification Constrain Visual Abilities?

2 Inter-Areal Correlations in Measures of Radial Cortical Magnification, Polar Cortical Magnification and Surface Area

2.1 Introduction

As described in the introduction, a link has been demonstrated between individual variability in perceptual abilities and structural and functional properties of cortical areas (Schwarzkopf et al., 2011). In recent years, cortical magnification has been one focus of research into this correlation (Duncan & Boynton, 2003, 2007). It has been argued that behavioural abilities are limited by cortical magnification within the task-relevant area (Duncan & Boynton, 2003). For example, individual variability in an acuity task was found to correlate with individual variability in cortical magnification in V1 (Duncan & Boynton, 2003). The replication of this limiting role for cortical magnification in other sensory domain (Duncan & Boynton, 2007) and species (Leingärtner et al., 2007) indicates that this phenomenon may also be found at higher level visual areas.

The possibility exists that, in the same way that V1 cortical magnification correlates with an individual's performance in a low level acuity task, cortical magnification further up the visual processing stream will correlate with more complex visual abilities. A hypothesis of this thesis states that behavioural abilities at an individual participant level will correlate with cortical magnification in the relevant visual area. For example, orientation discrimination thresholds for motion defined stimuli are expected to correlate with cortical parameters such as size and cortical magnification in regions underlying perception of motion defined boundaries, such as V3A (Larsson & Heeger, 2006).

Clarity of the interpretation of these potential higher level correlations will be impaired by a lack of understanding of the inter-dependence of visual area structure. If there is a high correlation between visual areas in levels of cortical magnification this will complicate conclusions regarding the specific role played by each visual area in limiting behavioural ability. If cortical magnification in all higher areas is correlated with cortical

magnification in V1 then it may not be possible to identify which visual area is driving a particular behavioural ability. Before correlations between behaviour and cortical magnification can be examined, this potential inter-dependence of visual areas must be addressed. Documentation of inter-areal correlation is the primary aim of this chapter.

2.1.1 Lower Visual Areas

The inter-areal correlations between the sizes of early visual areas have been well documented. Measures of cortical magnification are closely related to those of surface area, implying that cortical magnification will show similar inter-areal correlations. Inter-individual differences in visual areas have also been explored. A consistent and well established finding is the high levels of individual differences in V1 size. The surface area of this region can differ by as much as 3 times between individuals (Stensaas et al., 1974). This finding is supported by both early post-mortem studies (Brodmann, 1918) and later functional mapping investigations (Dougherty et al., 2003). The mechanisms associated with this size variability remain unknown, although explanations implementing cone density have been proposed (Wandell, Brewer, & Dougherty, 2005).

Importantly, V1 does not simply scale with brain size. It may be expected that individuals with large V1 simply have larger brains, however this is not evident. In fact, Schwarzkopf et al. (2011) found some indication of an inverse relationship between V1 surface area and overall cortical size. This finding suggests that the size of V1 is governed by complex mechanisms and offers no clear prediction of how this individual variability in size will progress in higher visual areas.

Variability in visual areas V2 and V3 has been less thoroughly examined. Dougherty et al. (2003) presented measurements of functionally defined V2 and V3 in the human cortex and consider correlations between these regions. In agreement with earlier research (Brodmann, 1918), Dougherty et al. (2003) found that variability between participants in V1 surface area was high. The size of this region varied by a factor of 2.5. This variability also progressed to later regions, with similar levels of individual differences seen in V2 and V3. There was a correlation between V1 size and V2 size. A correlation was also found between V2 size and V3 size. No correlation was observed between V1 size and

V3 size. It was suggested that at this point in the visual stream additional information is introduced, possibly pulvinar input (Sincich & Horton, 2002), thereby disrupting correlations between later areas and V1. Dougherty et al. (2003) also calculated cortical magnification measurements for V1, V2 and V3, finding similar levels of cortical magnification when overall surface size is accounted for.

The findings of Dougherty et al. (2003) indicate that whilst the surface area size may be correlated between V1 and V2, this simple scaling relationship most likely does not progress further than V2. The inter-areal correlations in visual maps higher than V3 remain unexamined. It is unknown both how maps correlate with one another and how much inter-individual variability exists in these relationships. Given the high individual variability in V1 surface area (Schwarzkopf et al., 2011), it seems likely that variability in other visual areas is also high. For this reason, it may be unwise to generalize from the modestly sized sample of Dougherty et al. (2003).

There has been some debate as to the underlying reasons for the V1-V2-V3 correlations. For decades, there has been an argument that visual areas should be considered inter-dependent. Some argue that areas sharing a common boundary should be defined as a single entity. There have been several terms proposed for these pairings including functional dyads (Gattass, Gross, & Sandell, 1981) and map clusters (Wandell et al., 2005). This view was extended to propose that visual areas V1, V2 and V3 not only shared qualitative features, but also possessed a common mathematical underpinning (Balasubramanian, Polimeni, & Schwartz, 2002). It has been shown that a single mathematical expression (termed Wedge-Dipole mapping), provides a good approximation of the topographic structure in monkeys primary visual cortex, as well as V2 and V3. The same function, simultaneously describe the topographic organization in all three areas (Balasubramanian et al., 2002). Balasubramanian et al. (2002) argued that early visual areas share a common pattern in measures of topographic anisotropy and shape.

Topographic anisotropy refers to the differences between radial cortical magnification and polar cortical magnification within a visual area. Typically, visual areas are somewhat compressed in the polar direction (perpendicular to the inter-areal boundaries), so have higher levels of radial than polar cortical magnification (Balasubramanian et al.,

2002). This relationship is typically expressed as a ratio of polar cortical magnification to radial cortical magnification (Adams & Horton, 2003b).

Balasubramanian et al. (2002) presented a 5 parameter wedge-dipole model that simultaneously summarized the retinotopy of V1, V2 and V3 of macaque monkeys. Later fMRI in humans confirmed that this visuotopic map complex also extended to humans (Polimeni, Balasubramanian, & Schwartz, 2006), with low inter-species variation in estimates of overall topography and local irregularities. The retinotopy in humans was similar to that of macaques. For example, higher isotropy exists near the internal horizontal meridian of V1 than near the V1-V2 border in both humans (Blasdel & Campbell, 2001) and squirrel monkeys (Adams & Horton, 2003b). The success of this model can be attributed to its ability to adjust to the local anisotropy. Previous models, such as conformal mapping (Schwartz, 1994), assumed isotropy. Conformal mapping models propose that visual space is represented in later visual areas in a qualitatively similar way in later visual areas as has been observed in V1, with a roughly equal representation of polar and eccentricity maps (Blasdel & Campbell, 2001). Others have argued that this assumption is false and renders conformal mapping inappropriate for descriptions of visual areas later than V1 (Polimeni et al., 2006).

Early efforts to document and explain this anisotropy have relied upon the columnar structures of V1 and V2 in the macaque. LeVay, Hubel, and Wiesel (1975) used the orientation of ocular dominance stripes in layer IV of the macaque V1 to test the hypothesis that a sub-columnar 1:2 anisotropy ratio existed, which translated to a 1:1 supra-columnar anisotropy following integration of the two monocular maps. The proposal that V1 has similar levels of compression in the radial and polar directions is supported by later studies (Blasdel & Campbell, 2001; Van Essen et al., 1984). There is some suggestion that greater isotropy is seen near the vertical meridian (1.15:1) than the horizontal meridian (1.5:1), perhaps due to the less consistent columnar pattern near the horizontal meridian (Blasdel & Campbell, 2001).

Tootell, Switkes, Silverman, and Hamilton (1988) also proposed a ratio reliant on the ocular dominance columnar structure, but presented measurements indicating a 1:1 sub-columnar ratio and a 2:1 overall ratio. They claimed that in macaque V1, at the level of the single column, there was no local anisotropy. Isotropic modelling of V1, e.g. the

model assumes a ratio of 1:1, is generally accurate for V1 (Adams & Horton, 2003b; Polimeni et al., 2006). For this reason, the non-isotropic overall estimate of Tootell et al. (1988) seem unlikely. There are multiple possible reasons for this discrepancy. Most likely, the methodologies used by Tootell et al. (1988) are limited. Tootell et al. (1988) acknowledged resolution ambiguity in the deoxyglucose techniques used to estimate cortical parameters and they noted that the anisotropy ratio estimated in their study could be as low as 1.5:1. Additionally, Tootell et al. (1988) computed their estimate based on assumptions regarding the causal relationship between cortical compression and ocular dominance stripes that has since been questioned (Adams & Horton, 2003a).

Delineation of anisotropy in extrastriate visual areas has remained less well understood. There has been some attempt to understand the anisotropy of this region in analogous terms to that of V1. V2 also shows a columnar cortical pattern, described as thin-thick-interstripe (Roe & Ts'o, 1995). As in V1, these stripes lie perpendicular to the polar representation. Roe and Ts'o (1995) identified a 2:1 sub-columnar anisotropy, resulting in a 6:1 supra-columnar anisotropy. Although, a later study conflicts with the triple stripe model (Felleman et al., 2015), questioning this anisotropy estimate.

The recent expansion of Wedge-Dipole mapping conflicts with previous columnar explanations of anisotropy. Polimeni et al. (2006) claim that anisotropy is dependent on the mathematical principles of the shared boundaries between V1 and V2 and between V2 and V3. The clear close association between the columnar structures of V1 and V2 and the polar maps is acknowledged (Polimeni et al., 2006) but a causal role for the ocular dominance columns such as the mechanism proposed by Tootell et al. (1988) is rejected. Research has indicated that the retinotopic organisation of V1 is consistent regardless of ocular dominance stripes (Adams & Horton, 2003a), supporting the argument that columnar structure does not play a causal role in anisotropy. A causal mechanism would indicate a close correlation between ocular dominance columns and the global topography of V1. In fact, there is high inter-individual variability in the expression of squirrel monkey V1 columns and very little variability in the shape of V1 (Adams & Horton, 2003a).

2.1.2 Higher Visual Areas

To date, research examining the relationship between visual areas has focused on lower tier regions (Dougherty et al., 2003). V1, V2 and V3 have been closely correlated in a variety of measures throughout the literature. One possibility is that this correlational relationship continues throughout the cortex, with V1 acting as a driving force to determine the retinotopic parameters of all later areas. The computational explanations of Polimeni et al. (2006) would not predict such a possibility. The mathematical inter-dependency of V1-V2-V3 would be disrupted by the inclusion of any later visual areas. A second possibility is that later visual areas function as independent entities, perhaps sharing some parameters with neighbouring regions but showing little inter- dependence with either the V1-V2-V3 complex or later regions. A third possibility is that later visual areas form a second, independent, complex and display inter-dependency as seen in V1-V2-V3. In this way, the wedge-dipole mapping may be a consistent design principle of the visual cortex (Polimeni et al., 2006).

To address these possibilities, a full analysis of correlations between cortical parameters of visual areas, including higher level retinotopic regions such as V3A, V4, LO1 and LO2, is required. The size and cortical magnification correlations seen for V1 with V2 and V2 with V3 (Dougherty et al., 2003) are expected to be replicated. However, the relationships between higher tier areas remain unknown, as do the relationships between higher tier areas and lower regions. Furthermore, given the inverse relationship between V1 size and overall visual cortex size (Schwarzkopf et al., 2011), no clear predictions about the direction of these potential correlations can be made.

2.1.3 Eye Surface Area

In addition to the hypothesised links between retinotopic areas, there is also some indication that the correlations between lower tier visual areas may also extend to earlier portions of the visual system such as the eye. The components of the subcortical early visual system have long been known to correlate in size. Andrews et al. (1997) examined a cross sectional area of the optic track, volumes of magnocellular and parvocellular layers and the surface area and volume of V1. There was a 2-3 fold difference in the size

of these areas between participants, but within participants all areas correlated with one another. This inter-dependency was reproduced at a neuronal level; Stevens (2001) demonstrated that the number of neurons in V1 correlated with the number of LGN neurons.

This work was expanded by Pearce and Dunbar (2012) to address eye size. It was found that individuals living in high latitude countries showed greater orbital volume (a measure closely associated with eye size; Pearce & Bridge, 2013). As eye size did not affect visual abilities, it was though that the large eyes compensated for low light levels in geographical areas of low light and short days. The subcortical elements of the visual system are tightly scaled, any individual variability is coordinated across the system (e.g. Andrews et al., 1997). For example, if a participant has a large V1, they will have a commensurately large lateral geniculate nucleus and optic tract (Andrews et al., 1997). If this tight-scaling expands to cortical elements then the compensatory role for the eye may also lead to higher level of grey matter in visual areas V1, V2 and V5/MT but not increased overall brain size (Pearce & Bridge, 2013).

An increase in grey matter would be expected to correlate with changes in both the surface area of visual areas and measures of cortical magnification. It is hypothesised that participants with small eyes may compensate for this deficit through changes in retinotopic organisation, a property through to have high plasticity (Godde, Leonhardt, Cords, & Dinse, 2002). This finding would expand the work of Pearce & Bridge (2013) to further characterise the relationship between eye size and cortical parameters.

To explore the relationship between eye size and the size and organization of other elements of the visual system I will compare eye size to multiple retinotopic measures of V1. I will estimate participant eye volume using the structural MRI data used to make the other retinotopic measures used in this chapter. I will examine the data for correlations between eye volume and V1 surface area, V1 width, V1 length, V1 radial cortical magnification and V1 polar cortical magnification Due to the exploratory nature of this hypothesis, no predictions will be made regarding the direction of these links.

2.2 Retinotopy Methods

2.2.1 Participants

14 subjects (5 males) participated in the experiment. Subjects were aged between 20 and 34. All participants had normal or corrected to normal vision. Ethical approval was granted by the Royal Holloway University Department of Psychology Ethics Committee. Written consent was obtained from all participants. Data collection was carried out in accordance with MRI safety guidelines.

2.2.2 MRI Acquisition

Data was collected on a 3T whole-body MR scanner (Magnetrom Trio; Siemens, Erlagen, Germany) at Royal Holloway University. All subjects participated in 2 scanning sessions. The first scan collected a high-resolution anatomical volume. A second scan obtained retinotopic data from the visual cortex. The 2 sessions took place on different days.

A T1 weighted structural brain image with whole brain coverage was obtained using an MDEFT sequence (Deichmann, 2006). The following parameters were used; voxel size= 1x1x1ms, repetition time (TR) = 7.9ms, time to inversion (TI) = 910ms, echo time (TE) = 2.5, flip angle= 16°. This data was used to visualise the flattened cortex. During collection of this anatomical data participants were instructed to lie as still as possible, no task was performed.

A second scanning session was carried out to obtain retinotopic data. Before retinotopic data collection began, a short (approximately 10 minutes) anatomical scan was performed. This served to allow co-registration between the previously collected MDEFT data and retinotopic data. This short anatomical scan collected a T1-weighted MPRAGE volume (magnetisation- prepared-rapid-acquisition gradient echo) with the head in the same position as the functional scan, allowing co-registration. This anatomical volume had a voxel size of 1x1x1mm, it had twice the inplane resolution of the functional scan. This anatomical volume allowed alignment of the functional data with the anatomical

MDEFT data, permitting later visualisation of the functional retinotopic data on the flattered cortical surface. An image registration algorithm (Nestares & Heeger, 2000) was used to align he anatomical and functional images across sessions.

Retinotopic scans were performed with a lower resolution than the MRAGE co-registration volume; a voxel size of 3x3x3mm was used. 24 slices were collected for each participant; these slices were approximately parallel to the calcarine sulcus and positioned to cover the temporal and occipital cortex. The following scan parameters were used; RT= 1500ms, TE= 30ms, flip angle= 75°, matrix= 64x64.

2.2.3 Cortical Surface Extracting and Analysis

Cortical surfaces were extracted from a high resolution T1-weighted image using SurfRelax (Larsson, 2001), (http://www.pc.rhul.ac.uk/staff/J.Larsson/software/surfrelax/doc/SurfRelax-HOWTO.html). This is public domain software and has the advantage of guaranteeing the correct spherical topology of the output surface whilst retaining high anatomical accuracy. For each hemisphere 4 surfaces are obtained. 2 surfaces corresponding to the inner grey/white cortex and 2 corresponding to the outer grey/pial cortex.

Acquisition of the flattened surface was performed in 4 steps. Firstly, pre- processing removed noise, intensity variation and all non-brain tissue from the image. Initial estimates of cortical surfaces were then made for each hemisphere. After hemisphere segmentation, the volume of white matter was extracted, and then the surface of the white matter volume was taken. The third step was to locate the boundary between the grey and white matter and the boundary between the grey and pial matter. At this stage manual inspection was required, and possibly also manual editing. For all hemispheres reported here, either no editing or minor editing was required. Fourthly, the data was prepared for visualisation and measurement. The cortex was inflated. The surface patch covering the occipital cortex (cortex within 10cm of the occipital pole) was cut and flattened. Calculation, measurements and visualization of the data was then performed on the flattened triangulated mesh representation.

2.2.4 Retinotopic Mapping

Retinotopic mapping was carried out using the procedures of Larsson and Heeger (2006). Visual areas were identified in 14 subjects through the measurement of BOLD activity during observation of checkerboard stimuli. Wedge and ring stimuli were presented in order to systematically activate multiple retinotopic maps in the occipital cortex. To map the visual field representation in the polar dimension, checkerboard wedges were presented rotating clockwise and counter-clockwise. To activate radial aspects of the maps, a checkerboard ring was displayed expanding or contracting. Using these stimuli, the temporal activation of each voxel allows a region of the cortex to be paired to point in the visual field, thereby identifying the retinotopic properties of the visual cortex and the boundaries between areas.

Visual stimuli were presented on a screen behind the scanner and viewed through a mirror. Stimuli consisted of a checkerboard pattern restricted to a ring or wedge. The wedges were 22.5 degrees polar angle and advanced by 22.5 degrees per TR. The wedges rotated in either a clockwise or anti-clockwise direction. The rings advanced between 0° and 13° degrees eccentricity in steps of 0.75 degree per TR. The rings expanded or contracted. The checkerboard pattern which filled the wedge and ring stimuli also moved within the ring or wedge apertures. Each radial checkerboard strip traversed towards or away from the centre of the screen at a speed of 2 degrees per second. The direction of movement was randomised. The checkerboard was coloured black and white and the contrast varied between trials (100%, 31%, 10% & 3%). The background of the screen remained a constant grey throughout. One scan was collected per contrast and direction (expanding/contracting rings, clockwise/anti-clockwise wedges).

In total, 16 runs were performed. The wedge stimuli were presented clockwise and counter-clockwise at each of the 4 contrasts. The ring stimuli were presented contracting and expanding at each of the 4 contrasts. Contrasts were presented in ascending order. Clockwise wedges and counter-clockwise wedges were presented first, followed by expanding rings and contracting rings. Stimuli was always presented in this order, there was no randomisation.

Data from the two stimulus directions were combined to estimate the response phase. The time series for the data collected during presentation of the clockwise wedge was time reversed and averaged with the data collected during the presentation of the counter-clockwise wedge. The same calculation was made for the expanding ring and contracting ring. In this way, the haemodynamic time lag for the 2 directions is thought to cancel each other out.

The average wedge time series and the average rings time series were submitted to travelling wave analysis. This process compared the time course of the fMRI data to the time course of stimuli presentation. Travelling wave analysis allows the estimation of the position in visual space to which each voxel maximally responds to, as it estimates the response amplitude, phase and coherence for the wedge time series (polar angle) and ring time series (eccentricity), which can be overlaid on top of the structural anatomy image. This analysis forms the basis for the visualization of the retinotopic maps (polar and eccentricity maps.) Only voxels with a coherence > 10% were included in the analysis. The assumption of this analysis is that the time series can be reasonably approximated by a sine wave.

Motion correction was performed on the functional data using FSL [Software Library of FMRIB (Functional Magnetic Resonance Imaging of the Brain), www.fmrib.ox.ac.uk/fsl]. The functional data was then aligned to the high- resolution MDEFT using the short anatomical volume collected within the functional scanning session.

2.2.5 Locating Visual Area Boundaries

The retinotopic data was displayed on the flattened cortical surface of the occipital lobe. Each hemisphere was visualised and analysed independently. Location of visual area boundaries was performed using SurfRelax (custom software in Matlab). Retinotopic maps were identified using 5 standard criteria (Larsson & Heeger, 2006; Wandell et al., 2007). Firstly, each visual area contained only one representation for each point in the visual field. Secondly, a substantial portion of the visual field was represented by each

area. Thirdly, the visual area showed an orderly representation of visual space, its organisation is contiguous in both eccentricity and polar angle. The MRI data showed the response phase to be progressing across the area in an orderly manner. Fourthly, discontinuities were seen at the edge of the visual area. In most cases, this materialized as a phase reversal in polar angle, with the adjacent area displaying a mirror image. However, this criterion can also be fulfilled by a reversal in eccentricity and a shared polar angle representation, as in V3A/V3B (Wandell et al., 2005). Finally, angular and radial components of the visual area must not be parallel to one another. Where there was controversy in the literature, for example the re-definition of V3B as the posterior section of LO1 (Larsson & Heeger, 2006; Smith, Greenlee, Singh, Kraemer, & Hennig, 1998), the conventions of Larsson and Heeger (2006) were followed.

Boundaries were drawn manually from the lowest eccentricity to the highest. Boundaries began immediately outside the foveal confluence and extended to the highest represented eccentricity (figure 2-1 & 2-2). Visual areas V1, V2d, V2v, V3d, V3v, V3A, V4, LO1 and LO2 were located in this way. 14 participants were analysed (28 hemispheres). All retinotopic maps were located in all participants.

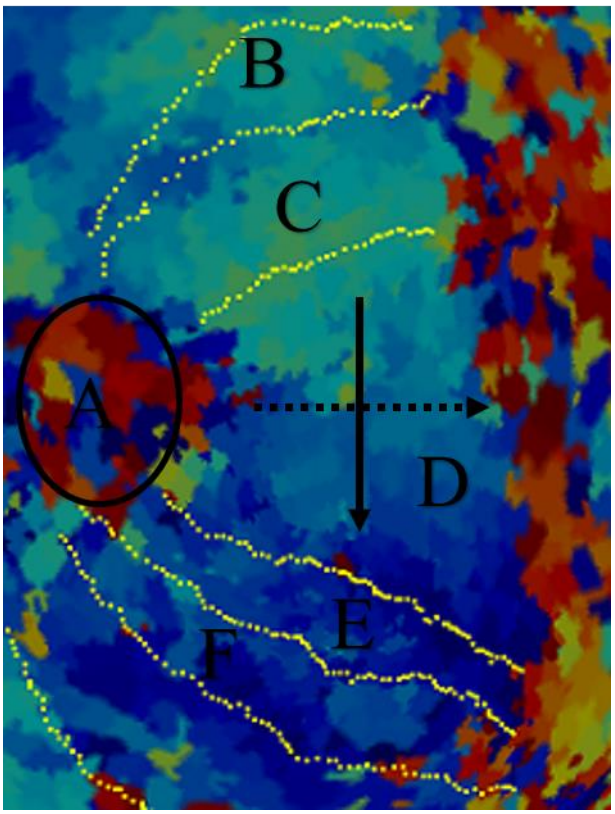

Figure 2-1 Retinotopic map (polar dimension) of the left hemisphere visual cortex displayed on an inflated cortex (displayed in SurfRelax). Figure shows foveal confluence (A), V3d (B), V2d (C), V1 (D), V2v (E) and V3v (F). The dotted arrow illustrates the direction of the radial dimension of the retinotopic map. The bold arrow illustrates the direction of the polar dimension of the retinotopic map. Yellow lines mark boundaries between visual maps determined by polar reversals. The upper meridian of the visual field is represented by light blue/green, the lower meridian is represented by dark blue.

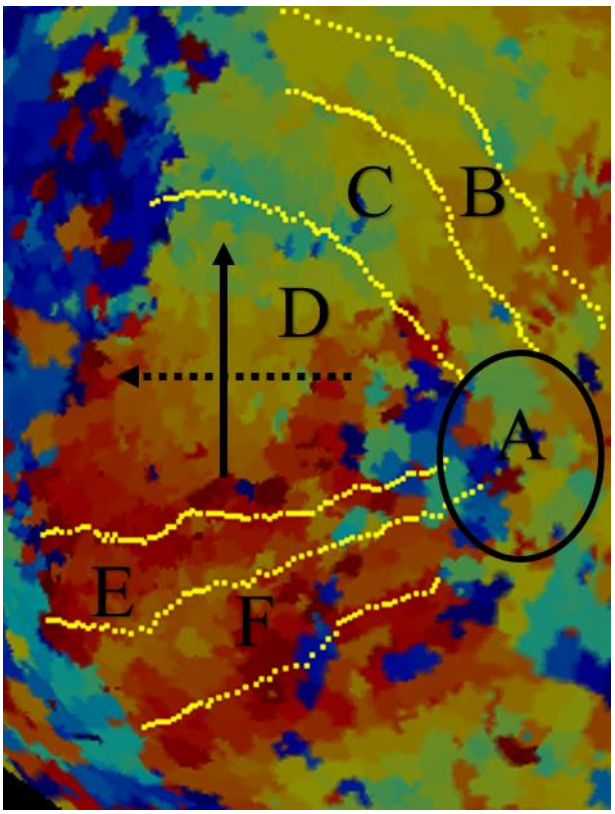

Figure 2-2 Retinotopic map (polar dimension) of the right hemisphere visual cortex displayed on an inflated surface (displayed in SurfRelax). Figure shows foveal confluence (A), V3d (B), V2d (C), V1 (D), V2v (E) and V3v (F). The dotted arrow illustrates the direction of the radial dimension of the retinotopic map. The filled arrow illustrates the direction of the polar dimension of the retinotopic map. Yellow lines mark boundaries between visual maps determined by polar reversals. The upper meridian of the visual cortex is represented by light blue/green, the lower meridian is represented by red.

2.2.6 Size Measures

The size of each visual area was measured. The measurement was made by manually drawing a boundary around the visual area ROIs. The ROIs used in the surface area measurement were identical to those used for cortical magnification measurements. The surface size was calculated as the number of vertices on the white matter surface within this boundary. As these vertices are evenly spaced, this value is approximately proportional to surface area. Within this participant sample, 1 vertex corresponded to 0.67mm² of cortex. Surface area estimates were calculated for eccentricity patches using the number of vertices within specific eccentricity range estimates from fMRI

(corresponding with the values used in subsequent psychophysical experiment; Chapters 3 & 4). Where analyses are performed across eccentricities, this surface area measure is computed as the sum of the eccentricity patches. The surface area of the full brain was also estimated.

Polar width was calculated as the average distance between the two meridian boundaries of the visual area. For example, for V1, the polar width was a measure from the boundary of V2d to the boundary of V2v. The polar width measure was parallel to the retinotopic polar map. Radial distance was calculated as the length of the visual area from the lowest eccentricity to the highest. Radial distance was parallel to the retinotopic radial map. As for the surface area measure, radial distance and polar width was estimated at eccentricities corresponding with subsequent psychophysical experiments. Again, where analyses are performed across eccentricities, this distance measure is computed as the sum of the eccentricity patches as is not directly comparable to width and distance measure in previous literature (e.g. Larsson & Heeger, 2006).

Polar width and radial distance were computed on the triangulated mesh representation of the cortex. The distance/width was calculated as the number of mesh steps between vertices. This value can then be converted to mm. 1mm is roughly equivalent to 1.2 mesh steps.

2.2.7 Raw Size Measures

Additionally, a raw size measure of surface area across all eccentricities within the ROI was calculated. This measure included all cortex between eccentricities of 0° and 13°. These estimates (table 2-1; figure 2-3) are consistent with previous estimates (Larsson & Heeger, 2006). These measures were calculated solely to confirm consistency with previous literature, they will not be used in the analyses reported here (or in the analyses reported in later chapters). Where analyses are performed across eccentricities, the size measurement is computed as the sum of the eccentricity patches.

Previous literature has suggested that V1 surface area correlates negatively with the overall size of the cortex (Schwarzkopf et al., 2011). This result was not repeated here.

All early visual regions were unrelated to an estimate of total brain surface area, although V3 showed a trend towards a correlation (V1, p=.34; V2, p=.13; V3, R=.37, p=.05). LO1 (p=.12) and LO2 (p=.78) were also unrelated. Conversely, V3A (R=.42, p<.05) and V4 (R=.41, p<.05) showed a weak but significant positive correlation with brain size.

Table 2-1 Estimates of surface area size (mm²) of visual areas V1, V2, V3, V3A, V4, LO1 and LO2

Hemisphere	V1	V2	V3	V3A	V4	LO1	LO2
Left	1860	1499	1161	482	538	331	254
SD	433	340	214	191	245	108	81
Right	1807	1592	1201	502	508	419	297
SD	370	444	187	195	198	162	122
Both	2737	2306	1763	734	781	559	411
SD	591	583	296	283	327	212	155
% of V1	100	84	64	27	29	20	15

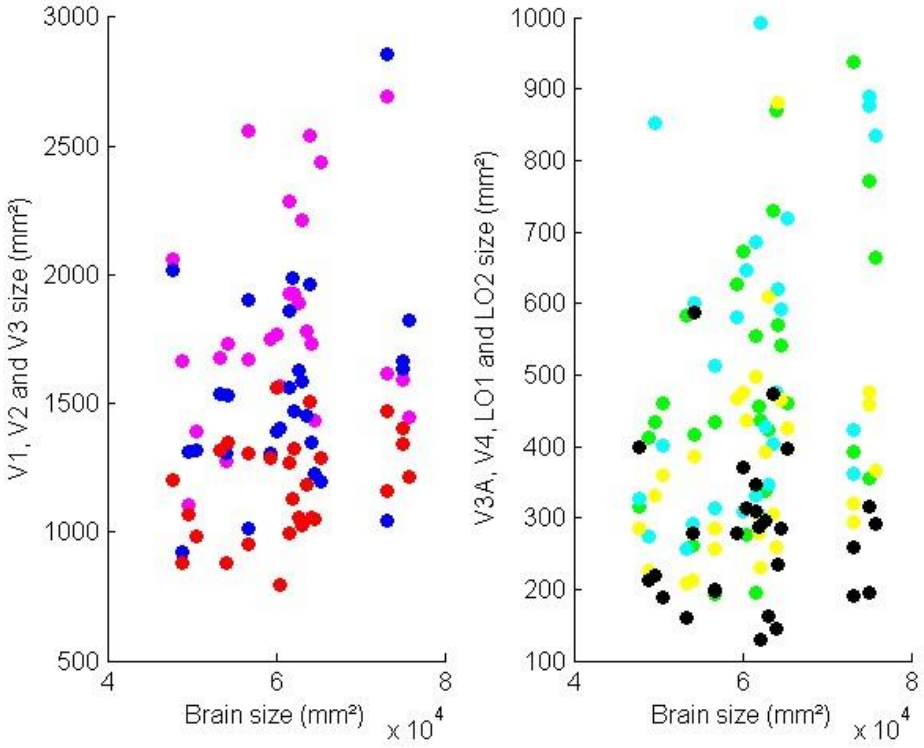

Figure 2-3 The relationship between visual areas V1 (magenta), V2 (blue), V3 (red), V3A (green), V4 (cyan), LO1 (yellow), LO2 (black) and total surface area of the brain (mm²). Raw size measures shown. Each data point represents a single hemisphere size measure for a single visual area.

2.2.8 Eye Surface Area

The surface area of the eye was computed from the anatomical images obtained in the anatomy scan. The image was first intensity corrected. The image was viewed at a horizontal angle and a scan was chosen in which the eyes were clearly visible. The centre of each eye was manually located and marked. The eye surface area was then computed through the exploitation of the differing intensities of the eye and the surrounding skull. A flood-fill algorithm was used to generate a volumetric representation of the inside of the eye (vitreous humour). The surface of this volume was extracted and elastically deformed to fit the retinal surface closely. Eye surface area was measured as the total surface area (mm²) of the deformed surface.

2.2.9 Cortical Magnification

Cortical magnification was calculated for each visual area. A radial measurement of magnification and a polar measurement were obtained for each visual area of each hemisphere. Radial cortical magnification was calculated by comparing the change in eccentricity with distance along the eccentricity dimension. Polar cortical magnification was calculated by comparing the change in polar angle with distance along the polar dimension. Three functions were fit to the data to produce cortical magnification values. A linear scaling function fit was obtained:

$$(1) \qquad D = a * \log(E) + b$$

Function 1 (linear scaling function) gave a measure of cortical magnification that was inversely proportional to eccentricity. Function 1 is shown in red in the lower left, centre and right plots of figures 2-4 to 2-12.

A second fit was obtained through a power function. This function described the local linear slope at each eccentricity. Radial cortical magnification was calculated in the same way, but used radial distance. This function was taken from Duncan and Boynton (2003). The power function is shown in black in the lower left, centre and right plots of figures 2-4 to 2-12. The linear scaling function and the power function produce one value of M for each visual area. Cortical magnification for each eccentricity was obtained by inserting the eccentricity value (*E*) into the formula produced by the function.

$$(2) \qquad D = a * E^b - c$$

A piecewise regression function gave 4 independent measures of cortical magnification, at eccentricities of 0.5°, 3°, 6° and 9° through a piecewise linear regression. The function was fit at eccentricities which corresponded to those used in subsequent psychophysical studies (Chapters 3 & 4). The piecewise regression function is shown by the blue line and blue data points in the lower left, centre and right plots of figures 2-4 to 2-12. This function was particularly illustrative for later visual areas, where the relationship between

increasing cortical magnification with decreasing eccentricity may not be as clear as in V1, V2 and V3.

All three fits of cortical magnification were obtained using the same data. The functions required 4 main inputs; radial distance, polar width, radial eccentricity, and polar eccentricity. In some cases (particularly V3A, LO1 and LO2), radial and polar coherence values could be added to the function to weight the fit such that high coherence points (strongly visually responsive) contributed most to the fit. Where coherence measures were used, the function plots show coloured data points. Coherence is represented using the Matlab Jet colourmap. Points of low coherence are represented by red, and points of high coherence are represented by blue. Generally, in most cases, data was first averaged into 10 eccentricity bins before fitting. In problematic cases (particularly V3A, LO1 and LO2) the bin number could be decreased to improve the fit (e.g. the values were binned into fewer bins prior to fitting). In most hemispheres, V3A, LO1 and LO2 used 5 bins prior to fitting. The fits produced by all three functions for a single hemisphere are displayed in figures 2-4 to 2-12.

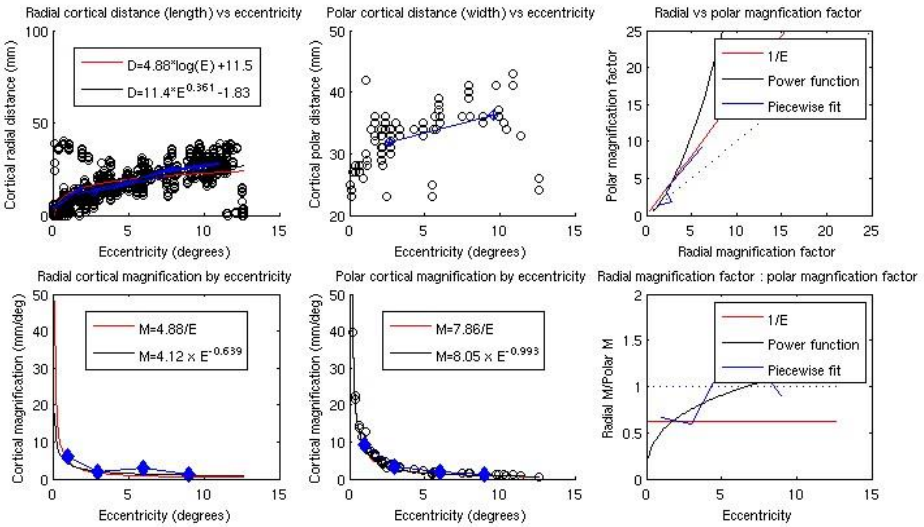

Figure 2-4 Left V1 cortical magnification function for participant HH

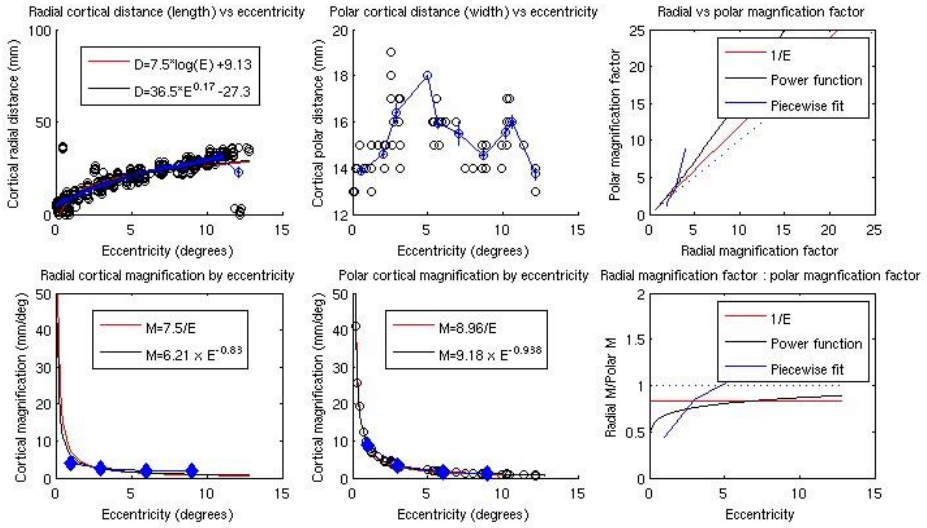

Figure 2-5 Left V2d cortical magnification function for participant HH

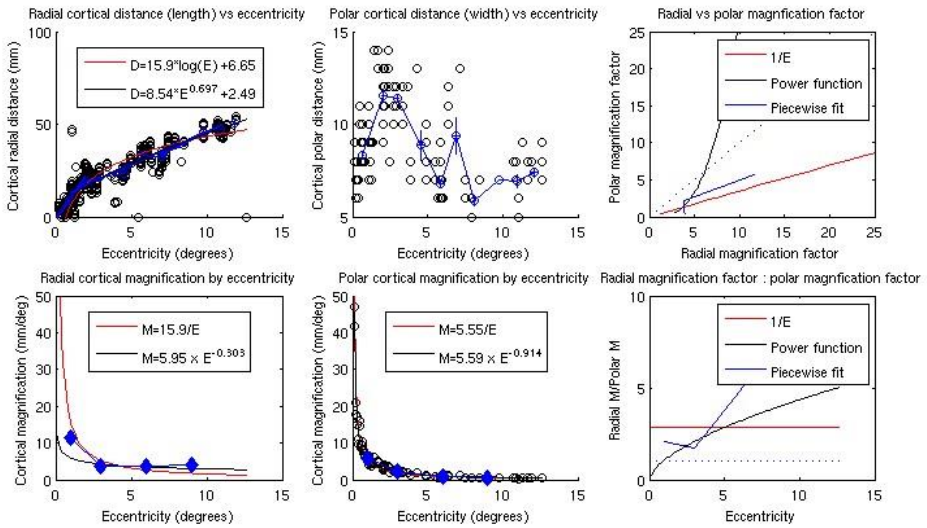

Figure 2-6 Left V2v cortical magnification function for participant HH

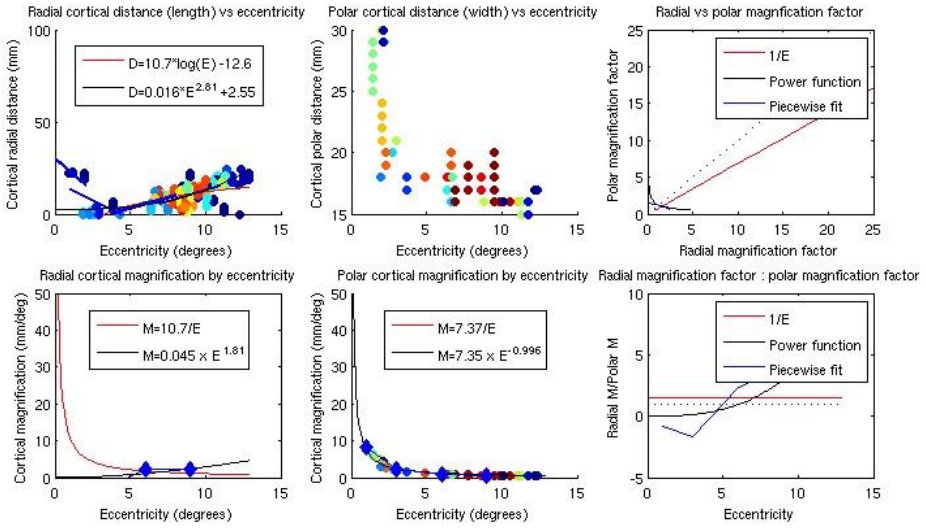

Figure 2-7 Left V3A cortical magnification function for participant HH

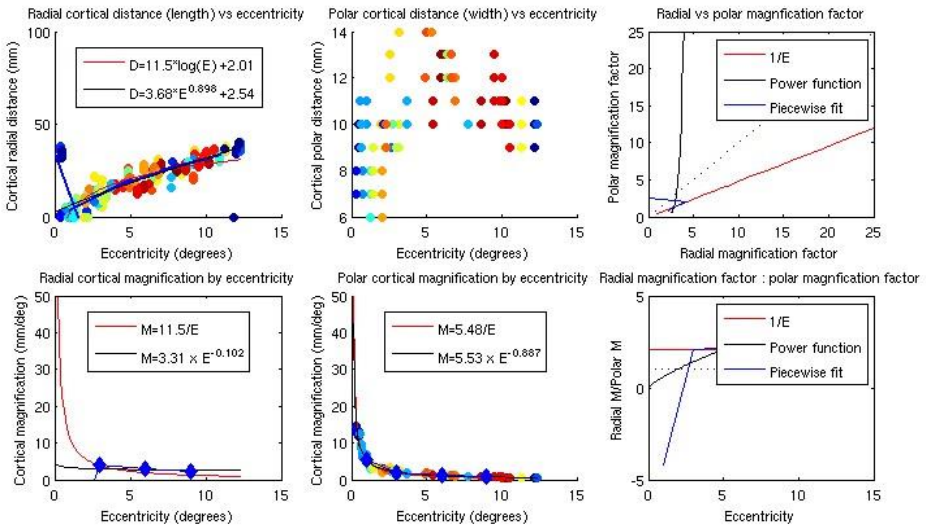

Figure 2-8 Left V3d cortical magnification function for participant HH

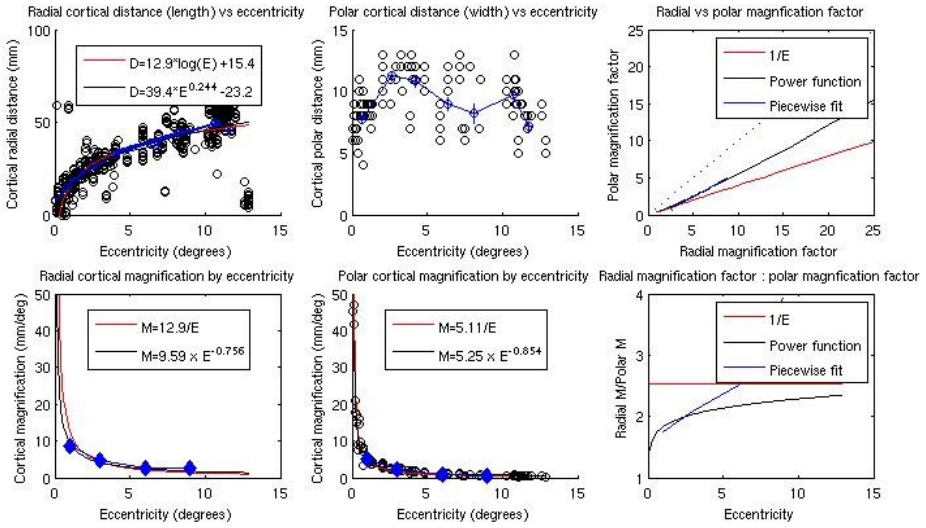

Figure 2-9 Left V3v cortical magnification function for participant HH

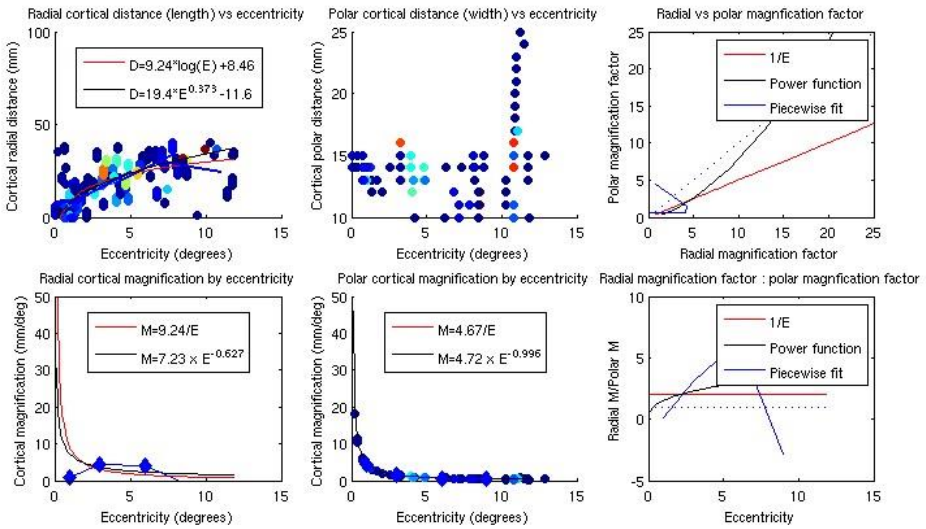

Figure 2-10 Left V4 cortical magnification function for participant HH

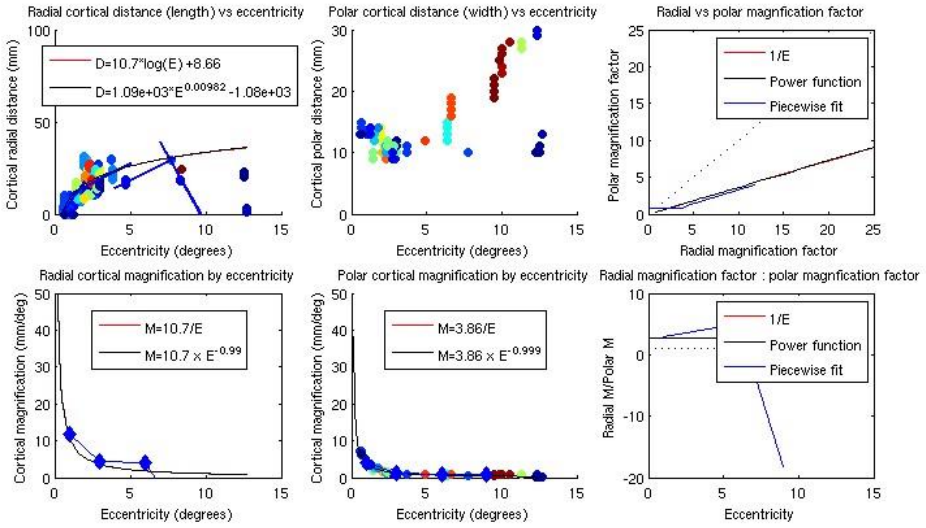

Figure 2-11 Left LO1 cortical magnification function for participant HH

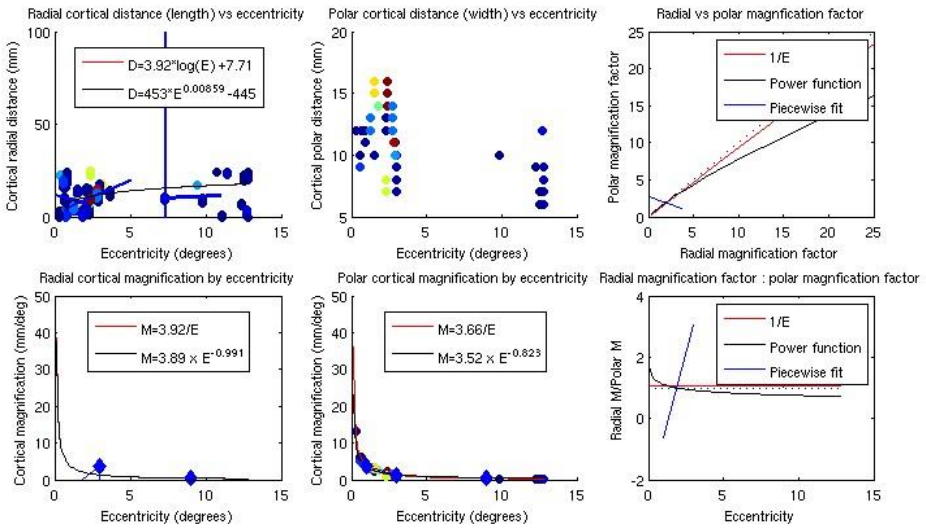

Figure 2-12 Left LO2 cortical magnification function for participant HH

2.3 Results

2.3.1 Cortical Magnification Analysis

Using each of the 3 functions, cortical magnification values were for obtained for each visual area at eccentricities of 0°, 3°, 6° and 9°. A radial and a polar measurement of

cortical magnification were computed using the fitted functions for the eccentricities corresponding to the extent of the stimulus used in the psychophysics studies (Chapter 3 & 4). Radial cortical magnification measures were analyzed separately from polar cortical magnification measures. 28 hemispheres were treated as independent data points. All analyses were conducted at a group level.

To investigate the hypothesis that V1 drives levels of cortical magnification in all later areas, a linear regression was performed to predict radial cortical magnification in V2, V3, V3A, V4, LO1 and LO2 from V1 radial cortical magnification. A second analogous linear regression was also performed with measures of polar cortical magnification.

Secondly, to identify clusters of visual areas, a series of principal component analyses (PCA) were run. PCA is a non-parametric method of identifying patterns within a data set, it is appropriate for data exploration and creating predictive models. This method used an orthogonal transformation to convert a set of correlated variables into linearly uncorrelated variables. Firstly, a principal component is extracted from the original data that explains the largest possible variance. Secondly, an additional principal component is extracted that explains the largest possible amount of the remaining variance but is constrained by the criterion that it must be uncorrelated with the first principal component. This process continues until all variance is explained. The end result is a group of uncorrelated principal components of the same number as original variables entered. These principal components show no multi- collinearity and are suitable for linear regression.

The variables submitted to the PCA were cortical magnification estimates from each of the 7 visual areas (V1, V2, V3, V3A, V4, LO1 and LO2). Each PCA received either cortical magnification estimates in the radial dimension or cortical magnification estimates in the polar dimension. In no PCA were both radial and polar estimates entered together. The principal components taken from the PCA were uncorrelated variables representing independent sources of variance. For example, given the strong effect of eccentricity present within the data it was expected that the first principal component extracted would represent this source of variance.

Visual areas were considered to form a cluster if they weighted the same component. To weight a component, a single visual area must account for more than 15% of the total component variance. This threshold was selected because if the variance of a component was weighted by all visual areas equally, each visual area would contribute approximately 15% of the variance.

A PCA was conducted on measures of radial cortical magnification from 7 visual areas (V1, V2, V3, V3A, V4, LO1 and LO2). A second PCA was conducted for 7 measures of polar cortical magnification. No rotation was used. The absence of a rotation decreased the likelihood of variables loading onto a single component and therefore minimised correlations. No minimum criterion for eigenvalues was used and small coefficients were not supressed. These criteria were selected to ensure that the large eccentricity effect did not mask the smaller influences of other shared variance. Bartlett's test of sphericity was performed to demonstrate that correlates between items were sufficiently large for PCA. In all analyses, Bartlett's value was sufficient so is not reported for individual items. Thirdly, correlations between the size measures of the visual areas were investigated. Three measures were compared; surface area, polar width and radial distance. For each parameter, a bivariate correlation was performed.

2.3.2 Cortical Magnification Summary

Radial and polar cortical magnification measures produced by each of the functions for each visual area were plotted across eccentricity (figure 2-15, 2-16 and 2-17). Mean measures at each eccentricity are shown, standard errors are also shown. Figures 2-13 and 2-14 demonstrate the different estimates produced by the 3 functions. All functions appropriately estimate V1 cortical magnification. Difficulties in fitting V3A were apparent across all functions, indicated by the negative estimates of cortical magnification. In terms of polar cortical magnification, the piecewise regression provides the best estimate. In terms of radial cortical magnification, the linear scaling and power functions appear most reliable.

Examination of figures 2-15, 2-16 and 2-17 clearly demonstrates that V3A showed a very different pattern of cortical magnification to the other visual areas mapped here. Unlike

other areas, in which polar and radial cortical magnification decreased concurrently with increasing eccentricity, V3A polar and radial cortical magnification showed independent patterns. In line with other areas, radial cortical magnification decreased with eccentricity. On the other hand, polar cortical magnification increased. This pattern is statistically significant for all 3 functions ($R=-.86$, $p<.001$; $R=-.51$, $p<.001$; $R=-.19$, $p<.05$). Generally, the eccentricity effect in V3A was much weaker than in other visual areas. Whilst some of the unusual attributes of V3A cortical magnification may be attributed to a failure of the functions to accurately fit, there is clearly a differentiation between the topographical anisotropy of V3A and other areas.

Cortical magnification estimates from all functions indicated that for V1, V2 and V3, radial cortical magnification was generally higher than polar. There is some inter-function variability in the eccentricity effect of this pattern, the linear scaling function indicated that the radial cortical magnification was higher than polar at the lowest eccentricity whilst the piecewise regression function demonstrated that polar was higher at the lowest eccentricity.

This difference is most likely due to the estimates of radial cortical magnification by the piecewise regression function. Unlike other function, the piecewise regression function produced estimates of radial cortical magnification that did not follow the established pattern (e.g. higher levels of cortical magnification at foveal locations). For early visual areas this pattern was constrained to the lowest eccentricity, but for V3A and LO2 the pattern existed across all eccentricities. The radial estimates produced by the piecewise regression function were consistent with the other functions and showed the expected pattern (e.g. higher cortical magnification at foveal locations).

Examination of the estimates of cortical magnification indicated that V1 has lower levels of cortical magnification than V2. V1 cortical magnification was significantly lower than that of V2 for all functions and in both the radial and polar dimensions ($p<.001$). V1 radial cortical magnification was significantly lower than V3 radial cortical magnification for all functions ($p<.001$). V1 polar cortical magnification was generally lower than V3 polar cortical magnification, but this reached significance only for the power function ($p<.01$).

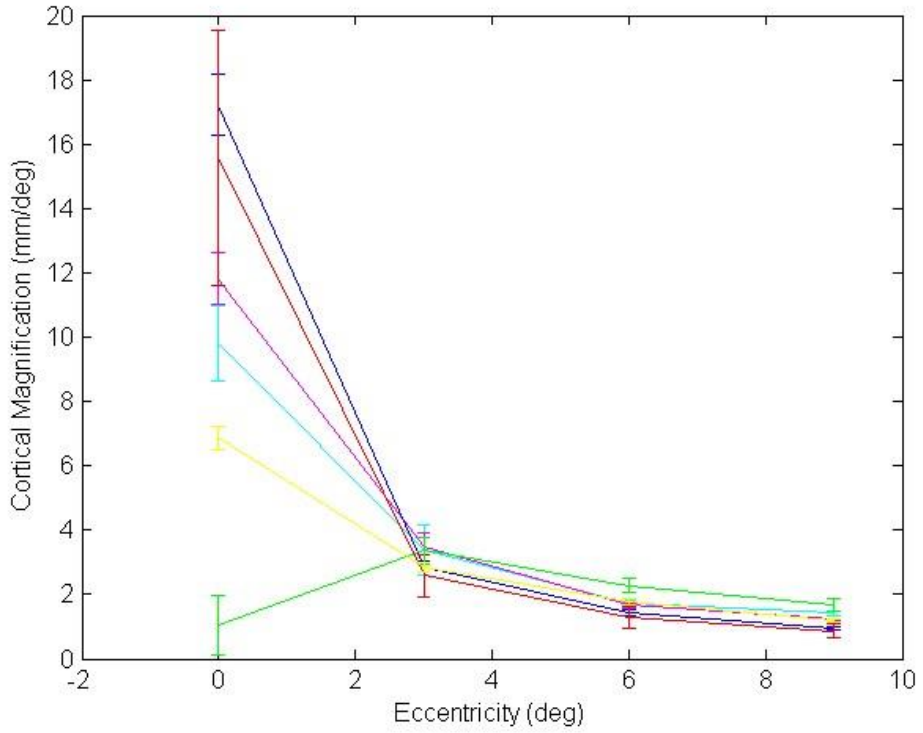

Figure 2-13 V1 cortical magnification (mm/deg) from 3 functions. Linear scaling function radial (blue) and polar (red); power function radial (cyan) and polar (magenta); piecewise regression function radial (green) and polar (yellow). Data averaged across 28 hemispheres. Standard errors shown.

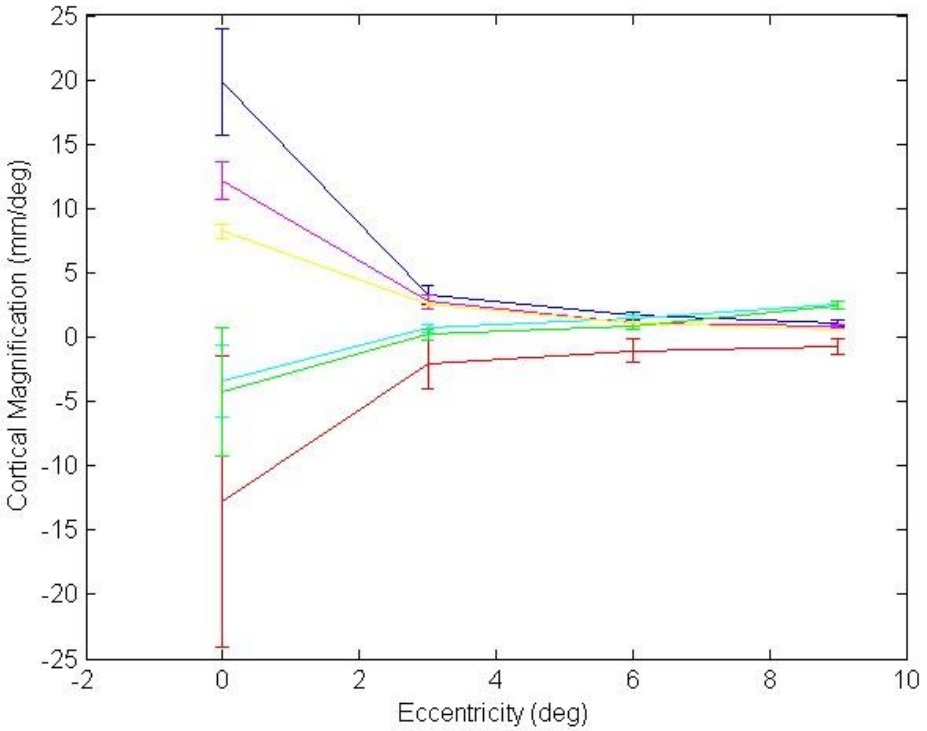

Figure 2-14 V3A cortical magnification (mm/deg) from 3 functions. Linear scaling function radial (blue) and polar (red); power function radial (cyan) and polar (magenta); piecewise regression function radial (green) and polar (yellow). Data averaged across 28 hemispheres. Standard errors shown.

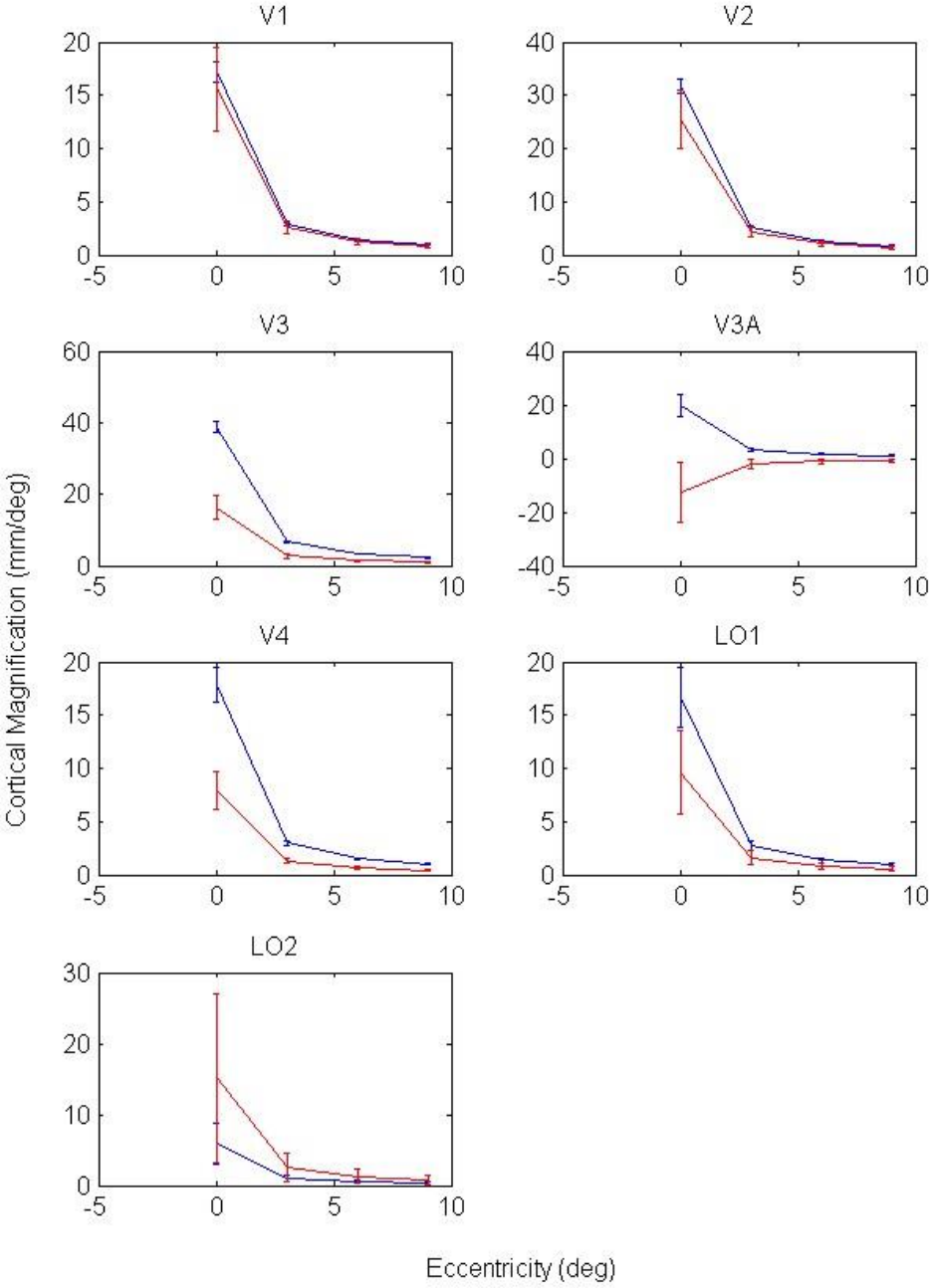

Figure 2-15 Radial (blue) and polar (red) cortical magnification (mm/deg) from the linear scaling function. Standard errors of the mean (across 28 hemispheres) shown

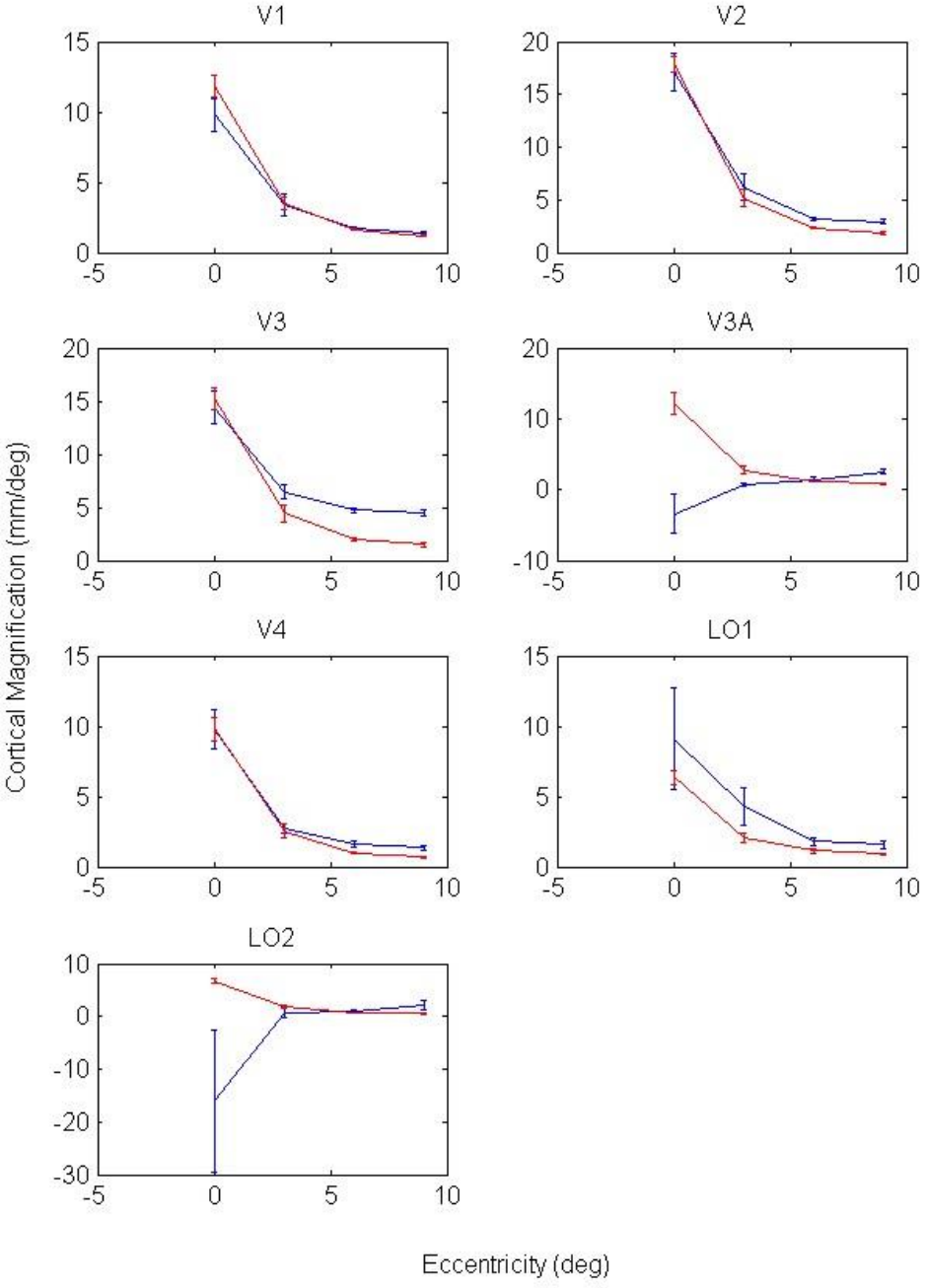

Figure 2-16 Radial (blue) and polar (red) cortical magnification (mm/deg) from the power function. Standard errors of the mean (across 28 hemispheres) shown.

.

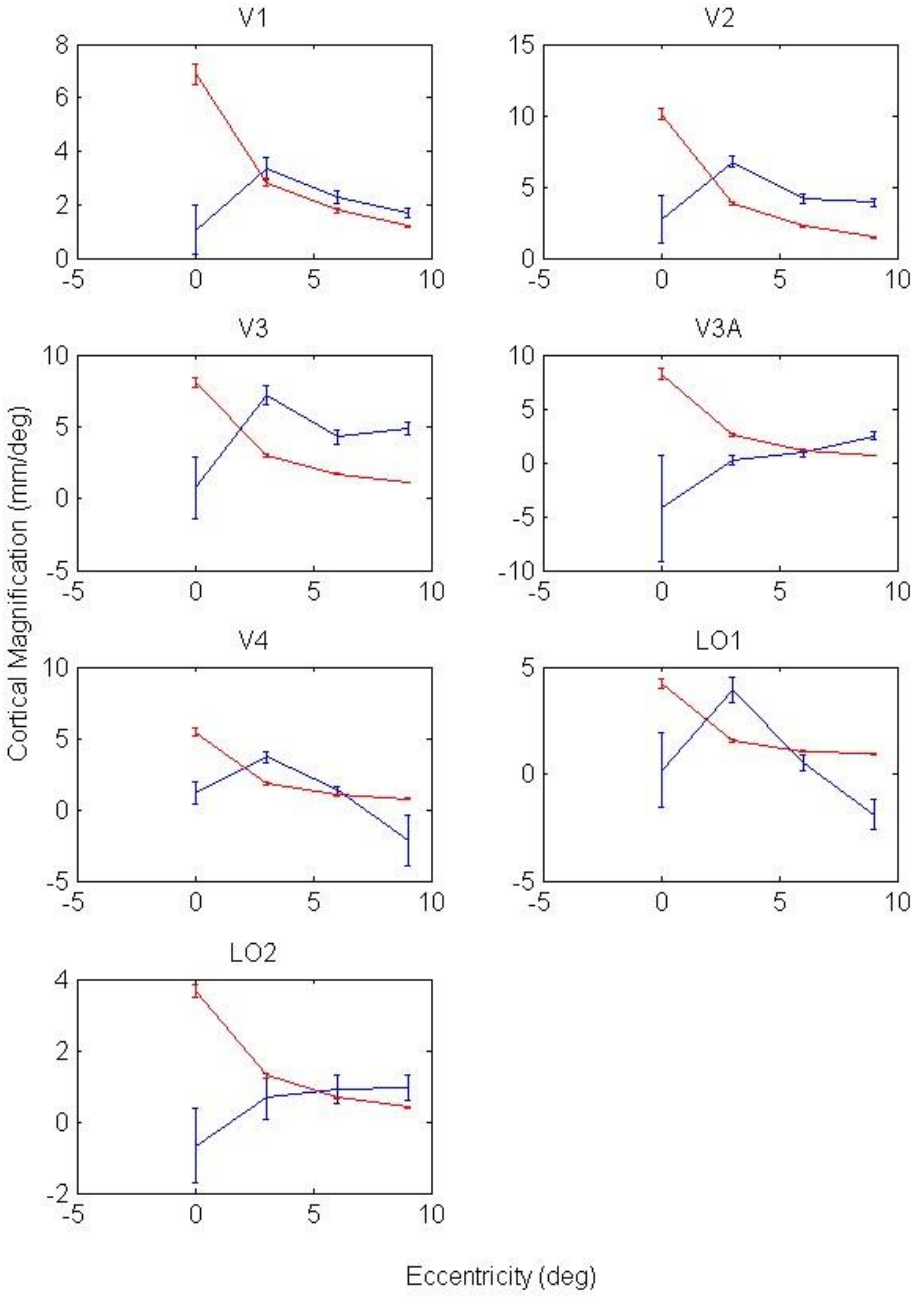

Figure 2-17 Radial (blue) and polar (red) cortical magnification (mm/deg) from the piecewise regression function. Standard errors of the mean (across 28 hemispheres) shown.

2.3.3 Principal Components Analysis

To identify clusters of visual areas, a PCA was conducted on all radial cortical magnification measures taken from the piecewise regression function (figure 2-18). This function was chosen because it was the most robust and assumption free. The second component accounted for 18.89% of the total variance and correlated with eccentricity (R=.3, p=.001), indicating that it represented the variability contributed to the PCA by eccentricity. Table 2-2 demonstrated that the first component was weighted by visual areas V1, V2 and V3 and accounted for 25.98% of the variance. The fourth component was weighted most strongly by LO1 and LO2, and to a lesser extent V3A. This component accounted for 13.87% of the variance. Neither component 1 nor component 4 correlated with eccentricity (p=.94; p=.46). It should be noted that the piecewise regression function is limited in its ability to fit V3A radial cortical magnification, so conclusions drawn from this PCA regarding links between V3A and other areas are inappropriate.

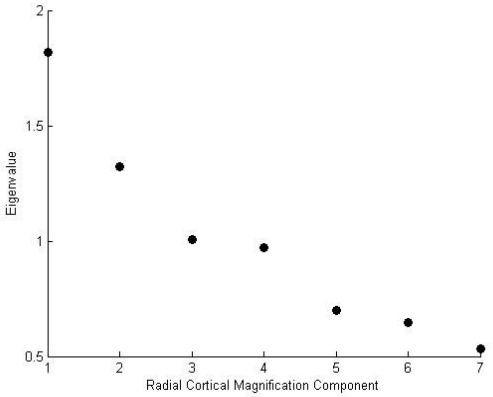

Figure 2-18 Radial cortical magnification (mm/deg; the piecewise regression function) scree plot. Each data point represents a principal component.

Table 2-2 Component matrix showing radial components extracted in a PCA of radial cortical magnification (mm/deg) from the piecewise regression function. Weightings of visual areas contributing more than 15% of the total component weight are highlighted.

	Component						
	1	2	3	4	5	6	7
V1r	.704	.301	.040	-.071	-.438	.279	.371
V2r	.744	.339	.092	.058	-.059	-.024	-.562
V3r	.721	-.026	.151	-.125	.487	-.372	.255
V3Ar	-.231	.397	.691	.438	.234	.246	.064
V4r	.383	-.703	-.062	.046	.265	.528	-.065
LO1r	.192	-.611	.260	.563	-.339	-.299	.018
LO2r	.109	.304	-.652	.660	.166	.018	.084

A second PCA was conducted on all measure of polar cortical magnification taken from the linear scaling function. The first 3 components correlated with the original eccentricity variable ($R=-.56$, $p<.001$; $R=-.21$, $p<.05$; $R=-.19$, $p<.05$) but not with one another. The 3 components explained a cumulative total of 77.13% of the variance. The seventh explained 0.543% of the total variance and did not correlate with eccentricity ($p=.96$). This component was weighted most strongly by V1 and V2 (table 2-3).

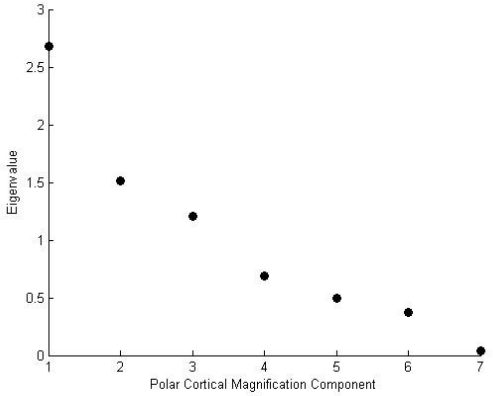

Figure 2-19 Polar cortical magnification (mm/deg; linear scaling function) scree plot. Each data point represents a principal component.

Table 2-3 Component matrix showing polar components extracted in a PCA of polar cortical magnification (mm/deg) from the linear scaling function. Weightings of visual areas contributing more than 15% of the total component weight are highlighted.

	Component						
	1	2	3	4	5	6	7
V1p	.888	-.231	-.139	.049	.301	.175	-.121
V2p	.946	-.186	-.144	-.044	.155	.044	.147
V3p	.727	.457	-.104	-.183	-.114	-.453	-.035
V3Ap	-.239	.675	-.370	.511	.294	-.039	.018
V4p	.643	.294	.351	.410	-.419	.184	-.004
LO1p	.026	.822	.159	-.462	.090	.278	.005
LO2p	.018	.005	.930	.108	.316	-.150	.008

These PCA analyses indicate that there is some shared variance between visual areas although the strongest finding is the effect of eccentricity. Eccentricity was a strong source of variance within each area and accounted for most of the variance in cortical magnification. Shared variance across the visual areas that was not due to eccentricity was relatively low.

2.3.4 Correlations between V1, V2 and V3

The PCA analysis indicated that V1, V2 and V3 shared variance in both the polar and radial cortical magnification dimensions. A series of linear regressions supported this close pairing between these 3 visual areas. Eccentricity was included as a covariate in these analyses to remove the dominant effect of eccentricity.

Using measures taken from the linear scaling function, V1 radial cortical magnification measures predicted radial cortical magnification of V2 (B=.27, SE=.05, β=.48, t=5.55, p<.001) at all eccentricities (0° R=.46, p<.05; 3° R=.46, p<.05; 6° R=.46, p<.05; 9° R=.46, p<.05), V3 (B=.2, SE=.05, β=.44, T=4.27, p<.001) but only at the lowest eccentricity (0° R=.42, p<.05; 3° p=.05; 6° p=.05; 9° p=.53) and V3A (B=.05, SE=.02, β=.09, T=2.57, p<.05) at all eccentricities (R=.42, p<.05; 3° R=.42, p<.05; 6° R=.42, p<.05; 9° R=.42, p<.05). The correlations are displayed in figure 2-20. The presence of correlations at specific eccentricities strengthens the claim for a close inter-areal relationship. The two regions are not linked solely by the common eccentricity effect of higher cortical magnification at peripheral locations.

Figure 2-20 displays clear clustering. There is an unexpected absence of data point representing V1 radial cortical magnification between approximately 5 and 10 mm/deg. It is likely that this reflects a limitation of the cortical magnification measurement techniques rather than a genuine characteristic of V1 cortical magnification, as this clustering in not present in estimates taken from the other 2 functions. It is possible that poor retinotopic mapping of the foveal confluence led to inaccurate estimates of cortical magnification at low eccentricities (where the missing data points would be expected to be found).

Similarly, figure 2-21 displays the findings that polar cortical magnification in V1 predicted polar cortical magnification in V2 (B=.75, SE=.03, β=1.09, T=24.26, p<.001) at all eccentricities (0° R=.92, p<.001; 3° R=.92, p<.001; 6° R=.92, p<.001; 9° R=.92, p<.001). V1 polar cortical magnification also predicted V3 (B=-.23, SE=.05, β=-.21, T=4.79, p<.001) and V3A (B=.04, SE=.01, β=.1, T=3.22, p<.01). The links between V1 and V3 and V3A were lost at specific eccentricities. (0° p=.3; 3° p=.3; 6° p=.3; 9° p=.3;

0° p=.44; 3° p=.44; 6° p=.44; 9° p=.44). The links identified here between polar cortical magnification in V1 and V3A are limited somewhat by the use of the linear scaling function, previously found to be suboptimal in estimating V3A polar cortical magnification.

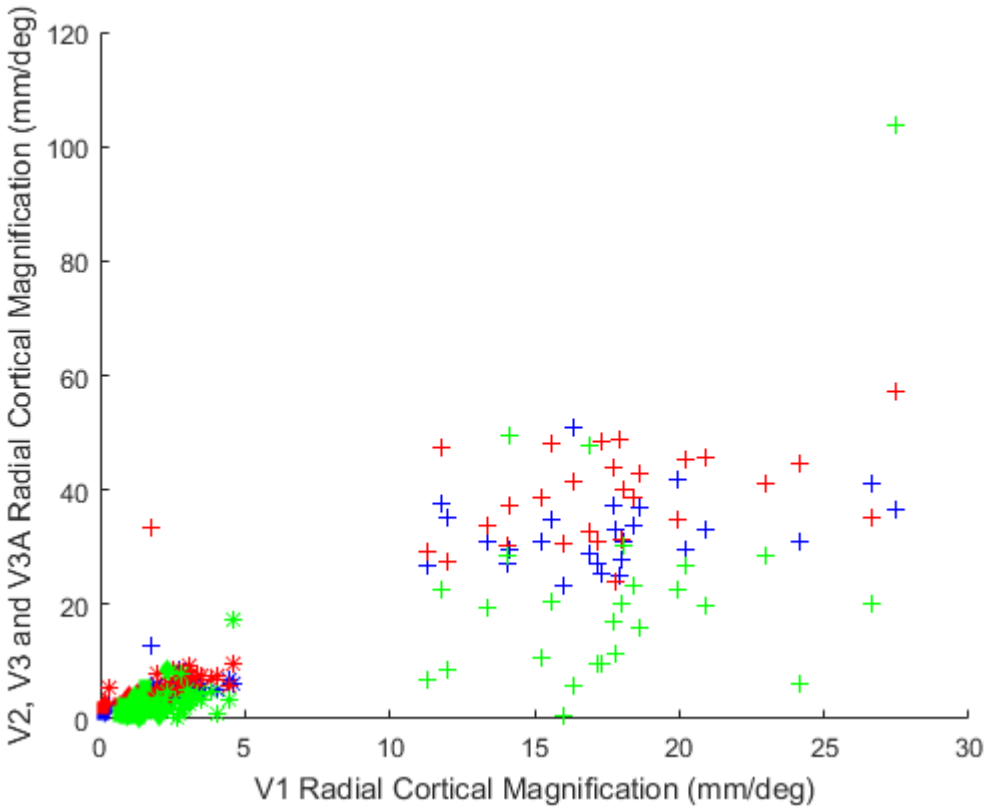

Figure 2-20 The relationship between V1 radial cortical magnification (mm/deg; the linear scaling function) and radial cortical magnification (mm/deg) in V2 (blue; p<.001), V3 (red; p<.001) and V3A (green; p<.01). Negative values are not shown on the plot. Each data point represents a single hemisphere at a single eccentricity patch. Eccentricities are represented by different symbols (0°+; 3°*; 6°♦; 9°■).

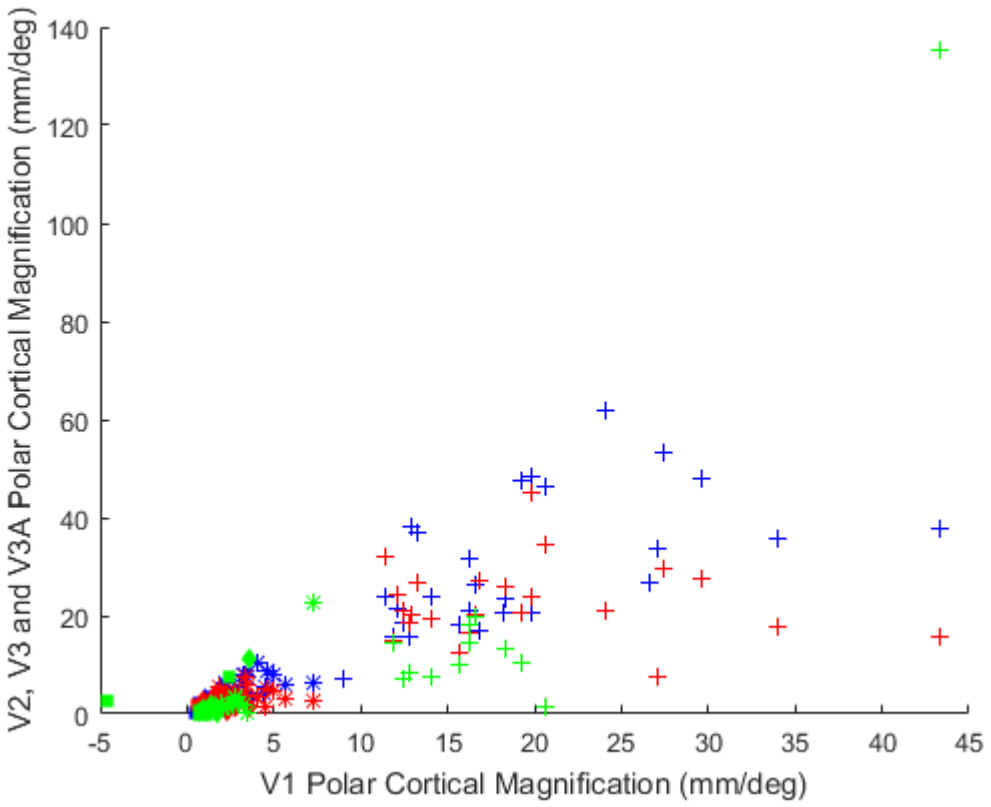

Figure 2-21 The relationship between V1 polar cortical magnification (mm/deg; the linear scaling function) and polar cortical magnification (mm/deg) in V2 (blue; p<.001), V3 (red; p<.001) and V3A (green; p<.01). Negative values are not shown on the plot. Each data point represents a single hemisphere at a single eccentricity patch. Eccentricities are represented by different symbols (0°+; 3°*; 6°♦; 9°■).

2.3.4.1 Size Measures

Multiple links between V1, V2 and V3 were identified in size measures of these visual areas. V1 size correlated with V2 size at a global level (figure 2-22; R=0.67, p<.001) and at low eccentricities (0° R=.57, p<.01; 3° R=.67, p<.001; 6° p=.09; 9° p=.1). Links were also seen between these two visual areas in measures of radial distance across all eccentricity (figure 2-23; R=.81, p<.001) and at all specific eccentricities (0° R=.79, p<.001; 3° R=.82, p<.001; 6° R=.57, p<.01; 9° R=.64, p<.001)

The links between V1 and V3 size measures were much weaker than those seen between V1 and V2. Again, it appears that the strongest source of shared variance is the eccentricity effect. At a global level, these areas correlated on measures of both surface

area (figure 2-24; R=.62, p<.001) and radial distance (figure 2-25; R=.41, p<.001). At specific eccentricities, the radial distance link was lost (0° p=0.78, 3° p=.33; 6° p=.56; 9° p=.64). The surface area link was also lost at all eccentricities but 3° (0° p=.07; 3° R=.49, p<.01; 6° p=.08; 9° p=.07). V1 and V3 did not correlate in measures of polar width (p=.83).

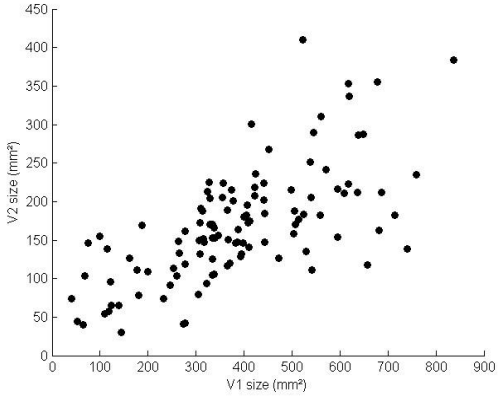

Figure 2-22 The relationship between V1 and V2 size (mm²; p<.01). Each data point represents a single hemisphere at a single eccentricity patch.

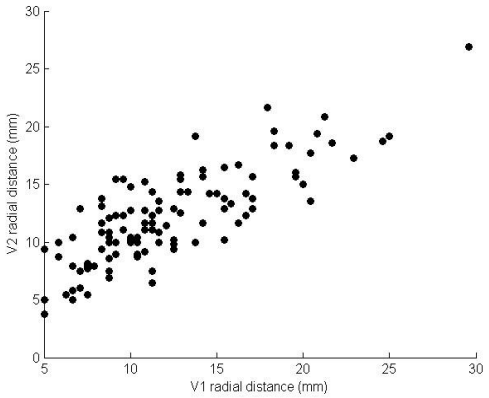

Figure 2-23 The relationship between V1 and V2 radial distance (mm; p<.001). Each data point represents a single hemisphere at a single eccentricity patch.

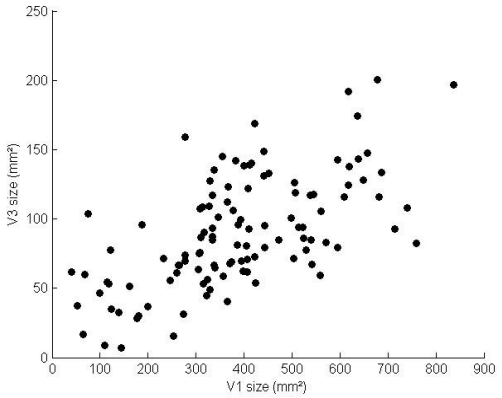

Figure 2-24 The relationship between V1 size and V3 size (mm²; p<.01). Each data point represents a single hemisphere at a single eccentricity patch.

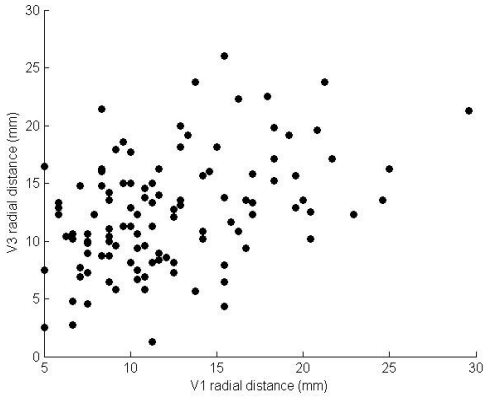

Figure 2-25 The relationship between V1 and V3 radial distance (mm; p<.001). Each data point represents a single hemisphere at a single eccentricity patch.

2.3.5 Correlations between LO1 and LO2

2.3.5.1 Cortical Magnification

Using the linear scaling function, a correlation was identified between radial cortical magnification in LO1 and radial cortical magnification in LO2 (figure 2-26; R=.41, p<.001). This link was lost at the level of specific eccentricities (0° p=.11; 3° p=.11; 6° p=.11; 9° p=.11). The link between LO1 and LO2 radial cortical magnification was not driven solely be the effect of eccentricity, it remained significant in a partial correlation controlling for the effect of eccentricity (R=.34, p<.001).

The link between LO1 and LO2 polar cortical magnification was also absent at specific eccentricities. Using measures from the piecewise regression function, a correlations was seen at a global level (figure 2-27; R=.87, p<.001) but absent at specific eccentricities (0° p=.55; 3° p=.07; 6° p=.65; 9° p=.54). The link between LO1 and LO2 polar cortical magnification remained when the effect of eccentricity was controlled for (R=.635, p<.001).

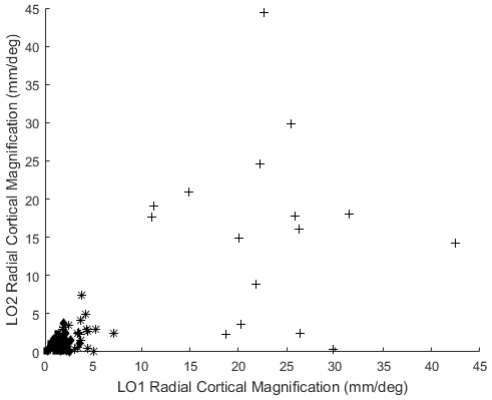

Figure 2-26 The relationship between LO1 and LO2 radial cortical magnification (mm/deg; the linear scaling function; p<.001). Each data point represents a single hemisphere at a single eccentricity patch. Negative cortical magnification values are not shown on the plot. Eccentricities are represented by different symbols (0°+; 3°*; 6°♦; 9°■).

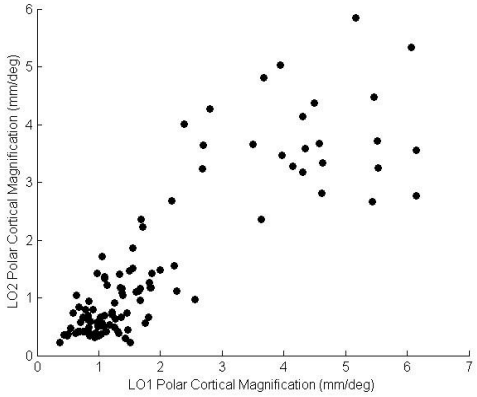

Figure 2-27 The relationship between LO1 and LO2 polar cortical magnification (mm/deg; the piecewise regression function; p<.001). Each data point represents a single hemisphere at a single eccentricity patch.

2.3.5.2 Size Measures

The size of LO1 was correlated with the size of LO2 at both a global level (figure 2-28; R=.65, p<.001) and at low eccentricities (figure 2-29; 0° R=.71, p<.001; 3° R=.69, p<.001; 6° p=.73; 9° p=.42). The presence of the link at solely low eccentricities is consistent with the overrepresentation of the fovea in LO1 and LO2 (Larsson & Heeger, 2006). Extensive links were also seen between LO1 and LO2 radial distance. Correlations were seen at a global level (figure 2-30; R=.77, p<.001) and at all eccentricities (figure 2-31; figure 2-32; 0° R=.78, p<.001; 3° R=.62, p<.001; 6° R=.65, p<.001; 9° R=.72, p<.001). The two visual areas showed no correlation in measures of polar width (p=.19).

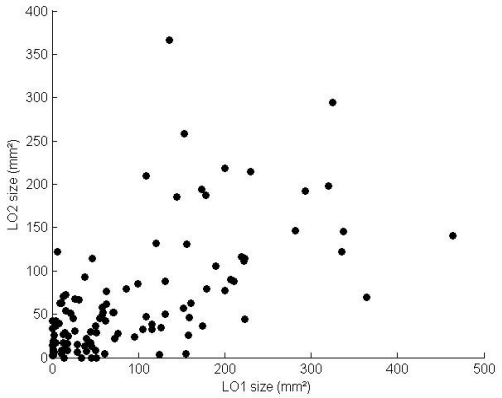

Figure 2-28 The relationship between LO1 and LO2 size (mm²; p<.001). Each data point represents a single hemisphere at a single eccentricity patch.

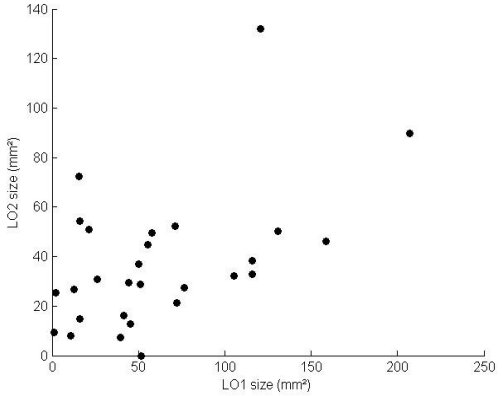

Figure 2-29 The relationship between LO1 and LO2 size (mm²) at 0° (p<.001). Each data point represents a single hemisphere at a single eccentricity patch.

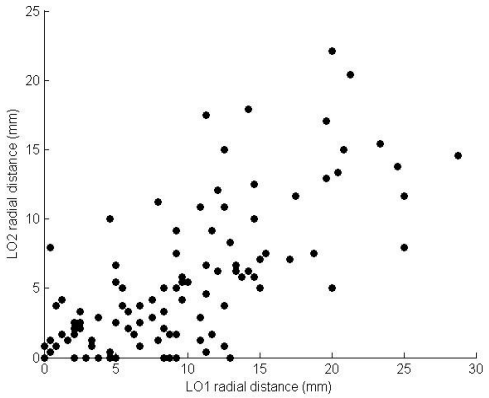

Figure 2-30 The relationship between LO1 and LO2 radial distance (mm; p<.001). Each data point represents a single hemisphere at a single eccentricity patch.

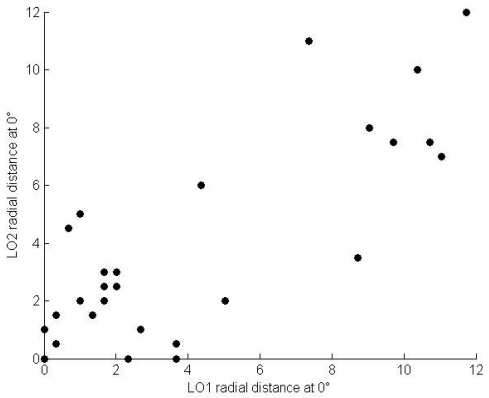

Figure 2-31 The relationship between LO1 and LO2 radial distance at 0° (mm; p<.001). Each data point represents a single hemisphere at a single eccentricity patch.

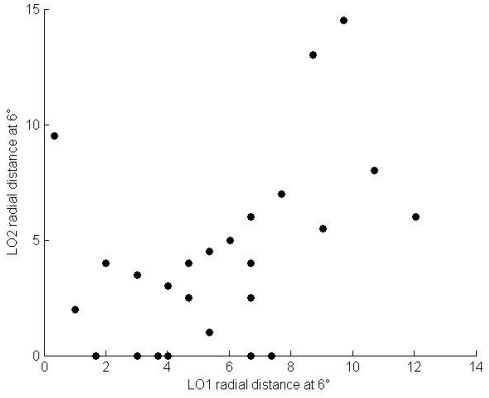

Figure 2-32 The relationship between LO1 and LO2 radial distance at 6° (mm; p<.001). Each data point represents a single hemisphere at a single eccentricity patch.

2.3.6 Correlations between V3A and Other Visual Areas

The linear regression performed using linear scaling function estimates of V3A radial cortical magnification demonstrated a link between V3A and V1 (figure 2-20). Additionally, using the linear scaling function, V3A radial cortical magnification was shown to correlate with LO1 radial cortical magnification ($R=.483$, $p<.001$). These links were absent at specific eccentricities (0° $p=.39$; 3° $p=.38$; 6° $p=.17$, 9° $p=.4$). Links between V3A and LO2 in measures of radial cortical magnification (linear scaling function) were absent ($p=.4$).

Exploration of links between V3A and other visual areas in measures of polar cortical magnification is limited somewhat by the failure of the linear scaling and power functions to successfully fit V3A. The piecewise regression function was the most successful of the 3 in describing V3A polar cortical magnification (indicated by an absence of negative estimates). Using the piecewise regression function, a linear regression was performed to predict V3A polar cortical magnification from all other visual areas (with eccentricity included as a covariate to remove the dominant effect of eccentricity). Both V2 ($B=.42$, $SE=.14$, $\beta=.45$, $p<.01$) and LO2 ($B=.87$, $SE=.33$, $\beta=.36$, $p<.05$) correlated with V3A. These links were lost at specific eccentricities for V2 (0° $p=.91$; 3° $p=.41$; 6° $p=.05$; 9° $p=.78$). A significant correlation remained between LO2 and V3A at 6° (0° $p=.73$; 3° $p=.99$; 6° $R=.51$, $p<.01$; 9° $p=.16$) but was driven by a single outlier.

In size measures, V3A showed a stronger link to LO1 than LO2. This is consistent with the general finding across analyses that adjacent areas correlate. The surface area ($R=-.19$, $p<.05$) and radial distance ($R=.66$, $p<.001$) of V3A correlated with LO1. This size correlation was absent at specific eccentricities (0° $p=.97$; 3° $p=.60$; 6° $p=.61$; 9° $p=.13$). The correlation between V3A and LO1 measures of radial distance was present at specific eccentricities (0° $R=.72$, $p<.001$; 3° $R=.62$, $p<.001$; 6° $R=.62$, $p<.001$; 9° $R=.58$, $p<.001$). The radial distance of V3A correlated with LO2 both across eccentricities ($R=.285$, $p<.01$) and at the lowest eccentricity (0° $R=.45$, $p<.05$; 3° $p=.72$; 6° $p=.81$, 9° $p=.86$). The size of LO1 did not correlate with the size of V3A ($R=-.15$, $p=.11$).

Extensive links between V3A and the V1-V2-V3 cluster were also seen. V3A correlated with V2 and V3 in surface area (figure 2-33; figure 2-34; $R=.26$, $p<.01$; $R=.49$, $p<.001$)

but not V1 (R=.15, p=.11). Links with V2 and V3 were lost at most specific eccentricities (0° p=.14; 3° p=.07; 6° p=.68; 9° p=.93; 0° p=.21; 3° p=.09; 6° p=.09) except V3 at 9° (R=.51, p<.01). Similarly, the radial distance of V3A correlated with V2 and V3 (figure 2-35; figure 2-36; R=.41, p<.001; R=.73, p<.001) but not with V1 (p=.08). The links between V3A radial distance and V2 and V3 were seen at most eccentricities (0° R=.44, p<.05; 3° R=.34, p<.05; 6° p=.50; 9° R=.47, p<.05; 0° R=.6, p<.001; 3° R=7, p<.001; 6° p=.08; 9° R=.65, p<.001). The polar width of V3A did not correlate with V1 (p=.82), V2 (p=.81) or V3 (p=.65).

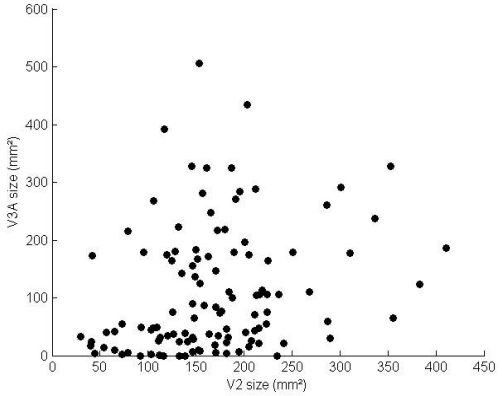

Figure 2-33 The relationship between V2 and V3A size (mm²; p<.01). Each data point represents a single hemisphere at a single eccentricity patch.

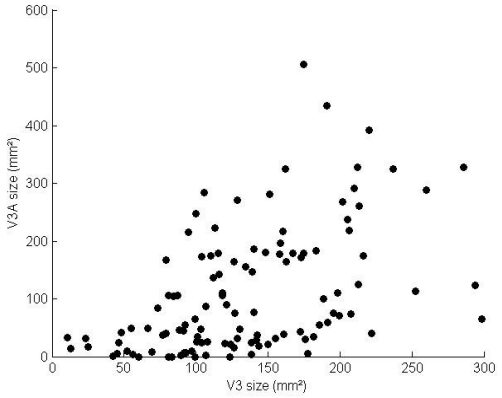

Figure 2-34 The relationship between V3 and V3A size (mm²; p<.001). Each data point represents a single hemisphere at a single eccentricity patch.

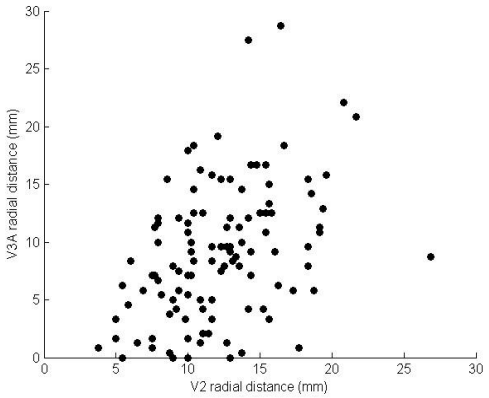

Figure 2-35 The relationship between V2 and V3A radial distance (mm; p<.001). Each data point represents a single hemisphere at a single eccentricity patch.

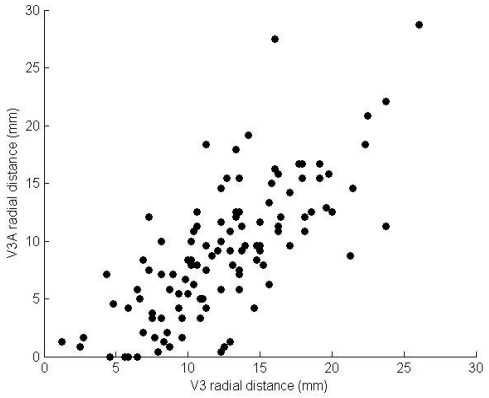

Figure 2-36 The relationship between V3 and V3A radial distance (mm; p<.001). Each data point represents a single hemisphere at a single eccentricity patch.

2.3.7 Correlations between Eye Size and Parameters of Retinotopic Maps

No links were identified between eye surface area and any parameter of V1. Eye surface area did not correlate with the size (figure 2-37; p=.29), radial distance (figure 2-38; p=.8) or polar width (figure 2-39; p=.09) of V1. Cortical magnification in V1 did not show any correlation with eye surface area. For example, using measures from the piecewise regression function, eye surface area was not linked to radial cortical magnification (figure 2-40; p=.45) or polar cortical magnification (figure 2-41; p=.58).

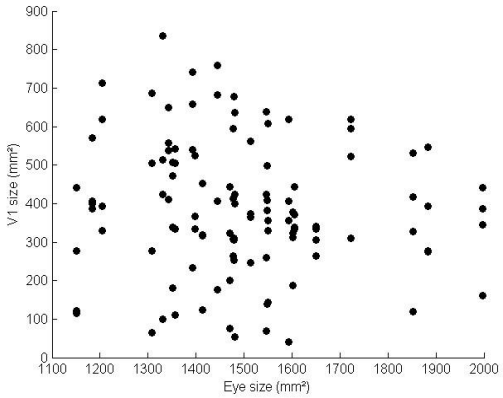

Figure 2-37 The relationship between eye surface area (mm²) and V1 size (mm²; p=.29). Each data point represents a single hemisphere at a single eccentricity patch.

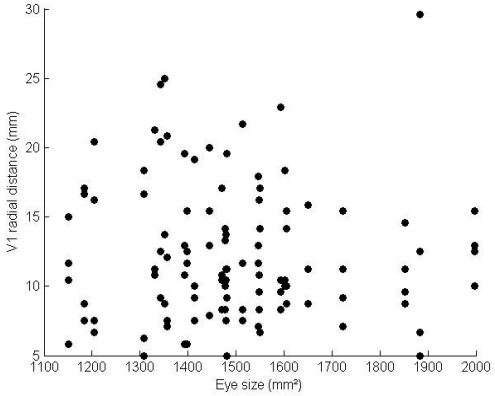

Figure 2-38 The relationship between eye surface area (mm²) and V1 radial distance (mm; p=.8). Each data point represents a single hemisphere at a single eccentricity patch.

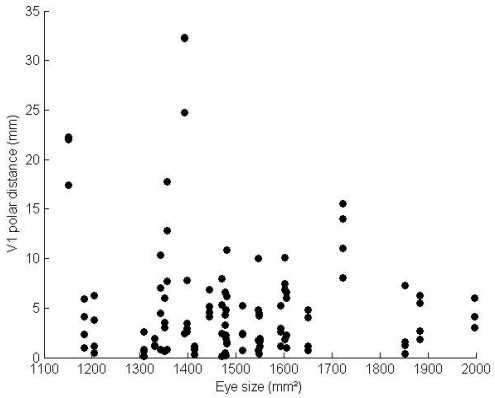

Figure 2-39 The relationship between eye surface area (mm²) and V1 polar width (mm; p=.09). Each data point represents a single hemisphere at a single eccentricity patch

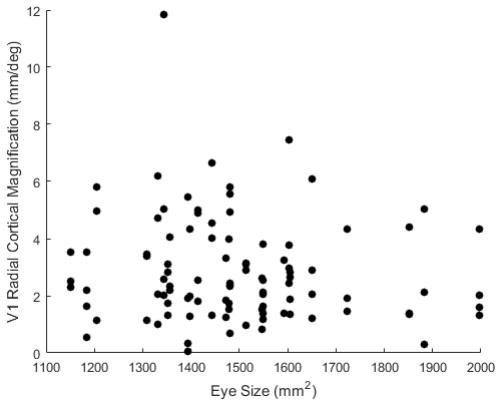

Figure 2-40 The relationship between eye surface area (mm²) and V1 radial cortical magnification (mm/deg; the piecewise regression function; p=.45). Each data point represents a single hemisphere at a single eccentricity patch. Negative cortical magnification values are not shown on the plot.

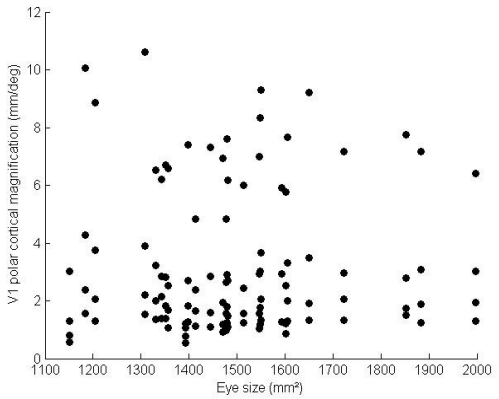

Figure 2-41 The relationship between eye surface area (mm²) and V1 polar cortical magnification (mm/deg; the piecewise regression function; p=.58). Each data point represents a single hemisphere at a single eccentricity patch.

2.4 Discussion

An exploration of inter-areal correlations across the visual system was performed for 28 hemispheres. Retinotopic areas V1, V2, V3, V3A, V4, LO1 and LO2 were included, in addition to the eye. Parameters included in this series of analyses were surface area size, radial distance, polar width, radial cortical magnification, polar cortical magnification and eye surface area. A cluster comprising of V1, V2 and V3 was identified. A secondary pairing, between LO1 and LO2 was also seen. An exploration of the role of V3A was

limited to some extent by a failure to accurately estimate cortical magnification in this map. There was an indication of an intermediary role for V3A, links were seen with both with V1-V2-V3 and LO1-LO2, at least in size measurements. The key finding of this study is that other than the V1-V2 link, inter-areal correlations are generally weak in both cortical magnification and size measures. Generally, the strong effect of eccentricity is the main common source of variance.

2.4.1 Early Visual Areas

The correlation between V1 and V2 and V3 is a consistent finding throughout the literature. It has been argued that these visual areas constitute a single map complex (Polimeni et al., 2006). Dougherty et al. (2003) found a strong correlation in surface size between V1 and V2 within individuals. Although V1 was not found to correlate with V3 in terms of surface size (Dougherty et al., 2003), a significant relationship was noted between V2 and V3. Furthermore, Dougherty et al. (2003) report that all 3 visual areas had similar levels of cortical magnification. Harvey and Dumoulin (2011) support this pairing both in terms of receptive field size and cortical magnification. It was argued (Harvey & Dumoulin, 2011) that V1 determines the architecture of later visual areas.

The data presented here replicates the relationship between V1, V2 and V3 although indicates that it may be weaker than previously suggested. In terms of size measurements, strong links were identified between V1 and V2, replicating previous findings (Dougherty et al., 2003). Both the surface area size and the radial distance correlated. V2 and V3 also demonstrated strong links in surface area size, radial distance and polar width. Analyses indicate that the V2-V3 correlations may be constrained to the central portion of the visual field. In terms of size measurements, the relationship between V1 and V3 was weak, corresponding with previous research (Dougherty et al., 2003).

Cortical magnification measurements also support a pairing of these 3 visual areas. In the radial dimension, links were clear between V1 and V2 and between V2 and V3. In the polar dimension the links were also evident between these areas. Unexpectedly, the polar cortical magnification correlation between V1 and V3 was inverse. Participants with high levels of polar cortical magnification in V1 had low levels in V3. This link is weak, it was

lost at specific eccentricities (although this may also be attributed to insufficient power). Furthermore, analysis of size V3 parameters did not mirror this link. For this reason, it is suggested that the V1-V3 link is driven largely by a failure of the functions to accurately estimate cortical magnification.

2.4.2 Eye Surface Area

Previous research suggests that the cortical magnification of V1 determines the properties of later visual areas (Dougherty et al., 2003). It was hypothesised that these correlations may begin earlier in the visual system than the retinotopic areas, such as the eye surface area. This hypothesis has not been supported here, conflicting with the proposal of Pearce and colleagues (2011; 2013). Neither the size nor the level of cortical magnification in V1 correlated with eye surface area.

Conclusions made regarding correlations between eye surface area and retinotopic parameters must be appropriately tentative. The investigation conducted here was solely exploratory. The eye surface area measurements taken were crude and the participant number was low. Particularly, comparisons with Pearce and Dunbar (2011) are limited due to the lack of geographical dissimilarity of the participants used here.

2.4.3 Higher Visual Areas

A map complex comprising V1, V2 and V3 has been suggested (Polimeni et al., 2006) and is moderately supported by the data presented here. Whether similar complexes exist at higher levels is unexplored in the literature. LO1 has previously been shown to be unrelated to the early complex (Harvey & Dumoulin, 2011), indicating that these later regions either form alternative complexes or are independent. A strong relationship was identified here between LO1 and LO2. These regions were similar in radial and polar measures of cortical magnification. Additionally, consistent with previous studies, LO1 and LO2 correlated in measures of size and radial distance (Larsson & Heeger, 2006).

An intermediate role was identified for V3A, particularly terms of surface area. V3A appeared to inherit radial cortical magnification from V1 and size measures of the two maps also correlated. V3A also showed extensive links with size measures of V2 and V3. Previous research has demonstrated links between V1 and intermediate maps such as V4 (Harvey & Dumoulin, 2011) so the links between V3A and the V1-V2-V3 cluster are not surprising. In addition to its involvement in the V1-V2-V3 cluster, V3A also showed links with LO1 and LO2 in measures of polar width, surface area and radial distance. Given the intermediate functional role of V3A in visual processing (Tootell et al., 1997) in addition to its intermediate physical location between dorsal V3 and LO1, its involvement in both the higher and lower complex is expected.

2.4.4 Intra-Individual Variability

The strongest finding presented here is the high variability within participants. Multiple links between visual areas were attributed to the common pattern of eccentricity. Due to the general pattern within the literature of considering group differences in correlations between visual areas (Dougherty et al., 2003), this eccentricity characteristic is largely unexplored. The study reported here looked at a wider range of eccentricities than has generally been considered. Within a single participant, measures of retinotopic parameters showed high variability. Figure 2-42 illustrates this high intra-individual variability. This intra-individual variability may account for the conflict between the data presented here and earlier research (Dougherty et al., 2003) in terms of inter- areal correlations. The strong effect of intra-individual variability within a single map is particularly pronounced in the polar direction, accounting for as much as two thirds of all variance in this dimension (table 2-2).

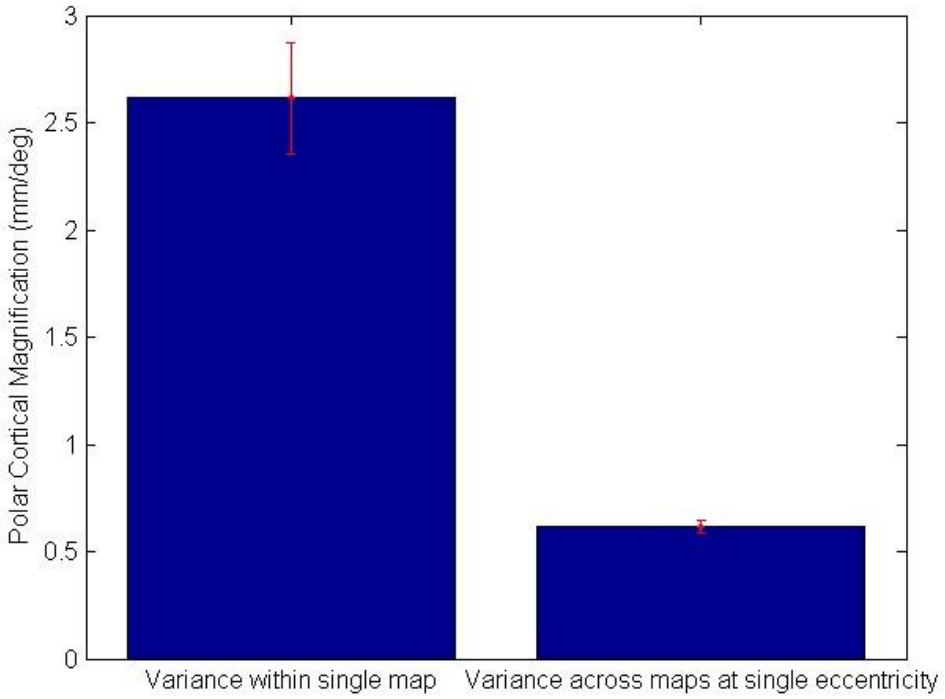

Figure 2-42 Comparison of variability in polar cortical magnification (piecewise regression function) across and between maps. Variance within a single map illustrates mean variability across all participants and eccentricities in left V1. Variance across maps illustrates mean variability across all participants and maps at 6°. Standard errors shown.

The finding that visual areas share relatively little variance other than the dominant effect of eccentricity informs speculation regarding the developmental pattern of the visual cortex. It was assumed that the cortical elements of visual system scale consistently across individuals, in an analogous fashion to subcortical structures (Andrews et al., 1997). It was also assumed that within a single area the levels of cortical magnification would increase in a consistent manner with distance from the fovea. The computational models of Polimeni et al. (2006) are reliant upon the presence of a pattern in inter-areal correlations. In fact, there appears to be a high level of variability at all levels.

2.4.5 Conclusions

Consideration of surface area size, radial cortical magnification and polar cortical magnification has supported the existence of a V1-V2-V3 complex. The involvement of eye surface area in this complex has been rejected. Correlations between visual areas later in the visual system have also been explored. A secondary complex has been identified, comprising LO1 and LO2. This complex may be analogous to that of V1-V2-V3. A strong effect of eccentricity has been identified, indicated substantial intra-individual variability in the representation of visual space within a single map.

Later studies within this thesis aim to correlate visual abilities with measures of radial and polar cortical magnification in retinotopic areas. The data presented here has implications for the conclusions that will be drawn from these later studies. Whilst it must be noted that no region throughout the visual cortex showed full independence from the others, these links were relatively weak in comparison to those suggested in previous studies (e.g. Polimeni et al., 2006). The development and organisation of higher-order areas is not simply driven by inheritance from V1. Performance reliant on characteristics of retinotopic areas may therefore be attributed to specific visual areas. If specific abilities rely on the function of a single area and the levels of these abilities are proportional to retinotopic parameters such as cortical magnification and surface area, identification of correlations between specific abilities and retinotopic parameters of specific maps should be possible.

3 Cortical Magnification in V3A and LO1 Constrains Performance in a Motion Defined Boundary, but not Luminance Defined Boundary, Orientation Discrimination Task

3.1 Introduction

Cortical magnification in V1 has been found to correlate with perceptual abilities reliant on this visual area (Duncan & Boynton, 2003). This chapter aims to expand the hypothesised constraining role of cortical magnification to intermediate maps. V3A has previously been associated with perception of coherent motion (Larsson, Heeger, & Landy, 2010). It is predicted that individual differences in perception of a motion defined boundary, but not a luminance defined boundary, will be correlated with individual differences in V3A retinotopic parameters.

3.1.1 V3A

Human V3A plays an important role in the perception of motion boundaries (Larsson et al., 2010). This region is located near the dorsal occipital cortex (Wandell et al., 2007). It is immediately bordering V3d. It was first mapped in rhesus monkeys by (Van Essen & Zeki, 1978), and despite its original name of V3 accessory, is in fact independent in both retinotopy (Gattass et al., 1988) and functional properties (Felleman & Van Essen, 1987). V3A is retinotopic. It has a continuous map of the contralateral hemisphere; it has a complete representation of the upper and lower quadrants of the visual field. It also differs from V1, V2 and V3 in its foveal representation. In humans, V3A has a foveal representation that is separate and displaced from that of V1-V3 (Larsson & Heeger, 2006). There is high individual variability in the clarity of this foveal representation (Larsson et al., 2010). Human V3A has larger receptive field sizes than V1 and high contrast sensitivity (Tootell et al., 1997).

Despite sharing retinotopic similarities with macaque V3A, human V3A differs from macaque V3A in functional characteristics. Unlike macaque, human V3A in highly sensitive to motion (Tootell et al., 1997). During the experience of motion after-effects induced by a visual illusion, MT showed the highest degree of activity. However, V3A also showed activation to a greater degree than V2, V3 and V1 (Tootell et al., 1995). Although this study was limited to some extent by attentional confounds, later research supports a role for V3A in motion perception (Braddick et al., 2001; Goebel, Khorram-Seffat, Muckli, Hacker, & Singer,1998).

More recently, the role of V3A has been linked to the processing of motion boundary stimulus (Larsson et al., 2010). Motion boundary stimuli are images in which an edge is created through local changes in visual motion direction. Orientation selectivity of V3A has been indicated through adaptation to motion- boundary gratings (Larsson et al., 2010). Unlike other regions which respond to motion, such as V1, V3A is able to differentiate between random and coherent movement (Braddick et al., 2001).

In addition to V3A specifically, the regions surrounding this map have also been linked with motion boundary perception. A region located dorsally and laterally to V3 has been acknowledged in recent decades as a key region of motion- boundary processing. The kinetic occipital area (KO) includes V3A, LO1 and parts of V3. It was found to respond more strongly to motion-boundary dot stimuli than dot stimuli without edges during passive viewing (Dupont et al.,1997; Van Oostende, Sunaert, Van Hecke, Marchal, & Orban, 1997). The region also responded to luminance defined gratings, unlike MT which favoured motion-defined gratings. This has led some to suggest that KO may play a general role in perception of any shape, not only those defined by motion (Zeki, Perry, & Bartels, 2003).

Single cell recording in macaques has indicated that, like humans, responses to motion-boundary stimuli are dispersed across the cortex. Sary, Vogels, Kovacs, and Orban (1995) report neural activity in inferior temporal cells. 27% of motion sensitive inferior temporal cells responded preferentially to a specific orientation. Although, the same percentage of luminance sensitive inferior temporal cells also responded preferentially to a specific orientation. Whilst there was a shorter latency value for luminance than motion, both

modalities elicited equally strong responses. It was concluded that this region is cue invariant in its coding of edges. Macaque V4d has also been implicated in the perception of motion boundaries (Mysore, Vogels, Raiguel, & Orban, 2006). Additionally, responses to motion boundaries have been found to be strong in V3 and V3A (Burkhalter & Van Essen, 1986; Zeki, 1978).

The utilization of macaque data to inform understanding of the human visual system, and V3A in particular is difficult for several reasons. Firstly, as previously discussed, it has not been confirmed that macaque V3A is fully homologous to human V3A in terms of functionality. Early studies suggest macaque V3A may be less motion selective than human V3A (Gaska, Jacobson, & Pollen, 1988; Tootell et al., 1997). Secondly, studies of the two species generally employ different methods leading to difficulties associated with cross- methodological comparisons (Larsson et al., 2010). Macaque studies utilize single cell recordings (Gaska et al., 1988) and measure orientation selectivity for boundaries of particular orientations. Human experiments, unable to measure single cells, rely on fMRI. fMRI studies identify regions demonstrating a stronger response to motion-boundaries stimuli than transparent motion stimuli. Despite these limitations, a recent study provides some indication that cross-methodological comparisons may be permitted. Human fMRI data indicates that the majority of regions that display greater activation in response to motion-boundary stimuli than transparent motion stimuli also show selectivity for boundary orientation (Larsson et al., 2010).

It has been demonstrated that multiple regions in the human cortex respond to motion boundary stimuli. These include areas within the established KO region, as well as additional locations (Larsson & Heeger, 2006). V3A is the most appropriate region to correlate with motion boundary behavioural thresholds as it is specialised for processing this form of stimuli (Larsson et al., 2010). The role of V3A in motion boundary perception is also of particular interest due to its intermediate position between early visual areas (e.g. V1, V2) and more complex processing in the inferior temporal cortex. As described in chapters 1 and 2, an aim of this thesis is to expand the link between V1 cortical magnification and simple perceptual abilities (Duncan & Boynton, 2003) to more complex processes. For this reason, the hierarchical position of V3A suggests it may be a suitable candidate. V3A has previously been proposed as a suitable location in which to

consider processing in higher cortical regions whilst using relatively simple stimuli (Tootell et al., 1997).

Specifically, if V3A is crucial for the processing of motion defined boundaries then performance in tasks reliant on this form of perception should correlate with cortical measures of this visual map. Variability in the retinotopy of V3A is expected to be reflected in behavioural variability between participants. If visual performance is dependent on the amount of neurons representing the stimulus (Duncan & Boynton, 2003) then high levels of cortical magnification should correlate with accurate perception of motion boundaries. Data addressing the extent of V3A variability between participants is mixed. Whilst earlier research (Larsson & Heeger, 2006) has indicated that there is high individual variability in the retinotopy of V3A, examination of figures 2-15, 2-16 and 2-17 suggest that within the data presented in this thesis V3A variability is not higher than variability of other visual areas.

3.1.2 Cortical Anisotropy

Early visual regions show some degree of anisotropy. This term describes the non-uniform retinotopic projection from the visual field to the cortex. This cortical anisotropy can be described using an anisotropy index (Adams & Horton, 2003b) of compression in the radial direction: compression in the polar direction. Analogously to the overrepresentation of the fovea described by cortical magnification, the cortex also has more surface area devoted to processing visual field points in certain directions (figure 3-1). Flattened maps of V1, V2 and V3 appear compressed in the direction perpendicular to the inter-area boundaries (Polimeni et al., 2006). There is more cortical surface, and therefore neurons, representing visual space in the radial direction (perpendicular to V1/V2 and V2/V3 borders) than representing visual space in the polar direction (parallel to V1/V2 and V2/V3 borders).

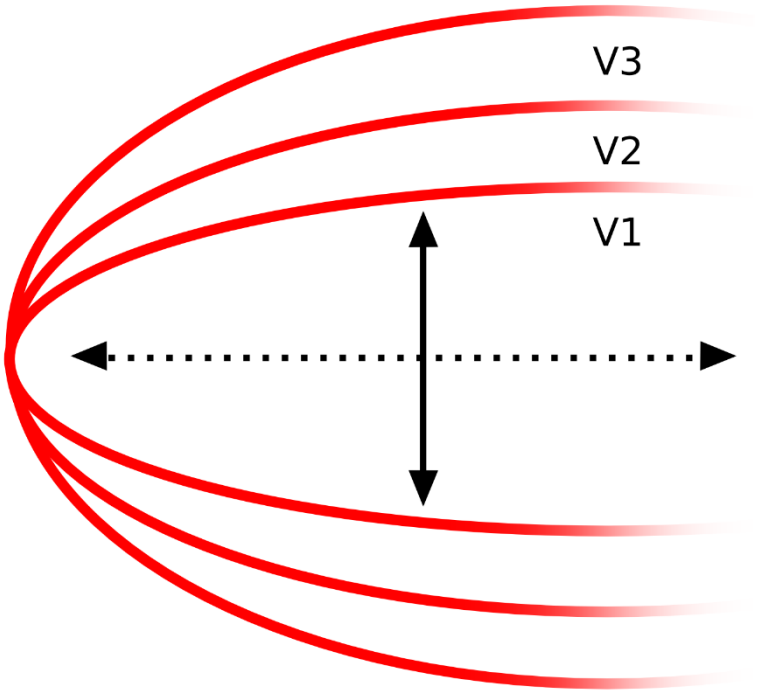

Figure 3-1 Illustration of cortical anisotropy. Compression is greater in the polar direction (solid arrow) than in the radial direction (dotted arrow).

Attempts have been made to quantify this ratio in early visual areas, but results lack convergence (Polimeni et al., 2006). LeVay et al. (1975) indicate that a 1:1 ratio exists in the macaque V1. Cortical magnification in the radial direction (parallel to the V1/V2 border) is equal to cortical magnification in the polar direction. Conversely, Tootell et al. (1988) suggest an index of 2:1 in the macaque, indicating that the representation of visual space is twice as compressed in the polar direction as the radial. Larsson and Heeger (2006) report a higher anisotropy of 3:1 in humans.

The early electrophysiological studies of Tootell et al. (1988) and LeVay et al. (1975) were constrained by their methodological limitations. They focused on a narrow strip near the V1/V2d border as this was the most convenient location due to the known columnar structure at this cortical point (Blasdel & Campbell, 2001). Using macaque optical recording, it was found that the cortical anisotropy ratio differed between points located near cortex representing the vertical meridian and points located near the horizontal meridian. Near the vertical meridian a ratio of 1.5:1 was identified, cortical magnification was higher in the radial direction than the polar direction. Near the horizontal meridian this ratio dropped to 1.15:1 (Blasdel & Campbell, 2001). Others have supported an

increased cortical magnification level in the proximity of the vertical meridian (Schwartz, 1994).

The cortical anisotropy of later visual areas has received less attention. V2 has been hypothesised, based on its biological structure, to have an anisotropy of 6:1 (Roe & Ts'o, 1995). Data supporting this particular estimate has not been found (Polimeni et al., 2006), but Larsson and Heeger (2006) present retinotopic data indicating anisotropy in the same direction (e.g. a higher level of compression in the polar direction compared to the radial). This high anisotropy predicts an increased compression, so lower cortical magnification, in the direction of the polar co-ordinates. This approximation is much higher than the highest estimate of cortical anisotropy in V1 (Larsson & Heeger, 2006). Levels of anisotropy in V3 have been less thoroughly documented, however observation of flattened maps (Horton & Hoyt, 1991a) indicate that some compression in the direction orthogonal to the V2/V3 border exists (Polimeni et al., 2006).

Despite the lack of convergence in V1 anisotropy ratio, early investigations generally agreed on the underlying causes of the topographical anisotropy. VI anisotropy was suggested to rely upon the columnar system of the visual area. The anisotropy was proposed to align with this structure (LeVay et al., 1975; Tootell et al., 1988). LeVay et al. (1975) argued for a process by which the topographic representation of layer IV created an anisotropy of 1:2, which when combined with the complete map from the other eye resulted in an overall anisotropy of 1:1. Tootell et al. (1988), argued for the opposite. They proposed that at a local level, single ocular dominance column stripes displayed an anisotropy of 1:1, resulting in an overall large anisotropy index of 2:1. To summarise, the debate centres on the anisotropic properties of the columnar system. A over representation of polar visual space would result in an overall non-anisotropic V1 (LeVay et al., 1975), an equal representation of radial and polar visual space would result in an overall compression of polar space in V1 (Tootell et al., 1988).

Retinotopic mapping has demonstrated that the pattern of anisotropy observed in V1 and V2 also exists later in the visual system. The representation of visual space, as in V1 and V2, is more compressed in the direction of polar angle co- ordinates than in the direction of eccentricity co-ordinates. Larsson and Heeger (2006) mapped visual areas V1, V2, V3, V3A, LO1 and LO2 and V4. Anisotropy in later areas was high. For example, in LO1,

1.5mm of cortex was devoted to processing 1 degree of visual space in the polar direction. In the radial direction, this ratio increased to 10mm of cortex for 1 degree of visual space.

Attempts have been made to understand V2 anisotropy through an understanding of columnar patterns. The striped structure of this region was thought to align with anisotropy, in a similar way to the alignment found in V1. Based on the finding that the sub-columnar structure was compressed in the direction orthogonal to the V2/V3 border at a ratio of 2:1, a supra-columnar ration was proposed as 6:1. However, this estimate was informed by the indication that each V2 column has 3 representations, thereby tripling any local anisotropy. This assumption has since been questioned, improved understanding of V2 structure has indicated that the 3-stripe pattern of V2 may be less consistent than previously assumed (Felleman et al., 2015).

Due to the absence of understanding regarding the structure of later visual areas, it is difficult to predict anisotropy in later visual areas, such as V3 and V3A. Although, Polemini et al. (2006) provide some indication that the cortical structure is not necessary in understanding anisotropy. Using Wedge-Dipole mapping, a model was created which successfully approximated macaque V1, V2 and V3. The model demonstrated that anisotropy at the V2/V3 border mathematically followed the ratio of anisotropy found at the V1/V2 border. This correlation suggests a weaker role for area-specific columnar structure than was previously assumed. Furthermore, evidence of an inheritance from V1/V2 to V2/V3 supports the suggesting that findings regarding anisotropy in early visual areas may be extrapolated to aid understanding of V3A.

3.1.3 Orientation Discrimination

Orientation discrimination tasks using motion defined stimuli are used to measure the orientation selectivity of the underlying processes. Participants are presented with a grating and asked to indicate its orientation. Correct identification of the orientation depends of successful visual processing of the grating, and therefore perception of the edges defined by the motion of the grating.

A consistent finding, both within motion defined grating studies and luminance defined grating studies, is that performance (discrimination thresholds) depends on the relative orientation of the stimulus. For adults, children and non-human primates, performance in a variety of tasks is better for stimuli presented at vertical or horizontal angles (Appelle, 1972). This well documented impediment (Campbell, Kulikowski, & Levinson, 1966; Heeley & Timney, 1988; Orban, Vandenbussche, & Vogels, 1984) in the ability to perceive oblique stimuli is known as the Oblique Effect (Appelle, 1972). The effect occurs only in the central visual field; disappearing at approximately 8 degrees eccentricity (Berkley, Kitterle, & Watkins, 1975).

In addition to this sensitivity to field-independent orientation, subjects also demonstrate impaired performance dependent on the orientation of stimuli relative to its position in the visual field (Sasaki et al., 2006). This is known as meridian relative sensitivity. A consistent finding is that performance is enhanced when the local pattern orientation matches the angular meridian. For example, the perception a grating positioned in the upper right quadrant of the visual field is more accurate at a 90 (figure 3-2, A) degree angle than at a 135 (figure 3-2, B) degree angle (Westheimer, 2005). However, preference for the stimulus oriented at a 90 degree angle will disappear if the grating is moved a new position in the upper left quadrant of the visual field (figure 3-2, C). In the first position, the 90 degree orientated stimuli is radial, whilst in its second position it is tangential.

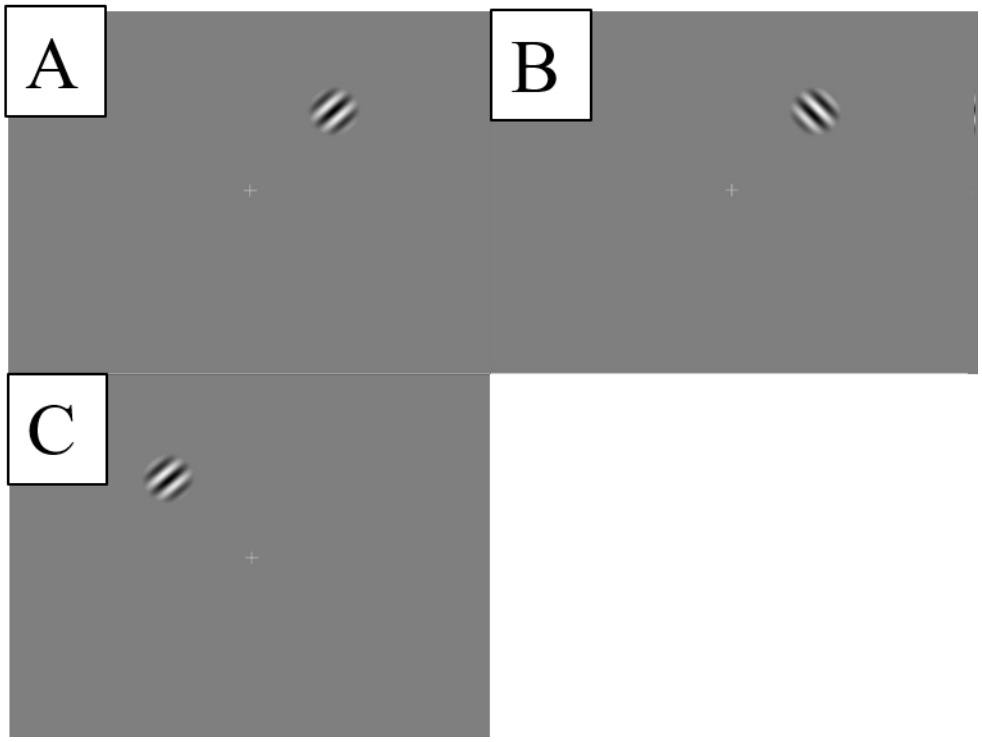

Figure 3-2 Illustration of meridian relative sensitivity. Perception is enhanced in figure A relative to figures B and C.

Rovamo, Virsu, Laurinen, and Hyvärinen (1982) established resolution thresholds for gratings in 3 positions and at 4 eccentricities. The Oblique Effect was observed at low eccentricities. At higher eccentricities (e.g. 20 degrees) an effect of meridian-relative anisotropy was seen. Resolution was better for meridian-parallel orientated stimuli than meridian-perpendicular bars. This increased sensitivity to orientations that are radial relative to the meridians of the visual field has been repeated (Sasaki et al., 2006; Westheimer, 2005).

Linking these two consistent patterns, the Oblique Effect and meridian-relative orientation sensitivity, to neural functioning has utilized both single-neuron measurements (De Valois, Yund, & Hepler, 1982) and MRI methodologies (Mannion et al., 2010). The correlations between oblique behavioural performance and neural activity seem to be somewhat more complex than those suggested to exist between meridian-relative behavioural performance and brain function.

Single-cell recordings have shown a preference in the macaque visual cortex to horizontal and vertical stimuli over oblique stimuli. De Valois et al. (1982) measured the activity of mainly foveal neurons during the presentation of variously oriented stimuli. Stronger neuronal activity was observed in response to the presentation of horizontal and vertical stimuli than oblique. Mansfield (1974) also documented a clear oblique effect at the level of individual neurons. Unlike De Valois et al. (1982), Mansfield considered the activity of neurons at higher eccentricities. It was found that the neuronal preference for oblique stimuli lessens greatly as distance from the fovea increases.

Whilst informative to some extent, these early investigations into the neural correlates of the behavioural Oblique Effect (De Valois et al., 1982; Mansfield, 1974) are severely compromised by their failure to account for meridian-relative anisotropies (Mannion et al., 2010). The design and interpretation of these studies were reliant on the assumption that the visual system is sensitive to orientations at only a field-independent level.

Mannion et al. (2010) account for this confound. Both global anisotropy (the Oblique Effect) and local anisotropy (meridian-relative) were investigated in humans using fMRI. Activation was measured in visual areas V1, V2, V3, V3A/B and V4 during presentation of sinosoidal gratings at various orientations. A clear effect of local anisotropy was found. All visual areas showed higher activation when the grating was presented in a radial position. This finding agrees with previous macaque investigations, in which a greater number of neurons responded to radial than tangential gratings (Leventhal, 1983). It also converges with behavioural findings (Furmanski & Engel, 2000). It was suggested that the preference for meridian relative radial gratings over tangential gratings may be related to the prevalence of radial orientations in natural scenes. Orientations radial to the image centre (Bruce & Tsotsos, 2006) and centre of gaze (Rothkopf, Weisswange, & Triesch, 2009) are common in natural scenes. Additionally, it has been suggested that radial orientations are also involved in computational processes such as establishing perspective (Rothkopf et al., 2009) and optic flow (Raemaekers, Lankheet, Moorman, Kourtzi, & Van Wezel, 2009).

The results of BOLD response during presentation of oblique-effect inducing stimuli were less consistent with past literature. Mannion et al. (2010) report lower activation in all visual areas in response to horizontal gratings. In single- cell recordings in the macaque

visual cortex, it was found that the greatest number of cells responded to horizontal stimuli, fewer to vertical and the least to oblique (Li, Peterson, & Freeman, 2003). The interpretation of this discrepancy is unclear, especially in light of the clear convergence of the local anisotropy findings with previous literature (Leventhal, 1983).

3.1.4 Predicted Correlations between V3A Cortical Magnification and Motion Perception

In summary, there is variability in visual area measurements defined by retinotopic mapping (Schwarzkopf et al., 2012) and this variability correlates with visual perceptual abilities (Duncan & Boynton, 2003), particularly for the parameter of cortical magnification. As outlined in Chapter 2, performance on a visual task was constrained by the amount of cortical tissue processing the stimulus. It is unknown whether this correlation extends to later visual areas, such as V3A, and the perceptual functions they are thought to underpin such as motion-boundary perception. Following from the findings of Duncan and Boynton (2003), a high number of orientation-tuned neurons in V3A are expected to be linked to good performance in a motion defined orientation discrimination task.

Furthermore, there is anisotropy in multiple regions of the visual cortex (Polimeni et al., 2006) and also anisotropy in perceptual abilities. Meridian- relative anisotropy in perceptual abilities has been linked to cortical activity (Mannion et al., 2010) but the relationship has not been fully described. It is possible that the ratio of cortical anisotropy is correlated with the radial/tangential perceptual differentiation. If, as the findings of Mannion et al. (2010) suggest, more neurons are tuned to optimally process radial orientations than tangential orientations, performance should be more accurate when the orientation of radial position stimuli are judged.

The cortical basis can be considered by exploring the link between cortical magnification and perceptual abilities in a task-specific way. Perception of a motion defined grating is thought to rely upon activity in V3A (Larsson et al., 2010), whilst a luminance defined grating correlates with activity in V1 (Mazer, Vinje, McDermott, Schiller, & Gallant, 2002). Cortical anisotropy is greater (e.g. the difference between M in the radial

dimension and the polar dimension is higher) in higher visual areas (Larsson & Heeger, 2006) than lower visual areas (Roe & Ts'o, 1995). For this reason, it is likely that the motion task, which relies upon the higher visual area, will show a greater difference in perceptual abilities for radial and tangentially orientated gratings than the luminance task, which relies on a lower visual area. Psychophysical performance in radial and tangential conditions is also expected to be preferentially constrained by either radial or polar cortical magnification. This hypothesis is speculative and exploratory, no predictions are made regarding the pairings between psychophysical conditions and dimensions of cortical magnification.

3.2 Methods

3.2.1 Measurement of Cortical Parameters

A subset of previously collected cortical magnification and size measurements were used (see Chapter 2 for collection and analysis details).

3.2.2 Psychophysical Measurement of Orientation Discrimination

3.2.2.1 Participants

Participants were aged between 20 and 34 years and had normal or corrected to normal eye sight. 10 subjects (5 males) participated in the luminance defined orientation task. 14 subjects (5 males) participated in the motion defined boundary orientation task. All 10 participants from the luminance defined boundary orientation task also took part in the motion defined boundary orientation discrimination task. Written consent was obtained from all participants. The experimental procedure was in accordance with the Declaration of Helsinki and was approved by the appropriate local ethics committee.

3.2.2.2 Orientation Discrimination Experimental Procedures

Testing took place in a quiet, dark room. Subjects sat 57cm from a screen and the head was stabilized through the use of a chin rest. Stimuli were binocularly viewed on 37cm by 30cm sized screen. Gamma correction of the screen was performed following luminance measurement using a Minolta LS-100 luminance meter. Stimuli were presented on an EIZO 660-M monochrome CRT monitor. There was a frame rate of 60.02Hz. Presentation of stimuli and acquisition of responses was carried out using Matlab 7.4.0 (R2007a) and MGL (http://www.pc.rhul.ac.uk/staff/J.Larsson/software.html) run on a Linux operating system.

3.2.2.3 Orientation Discrimination Stimuli

Experimental stimuli consisted of motion defined gratings (figure 3-3). The gratings were masked by a circular aperture, measuring 4 degrees of visual angle in diameter. Dots moved at a 45 degree angle to boundaries (alternating between 0 and 90 degree direction in adjacent stripes) so the net movement direction was identical for radial and tangential gratings. Dots moved at a speed of 3 seconds/degree. The grating consisted of 65 black dots. The phase of the dot position was randomised every 0.5s and the direction was reversed every 0.5s.

Control stimuli consisted of luminance defined gratings (figure 3-4). This grating was of equal size to the motion defined stimulus. This stimulus consisted of a sinusoidal grating pattern; luminance was modulated sinusoidally from white to black. The luminance contrast was 100%.

Figure 3-3 Motion defined boundaries stimulus. Black lines illustrate motion boundaries and black arrows illustrate direction of movement.

Figure 3-4 Luminance defined boundaries stimulus

The gratings (both luminance defined and motion defined) were located at one of four eccentricities. Dependent on the condition, the midpoint of the grating was at an eccentricity of 0°, 3°, 6° or 9 °. Gratings were displayed in either the upper right quadrant of the visual field or the upper left quadrant of the visual field. Central fixation of the

screen was marked by a white 1 degree by 1 degree fixation cross. The background was consistently mean luminance (26.1 cd).

3.2.2.4 Orientation Discrimination Task

The task was identical for both the condition using motion defined stimuli and the condition using luminance defined stimuli. Thresholds for the minimum perceivable difference in orientation between 2 gratings were obtained using a temporal two-alternative forced choice paradigm and a 1 up 2 down staircase with a maximum of 60 steps.

The procedure for a single trial is displayed in figure 3-5. One grating was displayed for 0.5s. This grating was displayed at an orientation of approximately 45 or 135 degrees (depending on the condition). The exact orientation of the first grating was determined by a randomized jitter of between -1 and 1 around 45 or 135 degrees (depending on the condition). Following this, there was an inter-stimuli interval of 0.5s in which a fixation cross was displayed. A second grating (at a different orientation to the first) was then displayed. The orientation of the second grating was determined by the staircase. Participants then made a button press response to indicate whether the second grating was clockwise or counter- clockwise in comparison to the first grating. Trials were self-paced. 60 pairs of gratings were presented in each block of trials. Each block produced 1 threshold value. This threshold value was the mean orientation difference across the last 20 trials of the block. Participants were instructed to keep their eyes focused on the fixation cross throughout the trials. This instruction was repeated regularly throughout the testing session.

Each testing sessions began with a short practice phase. This usually consisted of 1 block of trials, but occasionally lasted for 3 blocks for inexperienced subjects. In each testing session the grating was presented at 4 eccentricities. Each eccentricity was repeated 3 times. If a threshold was not achieved, the block was repeated. Failure to achieve a threshold was determined by inspecting the staircase output following each block of trails. Failure was common, approximately 4 trials per testing session were repeated. In total there were 12 blocks of trials. The testing sessions took approximately 50 minutes, including a break of 10 minutes half way through the experiment. Subjects attended either

4 or 8 testing sessions (depending on whether data for both the left and right visual fields was collected or only the right).

There was some concern that the inter-stimuli interval of 0.5s was insufficient to prevent adaptation. For this reason, additional piloting was performed for one participant (the author). Thresholds were obtained for radial and tangential motion and luminance conditions during right visual field presentation. This data is displayed Appendix A. The longer inter-stimuli break (2s) resulted in data similar to the shorter-stimuli break (0.5s).

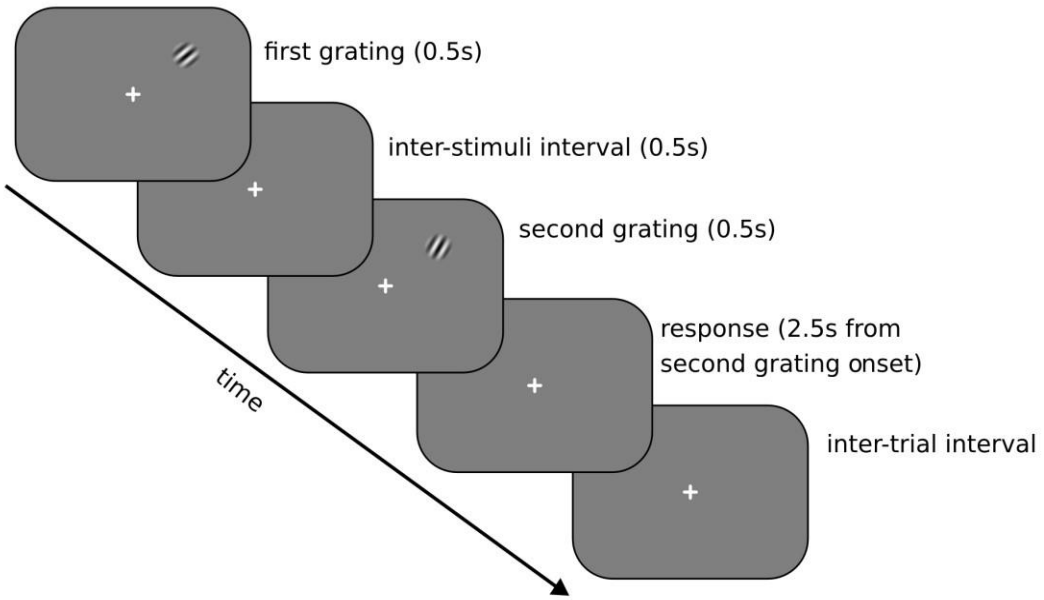

Figure 3-5 Orientation discrimination experimental paradigm: schematic representation of a single trial. Here, a luminance defined grating at a radial orientation in the right visual field is shown. Trials for all other condition followed an identical procedure.

3.2.2.5 Orientation Discrimination Experimental Design

Within each block of trials, the gratings were always at the same eccentricity and within the same quadrant of the visual field. Within each testing session, the gratings were always within the same quadrant of the visual field and of the same relative orientation (radial or tangential).

There were 4 conditions for each visual field location (right and left upper quadrants). These conditions were; luminance radial, luminance tangential, motion radial and motion tangential. As illustrated by figure 3-6, in the right visual field presentation sessions, the radial condition included stimuli at 45 degrees. In the left visual field presentation condition, radial stimuli were at 135 degrees.

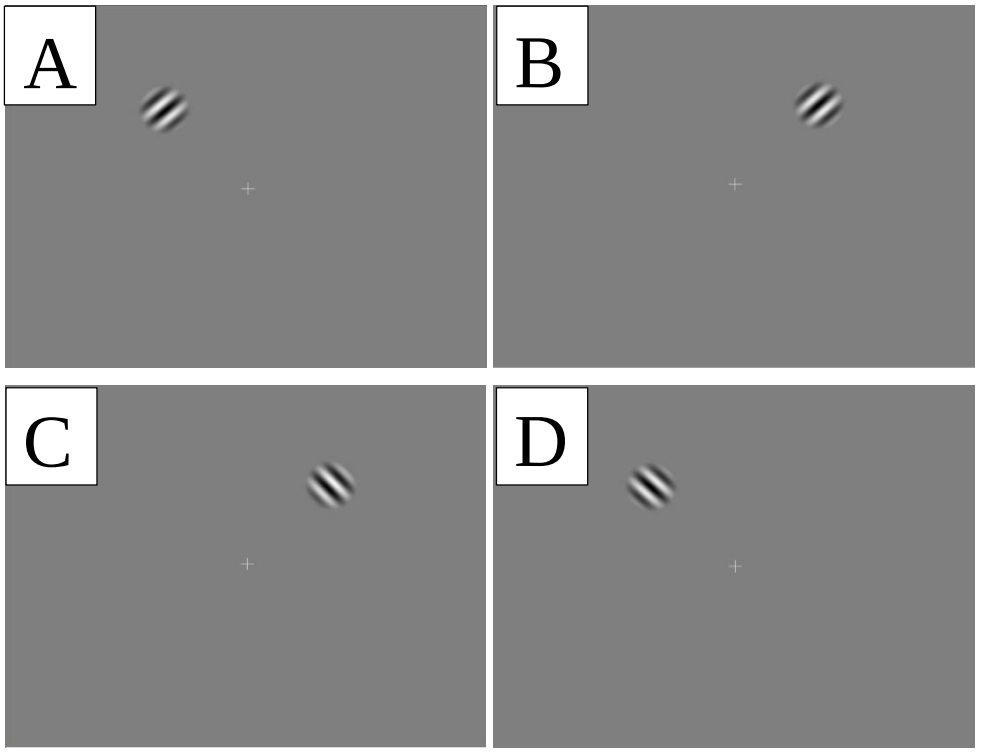

Figure 3-6 Position of luminance defined gratings at 9° (A) in the left tangential condition, (B) right radial condition, (C) right tangential condition and (D) left radial condition.

3.3 Results

In summary, the results presented in this chapter indicate that psychophysical performance in the motion defined boundary condition showed a greater level of anisotropy than the luminance defined condition. Orientation discrimination ability of a luminance defined grating was correlated weakly with cortical estimates of V2. Thresholds in the motion defined condition showed correlations with cortical estimates of V3A, V4, LO1 and LO2.

3.3.1 Psychophysical Measurement of Luminance Defined Boundary Orientation Discrimination

Each participant performed each condition (radial and tangential) of the discrimination task 3 times at each eccentricity; a mean was computed from these 3 values. For each participant in each visual field, 4 average thresholds were obtained. 3 participants performed the task in the right visual field only. 6 Participants performed the task in both the right and left visual fields. Left and right visual fields were treated as independent data points.

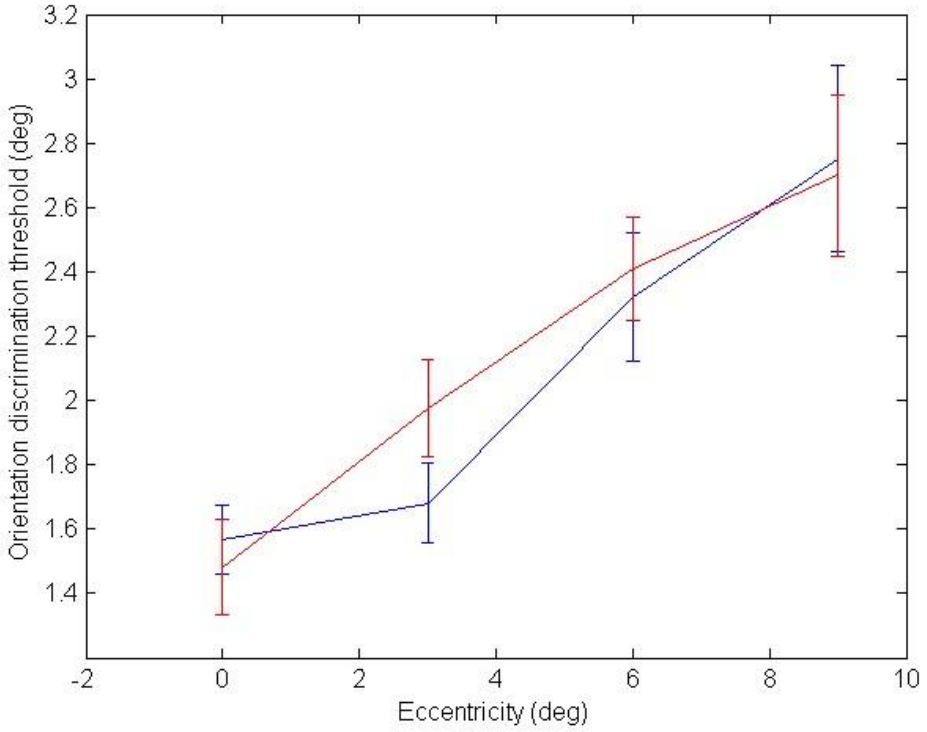

Figure 3-7 Average discrimination thresholds (25 hemifields) in an orientation discrimination task with luminance defined boundary stimuli. Tangential in red and radial in blue. Standard errors shown.

Figure 3-7 indicates a clear eccentricity effect in orientation discrimination performance, with little difference between radial and tangential conditions. A 2 way ANOVA was performed to examine the effects of condition (radial or tangential) and eccentricity (0°, 3°, 6° or 9°). The main effect of eccentricity indicated in figure 3-7 was statistically

significant (F (3,192) =16.31, p<.001). Planned contrasts indicated a significant difference between thresholds at 3° and 6° (p<.01). There was no main effect of condition (F (1,192) =0.21, p=.65), participants performed equally well the tangential and radial condition. There was no significant interaction between eccentricity and condition (F (3,192) =0.42, p=.74). Despite the lack of difference between tangential and radial conditions, the 2 conditions will still be examined separately in subsequent analyses to ensure consistency with the motion defined orientation discrimination task analyses and allow comparison between tasks.

3.3.2 The Relationship between Luminance Defined Boundary Orientation Discrimination and Cortical Parameters

Measures of radial cortical magnification were submitted to a series of linear regressions to predict thresholds in the luminance defined boundary orientation discrimination task (radial condition). One regression was performed for each of the functions. As for the radial psychophysical thresholds, radial cortical magnifications measures were submitted to a linear regression to predict tangential thresholds. Again, a linear regression for each function was computed. Eccentricity was included as a covariate in all linear regressions to remove this source of variance. Analogously to radial cortical magnification, polar cortical magnification was used to predict thresholds in both the radial and tangential psychophysical condition. Any significant predictors identified in these regressions were further explored through correlations at specific eccentricities.

A constraining role for size measures (e.g. the surface area, radial distance and polar width of maps) was also investigated. A series of bivariate correlations were performed to compare thresholds in both psychophysical conditions to radial distance, polar width and surface area. Again, significant links were further investigated at individual eccentricities.

Following the main analysis, the effect of power was explored. Radial and tangential psychophysical thresholds were combined and this measure (radial- tangential threshold) was examined for correlations with cortical magnification and size parameters. Generally, this secondary analysis produced results similar to the primary analysis. In this way, it

was confirmed that the lack of relationships in the main analysis was not due to insufficient power.

3.3.2.1 V1 Retinotopic Measures Did Not Correlate with Orientation Discrimination of Luminance Defined Boundary Stimuli

V1 cortical magnification did not correlate with performance in the luminance condition of the orientation discrimination task. This link was absent in all 3 functions. For example, using the linear scaling function, radial cortical magnification predicted neither radial psychophysical threshold (p=.18) nor tangential thresholds (p=.59). Similarly, polar cortical magnification did not predict thresholds in the radial (p=.31) or tangential (p=.1) condition. Size measure of V1 were similarly poor predictors. Radial psychophysical threshold were not linked to V1 size (R=.03, p=.77), radial distance (R=-.14, p=.17) or polar width (R=-.08, p=.45). Performance in the tangential condition were also unrelated to size (R=.06, p=.54), radial distance (R=-.13, p=.21) and polar width (R=.02, p=.83).

3.3.2.1.1 Radial and tangential thresholds combined

As radial and tangential psychophysical thresholds were not statistically different, these values were combined and counted as independent data points to improve power. Using estimates taken from the linear scaling function, the combined threshold (radial-tangential threshold) did not correlate with either V1 radial (p=.51) or polar (p=.25) cortical magnification. Cortical magnification measures from the 2 other functions also showed no correlation. Similarly, the radial-tangential threshold was uncorrelated with V1 surface area (p=.59), radial distance (p=.77) and polar width (p=.08).

3.3.2.2 V2 Retinotopic Measures correlate with Orientation Discrimination of Luminance Defined Boundary Stimuli

Links between V2 and psychophysical thresholds were not significant, although many showed a trend towards significance. Both radial cortical magnification, and to a lesser extent polar cortical magnification, showed a non-significant trend towards predicting psychophysical performance in the luminance defined boundary orientation discrimination task. Using measures from the linear scaling function, V2 polar cortical magnification showed a non-significant trend towards predicting performance in the

tangential condition (B=.04, SE=.02, β=.65, T=1.874, p=.06). This link was lost at all specific eccentricities (0° R=.31, p=.14; 3° R=.12, p=.58; 6° R=.12, p=.56; 9° R=.19, p=.35). V2 polar cortical magnification from the linear scaling function did not predict thresholds in the radial condition (p=.21).

Similarly, V2 radial cortical magnification measures taken from the piecewise regression function showed a non-significant trend toward predicting performance in the tangential condition (B=-.05, SE=.02, β=-.19, T=-1.95, p=.06) but no link with radial psychophysical threshold (p=.52). The relationship between radial cortical magnification and tangential thresholds was present at only the highest eccentricities (0° R=-.41, p<.05; 3° p=.39; 6° p=.43; 9° R=-.43, p<.05; figure 3-8). Although there was an indication of a link at 0°, this was due solely to negative values (a result of the failure of the function to fit).

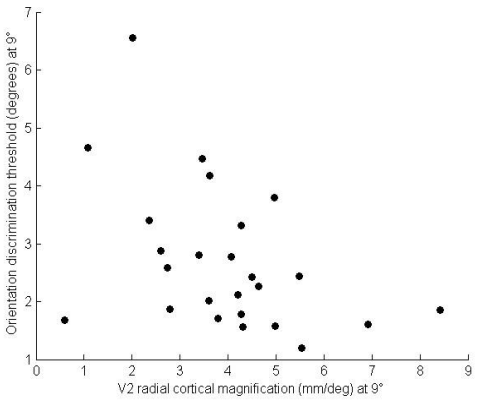

Figure 3-8 The relationship between radial cortical magnification (the piecewise regression function) in V2 at 9° eccentricity and psychophysical performance in an orientation discrimination task with luminance defined gratings (tangential condition) at 9° (p<.05). Each data point represents a single hemisphere at a single eccentricity patch.

Despite the multiple (but not significant) links between cortical magnification in V2 and psychophysical performance, no evidence of a predictive role for V2 size measures was identified. V2 surface area, radial distance and polar width predicted neither radial psychophysical performance (p=.68; p=.56; p=.19) nor the tangential condition (p=.54; p=.57; p=.9).

3.3.2.2.1 Radial and Tangential Thresholds Combined

To improve power, analyses were performed with radial and tangential thresholds combined. The links previously identified using the linear scaling function were not identified for either radial (p=.62) or polar (p=.15) measures. Links were also absent using measures taken from the other 2 functions. Surface area (p=.15), radial distance (p=.84) and polar width (p=.60) were uncorrelated with the radial-tangential threshold. This indicates that the correlation between polar cortical magnification and tangential thresholds (figure 3-8) are specific to orientation discrimination of tangentially presented stimuli.

3.3.2.3 LO2 Retinotopic Measures correlate with Orientation Discrimination of Luminance Defined Boundary Stimuli

Cortical magnification measures taken from multiple functions indicated a predictive role for LO2 polar cortical magnification in performance in the tangential psychophysical condition. This relationship was noted using the power function (B=.17, SE=.08, β=.45, T=2.11, p<.05). This link was seen at 3° (figure 3-9; R=.50, p<.05) 9° (figure 3-10; R=.59, p<.01). Although, examination of figure 3-9 indicates at this eccentricity the correlation is driven largely by an outlier. All relationship between LO2 polar cortical magnification and psychophysical performance suggested that high levels of cortical magnification were associated with high psychophysical thresholds (e.g. poor performance in the orientation discrimination task).

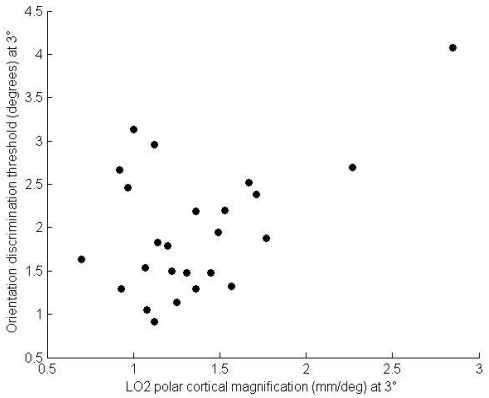

Figure 3-9 The relationship between polar cortical magnification (the power function) in LO2 at 3° eccentricity and psychophysical performance in an orientation discrimination task with luminance defined gratings (tangential condition) at 3° ($p<.05$). Each data point represents a single hemisphere at a single eccentricity patch.

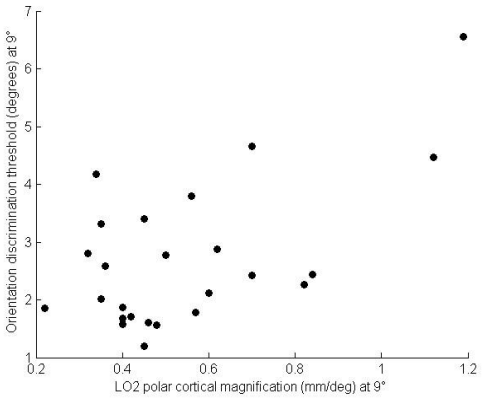

Figure 3-10 The relationship between polar cortical magnification (mm/deg; the power function) in LO2 at 9° eccentricity and psychophysical performance in an orientation discrimination task with luminance defined gratings (tangential condition) at 9° ($p<.01$). Each data point represents a single hemisphere at a single eccentricity patch.

Additionally, radial cortical magnification measures of LO2 taken from the piecewise regression function showed a trend towards predicting performancein the tangential condition (B=-.05, SE=.03, B=-.18, T=-1.92, p=.06). In conflict with the predictive role for polar LO2, participants with high levels of radial LO2 cortical magnification performed well in the orientation discrimination task. It is possible that the inverse predictive role for polar LO2 is driven by an intra-areal correlation with radial LO2 cortical magnification. Using the power function, participants with high levels of radial cortical magnification have low levels of polar cortical magnification (R=-.27, $p<.01$).

This link was also seen for the piecewise regression function measures (R=-.25, p<.05). It is hypothesised that the inverse link between psychophysical thresholds and LO2 polar cortical magnification is a result of this intra-areal link (e.g. high radial cortical magnification correlates both with low psychophysical thresholds and low polar cortical magnification. In this way, low polar cortical magnification and low psychophysical thresholds correlate but are not directly related).

Size measures of LO2 were poor predictors of psychophysical performance. Size, radial distance and polar width of LO2 did not correlate with either radial (p=.53, p=.07, p=.07) or tangential thresholds (p=.68, p=.2, p=.13).

3.3.2.3.1 Radial and Tangential Thresholds Combined

Increasing the power of the analysis through the use of the radial-tangential threshold revealed a stronger role for LO2. Using the piecewise regression function, thresholds were correlated with both radial (B=-.05, SE=.02, β=-.16, -2.53, p<.05) and polar (B=.36, SE=.17, β=.48, T=2.13, p<.05) cortical magnification. The opposing roles for cortical magnification in the 2 dimensions remained, good performance was correlated with high radial cortical magnification and low polar cortical magnification. Links between the psychophysical thresholds and LO2 size (p=.45) and polar width (p=.07) remained absent, but a correlation between thresholds and LO2 radial distance was identified (R=-.16, p<.05; figure 3-11). Large LO2 radial distance was associated with low thresholds (good performance). This link was lost at all eccentricities (0° p=93; 3° p=.71; 6° p=.09; 9° p=.28).

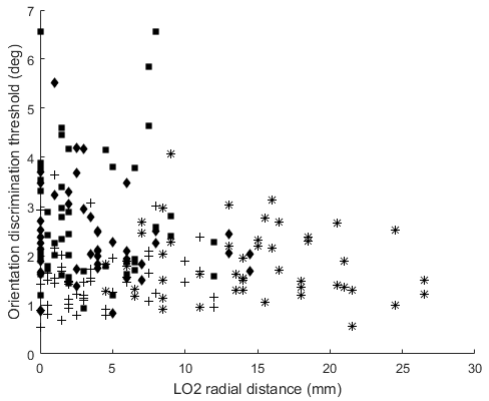

Figure 3-11 The relationship between LO2 radial distance (mm) and psychophysical performance in an orientation discrimination task with luminance defined gratings (radial-tangential combined; $p<.05$). Each data point represents a single hemisphere at a single eccentricity patch. Eccentricities are represented by different symbols (0°+; 3°*; 6°♦; 9°■).

3.3.2.4 Other Visual Areas and Orientation Discrimination of Luminance Defined Boundaries

No links were identified between any other visual area and psychophysical thresholds. Investigations were performed using all 3 functions but all relationships were not significant. For example, radial psychophysical thresholds could not be predicted from either the polar or the radial cortical magnification measures taken from the piecewise regression function (V3 p=64, p=.26; V3A p=.92, p=.416; V4 p=.45, p=.29; LO1 p=.19, p=.88). Similarly, tangential thresholds could not be predicted from either radial or polar cortical magnification (V3 p=.68, p=.81; V3A p=.92, p=.34; V4 p=.72, p=.94; LO1 p=.89, p=.66).

3.3.2.4.1 Radial and Tangential Thresholds Combined

The use of the radial-tangential threshold to improve power did not reveal any additional links between visual areas V3, V3A, V4 and LO1 and psychophysical data. For example, using the piecewise regression function neither radial cortical magnification (V3 p=.95; V3A p=.99; V4 p=.75; LO1 p=.38) nor polar cortical magnification (V3 p=.48; V3A p=.21; V4 p=.45; LO1 p=.67) correlated with the radial-tangential threshold.

In summary, performance in the orientation discrimination task using luminance defined stimuli is not strongly associated with any visual area. Weak links were identified between discrimination thresholds and cortical magnification in V2 and LO2. Figure 3-12 illustrates the similarities between the anisotropies of these areas in relation to the patterns seen the psychophysical data.

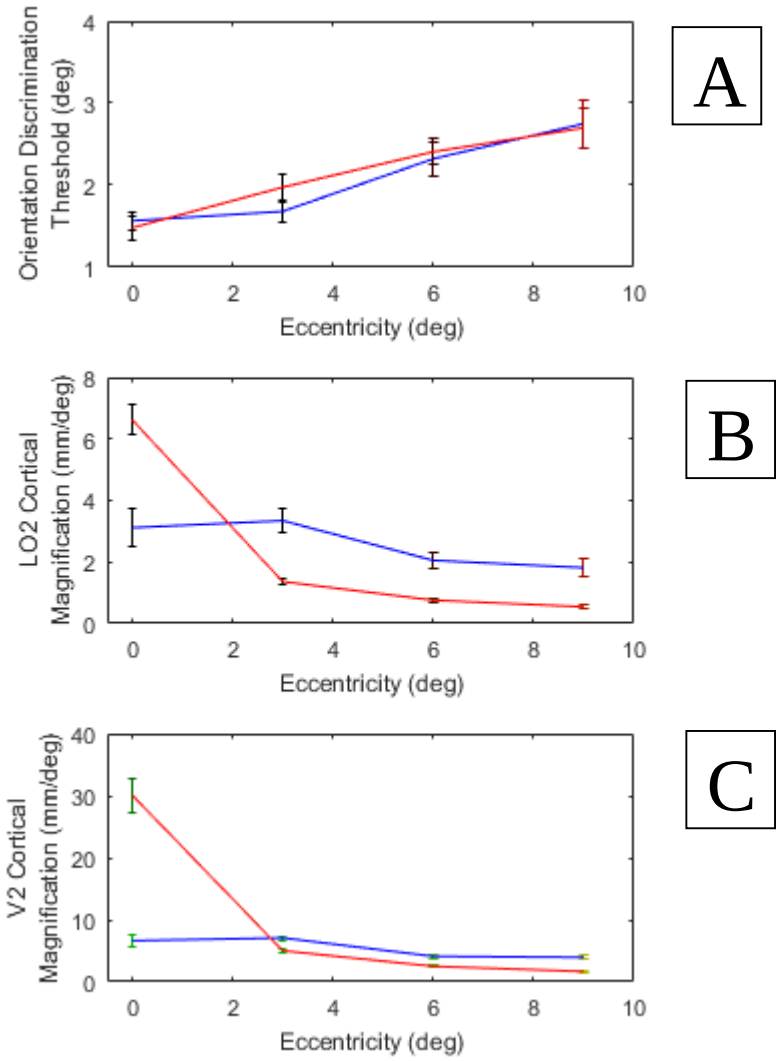

Figure 3-12 Psychophysical and cortical magnification (mm/deg) anisotropy. Average across 25 hemispheres. (A) Luminance defined boundary orientation discrimination thresholds. Tangential in red and radial in blue. Standard errors shown. (B) LO2 polar (red; the power function) and radial (blue; the piecewise regression function) cortical magnification. (C) V2 polar (red; linear scaling function) and radial (blue; piecewise regression function) cortical magnification. Negative data points not shown.

3.3.3 Psychophysical Measurement of Motion Defined Boundary Orientation Discrimination

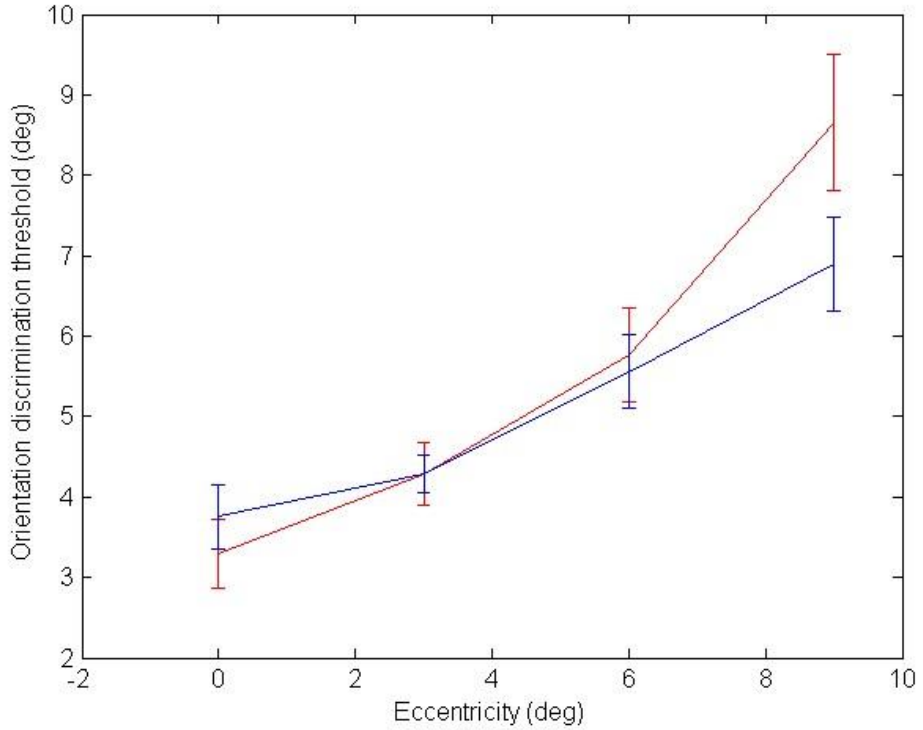

Figure 3-13 Average thresholds (15 hemifields) in an orientation discrimination task with motion defined boundary stimuli. Tangential in red and radial in blue. Standard errors shown.

Examination of figure 3-13 indicates a strong eccentricity effect in the psychophysical data, with higher thresholds at higher eccentricities. The effect of relative orientation appears more pronounced than in the luminance defined boundary data, particularly at higher eccentricities. A 2-way ANOVA was performed to investigate the effect of eccentricity (0°, 3°, 6° and 9°) and condition (radial and tangential) on psychophysical thresholds. There was a main effect of eccentricity ($F(3,112) = 26.05$, $p < .001$). Planned contrasts indicated a significant differences between 3° and 6° ($p < .05$) and between 6° and 9° ($p < .01$). There was no statistically significant main effect of condition ($F(1,112) = 1.079$, $p = .3$) and no interaction between eccentricity and relative orientation ($F(3,112) = 1.75$, $p = .16$). Although, consistent with the trend indicated in figure 3-13, a t-test indicated that there was a significant difference between radial and tangential thresholds at 9° ($p < .05$).

3.3.4 The Relationship between Motion Defined Boundary Orientation Discrimination and Cortical Parameters

Measures of radial cortical magnification were submitted to a series of linear regressions to predict thresholds in the luminance defined boundary orientation discrimination task (radial condition). One regression was performed for each of the functions. Generally only linear regressions with significant results are reported.

As for the radial psychophysical thresholds, radial cortical magnifications measures were submitted to a linear regression to predict tangential thresholds. Again, a linear regression for each function was computed. The relationship between polar cortical magnification and psychophysical thresholds was also investigated using a series of linear regression. As for radial cortical magnification, polar cortical magnification was used to predict thresholds in both the radial and tangential psychophysical condition.

3.3.4.1 V3A Retinotopic Measures correlate with Orientation Discrimination of Motion Defined Boundary Stimuli

Given the motion processing role of V3A (Larsson et al., 2010), correlations between retinotopic properties and psychophysical thresholds were expected in this visual area. Chapter 2 outlines the limitations of the cortical magnification functions in fitting V3A. The problems were particularly pronounced in the polar dimension, only the piecewise regression function sufficiently estimated this measure. Due to these issues, conclusions drawn from the analyses regarding V3A reported here must be tentative.

High levels of polar cortical magnification in V3A (measured using the linear scaling function) were associated with low thresholds ($B=-.03$, $SE=.01$, $\beta=-.33$, $T=-2.14$, $p<.05$). Participants with high levels of V3A polar cortical magnification performed well in the motion defined orientation discrimination task. The relationship was identified at only the lowest eccentricity (0° $R=-.53$, $p<.05$; 3° $p=.09$; 6° $p=.16$; 9° $p=.93$). This link was only seen for the radial psychophysical condition. No predictive role for polar cortical magnification was identified for performance in the tangential condition ($p=.66$). The piecewise regression function (which provides a superior estimate of polar cortical

magnification) showed no predictive role for V3A in either the tangential (p=.57) or radial condition (p=.56).

The presence of a link in the sub-optimal linear scaling function but not in the preferable piecewise regression function indicates that the links seen with psychophysical data do not represent a genuine relationship. The identification of the correlation at 0°, the eccentricity at which the linear scaling function gave the least coherent estimates (figure 2-12) supports this view. Additionally there is evidence that the correlation between polar cortical magnification and psychophysical thresholds is driven largely by negative outliers (a result of the failure of the function to fit). The link is lost when these negative values are removed (R=-.363, p=.38). However, examination of the polar width measurement of V3A demonstrated that large V3A polar width was linked to good performance in the radial condition (R=-.28, p<.05; figure 3-14) but not the tangential condition (R=-.1, p=.44). The consistency between size measures suggests that the cortical magnification correlation with V3A may have some level of reliability.

It is of interest that multiple hemispheres appear to have V3A polar widths of 0mm (figure 3-14). It is thought that this unexpected finding is a result of the non-perpendicular relationship between the radial and polar retinotopic maps in V3A. Unlike V1, V2 and V3, there is a high level of variability in the layout of the polar and radial maps in V3A. A non-perpendicular association between the radial and polar maps could lead to a measurement of 0mm.

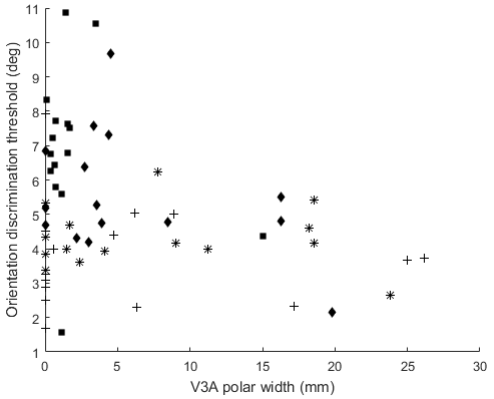

Figure 3-14 The relationship between polar width (mm) in V3A and psychophysical performance in an orientation discrimination task (radial condition) with motion defined boundaries ($p<.05$). Each data point represents a single hemisphere at a single eccentricity patch. Eccentricities are represented by different symbols (0°+; 3°*; 6°♦; 9°■).

Conversely, high levels of radial cortical magnification were linked to high thresholds. This unexpected pattern was seen across multiple functions. For both measures taken from the linear scaling function ($B=.06$, $SE=.03$, $\beta=.33$, $T=2.22$, $p<.05$) and the piecewise regression function ($B=.13$, $SE=.06$, $\beta=.24$, $T=2.05$, $p<.05$), participants with high levels of cortical magnification performed poorly in the radial condition of the psychophysical task. Measures taken from the linear scaling function indicated that this link was constrained to the lower eccentricities (0° $R=.57$, $p<.05$; 3° $R=.55$, $p<.05$; 6° $p=.18$; 9° $p=.66$; figure 3-15; figure 3-16). As indicated by figure 3-15, although the linear scaling function was generally successful at fitting V3A radial cortical magnification, a single negative data point was produced. The correlation between V3A radial cortical magnification and radial psychophysical thresholds remained following replacement of this data point with the mean of the remaining data points (0° $R=.56$, $p<.05$; 3° $R=.67$, $p<.01$).

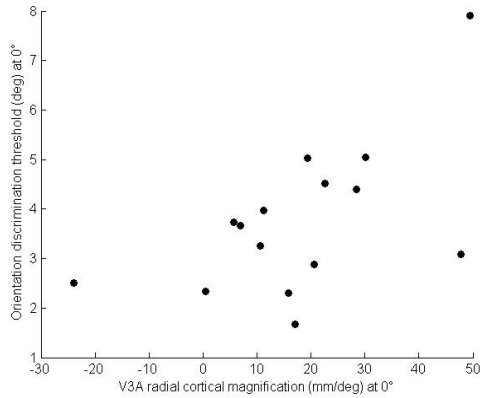

Figure 3-15 The relationship between radial cortical magnification (mm/deg; the linear scaling function) in V3A at 0° eccentricity and psychophysical performance in an orientation discrimination task with motion defined gratings (radial condition) at 0° ($p<.05$). Each data point represents a single hemisphere at a single eccentricity patch.

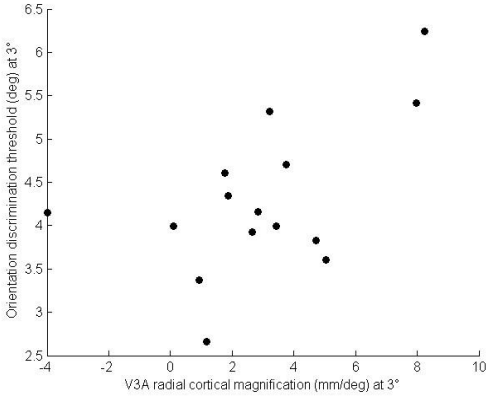

Figure 3-16 The relationship between radial cortical magnification (mm/deg; the linear scaling function) in V3A at 3° eccentricity and psychophysical performance in an orientation discrimination task with motion defined gratings (radial condition) at 3° ($p<.05$). Each data point represents a single hemisphere at a single eccentricity patch.

A similar link was not seen between tangential thresholds and cortical magnification measures from either the linear scaling function ($p=.55$) or the piecewise regression function ($p=.83$). Size measures of V3A were linked to orientation discrimination thresholds. Participants with a large V3A performed poorly in both the radial and tangential task conditions ($R=.55$, $p<.001$, figure 3-17; $R=.69$, $p<.001$, figure 3-18).

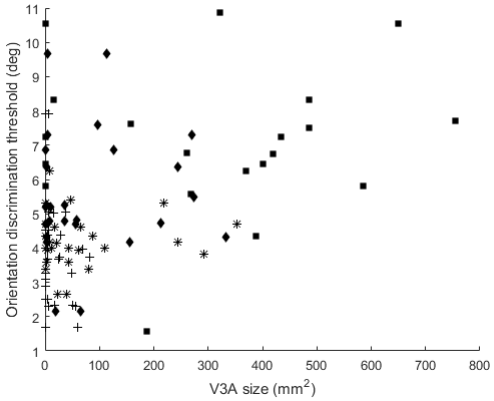

Figure 3-17 The relationship between V3A size (mm²) and psychophysical performance in an orientation discrimination task with motion defined gratings (radial condition; p<.001). Each data point represents a single hemisphere at a single eccentricity patch. Eccentricities are represented by different symbols (0°+; 3°*; 6°♦; 9°■).

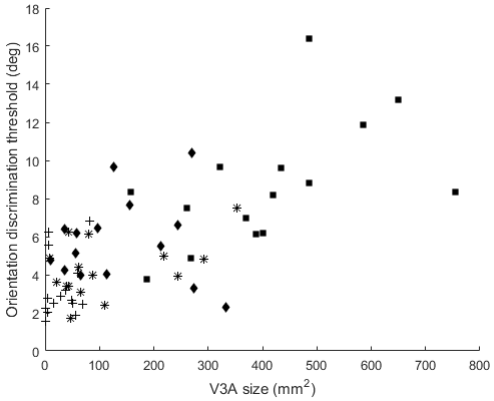

Figure 3-18 The relationship between V3A size (mm²) and psychophysical performance in an orientation discrimination task with motion defined gratings (tangential condition; p<.001). Each data point represents a single hemisphere at a single eccentricity patch. Eccentricities are represented by different symbols (0°+; 3°*; 6°♦; 9°■).

The conflicting roles for radial and polar cortical magnification in the constraint of psychophysical performance may be explained through examination of inter- and intra-areal correlations. Radial and polar measures obtained through the linear scaling function are inversely correlated for V3A. This is seen both across eccentricities (R=-.76, p<.001) and at specific eccentricities (0° R=-.92, p<.001; 3° R=-.92, p<.001; 6° R=-.92, p<.001; 9° R=-.92, p<.001).

3.3.4.1.1 Radial and Tangential Thresholds Combined

Despite the indication by figure 3-13, there was no statistically significant difference between radial and tangential thresholds. To improve power, radial and tangential thresholds were combined and the relationship between V3A and this variable was explored. Using values taken from the linear scaling function, both radial cortical magnification (B=-.15, SE=.05, β=-2.96, T=-2.96 p<.01) and polar cortical magnification (B=-.11, SE=.04, β=-.18, T=2.49, p<.05) correlated with the radial-tangential threshold. Whilst it is of interest that the increased power strengthens the results reported previously, it must be noted that the linear scaling function generally provided poor estimates of V3A polar cortical magnification. The more suitable function, the piecewise regression function, did not indicate any links between V3A cortical magnification and the radial-tangential threshold. The link between V3A size and thresholds remained (R=.62, p<.001). No significant correlations were seen between thresholds and V3A radial distance (p=.06) or polar width (p=.06), although trends were identified indicating that good performance was associated with small radial distance and large polar width. These trends mirror the previously documented opposing roles for radial and polar cortical magnification.

3.3.4.2 Retinotopic Measures of V4 correlate with Orientation Discrimination of Motion Defined Boundary Stimuli

An inverse relationship was also noted in V4 between cortical magnification levels and psychophysical performance. Participants with high levels of polar cortical magnification had higher thresholds in both the radial (figure 3-19; B=.22. SE=.09, β=.57, T=2.36, p<.05) and tangential conditions (figure 3-20; B=.27, SE=.13, β=.47, T=2, p<.05), using measures taken from the linear scaling function. The relationships between psychophysical performance and V4 could not be identified at specific eccentricities for either the radial condition (0° p=.89; 3° p=.26; 6° p=.58; 9° p=.98) or the tangential (0° p=.59; 3° p=.30; 6° p=.73; 9° p=.93). Figures 3-19 and 3-20 show unusual clustering around 0 and 15 mm/deg. There are very few polar cortical magnification measurements between 5 and 10 mm/deg. This mirrors the unexpected pattern seen in figure 2-20. As was explained in Chapter 2, it is though this characteristic is a result of methodological limitations that inaccurately inflate estimates of cortical magnification at cortex close to the foveal confluence.

Radial cortical magnification in this area showed no predictive role (p=.46; p=.71). The size data corresponds with these findings. Polar width was inversely correlated with tangential threshold (figure 3-21; R=.38, p<.01) and also radial thresholds (figure 3-22; R=.38, p<.01). Radial distance was not correlated with thresholds in either the radial (p=.11) or tangential condition (p=.3). In contrast to other parameters, the surface area size of V4 showed a positive relationship with psychophysical performance. Participants with a large V4 had lower thresholds in both conditions. This relationship was strongest for the radial condition (figure 3-23; R=-.29, p<.05), but a trend was also seen for the tangential condition (figure 3-24; R=-.23, p=.06).

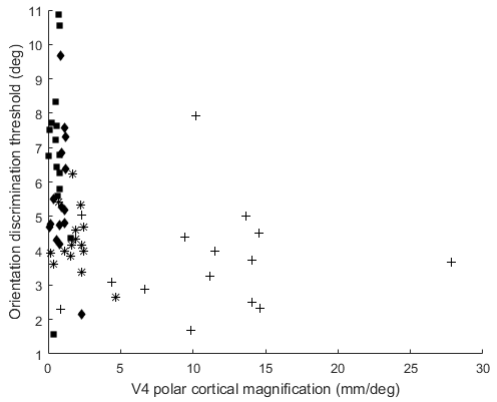

Figure 3-19 The relationship between polar cortical magnification (mm/deg; the linear scaling function) in V4 and psychophysical performance in an orientation discrimination task with motion defined gratings (radial condition; p<.05). Each data point represents a single hemisphere at a single eccentricity patch.

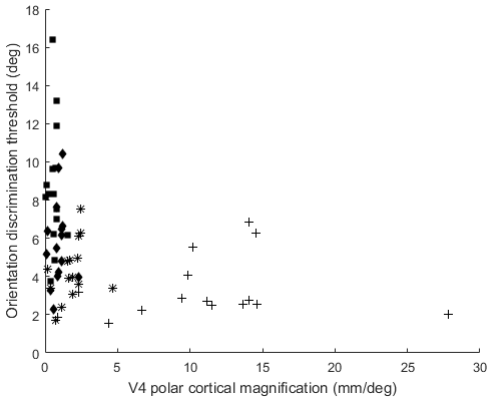

Figure 3-20 The relationship between polar cortical magnification (mm/deg; the linear scaling function) in V4 and psychophysical performance in an orientation discrimination task with motion defined gratings (tangential condition; $p<.05$). Each data point represents a single hemisphere at a single eccentricity patch. Eccentricities are represented by different symbols (0°+; 3°*; 6°♦; 9°■).

Given the lack of correspondence between the predictive role for V4 cortical magnification and the size measures of V4, it is possible that the inverse link between orientation discrimination and V4 cortical magnification is due to an inter-areal correlation (e.g. the link between polar cortical magnification and thresholds in indirect and not predictive). However, V4 polar cortical magnification taken from the linear scaling function did not inversely correlate with any visual area thought to constrain this task (V3A polar $p=.17$; LO1 radial $R=.29$, $p<.05$; LO2 polar $R=.57$, $p<.001$).

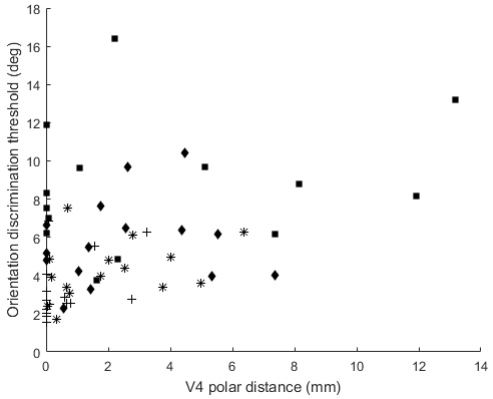

Figure 3-21 The relationship between polar width (mm) in V4 and psychophysical performance in an orientation discrimination task with motion defined gratings (tangential condition; p<.01). Each data point represents a single hemisphere at a single eccentricity patch.

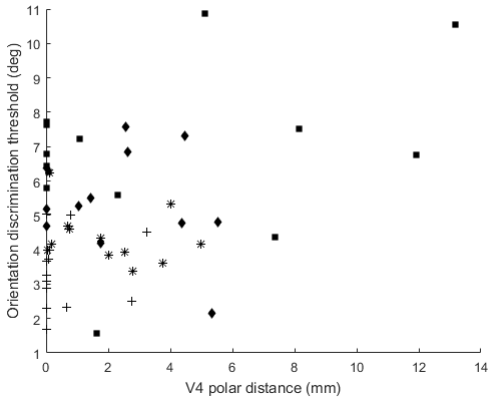

Figure 3-22 The relationship between polar width (mm) in V4 and psychophysical performance in an orientation discrimination task with motion defined gratings (radial condition; p<.01). Each data point represents a single hemisphere at a single eccentricity patch. Eccentricities are represented by different symbols (0°+; 3°*; 6°♦; 9°■).

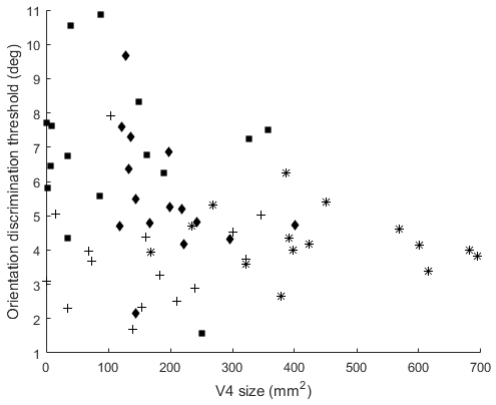

Figure 3-23 The relationship between V4 size (mm²) and psychophysical performance in an orientation discrimination task with motion defined gratings (radial condition; p<.05). Each data point represents a single hemisphere at a single eccentricity patch. Eccentricities are represented by different symbols (0°+; 3°*; 6°♦; 9°■).

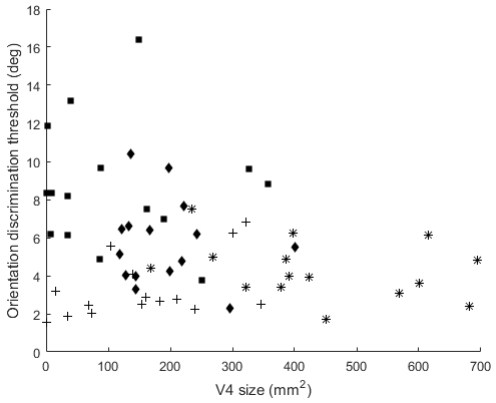

Figure 3-24 The relationship between V4 size (mm²) and psychophysical performance in an orientation discrimination task with motion defined gratings (tangential condition; p=.06). Each data point represents a single hemisphere at a single eccentricity patch. Eccentricities are represented by different symbols (0°+; 3°*; 6°♦; 9°■).

3.3.4.2.1 Radial and Tangential Thresholds Combined

Increasing the analysis power did not alter the results regarding V4. Using the linear scaling function, a correlation between V4 polar cortical magnification and radial-tangential thresholds was identified (B=1.28, SE=.19, β=.99, T=6.81, p<.001). The direction of this correlation was consistent with the previous analysis, high cortical magnification was associated with poor performance.

Radial cortical magnification remained unrelated to psychophysical performance. For example, using the linear scaling function no link was seen ($p=.53$). The links between thresholds and V4 surface area ($R=-.26$, $p<.01$) and V4 polar width ($R=.23$, $p<.05$) remained consistent with the previous analysis. No correlation was identified between radial-tangential thresholds and V4 radial distance ($p=.87$).

3.3.4.3 LO1 and LO2 Retinotopic Measures correlate with Orientation Discrimination of Motion Defined Boundary Stimuli

LO1 polar cortical magnification measures obtained using the piecewise regression function predicted tangential thresholds ($B=1.45$, $SE=.49$, $\beta=.77$, $T=3$, $p<.01$). Although figure 3-25 indicates that participant with high levels of LO1 polar cortical magnification performed well in the psychophysical task (they obtained low thresholds), the linear regression indicates that once the effect of eccentricity is removed this link reverses. This link reached significance only at 3° and was largely a result of negative values resulting from the failure of the function to fit (0° $p=.12$; 3° $R=.54$, $p<.05$; 6° $p=.59$; 9° $p=.06$). Polar cortical magnification did not predict radial thresholds ($p=.07$). LO1 radial cortical magnification did not predict performance in either condition ($p=.38$, $p=.99$).

LO2 polar cortical magnification measures taken from the linear scaling function predicted radial thresholds but not tangential thresholds ($B=-.09$, $SE=.04$, $\beta=-.37$, $T=-2.22$, $p<.05$; $p=.87$). Participants with high levels of LO2 polar cortical magnification performed well in the task. The link between polar cortical magnification and radial thresholds was seen at eccentricities of 3° ($R=-.55$, $p<.05$; figure 3-26) and 6° ($R=-.54$, $p<.05$; figure 3-27) but not 0° ($p=.41$) or 9° ($p=.53$). Radial cortical magnification did not predict psychophysical performance ($p=.95$; $p=.99$).

The size measures of these visual areas support the argument that LO1 and LO2 constrain psychophysical performance, particularly in the radial condition. LO1 size correlated with radial ($p<.05$; figure 3-28) but not tangential thresholds ($p=.09$). LO2 size did not predict performance ($p=.06$).

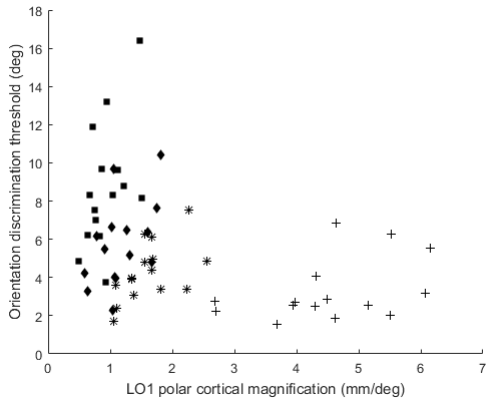

Figure 3-25 The relationship between LO1 polar cortical magnification (mm/deg; the piecewise regression function) and motion defined orientation discrimination thresholds (tangential thresholds; $p<.01$). Each data point represents a single hemisphere at a single eccentricity patch. Eccentricities are represented by different symbols (0°+; 3°*; 6°♦; 9°■). Negative values are not shown.

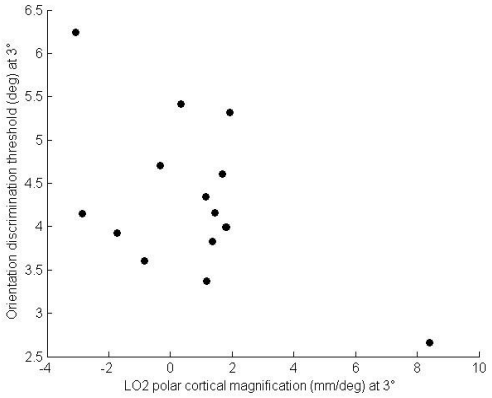

Figure 3-26 The relationship between polar cortical magnification (mm/deg; the linear scaling function) in LO2 at 3° eccentricity and psychophysical performance in an orientation discrimination task with motion defined gratings (radial condition) at 3°($p<.05$). Each data point represents a single hemisphere at a single eccentricity patch.

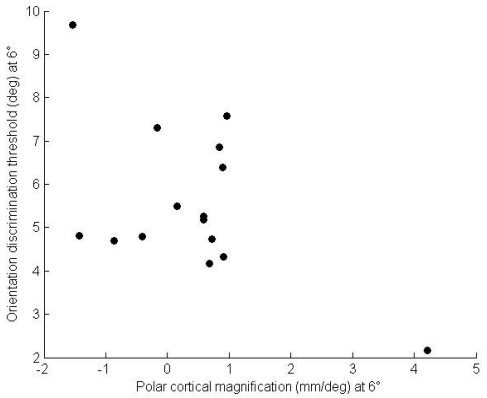

Figure 3-27 The relationship between polar cortical magnification (mm/deg; the linear scaling function) in LO2 at 6° eccentricity and psychophysical performance in an orientation discrimination task with motion defined gratings (radial condition) at 6° ($p<.05$). Each data point represents a single hemisphere at a single eccentricity patch.

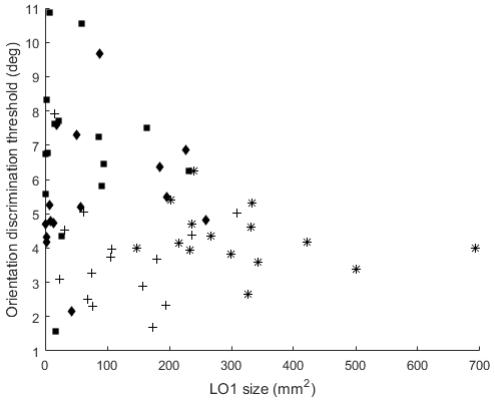

Figure 3-28 The relationship between LO1 size (mm^2) and psychophysical performance in an orientation discrimination task with motion defined gratings (radial condition; $p<.05$). Each data point represents a single hemisphere at a single eccentricity patch. Eccentricities are represented by different symbols (0°+; 3°*; 6°♦; 9°■).

3.3.4.3.1 Radial and Tangential Thresholds Combined

As before, radial and tangential psychophysical thresholds were combined to explore the effect of increased analysis power. The results for LO2 did not change following the increase in power. Polar cortical magnification values taken from the linear scaling function correlated with the radial-tangential thresholds ($T=-.29$, $SE=.14$, $\beta=-.24$, $T=-2.12$, $p<.05$) and radial cortical magnification values did not ($p=.15$). Similarly, the link between LO2 surface area and psychophysical thresholds remained absent ($p=.17$).

The relationship between LO1 and psychophysical data was effected by the increase in power. Unlike the previous analysis which identified a link between LO1 polar cortical magnification and tangential thresholds, using polar cortical magnification measures taken from the piecewise regression function LO1 did not correlate with the radial-tangential thresholds ($p=.67$). Conversely, a link between LO1 radial cortical magnification and radial-tangential thresholds was identified following the increase in power ($B=.32$, $SE=.07$, $\beta=.35$, $T=4.59$, $p<.001$). High levels of radial cortical magnification were correlated with high thresholds (poor performance).The link was present at only a single eccentricity (0° $p=.06$; 3° $p=.06$, 6° $R=.801$, $p<.001$, 9° $p=.07$). The link between LO1 size and psychophysical performance was lost following the merging of radial and tangential conditions ($p=.65$).

3.3.4.4 Other Visual Areas and Orientation Discrimination of Motion Defined Boundaries

All visual areas were explored for links with psychophysical thresholds. Other than the relationships of V3A, V4, LO1 and LO2 described above, no correlations were identified. Analyses were performed with all 3 functions, here results using the piecewise regression function are reported for illustrative purposes. Radial cortical magnification predicted neither radial nor tangential thresholds (V1 $p=.41$, $p=.33$; V2 $p=.77$, $p=.83$; V3 $p=.63$, $p=.58$). Similarly, polar cortical magnification did not predict radial and tangential thresholds (V1 $p=.92$, $p=.42$; V2 $p=.84$, $p=.49$; V3 $p=.69$, $p=.42$).

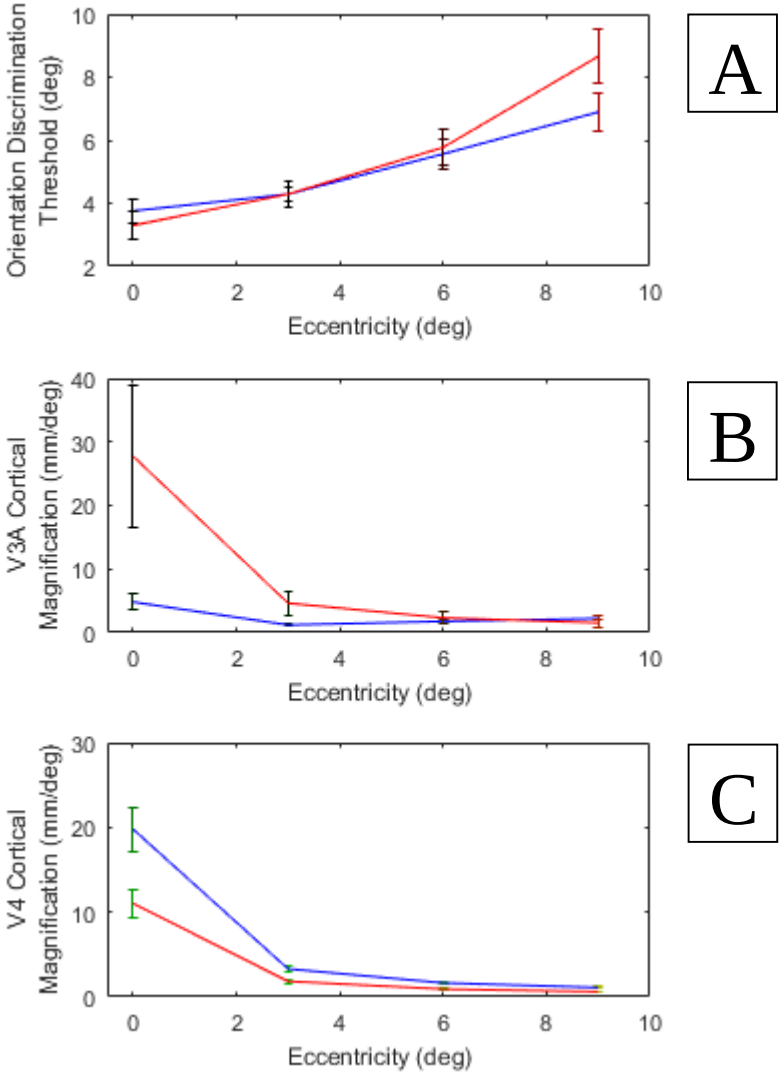

Figure 3-29 Psychophysical and cortical magnification (mm/deg) anisotropy. Average across 15 hemispheres. (A) Motion defined boundary orientation discrimination thresholds. Tangential in red and radial in blue. Standard errors shown. (B) V3A radial (blue; the piecewise regression function) and polar (red; the linear scaling function) cortical magnification. Standard errors shown. (C) V4 radial (blue) and polar (red) cortical magnification (the linear scaling function). Standard errors shown. Negative data points not shown.

3.4 Discussion

3.4.1 Key findings

Performance in a motion defined boundary orientation discrimination task, but not a luminance defined orientation discrimination task, was constrained by cortical magnification in motion sensitive areas. The direction of these correlations were inconsistent, unexpectedly in some cases high cortical magnification was associated with poor performance. This finding extends the work of Duncan and Boynton (2003), demonstrating that the constraining role for cortical magnification is also present in intermediate visual areas. The link between low level visual abilities and V1 (Duncan & Boynton, 2003) was not replicated here. Performance in the luminance defined orientation task was constrained primarily by V2 polar cortical magnification and this link was weak.

Whilst large inter-individual variability exists both in retinotopic properties of the visual areas measured here (Chapter 2) and performance in both orientation discrimination tasks (Chapter 3), these measures do not strongly correlate. It is likely that Duncan and Boynton (2003) found a stronger role for cortical magnification than was identified in the data presented here because they used a simpler task. The data presented in this chapter strongly indicates that the constraining role of cortical magnification in the visual cortex is less universal than was predicted. Conversely, the high intra-individual variability identified in both the cortical and psychophysical measures correlated strongly. In all analyses, the common effect of eccentricity was dominant and had to be removed before any other links were visible. The differences in performance between foveal and peripheral vision were correlated with the decrease in cortical magnification with movement towards the periphery. The intra-areal variability in perception was correlated with cortical magnification.

3.4.2 Anisotropy in Orientation Discrimination

For the motion defined condition, the psychophysical data displayed a clear eccentricity effect and also a trend towards higher thresholds (poorer performance) for tangential than radially oriented gratings. The eccentricity effect, that participants have better discrimination abilities when stimuli are presented at the centre of the visual field, is well established (Duncan & Boynton, 2003). The meridian-relative anisotropic effect, that performance is increased when the orientation of a stimulus matches its position in visual space, is also found in previous studies (Westheimer, 2005).

Additionally, the anisotropic trend increased at higher eccentricities. This increase corresponds with the findings of Rovamo et al. (1982). Rovamo and colleagues indicated that whilst the oblique effect was predominant at lower eccentricities, at higher eccentricities the meridian-relative anisotropic effect dominated. Rovamo et al. (1982) proposed that this change occurred at 20 degrees eccentricity, whilst the introduction of anisotropy occurred in this study at much lower eccentricities. This discrepancy may be due to different stimuli, Rovamo et al. (1982) used stationary gratings. The stationary luminance gratings used in the experiment reported here (e.g. the luminance defined boundary stimuli) also do not show a meridian-relative effect at these eccentricities.

Unlike in the motion defined condition, there was no anisotropy identified in the psychophysical thresholds for luminance defined gratings. Performance in the radial and tangential conditions was equal at all eccentricities. This disparity may be explained with reference to the hypothesized underlying cortical processes. As previously outlined, cortical anisotropy is expected to be greater at V3A than V1 and V2 based on the general pattern within the visual system (Larsson & Heeger, 2006; Roe & Ts'o, 1995). It is proposed that the motion task shows a greater difference in radial and tangential thresholds because it is reliant upon V3A, which has a high level of cortical anisotropy. Conversely, V1 has been identified in previous research (Duncan & Boynton, 2003) as the location of luminance defined boundary perception. V2, an area with similarly low levels of anisotropy, was found to constrain luminance defined orientation discrimination here.

On the other hand, few anisotropy based relationship were identified between cortical magnification and psychophysical conditions. It was hypothesised that dimensions of cortical magnification would be paired specifically and exclusively to the psychophysical orientation conditions. Radial cortical magnification would preferentially constrain either tangential thresholds or radial thresholds and polar cortical magnification would constrain the other. In fact, almost none of the links identified between cortical magnification and psychophysical thresholds showed the predicted anisotropy pattern. Generally, polar cortical magnification predicted thresholds in both the radial and tangential conditions.

The stronger predictive role for polar cortical magnification than radial is novel. Polar cortical magnification predicted performance in the motion defined boundary task. Any links with radial cortical magnification were attributed to the inverse correlation between radial cortical magnification and polar cortical magnification. It is argued that polar cortical magnification constrains performance because levels of polar cortical magnification are lower than radial, particularly in V3A. Although there is disagreement about the precise level of cortical anisotropy (Polimeni et al., 2006), generally later visual areas have higher overrepresentation of visual space in the radial direction. This finding is replicated in the data presented here (Chapter 2). Interestingly, the link between V3A polar cortical magnification and task performance is strongest at the lowest eccentricity. Chapter 2 (figure 2-14) indicate that polar differs from radial cortical magnification most greatly at the lowest eccentricity.

It is likely that cortical magnification is only a predictor of visual ability when overall levels of cortical magnification are low. Once cortical magnification reaches a critical level, any additional representation of visual space does not further improve ability. This explanation would also inform understanding of the failure to find any predictive role in other visual areas. Measures of cortical magnification in both the radial and polar cortical magnification of all other areas were higher than the estimates of V3A polar cortical magnification. Performance can be limited by an insufficient number of orientation-tuned neurons, but once a certain level is reached additional neurons do not further improve performance.

A clear and direct cortical basis for psychophysical anisotropy has not been identified here. Whilst there appears to be a broad link between the anisotropy of retinotopic areas

and the psychophysical tasks reliant on these areas, a specific mechanism cannot be proposed. It is likely that additional variables not measured here mediate the link between cortical anisotropy and impaired performance in the tangential condition.

3.4.3 Luminance Defined Boundary Orientation Discrimination

V2 polar cortical magnification constrained luminance defined boundary orientation discrimination. The involvement of this visual area was not expected, but is also not unprecedented. Edge detection is thought to occur in V2. Single cell recordings made in macaque V2 demonstrated that this area has orientation selectivity similar to that of V1, but greater contrast sensitivity than the earlier region. (Levitt, Kiper, & Movshon, 1994). The involvement of V2 in edge detection has also been identified in humans (Elder & Sachs, 2004).

Duncan and Boynton (2003) found that acuity of a luminance defined grating was constrained by V1 cortical magnification. The finding that a task dependent on V1 is constrained by cortical magnification in this area is not replicated here, despite similarities in the function used to compute cortical magnification. Correlations were also absent between size measures of the visual areas, such as surface area size, radial distance and polar width. This indicates that the absence of a link was not due to a failure of the 3 functions to fit the data.

Again, it appears that the prediction based on the findings of Duncan and Boynton (2003; 2007) over emphasised the role of cortical magnification as a constraining factor on sensory abilities. Recent attempts to replicate a group of studies showing a link between brain and behaviour have been unsuccessful. Boekel et al. (2015) repeated 5 correlational studies. The authors considered experiments from a variety of fields, including degree of distractibility, social network size and accuracy in perceptual decision making. MRI measures included cortical thickness (Westlye, Grydeland, Walhovd, & Fjell, 2011), tract strength (Forstmann et al., 2010), grey matter strength (Kanai, Bahrami, Roylance, & Rees, 2012; Kanai, Dong, Bahrami, & Rees, 2011) and diffusion measures of white matter pathways (Xu et al., 2012). The failure of the direct replications of Boekel et al.

(2015) indicate that the strong evidence for brain- behaviour links may be due to high proportion of false-positive findings.

Boekel et al. (2015) did not attempt to replicate any experiments addressing the cortical constraints on visual ability, although the criticisms made by the authors would be similarly applicable to this field. It should be noted that retinotopy has been shown by Schwarzkopf and Rees (2013) to be a more robust parameter from which to predict behavioural ability than the parameters used in the experiments Boekel et al. (2015) failed to replicate.

The psychophysical task used here was not directly analogous to the task found by Duncan and Boynton (2003) to be constrained by V1 cortical magnification. The previous study measured participant acuity. In the study reported here, orientation discrimination ability was measured. Although V1 is also thought to process stimuli of this type, the neural underpinnings of orientation discrimination differ. The link between retinotopy and acuity is clearly understood, the amount of cortex dedicated to the processing of each point in in the visual field affects the clarity of perception. Conversely, how the retinotopic parameters relate to orientation discrimination is unclear.

It has been argued that orientation perception is processed by an orientation map (Freeman, Brouwer, Heeger, & Merriam, 2011) which is separate from the retinotopic maps used here. The procedures of Freeman et al. (2001) were similar to the retinotopic mapping used here, but the stimulus was a large sinusoidal grating of various orientations. A topographic map of the orientation preferences of the cortex within V1 was established. If orientation perception is dependent on the orientation map rather than the retinotopic, cortical magnification would be expected to constrain performance. It would be of interest to explore the relationship between the parameters of the orientation map in V1 and performance in orientation perception psychophysical tasks. It is possible that as parameters of the retinotopic maps constrain acuity, parameters of the orientation maps limit perceptual abilities relating to orientation discrimination.

Freeman et al. (2011) present orientation maps with a radial bias. This bias is clearest in the periphery. The authors fail to identify this bias in more foveal locations, but argue that this failure should not be interpreted as confirmation of their absence. This radial bias is

difficult to integrate with the psychophysical data from the luminance defined orientation discrimination task seen here. If dependent on the orientation maps, the thresholds for the radially presented orientations would be expected to be lower than the tangentially presented stimuli, particularly at higher eccentricities. It is possible that the psychophysical performance is determined by a variety of factors, including the topographic organisation of both the retinotopic and orientation maps.

3.4.4 Motion Defined Boundary Orientation Discrimination

As expected, it was found that V3A correlated with performance in the motion condition, but not the luminance condition. V3A has been shown to have a specific role in the processing of motion boundary stimuli (Larsson et al., 2010). This finding expands the work of Duncan and Boynton (2003). It demonstrates that cortical magnification in intermediate visual areas constrains perceptual abilities in an analogous way to the bottleneck role for V1. This role for V3A was seen in both the radial and polar dimensions. Due to the limitations of polar measures taken from this area (see Chapter 2), the radial measure is argued to be a more robust estimate.

Unexpectedly, the links between V3A and psychophysical data were in the opposite direction to that expected. As outlined in Chapters 1 and 2, it was hypothesised that a high number of neurons in the visual area processing the task stimulus (e.g. high cortical magnification in motion sensitive areas) would result in improved performance in the task. V3A polar cortical magnification demonstrated this link, although the data was limited by methodological issues. Conversely, the more robust measure of radial cortical magnification correlated inversely with performance. Additionally, the surface area size of V3A also correlated inversely.

It is unknown how reduced cortical representation would result in improved perception. A possible explanation for this finding is the intra-areal correlation of V3A, radial and polar cortical magnification in this area correlate inversely (figure 2-13). It is possible that the primary predictor of performance is V3A polar cortical magnification, high levels of polar cortical magnification correlate with good performance. High levels of polar cortical magnification also correlate with low levels or radial cortical magnification. In

this way, good performance and low levels of radial cortical magnification correlate without the implication of any causal relationship. Improved estimation of polar cortical magnification in V3A will allow a direct examination of this suggestion.

Although, speculation that accurate discrimination is correlated primarily with high levels of polar cortical magnification is inconsistent with the links identified between size measures of V3A and orientation discrimination thresholds. The surface area of V3A was strongly and robustly correlated with motion boundary defined discrimination abilities. Participants with large V3A surface area performed poorly in this task. This was seen across both relative orientation conditions. The surface area measures were not confounded by methodological limitation in the way measures of polar cortical magnification were. Additionally, the size estimates are consistent with previous studies (Larsson & Heeger, 2006). It can be concluded that the correlation between small V3A surface area and good performance is reliable. This finding also strengthens the correlation between low radial cortical magnification and good psychophysical performance.

The unexpected role for V3A size is difficult to integrate with previous literature which has documented a positive correlation between the size and cortical magnification of retinotopic areas and visual abilities (Duncan & Boynton, 2003). It is possible that for less simple tasks than those used by Duncan & Boynton (2003), additional mechanisms mediate the link between psychophysical performance and cortical parameters. For example, whilst acuity was critical for the task used by Duncan and Boynton (2003), spatial integration may be necessary for orientation discrimination of motion defined boundaries. Accurate orientation discrimination of the motion defined boundary stimulus used in this experiment requires both spatial and temporal integration (Watamaniuk, Sekuler, & Williams, 1989). The stimulus consists of multiple inter-mingled dots of different directions. To obtain a percept of the global motion, the visual system must integrate these inter-mingled directions over multiple simultaneously presented dots and over multiple frames (Watamaniuk & Sekuler, 1992).

It is argued that spatial integration is facilitated by a smaller surface area. Schwarzkopf et al. (2011) report that participants with large V1 surface area are less perceptually influenced by the presence of objects surrounding a target. This indicates that they do not

integrate the surrounding stimuli into their percept of the target object. It has been suggested (Song, Schwarzkopf, & Rees,2013) that as the size of a visual area increases, the intra-cortical connections do not increase at the same rate (Ringo, 1991), therefore resulting in the neurons of larger visual areas being less well interconnected (Kaas, 2000). The lower level of neuronal interconnections may result in weaker spatial integration, these properties have been linked through a comparison of psychophysical investigation and cat neurophysiology (Gilbert, Das, Ito, Kapadia, & Westheimer, 1996).

This speculated differentiation between the influence of a large surface area on acuity perception (e.g. Duncan & Boynton, 2003) and spatial integration (e.g. the motion defined boundary orientation discrimination task used here) is consistent with the findings of Song et al. (2013). Song et al. (2013) investigated individual differences in V1 size, visual acuity, and susceptibility to context modulation. Participants with small V1 size showed higher levels of fine orientation discrimination (an ability necessary for good performance in the task used by Duncan & Boynton), whilst participants with large V1 size showed greater levels of contextual modulation (an ability necessary for successful perception of coherent motion; Watamaniuk & Sekuler, 1992).

In addition to the constraining role for V3A, the link with motion defined orientation discrimination ability was also seen at other intermediate areas. Polar cortical magnification in LO1 and LO2 also constraining boundary discrimination. Although it was hypothesised that relationships with the psychophysical data would be focused on V3A, it is not unexpected to identify a role for LO1 and LO2 in the perception of motion boundaries (Larsson et al., 2010). Due to the close pairing between LO1 and LO2 outlined in Chapter 2 it is difficult to identify whether this correlation is driven more strongly by one of these 2 areas. Given that LO1 correlates with performance in an unexpected direction, it seems likely that the link with LO2 is the primary predictor. Unlike V3A, the correlations between LO2 cortical magnification and orientation discrimination thresholds were in the expected direction. High levels of cortical magnification and correlated with good performance.

A link between V4 and performance in the motion defined boundary orientation discrimination task was identified. Again, this link was consistently in the opposite direction to that hypothesised. Participants with high levels of polar cortical magnification

performed poorly in both the radial and tangential condition of the psychophysical task. Unlike the inverse links identified for other visual areas, the role for V4 could not be attributed to inter- or intra-areal correlations. It is possible that the unusual links with V4 are due to an inter- areal correlation with an area that was not mapped. MT plays a key role in the perception of motion (Born & Bradley, 2005). In the macaque, V4 has connections with MT (Maunsell & Van Essen, 1983). A similar intra-cortical projection has also been hypothesised to exist in humans (Schmid et al., 2013).

It is arguable that firstly, high levels of cortical magnification in MT correspond to good perception of motion defined boundaries and secondly, MT and V4 are inversely correlated in measures of cortical magnification. The combination of these 2 effects would be an indirect and inverse link between motion perception and V4 cortical magnification, such as the link seen in this experiment. This suggestion is highly theoretical, confirmation would require further understanding of the retinotopic properties of MT and its relationship with other cortical areas.

3.4.5 Conclusions

The results presented here have increased the understanding of the link between cortical magnification and perception. Expanding the work of Duncan and Boynton (2003), a constraining role was identified for V3A, LO1 and LO2 in the perception of motion boundaries. Methodological limitations in obtaining cortical magnification measures of V3A prevented full exploration of this role. Additionally, V2 was found to correlate with orientation discrimination of luminance defined boundaries. It has also been demonstrated that variance in perceptual differences, particularly inter-individual variance, cannot be fully explained by neuronal density. Whilst the constraining role for cortical magnification exists past V1, the importance of this parameter in explaining variance in visual abilities has previously been overstated.

4 Shape Matching Ability is correlated with LO1 Polar Cortical Magnification

4.1 Introduction

Shape perception is one of the most complex tasks performed by the visual system. It is reliant on multiple steps throughout the visual stream (Poirier & Wilson, 2006), with a hierarchy of processing stages (Van Essen, Anderson, & Felleman, 1992). Successful shape perception requires the convergence of multiple aspects of the visual stimuli. This pathway is thought to originate in the occipital cortex, but extend into the ventral and lateral temporal lobe (Grill- Spector, 2003). Given the complex nature of shape perception, it is thought to occur in intermediate and higher level visual areas including V4, VO1, VO2, LO1 and LO2. The involvement and specificity of these regions had been described to some extent although remains unclear.

The locus of shape perception, and the more complex and memory reliant task of object recognition, have traditionally been attributed to the lateral occipital cortex (LOC; Grill-Spector et al., 1998). This region is functionally defined as the cortical location of object processing; it shows greater activation during the presentation of objects than during the presentation of scrambled images (Malach et al., 1995). Retinotopic mapping of this area has progressed slowly. Some have thought it to be less retinotopic than lower-tier visual areas. It has been argued that an eccentricity bias exists but a polar map is absent (Levy, Hasson, Avidan, Hendler, & Malach, 2001; Tootell & Hadjikhani, 2001; Tyler et al., 2005).

LOC was found to be somewhat modular, with different location within the complex responding to different aspects of the object. Given the complex nature of object recognition and the relatively large size of the region, this subdivision is not surprising. The anterior part of LOC was found to be more invariant to changes in object size and position than the posterior part (Grill-Spector et al., 1999; Sawamura, Georgieva, Vogels, Vanduffel, & Orban, 2005). Invariance to perspective is a necessity of object recognition, so this differentiation suggests that it may be the anterior part of LOC that underlies the

completion of object recognition, whilst the posterior regions play an accessory and preliminary role. This dissociation was supported by Stanley and Rubin (2005). They proposed that the posterior lateral part of LOC was required for processing abstract 2D shapes and familiar shapes, whilst the anterior ventral portion was activated only for familiar objects.

In recent years the retinotopy of LOC has been better defined, and previous failures to identify both orderly eccentricity and polar representations rectified (Larsson & Heeger, 2006). Multiple maps have been identified within LOC (Brewer & Barton, 2012) including LO1 and LO2. The advances in retinotopic understanding has aided the differentiation of LOC regions and indicated that it may be more appropriate to consider LOC a conglomerate of multiple regions rather than a single visual area (Larsson & Heeger, 2006).

4.1.1 The Role of LO1 and LO2 in Shape Perception

Larsson and Heeger (2006) investigated the retinotopic nature of LOC and identified 2 maps each possessing a full representation of the polar dimension of the visual field. LO1 and LO2 are adjacent maps in the posterior part of LOC. They share a foveal representation with V1, V2 and V3. LO1 shares a representation of the lower meridian with V3d and a representation of the upper meridian with LO2. LO2 is proximal to MT but does not extend into this region. In conflict with the previous suggestion, both an eccentricity and polar angle representation were identified. However, unlike other regions (Wandell, 1999), the polar angle and eccentricity maps are not orthogonal to one another. LO1 and LO2 are similar in size to one another, both approximately half the width of V1.

Individual differences in the sample used by Larsson and Heeger (2006) were high. 23% of hemispheres studied did not display LO1 and LO2 with standard retinotopic patterns. Despite stating that a full polar map was characteristic of these areas (Larsson & Heeger, 2006), only half of the participants showed a full representation of the contralateral visual field. In fact, 3 of the 30 hemispheres measured contained LO2 with only half the normal representation. Furthermore, the location of these maps was inconsistent, a finding attributed to the high variability in sulci surrounding LOC (Duvernoy, 1991). The

majority of these individual differences were attributed to methodological issues. Although given the confirmed variability of lower tier regions (Duncan & Boynton, 2003), it seems likely that at least a portion of the differences identified here reflected genuine inter-individual variability.

LO1 and LO2 are located in the posterior region on LOC. Functional investigations have identified this area of the cortex as correlating with perception of abstract 2D shapes and showing sensitivity to changes in object size (Kushnir, Grill-Spector, Mukamel, Malach, & Itzchakl, 1999; Sawamura et al., 2005; Stanley & Rubin, 2005). In other words, LO1 and LO2 are found in the region of LOC that is not the locus of object recognition but may play a role in shape perception.

The investigation of Larsson and Heeger (2006) further subdivided the posterior region of LOC, with LO1 and LO2 proposed to serve similar but functionally specific roles. LO1 showed selectivity for orientation, whilst LO2 was relatively orientation invariant (Larsson, Landy, & Heeger, 2006). LO2 also showed more responsiveness to objects. Whilst both LO2, and to a lesser extent LO1, showed indications of a role in object perception, neither region displayed the invariance to image transformation required for full object recognition (Larsson & Heeger, 2006). Larsson and Heeger (2006) suggested that the posterior portions of LOC, including LO1 and LO2, may extract complex shape information whilst the anterior portion performed the higher level function of object recognition. In this way, LO1 and LO2 are best described as intermediate visual processing regions.

The use of improved retinotopy methodology has allowed segmentation and understanding of functional specialisation in a region previously discussed as a single unit (Larsson & Heeger, 2006). This has aided understanding of conflicting results regarding the object recognition processes occurring in this region. Silson et al. (2013) further differentiate LO1 from LO2 using a TMS double dissociation paradigm. A 2 interval forced choice discrimination task was performed during application of TMS to either LO1 or LO2. The first psychophysical task involved observation of two radial frequency patterns of differing radial modulation amplitudes (Wilkinson, Wilson, & Habak, 1998). The higher the radial modulation amplitude, the spikier the shape appeared. Following presentation, participants were required to indicate which shape was spikier. A staircase

function obtained a measure of the smallest perceivable difference in radial modulation amplitude. The second psychophysical task required discrimination between 2 luminance defined gratings. Minimum perceivable difference in orientation was measured.

During transient LO1 lesions, performance was impaired for orientation discrimination. Shape discrimination performance was impaired by TMS applied to LO2. The double dissociation supports the argument that LO1 and LO2 serve distinct functions in the intermediary processing of objects (Silson et al., 2013). It also confirms the suggestions made regarding the position of LO2 later in the processing stream in comparison to LO1 (Larsson & Heeger, 2006).

4.1.2 The Role of VO1 and VO2 in Shape Perception

VO1 and VO2 were first mapped by Brewer et al. (2005). They are located in the ventral occipital cortex, anterior to V4 and on the fusiform gyrus. They are thought to constitute an independent cortical cluster and play an intermediary role in shape perception (Brewer et al., 2005). Due to the preliminary nature of investigations into the functional characteristics of these maps, evidence regarding the specificity of VO1 and VO2 is mixed (Arcaro et al., 2009).

In conflict with previous proposals (Halgren et al., 1999), Brewer at al. (2005) found that these areas showed clear and consistent retinotopic patterns across subjects. Both VO1 and VO2 represent the full contralateral visual field but focus on central visual space at the expense of more peripheral positions. The two regions share a foveal representation that is separate and distinct to that shared by V1, V2, V3 and V4; as well as independent of the V3A/B foveal representation. The lower vertical meridian of VO1 is shared with V4 and the upper vertical meridian is shared with VO2. The surface area (measured from 0° to 3° degrees eccentricity; Brewer et al., 2005) is smaller for VO1 and VO2 than V4. VO1 and VO2 are similar in size. Across 9 participants retinotopy was similar (Brewer et al., 2005) although the orientation of VO1 and VO2 relative to sulcal and gyral patterns differed. This between-participant consistency was also found by Acaro et al. (2009).

The object-responsive nature of the region of ventral occipital cortex anterior to V4 has been well documented. Despite failing to note the retinotopy of these maps, Halgren et al.

(1999) identified the general region of VO1 and VO2 as object responsive and labelled it the posterior collateral. The location of VO1 and VO2 is also similar to the collateral sulcus (Malach et al., 1995), found to be activated during the presentation of images of buildings. Additionally, clinical studies report that lesions to this area of the cortex result in impairments associated with recognition of colours, faces and objects (Damasio, Damasio, & Van Hoesen, 1982; James, Culham, Humphrey, Milner, & Goodale, 2003; Meadows, 1974).

To further specify the functional roles of VO1 and VO1 Brewer et al. (2005) compared activation for colour vs luminance stimuli and objects vs faces in VO1 and VO2. In both maps, a preference was found for objects over faces, particularly when the stimulus was presented peripherally. This preference was reversed at an area of the cortex slightly lateral to the maps. VO1 and VO2 both responded to colour. These findings led the authors to conclude that VO1 and VO2 are object selective.

A later study (Arcaro et al., 2009) questioned this object-selective role proposed by Brewer et al. (2005). The scope of stimulus categories correlated with VO1 and VO2 was expanded to included scrambled object images. In convergence with Brewer et al. (2005), both VO1 and VO2 were found to respond with greater activation to object than faces. However, no preference was seen for intact objects over scrambled objects. As this area of the cortex has been implicated in texture segregation and modulated selectively by attention (Kastner, De Weerd, & Ungerleider, 2000; Pinsk, Doniger, & Kastner, 2004), it was argued that VO1 and VO2 play an intermediate role in object perception and cannot be the locus of object perception itself.

4.1.3 The Role of V4 in Shape Perception

V4 is located near to the V1/V2/V3 cluster (Arcaro et al., 2009). It has clear retinotopy in both the eccentricity and polar dimensions that is consistent across individuals (Brewer et al., 2005). Unlike macaque V4, human V4 contains a full representation of the contralateral visual field. V4 represents the central portion of the visual field more fully than the periphery (Brewer et al., 2005). The representation of the lower vertical meridian is shared with VO1 and the upper vertical meridian is shared with ventral V3. The foveal

representation of the eccentricity map is shared with V1, V2 and V3. The eccentricity representation extends towards the collateral sulcus and is parallel with the eccentricity maps of V1, V2 and V3. The larger receptive field sizes found in V4 in comparison to earlier regions (Kastner et al., 2001; Press, Brewer, Dougherty, Wade, & Wandell, 2001; Smith, Singh, Williams, & Greenlee, 2001) indicates that it may have an integratory function.

This area of the cortex has also been strongly associated with colour processing. Lesions to the ventral occipitotemporal cortex, the general vicinity of V4, are accompanied by achromatopsia (impaired colour perception). In healthy individuals it has been noted that fMRI BOLD responses are stronger during presentation of a colour defined pattern than a luminance defined pattern (Bartels & Zeki, 2000; Lueck et al., 1989; McKeefry & Zeki, 1997). This preference is also noted at the level of the single neuron (Schein & Desimone, 1990).

The role for V4 in both colour and object processing has been questioned by recent investigations. When V4 was defined retinotopically it showed no preference (as measured by BOLD response during presentation) for colour over luminance stimuli or object over face stimuli (Brewer et al., 2005). The lack of preference for object over face stimuli was confirmed by Acaro et al (2009). Additionally, it was found that as for VO1 and VO2 measured in the same experiment, V4 showed no preference for intact objects over scrambled objects (Arcaro et al., 2009).

4.1.4 Individual Differences in the Cortical Constraint of Shape Perception

Duncan and Boynton (2003) found that early retinotopic regions constrained participant behavioural abilities in associated tasks (see Chapter 3). Specifically, the measure of M (cortical magnification) was thought to limit perceptual functioning. This cortical-perceptual pairing has been extended to later visual regions (Chapter 3). Now that the clear retinotopic organisation of cortical regions underlying shape perception has been demonstrated (Brewer et al., 2005; Larsson & Heeger, 2006) it is possible to extend the hypothesis regarding the constraining properties of cortical magnification to these

regions. The high level of inter-individual retinotopic variability in intermediate areas (Larsson & Heeger, 2006) is expected to be reflected in perceptual measures.

Following from the work of Duncan and Boynton (2003), it is thought that individual differences in shape matching ability will correlate with individual differences in measures of cortical magnification. This experiment will investigate the prediction that participants with more neurons in shape processing areas of the brain (higher cortical magnification) will perform better in a task reliant on shape processing. The constraint imposed by limited cortical representation may also be seen at an intra-individual level. The increase in accuracy with movement of the location of the stimulus towards the centre of the visual field is expected to correlate with increases in cortical magnification with movement towards the foveal representation. For example, intermediate visual areas have particularly exaggerated over-representation of the fovea (VO1 and VO2, Brewer et al., 2005; LO1, Larsson & Heeger, 2006). Perceptual tasks reliant on these regions may be expected to show a foveal bias to a greater extent than tasks reliant on earlier maps.

4.2 Methods

4.2.1 Participants

Data was collected from 11 participants (3 males). Of the participant group used here, 6 (3 males) also took part in the experiment reported in Chapter 3 and all 11 participants took part in the experiment reported in Chapter 2. All participants had normal or corrected to normal vision and were aged between 21 and 34. Written consent was obtained from all participants. The experimental procedure was in accordance with the Declaration of Helsinki and was approved by the appropriate local ethics committee.

4.2.2 Measurement of Cortical Parameters

Retinotopy data was collected using the methods outlined in Chapter 2. Cortical magnification measurements of V1, V2, V3, V3A, LO1, LO2 and V4 were made in both

the radial and polar directions. These visual areas were clearly defined in all participants. VO1 and VO2 could not be identified in the majority of participants so were excluded from all analyses.

4.2.3 Psychophysics Measurement of Shape Matching Ability

4.2.3.1 Shape Matching Experimental Procedures

Testing took place in a quiet, dark room. Subjects sat 57cm from a screen and the head was stabilized through the use of a chin rest. Stimuli were binocularly viewed on 37cm by 30cm sized screen. Stimuli were presented on an EIZO 660-M monochrome CRT monitor which had been gamma corrected. There was a frame rate of 60.02Hz. Presentation of stimuli and acquisition of responses was carried out using Matlab 7.4.0 (R2007a) and MGL (http://www.pc.rhul.ac.uk/staff/J.Larsson/software.html) run on a Linux operating system.

4.2.3.2 Shape Matching Stimuli

Experimental stimuli consisted of radial frequency pattern modulated shapes (figure 4-1). The stimulus had a peak spatial frequency of 0.5 cpd, a radius of 2 degrees of visual angle and a contrast of 100%. Stimuli were generated in an analogous way to Silson et al. (2013) but used 3 independently modulated spatial frequencies (0, 3 and 7 cycles per stimulus). The shapes were located at various eccentricities. Dependent on the condition, the midpoint of the grating was at an eccentricity of 0°, 3°, 6° or 9 °. Gratings were displayed in either the upper right quadrant of the visual field or the upper left quadrant of the visual field. Central fixation of the screen was marked by a white 1 degree by 1 degree fixation cross. The background was consistently mean luminance (21.6 cd).

Figure 4-1 Radial frequency modulated shape stimulus

4.2.3.3 Shape Matching Task

Thresholds for the minimum perceivable difference in radial amplitude between 2 shapes were obtained using a temporal 2-alternative forced choice paradigm and a 1 up 2 down staircase. A schematic representation of a single trial is displayed in figure 4-2. One shape was displayed for 0.5s. There was an inter- stimuli interval of 0.5s in which a fixation cross was displayed. A second shape (of different radial amplitude to the first) was then displayed. The second grating was rotated 45 degrees in comparison to the first. Participants then made a button press response to indicate whether the second grating was the same or different to the first shape, for which 2.5s was permitted. Participants had control over the onset time of the next trial, indicating via a second button press that they were prepared for another trial. 60 pairs of shapes (60 trials) were presented in each block of trials. Each block produced 1 threshold value.

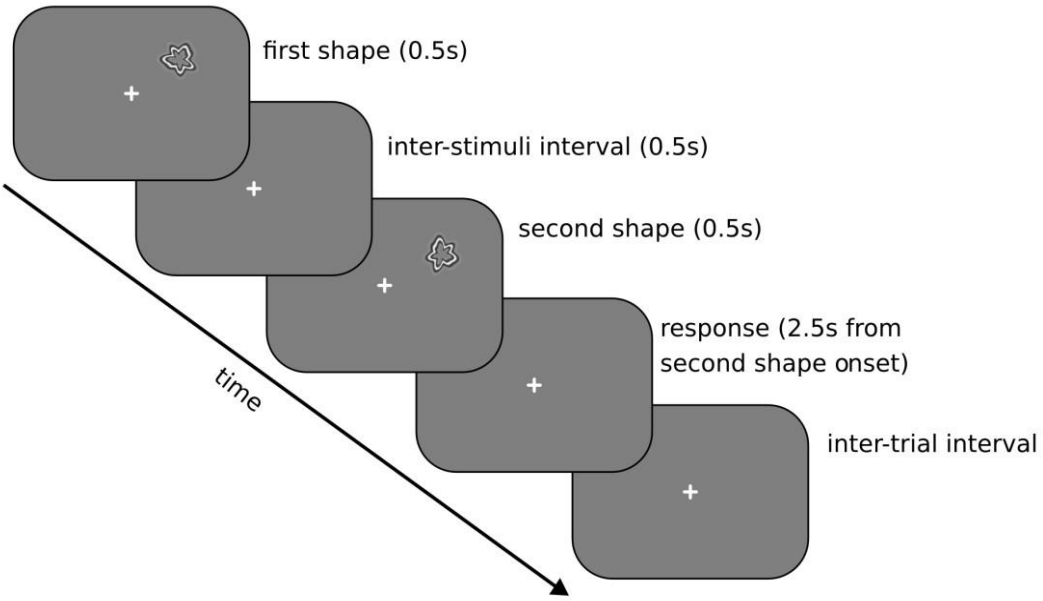

Figure 4-2 Shape matching experimental paradigm: schematic representation of a single trial. Here, the stimulus is shown the right visual field is shown. Trials for the left visual field presentation condition followed an identical procedure.

Participants were instructed to keep their eyes focused on the fixation cross throughout the trials. This instruction was repeated regularly throughout the testing session. Participants were informed that the second shape may be rotated in comparison to the first, but that the rotation should not be considered during the judgement of similarity. They were told that if the 2 shapes were identical except for the rotation, they should indicate that the 2 shapes are identical.

Each testing session began with a short practice phase. This usually consisted of 1 block of trials, but occasionally lasted for 3 blocks of trials for inexperienced subjects. In each testing session the grating was presented at 4 eccentricities. Each eccentricity was repeated 4 times. If a threshold was not achieved, the block was repeated. Failure to achieve a threshold was determined byinspecting the staircase output following each block of trails. In total there were 16 blocks of trials. The testing sessions took approximately 60 minutes, including a break of 10 minutes half way through the experiment. Participants attended 2 testing sessions.

4.2.3.4 Experimental Design

This task was carried out at a range of eccentricities (0°, 3°, 6°, 9°) and in 2 quadrants of the visual field (upper left and upper right). Within each block of trials, the gratings were always at the same eccentricity and within the same quadrant of the visual field. Eccentricity was changed between blocks in a semi- randomised fashion. Blocks of the same eccentricity were not performed consecutively. Within each testing session, the gratings were always within the same quadrant of the visual field.

4.3 Analysis and Results

In summary, the results of this experiment demonstrated a weak correlation between LO1 cortical magnification and shape matching thresholds. A non-significant trend suggested that participants with low LO1 polar cortical magnification accurately matched shapes. Visual areas V4 and LO2 were unrelated to psychophysical thresholds.

4.3.1 Psychophysical Measurement of Shape Matching Ability

Psychophysical data for this experiment was analysed analogously to the data reported in Chapter 3. Hemifields were treated as individual participants. Preliminary analysis of the psychophysical data identified a single data point as an outlier. This data point fell more than 1.5 times the interquartile range above the third quartile. This data point was replaced with the mean of the remaining data points in the condition. The mean for each participant at each eccentricity was taken from 4 thresholds (figure 4-3). An ANOVA demonstrated a main effect of eccentricity ($F(3,84)=16.47$, $p<.001$). Planned contrasts indicated that thresholds were higher (poorer performance) at 6° (M=0.5, SE=0.03) than 3° (M=0.39, SE=0.03). This relationship was significant ($p<.001$). Thresholds were higher (poorer performance) at 9° (M=0.65, SE=0.04) than 6° ($p<.001$).

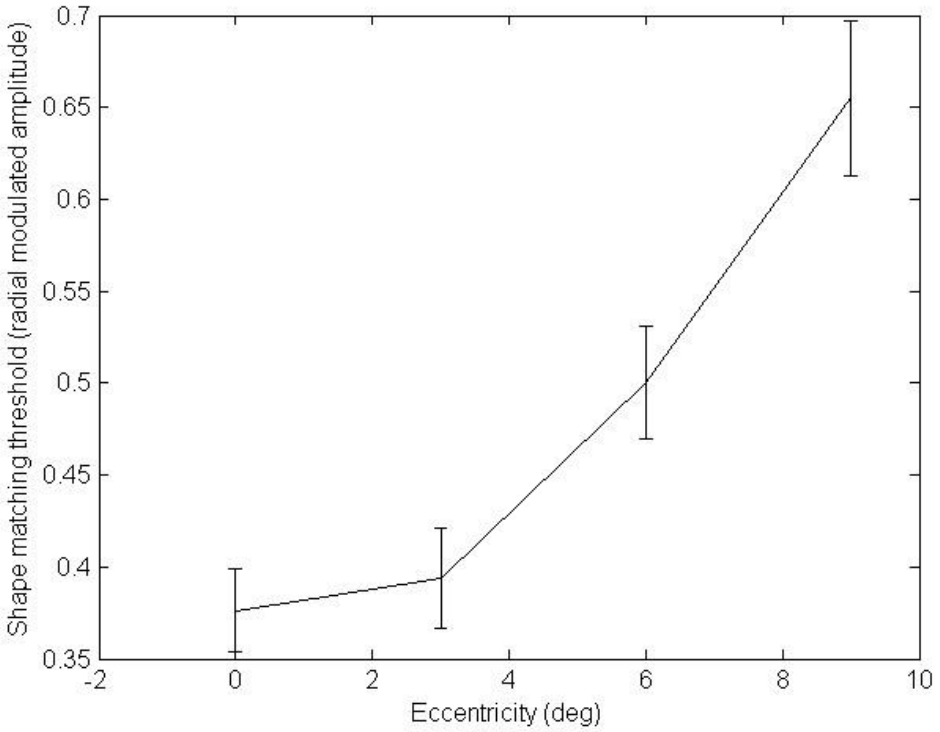

Figure 4-3 Average shape matching thresholds (22 hemispheres). Standard errors shown.

4.3.2 Analysis of Visual Areas

Radial cortical magnification measurements from 7 visual areas were submitted to a linear regression to predict performance in a shape matching task. A regression was performed for each of the 3 functions. Polar cortical magnification measurements from 7 visual areas were submitted to a linear regression to predict performance in a shape matching task. A regression was performed for each of the 3 functions. Bivariate correlations were performed between psychophysical data and the surface areas of all visual areas. Analogous correlations were also run for radial distance and polar width.

Eccentricity was included as a covariate in all linear regressions to remove this source of variance from the analysis. For the linear scaling function, power function and piecewise regression function, eccentricity was the dominant source of variance in both the radial (B=.05, SE=.01, β=.83, T=5.32, p=.001; B=.04, SE=.01, β=.72, T=.57, p<.01; B=.03,

SE=.01, β=.61, T=6.3, p<.001) and polar dimension (B=.03 SE=.01, β=.6, T=5.34, p<.001; B=.05, SE=.01, β=.73, T=4.77, p<.001; B=.05, SE=.01, β=.7, T=3.71, p<.001).

4.3.2.1 LO1 Retinotopic Measures Correlate with Shape Matching Ability

A link was identified between LO1 polar cortical magnification taken from the piecewise regression function and shape matching thresholds (figure 4-5; B=.05, SE=.03, β=.42, T=1.86, p=.07). This relationship did not reach significance. Participants with high levels of LO1 cortical magnification had higher psychophysical thresholds (e.g. poorer performance). Figure 4-5 suggests that participants with high levels of LO1 cortical magnification had low thresholds, but the linear regression indicates that once the dominant effect of eccentricity is removed this relationship reverses. This relationship could not be identified at specific eccentricities (0° p=.78; 3° p=.99; 6° p=.17; 9° p=.31). Figure 4-6 illustrates the similarity between the LO1 polar cortical magnification eccentricity effect and the psychophysical data (figure 4-3). An analogous role for radial cortical magnification in LO1 was not seen (p=.099).

In addition to the trend towards a predictive role for cortical magnification, the size measures of LO1 were also linked to psychophysical thresholds. Participants with low thresholds (e.g. good performance) had large LO1 surface areas (figure 4-4; R=-.27, p<.05). This link was not seen at specific eccentricities (0° p=.87; 3° p=.80; 6° p=.68; 9° p=.44). It is possible that this relationship is driven solely by the global eccentricity effect. This suggestion is supported by the fact that the correlation is lost when eccentricity is controlled for (p=.35). Both the psychophysical thresholds and the size of the cortex representing visual space are correlated with eccentricity. Neither radial distance (p=.49) nor polar width (p=.26) correlated with shape matching thresholds.

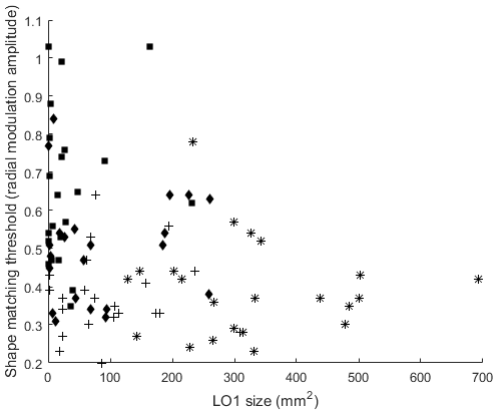

Figure 4-4 The relationship between LO1 size (mm²) and shape matching thresholds (p<.05). Good performance in the shape matching task was associated with large LO1 surface area. Each data point represents a single hemisphere at a single eccentricity patch. Each data point represents a single eccentricity patch for a single participant. Eccentricities are represented by different symbols (0°+; 3°*; 6°♦; 9°■).

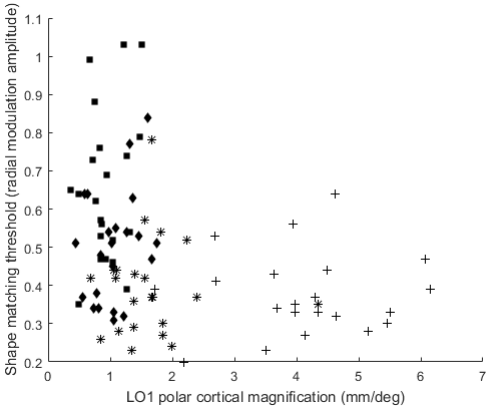

Figure 4-5 The relationship between LO1 polar cortical magnification (mm/deg; the piecewise regression function) and shape matching thresholds (p=.07). Good performance in the shape matching task was associated with high levels of cortical magnification. Each data point represents a single hemisphere at a single eccentricity patch. Each data point represents a single eccentricity patch for a single participant. Eccentricities are represented by different symbols (0°+; 3°*; 6°♦; 9°■).

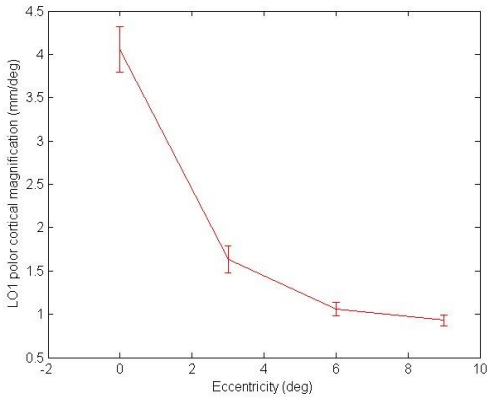

Figure 4-6 Average LO1 polar cortical magnification (mm/deg) across eccentricities of 0°, 3°, 6° and 9° (22 participants; the piecewise regression function). Standard errors shown.

4.3.2.2 LO2 and V4 Cortical Magnification does not correlate with Shape Matching Ability

LO2 and V4 are thought to have a role in shape matching. Previous studies indicate a role in intermediate visual processing for V4 (Kastner et al., 2001). LO2 has been associated with object processing (Larsson & Heeger, 2006). Surprisingly, cortical magnification in neither LO2 nor V4 correlated with psychophysical thresholds. For example, using measures taken from the piecewise regression function, V4 radial ($p=.14$) and polar cortical magnification ($p=.71$) did not correlate with performance. LO2 radial ($p=.14$) and polar ($p=.92$) cortical magnification were also poor predictors.

Conversely, the size measures of these visual areas correlate with psychophysical thresholds. Participants with large LO2 radial distances had low psychophysical thresholds (e.g. good shape matching ability). This was seen at a global level ($T=-.28$, $p<.01$; figure 4-7) but not at specific eccentricities (0° $p=.27$; 3° $p=.89$; 6° $p=.59$; 9° $p=.79$).

The predictive role for size measures of V4 is less clear. The radial distance of V4 did not correlate with thresholds ($p=.5$). The surface area V4 predicted thresholds when the analysis was run across eccentricities ($R=-.21$, $p=.05$; figure 4-8), although the link did not reach significance. At specific eccentricities no links were seen (0° $p=.98$; 3° $p=.96$; 6° $p=.98$; 9° $p=.28$). In contrast, the polar width measure of V4 indicates that a larger V4

is associated with poor performance in the shape matching task (R=.33, p<.01; figure 4-9). Again, this predictive role was lost at specific eccentricities (0° R=-.07, p=.77; 3° R=.16, p=.46; 6° R=.3, p=.17; 9° R=.43, p=.05).

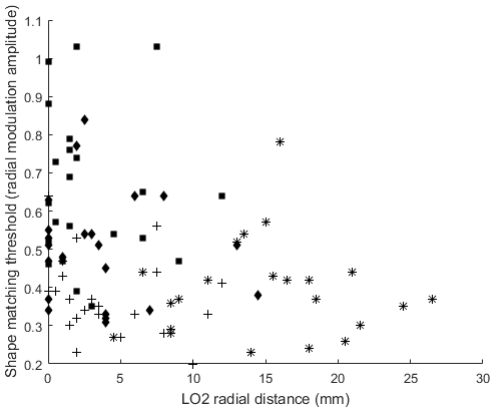

Figure 4-7 The relationship between LO2 radial distance (mm) and shape matching thresholds (p<.01). Each data point represents a single hemisphere at a single eccentricity patch. Each data point represents a single eccentricity patch for a single participant. Eccentricities are represented by different symbols (0°+; 3°*; 6°♦; 9°■).

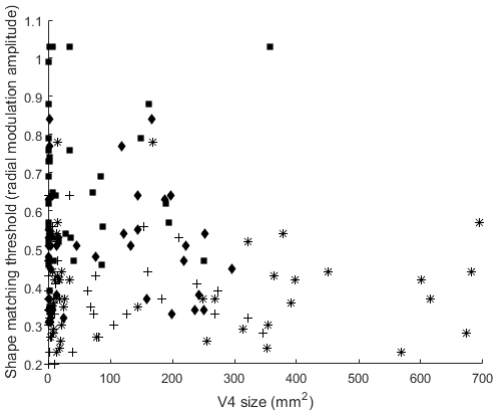

Figure 4-8 The relationship between V4 size (mm²) and shape matching thresholds (p=.05). Each data point represents a single hemisphere at a single eccentricity patch. Each data point represents a single eccentricity patch for a single participant. Eccentricities are represented by different symbols (0°+; 3°*; 6°♦; 9°■).

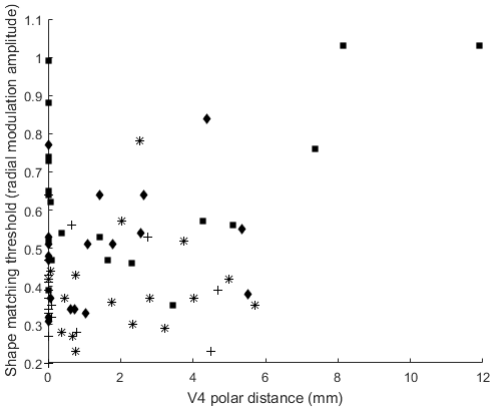

Figure 4-9 The relationship between V4 polar width (mm) and shape matching thresholds (p<.01). Each data point represents a single hemisphere at a single eccentricity patch. Each data point represents a single eccentricity patch for a single participant. Eccentricities are represented by different symbols (0°+; 3°*; 6°♦; 9°■).

4.3.2.3 V3A Retinotopic Measures Correlate with Shape Matching Ability

Given the intermediate nature of this visual area, V3A was examined for a predictive role in shape matching ability. V3A cortical magnification was a poor predictor of performance. The piecewise regression function was the only function to provide sufficiently accurate estimates of V3A cortical magnification. Using this function, neither V3A polar cortical magnification (p=.12) nor radial cortical magnification (p=.35) correlated with shape matching thresholds. Conversely, size measure of V3A were good predictors of performance. V3A size correlated with thresholds (B=.00, SE=.00, β=.5, T=4.37, p<.001). This link was strongest at the highest eccentricity (figure 4-10; 0° R=.22, p=.34; 3° R=-.15, p.51; 6° R=-.07, p=.77; 9° R=.62, p<.01). Poor performance was associated with a large V3A surface area. V3A radial distance also showed a trend towards a correlation with shape matching ability (B=.01, SE=.01, β=.29, SE=1.73, p=.09).

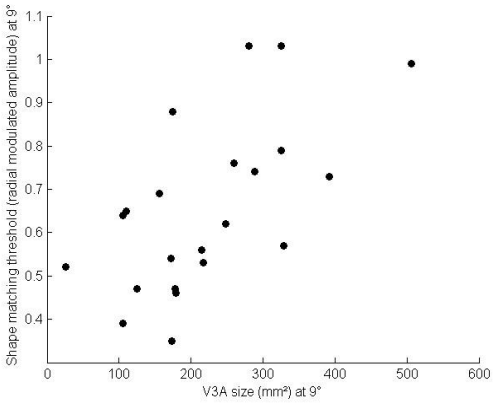

Figure 4-10 The relationship between V3A size (mm²) and shape matching thresholds at 9° ($p<.01$). Each data point represents a single hemisphere at a single eccentricity patch.

4.4 Discussion

Perceptual thresholds in a shape discrimination task displayed a clear eccentricity effect. Thresholds were lower in the fovea than the periphery. Analysis demonstrated that psychophysical performance was not significantly correlated with cortical magnification of any visual area, although a trend with LO1 was noted. This finding indicates that the constraining role of cortical magnification in V1 (Duncan & Boynton, 2003) may extend to higher tier visual areas, but is much weaker at these locations. Mirroring Chapter 3, inter- individual variability exists in both cortical and behavioural measures, but these values do not correlate. Also following the findings of Chapter 3, a strong effect of eccentricity was identified in both the retinotopic and psychophysical data. Generally this source of variance drove correlations between cortical and perceptual measures.

Levels of polar cortical magnification in LO1 were associated with performance in the shape matching task. This relationship was not significant so speculation must be tentative. Unexpectedly, once the common effect of eccentricity was removed participants with higher levels of LO1 polar cortical magnification performed poorly in the shape matching task. The identification of this link in LO1 is difficult to understand. LO1 was not expected to constrain task performance. The double dissociation demonstrated by Silson et al. (2013) indicated that LO1 does not process radial frequency shapes.

Additionally, it is inconsistent with the general hypothesis that a higher number of neurons representing the stimulus results in better perception.

It should be noted that the retinotopic mapping of LO1 may have been limited to some extent by methodological issues. Past literature highlights the problems associated with establishing the retinotopic parameters of this area. For example, early descriptions of LOC (Tyler et al., 2005) claimed no polar map existed in this area. However, the retinotopic methods used here have successfully delineated a clear LO1 map in all participants. Although Chapter 2 (figure 2-11) demonstrates that the function was successfully fit to this visual area, the lack of uniformity of this region must be acknowledged and may have contributed to the lack of statistical significance in the relationship between LO1 and psychophysical thresholds.

Despite the close relationship between LO1 and LO2 outlined in Chapter 2, LO2 cortical magnification showed no relationship with the psychophysical data. Radial and polar cortical magnification links were absent and the size measures of LO2 showed only a weak role. The absence of a strong correlation between LO2 cortical parameters and shape matching ability conflicts with the work of Silson et al. (2013). The task here is very similar to the task shown by Silson et al. (2013) to be disrupted following TMS to LO2. Similarly, despite the evidence of a role for V4 in intermediate visual processing (Brewer et al., 2005), psychophysical thresholds did not correlate with cortical magnification of this visual area.

It is possible that performance in complex tasks is not simply constrained by the properties of any one single area. For example, a relatively complex task such as object discrimination is reliant on multiple areas (Brewer et al., 2005; Larsson & Heeger, 2006). It can be argued that complex tasks are constrained by cortical magnification to the same extent as low level task. Although, in the case of complex tasks, this constraining role is dispersed across multiple visual areas. In this way, the constraining role in a single visual area is too small to identify. To fully understand this dispersed role, all visual areas underlying the task must be accurately identified and mapped. This complex is likely to include VO1 and VO2, areas excluded from this analysis due to a failure to identify in a sufficient number of participants.

It is of interest that V3A surface area was inversely correlated with shape matching ability. Participants with a large V3A had higher thresholds in the psychophysical task. Again this is inconsistent with the hypothesis that visual performance is facilitated by a higher number of neurons processing the task stimulus. However, it is consistent with the findings of Chapter 3. In addition to shape matching ability, a small V3A surface area has also been associated with orientation discrimination of a motion defined boundary. Whilst understanding of this counter-intuitive link is beyond the scope of this experiment, it is noteworthy that the retinotopic characteristics that inhibit low level tasks (e.g. small surface area) appear to be beneficial in intermediate tasks.

Consideration of the data presented here with the findings outlined in the previous chapter supports the argument that Duncan and Boynton (2001) may have overstated the predictive role of cortical magnification in visual abilities. Neither shape matching (Chapter 4) nor orientation discrimination (Chapter 3) were strongly associated with this retinotopic parameter. The link was particularly absent in higher tier visual areas. Whilst it is evident that inter- individual difference exist in both psychophysical and cortical magnification measures, these characteristics correlate only weakly. Visual abilities are mediated to some extent by the amount of cortex processing the stimulus, but there are most likely multiple additional factors contributing to this variability.

Part II: Do Population Receptive Field (pRF) Centre Size, Surround Size and Ratio Constrain Visual Abilities?

5 Population Receptive Field (pRF) Surround Size of V1 Correlates with First Order Surround Suppression

5.1 Introduction

Surround suppression is a form of visual context modulation (Bair et al., 2003). The presence of a stimulus directly outside the classical receptive field prevents a response to a stimulus located within the classical receptive field (Bair et al.,2003). The behavioural consequences of surround suppression are well established. Perception of a stimulus can be affected by the presence of other stimuli nearby (Xing & Heeger, 2001).

Research into surround suppression has generally focused on first order stimuli. A first order stimulus, such as a luminance defined grating, is detected by comparing light and dark (Baker & Mareschal, 2001). It can be processed by V1 orientation-tuned neurons (Hubel & Wiesel, 1962). When a first order grating is surrounded by a grating of higher contrast, the target grating will appear to be of a lower contrast than if it is displayed alone (Chubb et al.,1989). The higher the surround contrast, the greater the suppressive effect (Olzak & Laurinen, 1999). This effect requires collinearity of the target and the surround (Xing & Heeger, 2000). Small differences between the relative orientation and spatial frequency of the surround and the target will weaken the suppressive effect (Chubb et al., 1989; Solomon, Sperling, & Chubb, 1993). An analogous but opposite effect also exists. Surround enhancement occurs when the target grating is of a higher contrast than the surround grating. The target is perceived to be of a greater contrast because of the presence of the surround (Cannon & Fullenkamp, 1993). Co-linearity of surround and target is more critical for enhancement than suppression (Xing & Heeger, 2000).

Psychophysical measures of surround suppression are thought to reflect the functioning of individual neurons in the visual cortex. A cell's classical receptive field is the region of visual space to which stimulation will result in activity of the cell (Victor, Purpura, Katz,

& Mao, 1994). Stimulation immediately outside the classical receptive field will inhibit the cell, causing a negative response. At the foveal representation, receptive field sizes are small. Receptive field sizes increase with distance from the foveal representation (Hubel & Wiesel, 1974). The eccentricity effect in psychophysically measured surround suppression mirrors the pattern of receptive field sizes on the cortex. Surround suppression is greatest in the periphery (Xing & Heeger, 2000). At low eccentricities the influence of the surround on the target is low.

V1 is thought to be the locus of first order contrast surround suppression. Zenger-Landolt and Heeger (2003) measured BOLD response during observation of luminance defined gratings both with and without a high contrast surround. In replication of previous results (Xing & Heeger, 2000), contrast of the target appeared lower in the presence of a surround. Additionally, the fMRI response was lower when the surround was present. This pattern was strongly associated with V1, this region accounted for 96.5% of the variance (Zenger- Landolt & Heeger, 2003).

Single cell recordings in macaque V1 have also demonstrated the role of this visual area in first order surround suppression. The presence of a high contrast surround near to a cell's receptive field decreased the response of the neuron (Levitt & Lund, 1997). The suppressive effect is strongest when the stimulus matches the neuron's preferred orientation and spatial frequency (Cavanaugh et al., 2002; DeAngelis et al., 1994; Knierim & Van Essen, 1992). This mirrors the importance of collinearity between surround and target seen in psychophysical experiments (Xing & Heeger, 2000).

Population receptive field modelling (pRF; Dumoulin & Wandell, 2008) is an analysis technique that allows understanding of the neural properties of the visual cortex. Using retinotopic data collected during MRI, the size of receptive fields can be measured. Retinotopic data can be collected with standardized methods (see Chapter 2), or alternatively using bars at different positions and orientations (Harvey & Dumoulin, 2011). Unlike standard retinotopic mapping which pairs a single voxel to a single point in space to which it responds most strongly, pRF modelling fits a Gaussian receptive field function to each voxel time series. In this way, the full receptive field of each neuron can be described. This analysis is possible through an understanding of the effect of receptive

field parameters and the relative amount of active versus inactive epochs in fMRI data (Smith et al., 2001).

Traditionally, receptive fields were measured for single cells. Single cell recordings indicated that the size of these visual fields increased with progression through the visual cortex, with smaller sizes in V1 than V3 (Burkhalter, Felleman, Newsome, & Van Essen, 1986; Burkhalter & Van Essen, 1986; Gattass, Sousa, & Rosa, 1987). Additionally, the receptive fields were smaller in the fovea and larger in the periphery of vision. The introduction of pRF modelling (Dumoulin & Wandell, 2008) has allowed expansion of the small scale single electrode measures to larger portions of the cortex. Data collected from V1, V2 and V3 has demonstrated cross-methodological validity (Dumoulin & Wandell, 2008). For example, the pRF size measurements obtained by Dumoulin & Wandell (2008) in V1, V2 and V3 are similar to estimates obtained using neurophysiological methods (Yoshor, Bosking, Ghose, & Maunsell, 2007).

A later development in this technique enabled a more detailed exploration of receptive field properties. It is well established that stimulation directly outside the receptive field decreases activity of the cell (Cavanaugh et al., 2002). Zuiderbaan et al. (2012) presented a modelling technique that accounts for this suppressive effect. Unlike previous pRF models (Dumoulin & Wandell, 2008), the Zuiderbaan et al. (2012) method accounts for decreased BOLD responses that fall below baseline through the use of a circular symmetric difference-of- Gaussian function. These improvements provided a better estimate of receptive field activity in visual areas V1, V2 and V3. The surround size of the receptive field, the centre size of the receptive field and the suppression index (the ratio of surround to centre) can be estimated.

The methods used by Zuiderbaan et al. (2012) estimate the pRF suppression index by computing a ratio between the size and amplitude of the receptive field and the size and amplitude of the negative surround. This analysis method makes several assumptions about the parameters of the receptive field. The size of the negative surround is larger or equal to the size of the receptive field, and the amplitude of the surround is negative with an absolute value smaller than that of the receptive field amplitude. Importantly, this method assumes a circular receptive field shape. It may not be an appropriate model for highly anisotropic pRFs.

The limitations placed on pRF estimates by this assumption of isotropy can be overcome by adopting a model-free, data-driven approach (Greene, Dumoulin, Harvey, & Ress, 2014; Pizzorni-Ferrares & Larsson, 2014). In this way, the asymmetric nature of receptive fields can be described. For example, Pizzorni- Ferrarese and Larsson (2014) report an increase in the anisotropy of both centre and surround size with increasing eccentricity for V1, V2, V3 and V3A. Additionally, at later maps receptive field shapes are more elongated.

Research from single cell recording, psychophysics and pRF analyses has converged to show a clear link between perceptual surround suppression and cortical parameters of receptive fields in V1. This indicates that V1 mediates surround suppression. Other retinotopic properties of V1, such as cortical magnification, have been shown to constrain perceptual abilities (Duncan & Boynton, 2003). The development of pRF methodology provides an opportunity to demonstrate that receptive field parameters also constrain the perceptual phenomenon of surround suppression. In this experiment I investigated the hypothesis that small receptive field sizes and high surround/centre ratios will correlate with low levels of surround suppression in a psychophysical first order contrast matching task. Past research has localised first order surround suppression to V1, so the majority of relationships were expected here.

5.2 Estimation of Population Receptive Fields

5.2.1 MRI Acquisition

The data used in the pRF analysis was identical to that used in Chapters 2, 3 and 4. The visual stimuli used were clockwise and anti-clockwise wedges and contracting and expanding rings. See Chapter 2 for a full description of data collection procedures.

5.2.2 Cortical Surface Extraction and Analysis

MRI data was processed to obtain flattened cortical surfaces. The full methods are outlined in Chapter 2.

5.2.3 Retinotopic Mapping

Visual areas were identified on the flattened cortical surfaces using the methods outlined in Chapter 2. Visual areas V1, V2d, V2v, V3d, V3v and V3A were identified on both hemispheres of each participant. Although using the same data and methods as the experiment reported in Chapter 2, the ROIs used here were drawn independently of the previous experiments.

5.2.4 pRF Model

The pRF estimation was performed for each visual area. Estimates from the two hemispheres and from dorsal and ventral portions of V2 and V3 were combined. Estimates were made using a model-agnostic data-driven approach (Pizzorni- Ferrares & Larsson, 2014). Unlike the methods of Zuiderbaan et al. (2012) and also the model-free approach of Greene et al. (2014), no assumptions about the haemodynamic response function (HDF) were made.

Firstly, an initial estimate of the pRF position was obtained. Estimates of both population receptive fields and HDF were made through a comparison of response amplitude across time via a reverse correlation. HDF estimate was obtained by linear deconvolution, systematically shifting the onset of the HDF along all positions in visual space. Given that our stimuli consisted on moving wedges and expanding rings, two separate responses were expected over time in the responsive voxel, one associated with the polar dimension and the second with the radial dimension. The search space consisted on a 16x16 kernel showing time (HDF) against space (pRF, polar and radial dimension). The peak of the pRF estimate occurred at 6 seconds. The polar and radial pRFs corresponding to this HDF time point were selected.

Secondly, a single 2D Gaussian was fitted to the obtained kernel for all the voxels (figure 5-1). This single 2D Gaussian estimated pRF parameters in the traditional way (Dumoulin & Wandell, 2008). Crucially, the method used here fit a Gaussian for the polar and radial dimensions separately, thereby allowing estimation of size independently in each dimension.

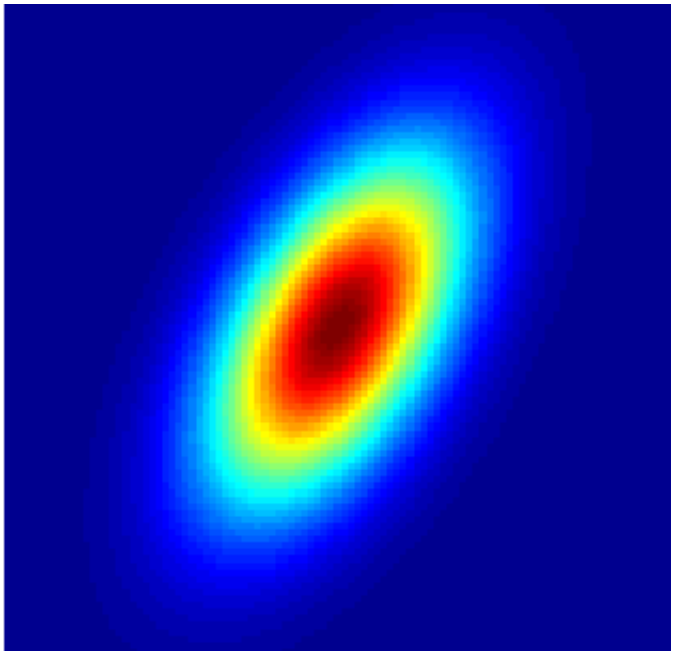

Figure 5-1 Illustration of 2D Gaussian pRF

The analysis provides 4 parameters of the receptive field; position along x and y axes, amplitude and size (along the radial and polar dimensions). The size measurement corresponded to the width of the Gaussian. The single Gaussian estimate can describe the positive response of the central portion of the receptive field only.

Thirdly, the difference between 2 Gaussians was fitted (DoG model). This model allows estimation of the negative surround of the receptive field. Like the single Gaussian estimate, this model also describes the positive centre of the receptive field. The use of the DoG model allowed estimation of a suppressive surround. The size measurements produced by the DoG model correspond to the width of the negative Gaussian (the surround size) and the width of the positive Gaussian (the centre size).

The pRF suppression ratio (surround/centre ratio) was computed using the size (SS) and amplitude (AS) of the surround and the size (SC) and amplitude (AC) of the centre.

$$(1)\ pRF\ Ratio = \frac{AS \cdot (SS)^2}{AC \cdot (SC)^2}$$

These pRF parameter estimates were made for the full visual field at a contrast of 100%. Both eccentricity and polar angle maps were created to show the pRF representation across the cortex. The polar dimension of pRF data was not used in the experiments reported in this thesis. All analysis reported here refer to eccentricity measures only. The radial pRF was selected to allow comparison with psychophysical data, which was collected across eccentricities. The exclusion of polar data limits interpretation to some extent, as the anisotropy of the receptive field is not accounted for. 3 characteristics of the receptive fields were obtained from this analysis; centre size (CS), surround size (SS) and pRF suppression ratio (surround/centre ratio).

5.3 Psychophysical Estimation of First Order Surround Suppression

5.3.1 Participants

11 Participants (3 males) took part in this experiment. All participants had also taken part in experiments reported in Chapters 2, 3 and 4. All participants had normal or corrected to normal vision and were aged between 22 and 35. Written consent was obtained from all participants. The experimental procedure was in accordance with the Declaration of Helsinki and was approved by the appropriate local ethics committee.

5.3.2 First Order Surround Suppression Experimental Procedures

Psychophysical testing took place in a quiet, dark room. Participants sat 57cm from a screen and the head was stabilized through the use of a chin rest. Stimuli were binocularly viewed on 37cm by 30cm sized screen. Stimuli were presented on an EIZO 660-M monochrome CRT monitor which had been gamma corrected. The monitor was linearized. There was a frame rate of 60.02Hz. Presentation of stimuli and acquisition of responses was carried out using Matlab 7.4.0 (R2007a) and MGL (http://www.pc.rhul.ac.uk/staff/J.Larsson/software.html) run on a Linux operating system.

5.3.3 First Order Surround Suppression Stimuli

Target stimuli consisted of luminance defined gratings. The gratings were masked by a circular aperture, measuring 3 degrees of visual angle in diameter. This stimulus consisted of a sinusoidal grating pattern; luminance was modulated sinusoidally from white to black. The spatial frequency of the grating was 2 cpd. In the surround suppression condition, the first target in each trial was surrounded by a high contrast grating (80%), with the same spatial frequency and phase as the target, displayed with an annulus (inner diameter 4 degrees, outer diameter 11 degrees). The parameters of the surround were identical to the parameters of the target except for size and contrast level. The target and surround were separated by a 0.5 degree blank space with the same luminance as the background (figure 5-2). The edges of the target and surround stimuli were blurred to yield a soft edge. In the control condition, both the target and the matching grating were displayed in isolation (figure 5-3).

The gratings (both alone and with a surround) were located at eccentricities of 0°, 3°, 6° or 9°. Gratings were displayed in either the upper right quadrant of the visual field or the upper left quadrant of the visual field. Central fixation of the screen was marked by a white 1 degree by 1 degree fixation cross. The background was consistently mean luminance (21.6 cd).

Figure 5-2 First order surrounded stimulus

Figure 5-3 First order control stimulus

5.3.4 First Order Surround Suppression Task

Perceived contrast thresholds for the matching grating were obtained using a temporal 2-alternative forced choice paradigm and a 1 up 1 down staircase. A schematic

representation of a single trial is displayed in figure 5-4. The target grating was displayed for 0.5s. There was an inter-stimulus interval of 0.5s in which a fixation cross was displayed. A second grating (of a different contrast to the first) was then displayed. This was the matching grating. Participants then made a button press response to indicate whether the second matching stimulus was the same or different to the first target stimulus, for which 2.5s was permitted. Participants had control over the onset time of the next trial, indicating via a second button press that they were prepared for another trial.

In the experimental conditions, the first centre grating (the target stimulus) was shown in the presence of a surround and the second centre grating (the matching stimulus) was alone. The staircase modulated the contrast of the matching stimulus. The difference in contrast between the 2 gratings started at 30% (with a random jitter of between 5 and -5) and increased or decreased in increments of 1. The target and the surround of the target stimulus remained a constant contrast throughout. The target had a contrast of 40% and the surround had a contrast of 80%. In the control conditions, neither the target nor the matching grating had a surround. 60 pairs of gratings were presented in each block of trials. Each block produced 1 threshold value, the perceived difference in contrast between the target and matching stimuli. The threshold was computed as the average of the last 20 trials.

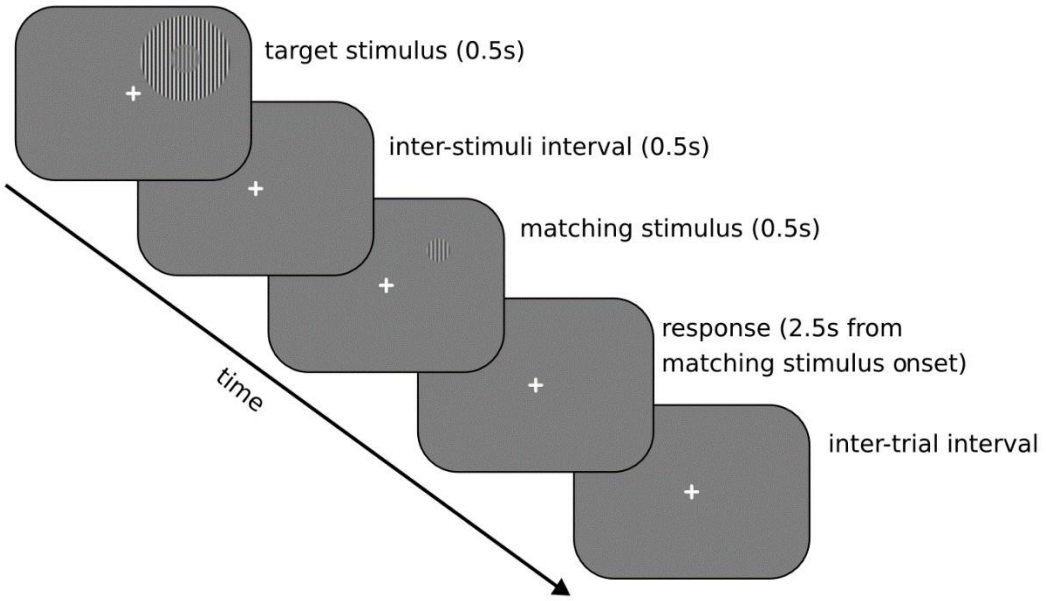

Figure 5-4 First order surround suppression experimental paradigm: a schematic representation of a single trial. A trial from the surrounded condition is shown. Control trials were identical but the target stimulus did not have a surround.

Participants were instructed to keep their eyes focused on the fixation cross throughout the trials. This instruction was repeated regularly throughout the testing session. The instruction; “Press 1 if the second grating has a higher contrast than the first, 3 otherwise”, was presented at the beginning of the testing session verbally. It was also presented visually at the start of each block of trials. In experimental trials, participants were informed that they should make their decisions based on the contrast of the target stimulus, and ignore the surround stimulus as much as possible.

Each testing session began with a short practice phase. This usually consisted of 1 block of trials, but occasionally lasted for 3 blocks of trials for inexperienced subjects. In each testing session the grating was presented at 4 eccentricities. Each eccentricity was repeated 5 times. If a threshold was not achieved, the block was repeated. Failure was rare. In total there were 20 blocks of trials. The testing sessions lasted approximately 60 minutes, including a short break half way through the experiment. Subjects attended 4 testing sessions.

5.3.5 First Order Surround Suppression Experimental Design

The task was performed at an eccentricities of 0°, 3°, 6° and 9°, in 2 quadrants of the visual field (upper left and right). Within each block of trials, the gratings were always at the same eccentricity and within the same quadrant of the visual field. Within each testing session, the gratings were always within the same quadrant of the visual field and of the same experimental condition (control or surrounded).

5.4 Results

The data reported here demonstrates that pRF surround size and centre size of V1 correlate with psychophysical measures of surround suppression. High levels of first order surround suppression are associated with large V1 surround size and large V1 centre size.

5.4.1 Psychophysical Measurement of First Order Surround Suppression

Each participant performed each condition (control and surrounded) of the contrast matching task 5 times at each eccentricity; a mean was computed from these 5 values. For each participant in each visual field, 4 average thresholds were obtained. All participants performed the task in both the right and the left visual field. Results from the two visual fields were averaged.

Psychophysical measures of suppression (SS_1) for each block were calculated by dividing the staircase output (the matching contrast; Cmatch) by the contrast of the target stimulus (the test contrast; Ctest). This was a ratio of the matching contrast and the test contrast (figure 5-5). A value of 1 indicated that no surround suppression had occurred within the trial, the participant perceived the second stimulus as equal to the first stimulus. Generally, values lower than 1 indicate surround suppression (although this ratio does not account for the suppressive effect of adaptation, which may also result in values lower

than 1). This suppression ratio is consistent with past research (Xing & Heeger, 2001). An analogous suppression ratio (SC_1) was computed for the control trials (figure 5-6).

(1) $SS_1 = \frac{Cmatch}{Ctest}$

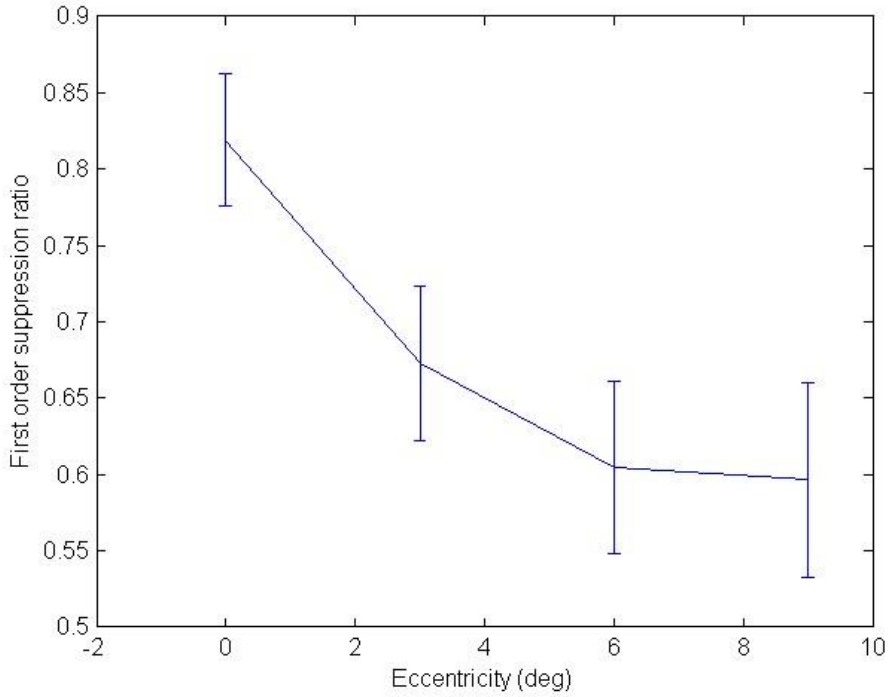

Figure 5-5 Average psychophysical suppression ratio (11 participants) in a first order contrast matching task (SS_1). Standard errors shown

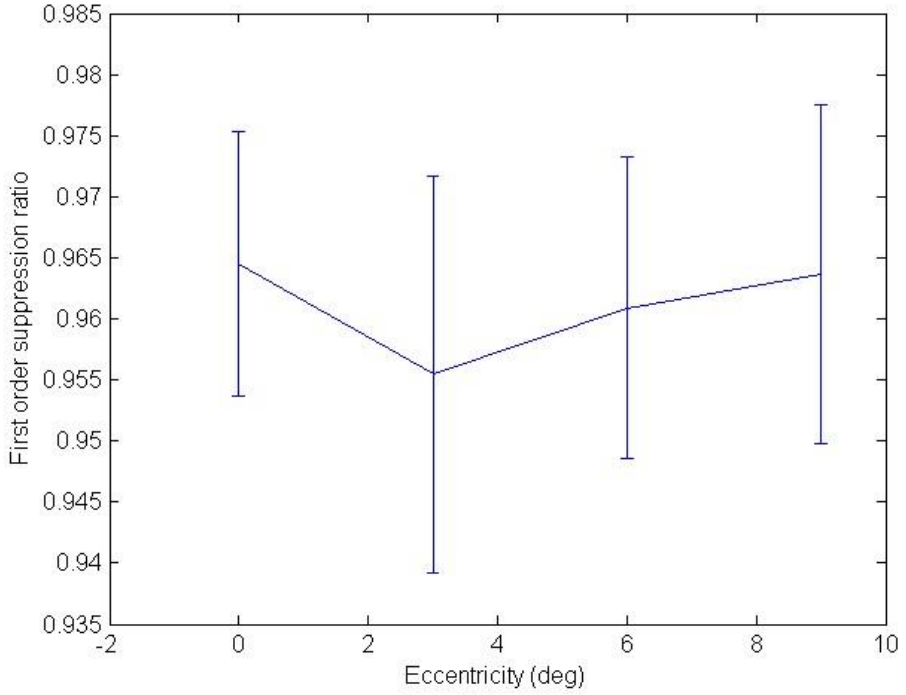

Figure 5-6 Average psychophysical suppression ratio (11 participants) in a first order contrast matching control task (SC_1). Standard errors shown.

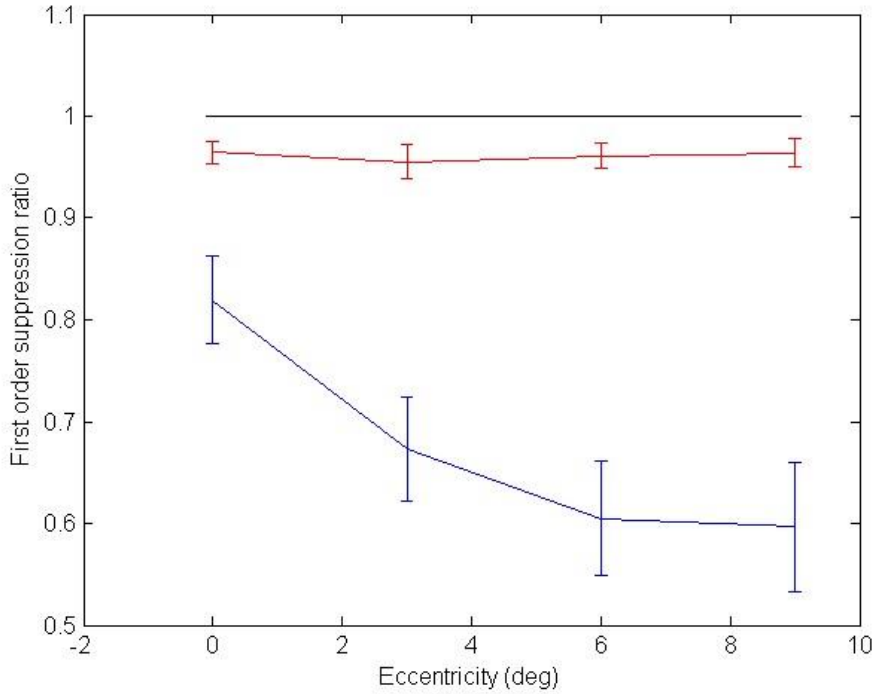

Figure 5-7 Average psychophysical suppression ratio (11 participants) in control (SC_1; red) and surrounded condition (SS_1; blue). The black plot shows hypothetical performance in which the test contrast is perceived as equal to the matching contrast (SS_1= 1). Standard errors shown.

A suppression index (SI_1) was calculated for each participant at each eccentricity by dividing the suppression ratio in the surrounded condition by the suppression ratio in the control condition at the equivalent eccentricity. This corrected for the eccentricity-specific effects of adaptation in contrast matching within trial adaptation. This value was then subtracted from 1. This number represents the increase in matching thresholds with the introduction of a surround stimulus. A high value indicates that the introduction of a surround has had a high impact on the perceived contrast. This suppression index distinguishes the suppression due to the presence of a surround from the suppression due to adaptation and is consistent with past research (Xing & Heeger, 2001). Figure 5-8 indicates a strong effect of eccentricity. An ANOVA demonstrated that this main effect was significant ($F(3,40)=4.12$, $p<.05$). Planned contrasts indicated that the index at 0° ($M=.15$, $SE=.04$) was smaller than indices at 3° ($M=3$, $SE=.04$, $p=.05$), 6° ($M=.37$, $SE=.06$, $p<.01$) and 9° ($M=.38$, $SE=.06$, $p<.01$).

(2) $SI_1 = 1 - (\frac{SS_1}{SC_1})$

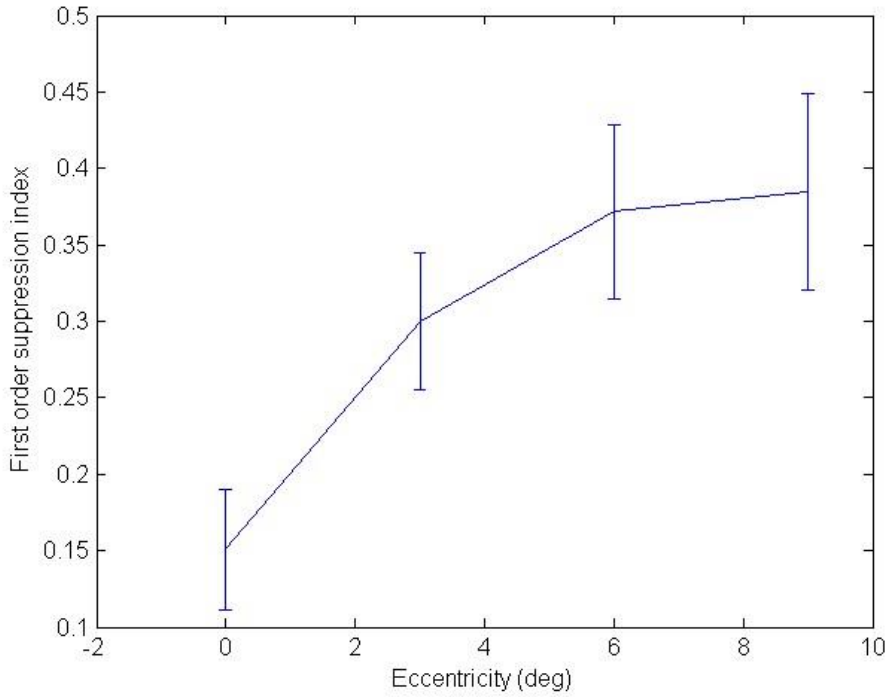

Figure 5-8 Average first order surround suppression index (11 participants). Standard errors shown.

5.4.2 Summary of pRF Surround Size, Centre Size and Surround/Centre Ratio

Estimates of centre size, surround size and surround/centre ratio were made in visual areas V1, V2d, V2d, V2v, V3d, V3v and V3A of the same 11 participants used in the psychophysical task. For all analyses, dorsal and ventral portions of the visual areas were summed. Centre size is an estimate of the width of the excitatory centre region of the pRF. Surround size is an estimate of the width of the inhibitory surrounding Gaussian of the pRF. The suppression ratio is a measure of the relative difference between centre and surround sizes. The 3 pRF parameters were binned to match the eccentricities of the psychophysical stimulus patches (0°, 3°, 6° and 9°). To explore differences in measures of pRF, 2-way ANOVAS were run with visual areas and eccentricity as factors.

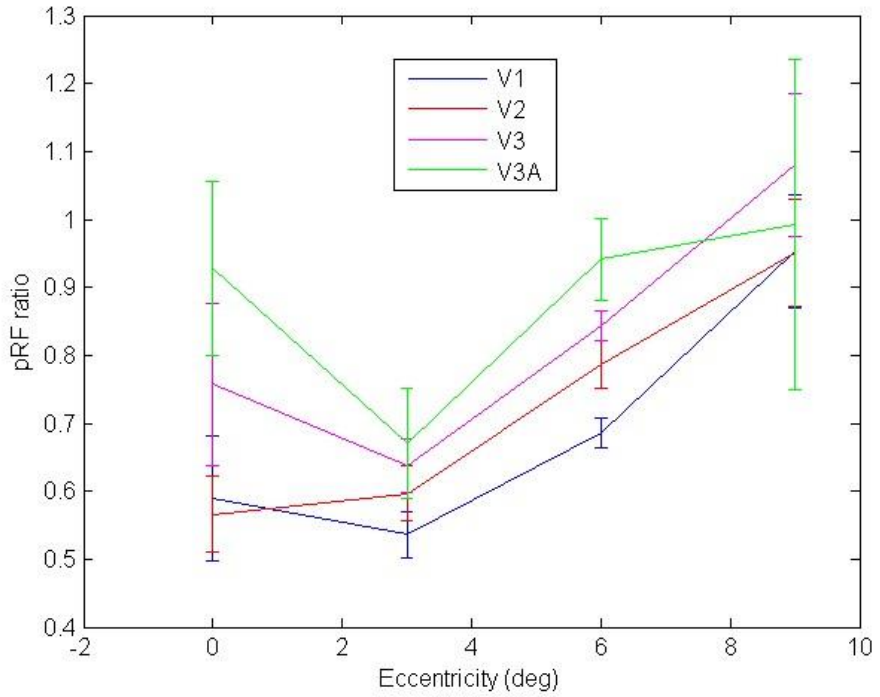

Figure 5-9 Average pRF surround/centre ratio for visual areas V1, V2, V3 and V3A (11 participants). Standard errors shown.

Figure 5-9 illustrates surround/centre ratios in visual areas V1, V2, V3 and V3A at 4 eccentricities. A 2-way ANOVA demonstrated a main effect of visual area ($F(3,160)=3.59$, $p<.05$). The pRF surround/centre ratio in V1 ($M=.71$, $SE=.04$) was significantly lower than the pRF surround/centre ratio in V3A ($M=.88$, $SE=.07$; $p<.01$). There was also a main effect of eccentricity ($F(3,160)=12.18$, $p<.001$). Ratios were lower at lower eccentricities. This difference was significant between 0° and 9° ($p<.001$), 3° and 6° ($p<.05$), 3° and 9° ($p<.001$) and between 6° and 9° ($p<.05$).

Surround/centre ratios for all visual areas were submitted to a bivariate correlation. V1 correlated strongly with both V2 ($R=.81$, $p<.001$) and V3 ($R=.7$, $p<.001$). V1 also correlated with V3A ($R=.36$, $p<.05$). Centre/surround ratio of V2 correlated with V3 ($R=.63$, $p<.001$) but not V3A ($R=.15$, $p=.33$). V3 did not correlate with V3A ($R=.28$, $p=.07$). The correlation between V1 and V2 limits linear regression analyses using this data as collinearity is introduced. The weaker correlations between later areas are less problematic. Surround/centre ratios for V1, V2, V3 and V3A were not strongly correlated with either eccentricity ($R=.6$, $p<.001$; $R=.64$, $p<.001$; $R=.43$, $p<.01$; $R=.12$, $p=.49$) or eccentricity squared ($R=.6$, $p<.001$; $R=.66$, $p<.001$; $R=.49$, $p<.01$; $R=.15$, $p=.33$).

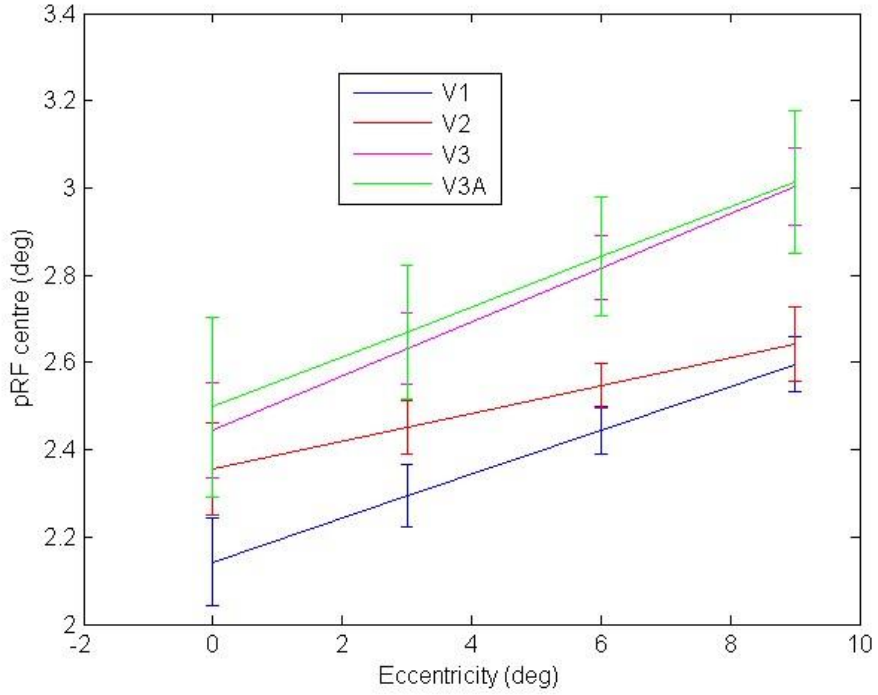

Figure 5-10 Average pRF centre size (deg) for visual areas V1, V2, V3 and V3A (11 participants) Standard errors shown.

Figure 5-10 indicates that centre size increases with eccentricity. A 2-way ANOVA demonstrated a main effect of eccentricity ($F(3,160)=12.89$, $p<.001$). Centre size was smaller at 0° (M=2.36, SE=.07) than 3° (M=2.51, SE=.05, $p<.001$), 6° (M=2.66, SE=.05, $p<.001$) and 9° (M=2.81, SE=.06, $p<.001$). Centre size at 3° was smaller than centre size at both 6° ($p<.001$) and 9° ($p<.001$). Centre size at 6° was smaller than centre size at 9° ($p<.001$).

A main effect of visual area was also identified ($F(3,160)=11.53$). Centre size in V1 (M=2.37, SE=.04) was smaller than centre size in V2 (M=2.49, SE=.04, $p<.05$), V3 (M=2.72, SE=.05, $p<.001$) and V3A (M=2.76, SE=.09). V2 centre size was smaller than both V3 ($p<.001$) and V3A ($p<.01$). No interaction between eccentricity and visual area was seen ($p=.99$).

Centre sizes for all visual areas were submitted to a bivariate correlation. V1 centre size correlated with V2 ($R=.63$, $p<.001$), V3 ($R=.61$, $p<.001$) and V3A ($R=.39$, $p<.01$). V2 centre size correlated with V3 centre size ($R=.48$, $p<.01$) but not V3A centre size ($R=.09$, $p=.56$). V3 centre size correlated with V3A centre size ($R=.59$, $p<.001$). Whilst

significant correlations exist between visual areas in measures of centre size, these links are not considered strong enough to limit subsequent linear regression analyses using this data. V1, V2, V3 and V3A centre size were not strongly correlated with either eccentricity (R=.58, p<.001; R=.39, p<.01; R=.59. p<.001; R=.34, p<.05) or eccentricity squared (R=.56, p<.001; R=.38, p<.05; R=.57, p<.001; R=.33, p<.05).

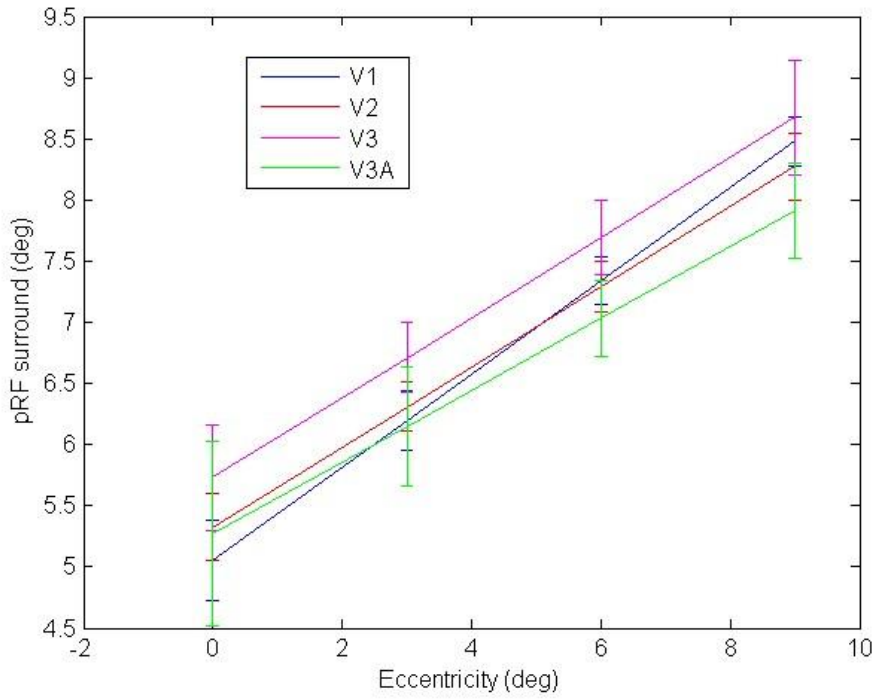

Figure 5-11 Average pRF surround size (deg) for visual areas V1, V2, V3 and V3A (11 participants). Standard errors shown.

Figure 5-11 displays pRF surround size of visual areas V1, V2, V3 and V3A. A 2-way ANOVA indicated a main effect of eccentricity ($F(3,160)=50.15$, $p<.001$). Surround size at 0° (M=5.35, SE=.24) was smaller than surround size at 3° (M=6.34, SE=.16, p<.001), 6° (M=7.33, SE=.13, p<.001) and 9° (M=8.34, SE=.17, p<.001). Surround size at 3 was smaller than surround size at both 6° (p<.001) and 9° (p<.001). Surround size was smaller at 6° than at 9° (p<.001). There was no main effect of visual area (p=.12) and no interaction (p=.99).

A bivariate correlation of surround size in all visual areas showed multiple strong links. V1 correlated strongly with both V2 (R=.88, p<.001) and V3 (R=.82, p<.001). A link was also seen between V1 and V3A (R=.53, p<.001). V2 correlated with V3 (R=.83, p<.001)

and V3A (R=.53, p<.001). V3 correlated with V3A (R=.41, p<.01). Linear regressions reported in Chapters 5, 6 and 7 will be limited to some extent by the collinearity of surround size across visual areas. The links between V1, V2 and V3 are particularly problematic.

Additional analyses indicated that the surround size of V1 and V2 correlated strongly with both eccentricity (R=.85, p<.001; R=.82, p<.001) and eccentricity squared (R=.82, p<.001; R=.79, p<.001). For this reason, eccentricity and eccentricity squared will be included as additional covariates in subsequent linear regression analyses. V3 and V3A surround size were not strongly correlated with either eccentricity (R=.67, p<.001; R=.52, p<.001) or eccentricity squared (R=.65, p<.001; R=.49, p<.01).

5.4.3 The Relationship between pRF Surround Size and First Order Surround Suppression

The first order surround suppression index is a measure of the difference between luminance matching without a surround and luminance matching with a surround. A high suppression index indicates a high amount of perceptual suppression. pRF surround sizes in V1, V2, V3 and V3A were submitted to a linear regression to predict first order surround suppression indices (table 5-1). Eccentricity squared and eccentricity were included in this linear regression as additional covariates to remove the confounding, non-linear and linear effects of eccentricity. First order surround suppression index (SI_1) correlated with pRF surround size in V1 (T=2.21, p<.05; figure 5-12). Participants with high surround suppression had large V1 pRF surround sizes. The link between perceptual suppression and V1 is consistent with previous research (Zenger-Landolt & Heeger, 2003). Additional analyses were performed at 4 eccentricities. The link between first order surround suppression indices and V1 pRF surround size was non-significant at all eccentricities (0° p=.08; 3° p=.32; 6° p=.33; 9° p=.11).

As mentioned above, a bivariate correlation indicated that visual areas correlated in measures of surround size. The linear regression is limited to some extent by the presence of collinearity. The link between V1 and V2 was particularly strong (R=.88, p<.001). It is therefore difficult to confirm whether the link between perceptual surround suppression

and pRF surround size was driven by V1 or by V2. Additionally, conclusions drawn from this finding must be tentative as V1 and V2 also correlated with eccentricity and eccentricity squared. Although, a partial correlations controlling for eccentricity and eccentricity squared demonstrated that the first order suppression index correlated with V1 surround size (R=.4, p<.01) but not V2 surround size (R=.12, p=.45).

Table 5-1 First order suppression index predicted from pRF surround size (deg). *p<.05 **p<.01 ***p<.001.

Model	B	SE	β
Constant	-.135	.192	
Eccentricity	.037	.028	.648
Eccentricity^2	-.004	.003	-.630
V1 Surround Size	.092	.042	.728*
V2 Surround Size	-.066	.045	-.465
V3 Surround Size	.034	.029	.293
V3a Surround Size	-.004	.015	-.042

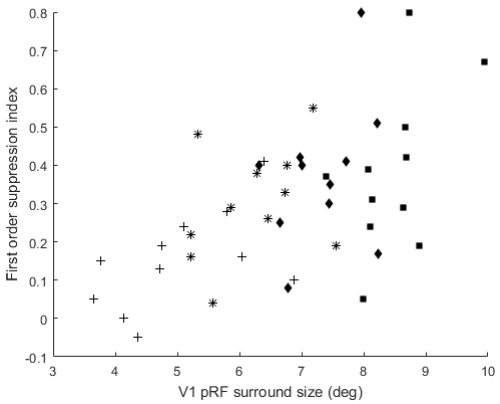

Figure 5-12 The relationship between first order surround suppression index and V1 pRF surround size (deg; p<.001). Each data point represents a single eccentricity patch for a single participant. Eccentricities are represented by different symbols (0°+; 3°*; 6°♦; 9°■).

5.4.4 The Relationship between pRF Centre Size and First Order Surround Suppression

A linear regression was performed to predict surround suppression from pRF centre size (table 5-2). V1 pRF centre size correlated with first order suppression indices (SI_1). High indices were associated with large V1 centre sizes ($T=3.15$, $p<.01$; figure 5-13). Participants with large V1 centre size experienced high levels of perceptual suppression. This link was identified only at 0° ($R=.619$, $p<.05$). It was non-significant at all other eccentricities (3° $p=.14$; 6° $p=.46$; 9° $p=.09$). The link between pRF centre size and surround suppression is unexpected and most likely driven by the positive correlation between measures of centre size and surround size. A correlation controlling for the effects of eccentricity and eccentricity squared demonstrated a strong link ($R=.54$, $p<.001$).

Table 5-2 First order suppression index predicted from pRF centre size (deg). *p<.05 **p<.01 ***p<.001.

Model	B	SE	β
Constant	-.478	.269	
Eccentricity	.044	.024	.779
Eccentricity²	-.004	.003	-.630
V1 Centre Size	.378	.120	.580**
V2 Centre Size	-.066	.115	-.094
V3 Centre Size	-.092	.102	-.171
V3a Centre Size	.080	.053	.238

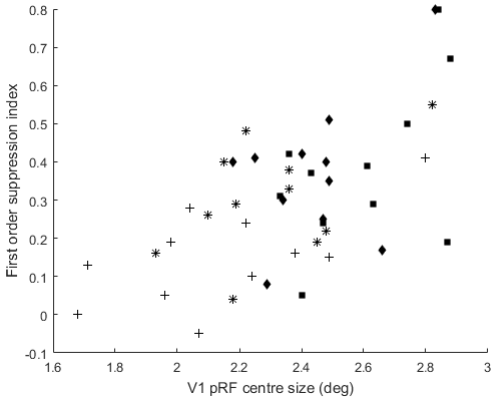

Figure 5-13 The relationship between first order surround suppression index and V1 pRF centre size (deg; p<.001). Each data point represents a single eccentricity patch for a single participant. Eccentricities are represented by different symbols (0°+; 3°*; 6°♦; 9°■).

5.4.5 The Relationship between pRF Surround/Centre Ratio and First Order Surround Suppression

The pRF surround/centre ratio did not correlate with the first order suppression index (SI_1). Estimates of pRF surround/centre ratio did not predict perceptual surround suppression in any area (table 5-3). This included both V1 (p=.37) and V2 (p=.37). Again, this linear regression was limited to some extent by the presence of collinearity. V1 surround/centre ratio correlated strongly with V2 surround/centre ratio (R=.81, p<.001).

Table 5-3 First order suppression index predicted from pRF surround/centre ratio sizes. *p<.05 **p<.01 ***p<.001.

Model	B	SE	β
Constant	.222	.111	
Eccentricity	.045	.029	.803
Eccentricity²	-.002	.003	-.308
V1 Centre Size	-.187	.207	-.258
V2 Centre Size	.202	.221	.250
V3 Centre Size	-.110	.123	-.179
V3a Centre Size	.009	.061	.023

5.5 Discussion

The experiment reported here showed that individual differences in V1 receptive field parameters predicted perceptual susceptibility to first order surround suppression. V1 pRF surround size was closely related to surround suppression in a psychophysical task. Previous research has indicated that V1 is the cortical locus of first order surround suppression (Levitt & Lund, 1997), the results outlined here support this proposal. More broadly, this experiment also expanded the finding of Duncan and Boynton (2003), that retinotopic parameters can constrain low level visual abilities. In an analogous way to the constraint imposed on acuity by cortical magnification (Duncan & Boynton, 2003), pRF surround size limited perceptual surround suppression.

The identification of a correlation between pRF surround size and perceptual surround suppression expands understanding of the cortical basis of surround suppression by bridging human fMRI studies (Zenger-Landolt & Heeger, 2003) and animal neurophysiological experiments (Levitt & Lund, 1997). Zenger- Landolt and Heeger (2003) reported a strong link between V1 and surround suppression. BOLD responses in V1 were suppressed when a target grating was presented with surround. The data presented in this chapter confirmed that the BOLD response suppression identified by Zenger-Landolt and Heeger (2003) was due to the receptive field properties of the V1 neurons described by Levitt and Lund (1997). It also supports the assertion of Zenger-Landolt and Heeger (2003) that perceptual suppression of first order stimuli is closely linked to V1 activity.

A link was also noted between V1 centre size and first order surround suppression. Participants with large V1 centre size experienced higher levels of perceptual surround suppression. I argue that this relationship is most likely a result of the close correlation between V1 centre and surround size. Participants with large V1 centre size had large V1 surround size, even when the effect of eccentricity was controlled for.

High intra-individual variability was seen in both psychophysical abilities and pRF surround size, centre size and ratio. The effect of eccentricity was dominant in all measures. Mirroring the cortical magnification experiments (Chapters 2 & 3), retinotopic

measures predicted intra-individual variability in perception. Despite this strong effect, it was not the sole sources of variance. Following removal of eccentricity through its inclusion as a covariate in the linear regressions reported here, a relationship between pRF surround size and psychophysical surround suppression remained.

Broadly, the experiment reported here provides confirmation that pRF is a suitable method by which to directly compare the parameters of receptive fields to the psychophysical phenomenon of surround suppression, unifying data from the fields of neurobiology and perceptual psychology. This presents novel opportunities for researching the neurophysiological basis of individual differences in perceptual abilities. Future research should expand the use of pRF methods to the exploration of more complex visual tasks.

pRF size and cortical magnification are not independent of one another. At higher eccentricities receptive field sizes are larger (Hubel & Wiesel, 1974) and cortical magnification is lower (Duncan & Boynton, 2003). Harvey et al. (2011) demonstrated that individual variations in V1 cortical magnification, V1 pRF size and V1 surface area are correlated. The close association between these retinotopic characteristics must be considered when examining the correlation between perceptual abilities and pRF size. Ideally, future research should examine the possibility that the perceptual ability is predicted more strongly by either cortical magnification or surface area. Both these characteristics have been previously shown to correlate with visual abilities (Duncan & Boynton, 2003; Schwarzkopf et al., 2011).

6 Population Receptive Field (pRF) Surround Size of V1 Correlates with Second Order Surround Suppression

6.1 Introduction

Under certain conditions, the presence of a surround will influence the perception of the contrast of a target stimulus (Chubb et al., 1989). Understanding of this phenomenon has generally been confined to first order stimuli (Cannon & Fullenkamp, 1993; Olzak & Laurinen, 1999). Recent work has attempted to expand investigation of this phenomenon to more complex visual stimuli. The locus of second order surround suppression is less well specified than that of first order. Psychophysical investigations of the suppressive interaction between first and second order stimuli indicate different underlying mechanisms (Ellemberg, Allen, & Hess, 2004; Morgan et al., 2000). This study aims to investigate whether the correlation between pRF estimates (surround size, centre size) and first order surround suppression is also seen for stimuli thought to engage higher levels of visual processing mechanisms.

Unlike first order stimuli, which can be detected by comparing light to dark and is therefore reliant solely on V1 neurons (Larsson et al., 2006), second order stimuli requires additional processing at later visual areas (Larsson et al., 2006). Second order stimuli are created through differences in texture between the stimulus and the background, features that cannot be processed by V1. These textures may comprise of local changes in orientation, spatial frequency or contrast (Wang, Heeger, & Landy, 2012). Whilst first order gratings are created through differences in luminance, in a second order grating the sum of the luminance across the stripes must equal the luminance level of the background.

Wang et al. (2012) describe the critical parameters required for second order surround suppression. Two forms of second order gratings were used; contrast modulated and orientation modulated. Using experimental procedures analogous to first order surround

suppression research (Cannon & Fullenkamp, 1991; Zenger-Landolt & Heeger, 2003) it was demonstrated that second order surround suppression occurs in the same way as first order suppression. Contrast modulated stimuli showed the orientation specificity of first order surround suppression (Xing & Heeger, 2000), but orientation modulated stimuli did not. Others suggest that that second order suppression is less sensitive to differences in orientation and spatial frequency between a target and a surround than first order suppression (Ellemberg et al., 2004).

Second order suppression occurs within a broader range of spatial frequencies and orientations than first order (Ellemberg et al., 2004). There is also an asymmetrical pattern seen in first and second order interaction. Perceived contrast of a second order stimulus can be disrupted by the presence of a first order surround, but the opposite effect is absent (Ellemberg et al., 2004). This indicates that the two forms of suppression are reliant on different mechanisms.

Investigations into the cortical basis of second order suppression are mixed in regards to providing support for the proposal that it is distinct from first order. Single cell recording has identified neurons in multiple visual areas that respond preferentially to second order stimuli. These include V2 (Rossi, Desimone, & Ungerleider, 2001) and MT (O'Keefe & Movshon, 1998). Human imaging studies provide inconsistent information about the cortical locus of first and second order suppression. Multiple investigations conclude that first and second order motion are processed in analogous ways (Dupont, Sáry, Peuskens, & Orban, 2003; Nishida, Sasaki, Murakami, Watanabe, & Tootell, 2003; Seiffert, Somers, Dale, & Tootell, 2003). For example, Seiffert et al. (2003) compared activation in V1, V2, V3, VP, V4v, V3A, LO and MT/MST during observation of first order motion to activation during observation of second order motion. Both conditions elicited similar responses across all visual areas.

Conversely, other studies indicate discrete and separate cortical loci for first and second order motion. Smith et al. (1998) identified a stronger response in V3 and V3A/B during observation of second order motion stimuli in comparison to first order. This result is supported by a similar finding presented by Wenderoth, Watson, Egan, Tochon-Danguy, and O'keefe (1999). Positron emission tomography (PET) activation was stronger in V3 during presentation of a second order plaid pattern than during presentation of a first

order pattern (Wenderoth et al., 1999). Perception of first order motion, but not second order, has been associated with V1 activity (Dumoulin, Baker, Hess, & Evans, 2003).

It is possible that human imaging studies have failed to provide a clear consensus on the locus of first and second order perception because although separate subpopulations of neurons are responsible for processing first and second order stimuli, these neurons are intermingled within visual areas (Larsson et al., 2006). For this reason, it may be more appropriate to use adaptation studies to investigate the neural loci of first and second order perception. Larsson et al. (2006) used an adaptation task to measure BOLD response during presentation of orientation modulated and contrast modulated textures. Unlike first order stimuli, second order stimuli showed greater adaptation in VO1 that V1. Perception of contrast modulated texture also correlated with adaptation originating in V3A/B and LO1 (Larsson et al., 2006).

It is likely that the regions underlying the processing of second order stimuli will also be the locus of second order surround suppression. To date, this hypothesis has not been directly tested. Britten and Heuer (1999) compared the interaction between multiple small Gabor stimuli presented in a single MT receptive field. Suppression was identified, neuronal responses during presentation of multiple stimuli simultaneous were less than responses to the component stimuli (e.g. the summed response of 2 stimuli presented in isolation). Although given the direct input to MT from V1 it is unknown whether the suppressive effect originated in MT or was inherited from the well- established normalization processes of V1 (Wang et al., 2012). The study presented in this chapter expanded the work of Britten and Hueur (1999) to better localise the visual area underlying second order suppression.

As for first order surround suppression, estimating population receptive field properties from fMRI data (pRF) may also inform the cortical underpinnings of second order surround suppression. The use of this technique in visual areas likely to underlie second order surround suppression (VO1, LO1, V3A/B) has not been investigated. Given the limitations of psychophysics in distinguishing between inherited surround suppression and local surround suppression at higher tier visual areas (e.g. Britten & Heuer, 1999), pRF estimation may provide an opportunity to better define the nature of second order surround suppression.

In this experiment I used estimates of surround suppression based on pRF methods to determine whether psychophysical thresholds correlated with surround suppression in specific cortical areas to identify a likely locus for second order processing mechanisms. pRF estimates of receptive field surround size, centre size and surround/centre ratios were measured for early visual areas V1, V2 and V3, in addition to intermediate visual area V3A. It was hypothesised that analogously to the constraint exerted on first order surround suppression by V1 receptive field properties (Chapter 5), second order surround suppression is limited by receptive field characteristics of later visual areas.

6.2 Estimation of pRF Surround Size, Centre Size and Surround/Centre Ratio

The pRF data (surround size, centre size, surround/centre suppression ratio) used here is taken from Chapter 5. See previous chapter for full details. Analysis methods were identical.

6.3 Psychophysical Estimation of Second Order Surround Suppression

This experiment was similar to the experiment reported in Chapter 5 in all respects but stimuli. The experimental procedures, task, participant group and experimental design were identical. See Chapter 5 for details.

6.3.1 Second Order Surround Suppression Stimuli

Stimuli consisted of contrast-modulated sinusoidal gratings generated as described in Larsson et al. (2006) by modulating the luminance contrast of an isotropic band-pass filtered noise carrier with a 50% contrast, 8cpd spatial frequency and 1 octave bandwidth (figure 6-2). Modulator frequency was 2cpd.

Target gratings were presented within a 3 degree wide circular aperture. In the surround suppression condition, the first target in each trial was surrounded by a high contrast grating (100%), with the same spatial frequency and phase as the target, displayed within an annulus (inner diameter 4 degrees, outer diameter 11 degrees). The parameters of the surround were identical to the parameters of the target except for size and contrast level (figure 6-1). The target and surround were separated by a 0.5 degree blank space with the same luminance as the background (21.6 cd). The edges of the target and surround stimuli were blurred to yield a soft edge. In the control condition, both the target and the matching grating were displayed in isolation (figure 6-3).

The target central stimulus had a constant contrast of 90% throughout the experiment. The surround of the target stimulus had a constant contrast of 100% throughout. There was a contrast difference of 85% between the target stimulus and the matching stimulus at the beginning of the trial (with a random jitter of between 5 and -5). The contrast of the matching stimulus was modulated in increments of 2% in response to the accuracy of participant responses.

The midpoint of the gratings (both alone and with a surround) were located at eccentricities of 0°, 3°, 6° or 9 °, dependent on condition. Gratings were displayed in either the upper right quadrant of the visual field or the upper left quadrant of the visual field. Central fixation of the screen was marked by a white 1 degree by 1 degree fixation cross. The background was consistently mean luminance (21.6 cd).

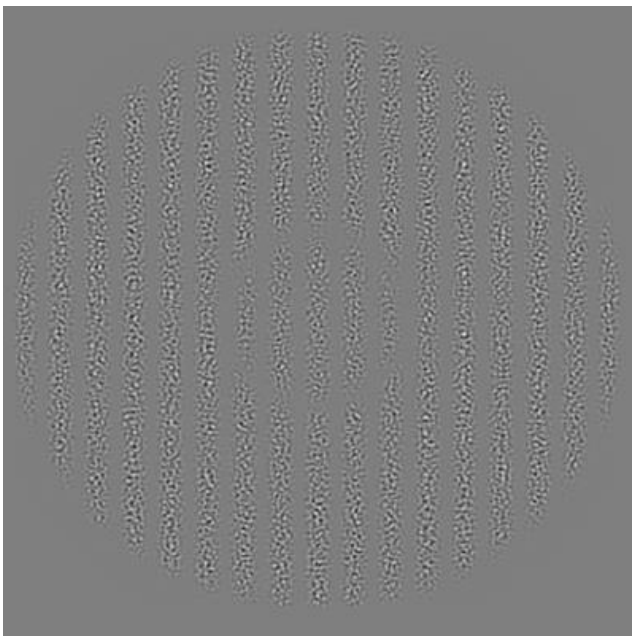

Figure 6-1 Second order surrounded stimulus

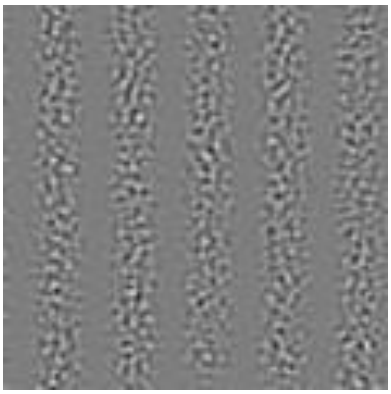

Figure 6-2 Magnified second order contrast-modulated pattern

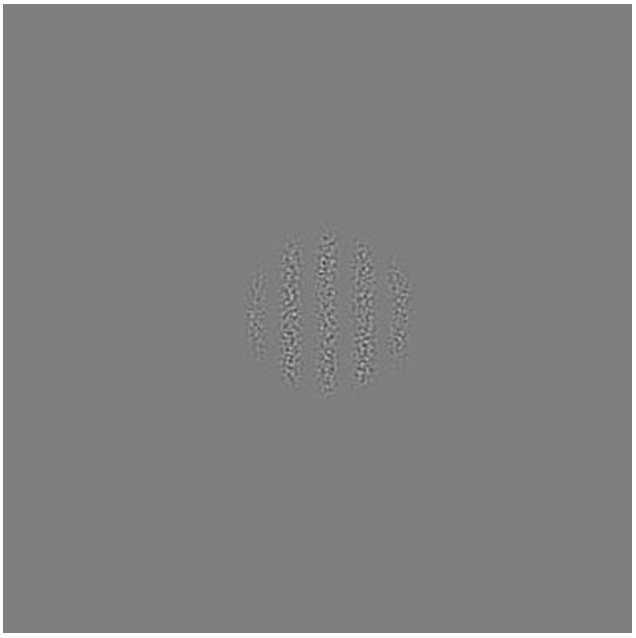

Figure 6-3 Second order control stimulus

6.4 Results

The results of this experiment indicated a correlation between V1 pRF surround size and second order surround suppression. Mirroring the link seen between V1 and first order, a large pRF surround size was associated with a high level of psychophysical second order surround suppression. Unlike first order suppression, no links were identified between V1 centre size and second order surround suppression.

6.4.1 Psychophysical Measurement of Second Order Surround Suppression

Each participant performed each condition (control and surrounded) of the discrimination task 5 times at each eccentricity; a mean was computed from these 5 values. For each participant in each visual field, 4 average thresholds were obtained. All participants performed the task in both the right and the left visual field. Results from the two visual fields were averaged.

A psychophysical suppression ratio (SS_2) for each block was calculated by dividing the staircase output (the matching contrast; Cmatch) by the contrast of the test stimulus (Ctest). Generally, a value of 1 indicated that the presence of a surround for the matching stimulus had not influenced the perceived contrast. Values lower than 1 indicated surround suppression. Computing suppression in this way is consistent with both the investigation into the correlation between first order surround suppression and pRF parameters (Chapter 5) and past research (Xing & Heeger, 2001). An analogous psychophysical suppression ratio (SC_2) was computed for the control condition. Comparing the control data (SC_2) in figure 6-4 to the control data (SC_1) in figure 5-6 indicates a higher level of within trial adaptation for second order perceived contrast.

(1) $SS_2 = \frac{Cmatch}{Ctest}$

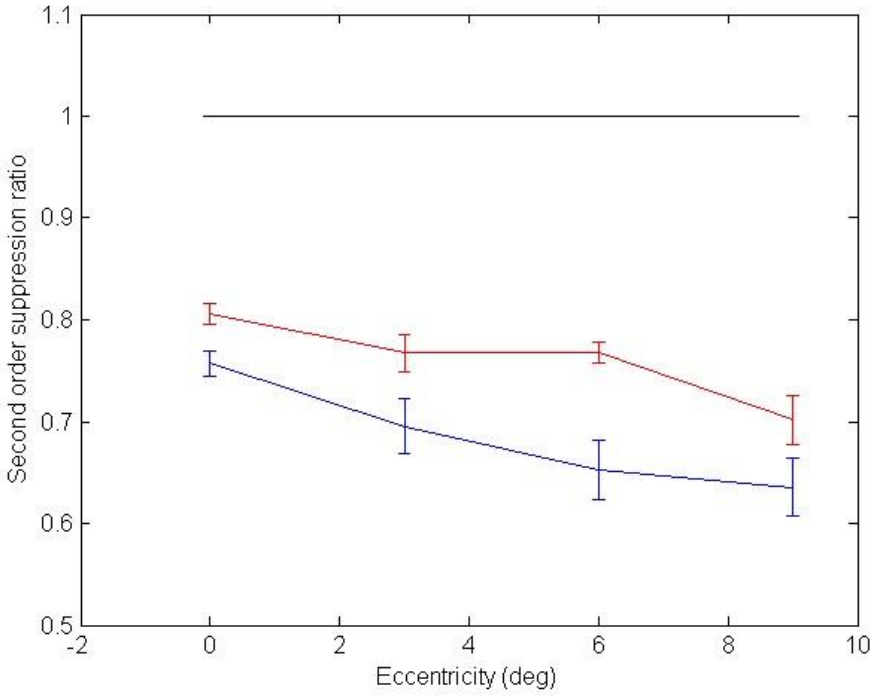

Figure 6-4 Average surround suppression ratio in a second order contrast matching task (11 participants). SC_2 in red and SS_2 in blue. Hypothetical performance in which perceived contrast of the matching stimulus is identical to the true contrast of the target (SS_2 =1) is in black. Standard errors shown.

A 2-way ANOVA was performed to examine interactions between the effects of eccentricity and the presence of a surround on perceived contrast. As indicated by figure 6-4, there was a significant main effect of eccentricity ($F(3, 80)= 9.62$, $p<.001$). Lower eccentricities were associated with higher suppression ratios. Planned contrasts revealed that the suppression ratio was significantly higher at 0° than 3° ($p<.05$). The suppression ratio was significantly higher at 6° than 9° ($p<.05$). There was also significant main effect of the presence of a surround ($F(1, 80)=24.47$, $p<.001$). The suppression ratio was lower when the match stimulus was surrounded (M=.69, SE=.01) than when it was presented alone (M=.76, SE=.01). There was no interaction between eccentricity and the presence of a surround ($p=.49$).

A suppression index (SI_2) was computed by dividing the surrounded suppression ratio by the control suppression ratio at the analogous eccentricity. This corrected for the eccentricity-specific effects of within trial adaptation. This value was then subtracted from 1. A high index indicates that the presence of a surround had a large impact on the

perceived contrast of the matching stimulus. Figure 6-5 indicates a strong effect of eccentricity in this index. In contrast with the first order surround suppression index, this relationship is not linear. An ANOVA indicated no statistically significant main effect of eccentricity (p=.09).

(2) $SI_2 = 1 - (\frac{SS_2}{SC_2})$

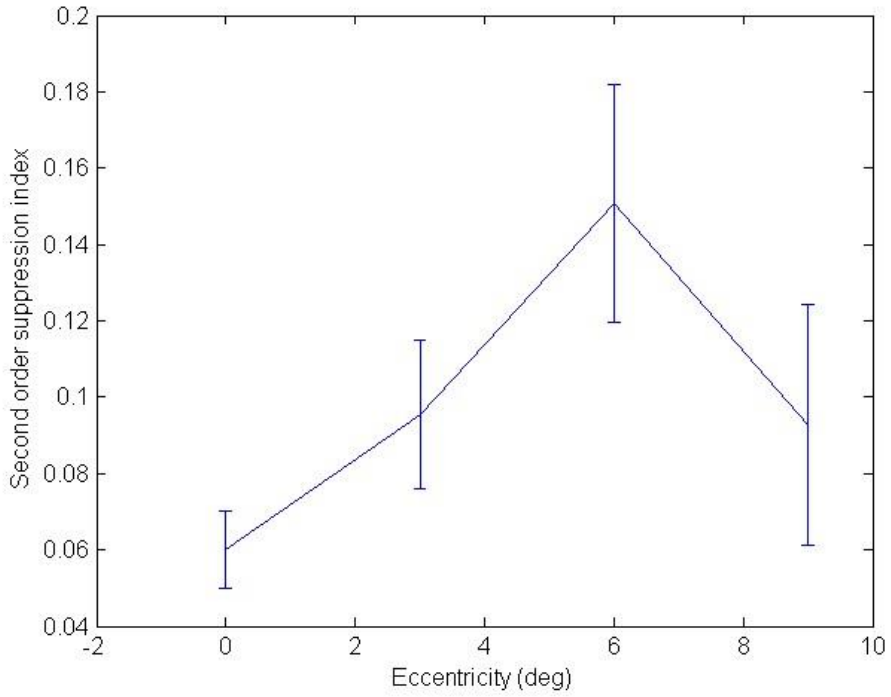

Figure 6-5 Average surround suppression index (SI_2; 11 participants). Standard errors shown.

6.4.2 The Relationship between pRF Surround Size and Second Order Surround Suppression

pRF surround sizes for visual areas V1, V2, V3 and V3A were submitted to a linear regression to predict psychophysical suppression indices (table 6-1). Eccentricity squared and eccentricity were included in this linear regression as additional covariates to remove the confounding, linear and non-linear effects of eccentricity. V1 was the only area to predict the psychophysical suppression (T=2.47, p<.05; figure 6-6). High perceptual

surround suppression was associated with large V1 surround size. This link was absent at specific eccentricities (0° p=.23, 3° p=.59, 6° p=.39, 9° p=.16). Due to the involvement of V3A in perception of second order stimuli (Larsson et al., 2006), correlations were expected in this area. V3A surround size did not correlate with the second order suppression index (p=.97).

As described in Chapter 5, V1 and V2 correlated strongly in measures of pRF surround size (R=.88, p<.001). It is difficult to separate the predictive role of V1 surround size from the role of V2 surround size. Furthermore, both V1 and V2 surround size correlated with eccentricity and eccentricity squared, suggesting that the link reported here may have been driven by the effect of eccentricity. The link between V1 surround size and perceptual suppression was lost when a partial correlation was performed controlling for the effects of eccentricity and eccentricity squared (p=.11).

Table 6-1 Second order suppression index predicted from pRF surround size (deg). *p<.05 **p<.01 ***p<.001.

Model	B	SE	β
Constant	.001	.096	
Eccentricity	.021	.014	.850
Eccentricity²	-.003	.001	-.967
V1 Surround Size	.052	.021	.917*
V2 Surround Size	-.030	.023	-.468
V3 Surround Size	-.009	.015	-.179
V3a Surround Size	.000	.008	.006

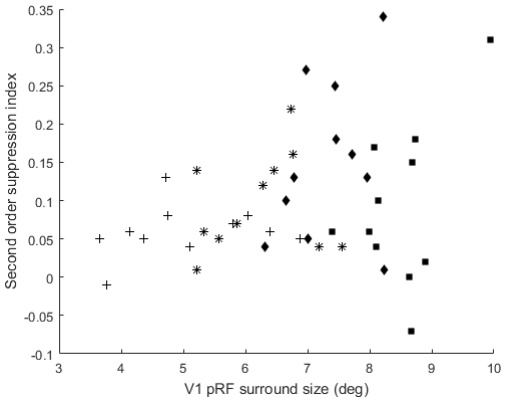

Figure 6-6 The relationship between second order surround suppression index and V1 pRF surround size (deg; p<.05). Each data point represents a single eccentricity patch for a single participant. Eccentricities are represented by different symbols (0°+; 3°*; 6°♦; 9°■).

6.4.3 The Relationship between pRF Centre Size and Second Order Surround Suppression

Second order surround suppression indices (SI_2) did not correlate with pRF centre size. Neither V1 (p=.82), V2 (p=.39), V3 (p=.85) nor V3A (p=.88) were correlated with the psychophysical suppression index (table 6-2).

Table 6-2 Second order suppression index predicted from pRF centre size (deg). *p<.05 **p<.01 ***p<.001.

Model	B	SE	β
Constant	.181	.153	
Eccentricity	.030	.014	1.194*
Eccentricity²	-.003	.001	-.967
V1 Centre Size	-.016	.068	-.053
V2 Centre Size	-.057	.066	-.181
V3 Centre Size	.011	.058	.047
V3a Centre Size	.005	.030	.031

6.4.4 The Relationship between pRF Surround/Centre Ratio and Second Order Surround Suppression

pRF surround/centre ratio measures were unrelated to second order surround suppression indices. Links were absent for all visual areas (V1 p=.27, V2 p=.12, V3 p=.16, V3A p=.97). Problematic levels of collinearity were present between parameters of this linear regression. V1 surround/centre ratio correlated strongly with V2 surround/centre ratio (R=.81, p<.001).

Table 6-3 Second order suppression index predicted from pRF surround/centre ratio. *p<.05 **p<.01 ***p<.001.

Model	B	SE	β
Constant	.091	.051	
Eccentricity	.018	.013	.718
Eccentricity²	-.001	.001	-.510
V1 Ratio	-.113	.096	-.349
V2 Ratio	.161	.102	.446
V3 Ratio	-.081	.057	-.295
V3a Ratio	-.001	.028	-.006

6.5 Discussion

The psychophysical literature regarding second order surround suppression is sparser than that addressing first order surround suppression. The data presented here further characterises this perceptual process. At lower eccentricities, between 0° and 6°, second order surround suppression mirrored first order surround suppression (Xing & Heeger, 2000). The amount of suppression increased with eccentricity. This finding addresses the predictions of Wang et al. (2012), confirming that the strength of second order surround suppression increase in the periphery.

In contrast with first order surround suppression, the second order suppression index decreased at 9°. Surround suppression at the furthest eccentricity measured was lower than the suppression at 6°, a reverse of the general eccentricity pattern. This finding can be attributed to performance in the control task, from which the suppression index was computed. When the second order stimuli is presented without a surround, performance in the periphery differs from performance in the fovea.

It is argued that the unusual eccentricity effect of the second order suppression index reflects a failure to accurately measure contrast matching ability in peripheral vision. Despite extensive pilot testing to identify suitable stimulus parameters, participants reported difficulty in perceiving the second order control stimulus when it was presented at 9°. Figure 6-5 indicates that the error at 9° was not larger than the error at other eccentricities, suggesting that repeating this condition additional times would not aid this limitation. It is possible that due to the high task difficulty, participants in the 9° condition failed to fixate at the centre of the screen and instead directed their gaze to the stimulus itself. Future research should use eye tracking measures to explore this possibility. The task difficulty may reflect the visual field representation of underlying cortical regions. For example, LO1 has been proposed a possible locus of second order perception (Larsson et al., 2006) and this retinotopic map over represents lower eccentricities (Larsson & Heeger, 2006).

In terms of links with pRF parameters, second order surround suppression shows a very similar pattern to first order (Chapter 5). The pRF data presented in this chapter shows a clear and positive link with V1 surround size. Participants with large V1 pRF surround size had high levels of perceptual suppression. No links were seen between second order surround suppression and any visual area later than V1. Analyses were limited to some extent by the strong correlation between V1 surround size and V2 surround size. It is possible that this collinearity masked relationships between perceptual surround suppression and V2.

It is surprising that all links were constrained to pRF estimates of the earliest visual area. It was hypothesised that the regions underlying the perception of second order stimuli would also be the locus of second order surround suppression. V3A (Larsson et al., 2006) and V2 (Rossi et al., 2001) have been shown to correlate with the perception of second order patterns. Instead, the data presented here indicates that V1 modulates perceptual suppression regardless of the complexity of the stimulus. In this way, the receptive field properties of V1 act as a bottle neck for contextual modulation throughout the visual cortex. This proposal does not conflict with the argument that second order surround suppression undergoes a second stage of processing at a later visual area (Ellemberg et al., 2004).

The finding that V1 receptive field properties constrain all surround suppression regardless of complexity is not consistent with the conclusions drawn from previous research, but also does not necessarily conflict with the data. For example, Britten and Heuer (1999) argued that the perceptual suppression of stimuli presented in an MT receptive field was evidence of contextual modulation at a visual area later than V1. The finding reported in this chapter suggests that the effect reported by Britten and Heuer (1999) may instead have been inherited from V1.

It is possible that whilst later regions are involved in second order surround suppression, at intermediate regions pRF parameters do not constrain psychophysical performance in such a straightforward way as is seen in V1. This would mimic the pattern seen between cortical magnification and visual ability. Duncan and Boynton (2003) demonstrated a strong link between V1 and perceptual abilities, but correlations between cortical magnification in later visual areas and perceptual abilities were weaker (Chapters 3 & 4). With progression through the cortex, it appears that it is more difficult to link specific abilities to specific areas. The findings of Larsson et al. (2006) also indicate that correlations may be seen between pRF measures in VO1 and LO1 and second order surround suppression. Unfortunately, as pRF parameters were not measured in VO1 and LO1, this hypothesis cannot be fully addressed.

In general, it appears that second order surround suppression is not a separate and distinct process to first order suppression. Psychophysically, the 2 processes show a similar pattern, at least at lower eccentricities. Unexpectedly all links between pRF estimates and second order suppression are located in V1. The later visual area previously linked to the perception of second order stimuli (Larsson et al., 2006) did not constrain second order surround suppression.

7 Individual Differences in Crowding are correlated with V1 pRF Centre Size

7.1 Introduction

Crowding describes the impairment in identifying a target when it is surrounded by other objects. In isolation, the target would be easily identifiable (Sayim, Greenwood, & Cavanagh, 2014). Specifically, the inability to recognise the target is caused by the disruptive influence of surrounding objects, not limited visual acuity. Unlike ordinary masking, crowding disrupts identification but not detection (Pelli, Palomares, & Majaj, 2004). Crowding is strongest in peripheral vision (Flom et al., 1963).

In addition to suppressing perceptual experience, the presences of additional stimuli can also suppress cortical activity. The neural location of the underlying cause of correlations between cortical suppression and perceptual suppression remains unconfirmed. Unlike first order surround suppression which is clearly localised to V1 (Zenger-Landolt & Heeger, 2003), the locus of crowding is poorly understood (Whitney & Levi, 2011).

There is some debate as to the earliest visual area involved in this phenomena. Due to the dichoptic nature of crowding (Tripathy & Levi, 1994), the process is known to occur in the cortex. Kastner, De Weerd, Desimone, and Ungerleider (1998) presented multiple complex stimuli simultaneously. fMRI responses in V1, V2, V4 and TEO were weaker during simultaneous presentation than when stimuli were presented alone or in succession. The presence of additional objects suppressed the cortical response. The differential responses in V1 to crowded and non-crowding stimuli indicate that crowding may occur as early as V1.

Later research expanded the work of Kastner et al. (1998) to investigate the presence of crowding in additional visual areas. Evidence of crowding was also noted in V3A and MT (Kastner et al., 2001). This indicates that both early and intermediate cortical areas are susceptible to the influence of crowding. Some have also argued that the process can been seen in later visual areas underlying object recognition (Louie et al., 2007).

Recognition of a face in peripheral vision was more highly impaired when the target was surrounded by upright faces than when it was surrounded by inverted faces (Louie et al., 2007).

In contrast to the V1 locus of proposed by Kastner et al. (1998), others have reported no evidence of crowding in this visual area (Arman et al., 2006). Arman et al. (2006) compared BOLD response in visual areas V1, V2, V3, V3A, V4 and LOC during a letter recognition task eliciting crowding and a letter recognition task without crowding. There was no difference in V1 activity between conditions. For later visual areas crowding related activity was consistent with the findings of Kastner et al. (1998, 2001), the effects of crowding were dispersed across multiple maps.

Crowding may originate as a result of low level processes. Parkes, Lund, Angelucci, Solomon, and Morgan (2001) proposed spatial pooling as a possible explanation. During observation of a collection of objects, textural analysis occurs. Instead of examination of a single object, the average properties of the full collection is computed. For example, when looking at a group of tilted lines, the mean orientation can be estimated (Dakin & Watt, 1997). In this way, the properties of the target are identified but this information does not reach conscious perception because it is pooled with other information at an early stage in the visual system.

Later studies conflict with the spatial pooling explanation of Parkes et al. (2001). Livne and Sagi (2007) investigated orientation and contrast discrimination for crowded Gabor patches. The 8 surrounding patches were positioned to produce either a global smooth contour or a random arrangement. The mean orientation of the flankers remained consistent throughout. The crowding effect was stronger for the smooth contour arrangement. This conflicts with the crowding explanation of Parkes et al. (2001) as although the mean orientation was identical in the smooth and random conditions, the crowding effect differed.

An alternative explanation similar to the spatial tuning hypothesis (Parkes et al., 2001) has been suggested by Levi (2008). Whilst some combining of the multiple signals occurs, the influence of each flanker is not equal. According to the “maximum rule” (Levi, 2008), all components of the image are analysed independently. However, unlike

the spatial pooling explanation of Parkes et al. (2001), only the detector with the greatest strength feeds forward to the next stage of processing.

MRI data supports the argument that crowding can be linked to low level cortical parameters. Crowding has been attributed to large receptive fields. This hypothesis states that when the target and the flankers are positioned within the same receptive field, perception of the target is compromised. Kastner et al. (2001) demonstrated that the spacing of simultaneously presented stimuli correlates with the suppression of BOLD response, a cortical marker of crowding. The spaces required for disruption matched the estimated receptive field sizes of each visual area. For example, the fMRI response in V2 was diminished at a spatial separation of 2-4 degrees, corresponding with the receptive field size recorded in physiological research (Gattass et al., 1981).

The evidence regarding the cortical basis of crowding has led some to believe that surround suppression and crowding share a common mechanism, most likely involving the retinotopic organisation of receptive fields. Conceptually, crowding appears very similar to surround suppression. In both cases, the identification of a target is disrupted by the close proximity of additional stimuli, particularly in the periphery (Flom et al., 1963; Snowden & Hammett, 1998).

Independent psychophysical investigations into crowding and surround suppression have demonstrated several similarities. Both processes scale with eccentricity. Bouma's law (Bouma, 1970) states that in crowding, the distance between flanker and target increases with movement towards the periphery. For full visual isolation, the flankers must be presented within a distance equal to 50% of the target's location. For example, crowding will occur if flankers of a target at 6° are located at a distance of less than 3° from the target. This eccentricity relative effect is also seen for surround suppression (Petrov & McKee, 2006). Surround suppression declines as the distance between the target and the surround increase. The proximity between target and surround required for suppression decreases at greater eccentricities.

Others argue that crowding and surround suppression are distinct and separate processes. An investigation of crowding and surround suppression using comparable stimuli supports this argument (Petrov et al., 2007). Inward- outward anisotropy is present in crowding but not surround suppression. Perception of a target with a half-annulus high

contrast surround is not affected by the location of the surround. Perception with a surround annulus positioned outwards relative to fixation was equal to perception with an inward surround. Conversely, when a contrast defined grating was crowded by a checkerboard flanker, performance was effected by the position of the flanker relative to fixation. An outward flanker caused greater levels of crowding. It has been argued that this form of anisotropy should be used as the litmus test for crowding (Levi, 2008).

Stronger links can be drawn between the two processes by understanding the underlying neurological processes. Surround suppression is correlated with multiple dimensions of population receptive fields (pRF). Earlier chapters (5 & 6) demonstrated that individual variation in surround suppression susceptibility is correlated with the surround size of receptive fields. If crowding susceptibility can be linked to these retinotopic properties, it would indicate that surround suppression and crowding may be different levels of the same phenomenon.

Cai, He, and Fang (2014) presented crowded stimuli to participants during collection of fMRI data. Both the target and the flankers consisted of sine wave gratings. Flankers were presented either perpendicularly or parallel relative to the target, producing weak or strong crowding. V2 voxels responded in a condition-specific way. A pRF analysis technique demonstrated that the pRF size of the strong crowding responsive voxels were larger than the pRF sizes of the voxels which showed activation in the weak crowding condition. This study indicates that crowding is closely associated with receptive field sizes. It also suggests that any cortical correlations of individual differences in crowding susceptibility will be located in V2.

The findings of Cai et al. (2014) are limited by the pRF techniques used. They performed analyses with a single measure of receptive field size, they did not estimate surround size specifically. The use of recent advances in pRF mapping (Zuiderbaan et al., 2012) allows measures of surround size, centre size and surround/centre ratio to be taken. As surround size has been shown to be particularly important in predicting perceptual surround suppression (Chapter 5), this measure would also be expected to correlate with crowding.

7.2 Estimation of pRF Surround Size, Centre Size and Surround/Centre Ratio

The pRF data used here is taken from Chapter 5. See Chapter 5 for full details. Analysis methods were identical.

7.3 Psychophysical Measurement of Crowding

7.3.1 Participants

9 participants (2 males) took part in this experiment. All participants used in the experiment reported here also participated in the experiments reported in Chapters 2, 3, 4, 5 and 6. All participants had normal or corrected to normal vision and were aged between 22 and 35. Written consent was obtained from all participants. The experimental procedure was in accordance with the Declaration of Helsinki and was approved by the appropriate local ethics committee.

7.3.2 Crowding Experimental Procedures

Testing took place in a quiet, dark room. Subjects sat 57cm from a screen the head was stabilized through the use of a chin rest. Stimuli were binocularly viewed on 37cm by 30cm sized screen. Stimuli were presented on an EIZO 660-M monochrome CRT monitor which had been gamma corrected. There was a frame rate of 60.02Hz. Presentation of stimuli and acquisition of responses was carried out using Matlab 7.4.0 (R2007a) and MGL (http://www.pc.rhul.ac.uk/staff/J.Larsson/software.html) run on a Linux operating system.

7.3.3 Crowding Control Stimuli

Control stimuli were taken from Chapter 4. Stimuli consisted of radial frequency pattern modulated shapes (figure 7-1). The stimulus had a peak spatial frequency of 0.5 cpd, a contrast of 100% and a mean radius of 2 degrees of visual angle. Stimuli were generated in an analogous way to Silson et al. (2013) but used 3 independently modulated radial frequencies (0, 3 and 7 cycles per stimulus). The shapes were located at various eccentricities. Dependent on the condition, the midpoint of the shape was at an eccentricity of 0°, 3°, 6° or 9°. Shapes were displayed in either the upper right quadrant of the visual field or the upper left quadrant of the visual field. Central fixation of the screen was marked by a white 1 degree by 1 degree fixation cross. The background was consistently mean luminance (21.6 cd). At all times in the control condition there was no more than 1 radial frequency shape displayed.

Figure 7-1 Crowding control stimulus. Single radial modulated shape.

7.3.4 Crowded Stimuli

Crowded stimuli were identical to control stimuli, but the first (test stimulus) and second (matching stimulus) shapes was surrounded by 2 additional shapes (flankers). The flankers were positioned tangentially on the screen (e.g. If the target was positioned in the

upper left quadrant of the visual field then the flankers were positioned at 45° and 225° relative to the target; figure 7-2). The flankers were placed along the tangent line. The distance between the target and the flankers remained constant throughout all crowded trials. The distance was 2.4 degrees from the centre of the target shape. The matching stimulus was presented with the same flankers as the target stimulus.

All flanker parameters except radial frequency and position were identical to the parameters of the target shape (e.g. radius, peak spatial frequency, contrast). The radial frequency of the flankers was randomly computed at the start of each trail. The radial frequency of the flankers was computed independently to that of the target shape, resulting in the flankers appearing dissimilar to the target shape. Depending on the randomized of the radial frequency of the flankers, the dissimilarity between the target and the flankers differed. For example, in figure 7-2 the flankers appear almost identical to the target but in other trials the flankers looked very different to the target.

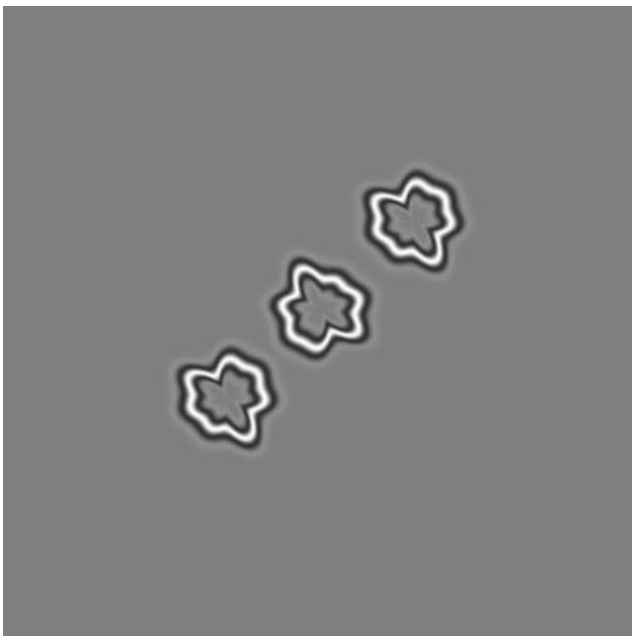

Figure 7-2 Crowded stimulus. Target radial modulated shapes with 2 flanker radial modulated shapes. This figure represents the position of the stimulus in the upper-left visual field presentation condition.

7.3.5 Crowding Task

Participants performed a temporal two-alternative forced choice shape matching task, judging whether two sequentially presented stimulus patters were the same. Thresholds for the minimum perceivable difference in radial amplitude between the test stimulus and matching stimulus were obtained using a 1 up 2 down staircase with increments in radial amplitude of 0.07. The difference in radial amplitude between the test and matching stimuli at the start of each trial was 0.5. Participants compared the test stimulus to the matching stimulus, whilst ignoring the flankers. The first shape (test stimulus) was displayed for 0.5s. There was an inter-stimuli interval of 0.5s in which a fixation cross was displayed. A second shape (of a different radial amplitude to the first) was then displayed. The second shape was the matching stimulus. The second shape was rotated 45 degrees in comparison to the first. Participants then made a button press response to indicate whether the matching stimulus was the same or different to the target stimulus, for which 2.5s was permitted. Participants had control over the onset time of the next trial, indicating via a second button press that they were prepared for another trial. 60 pairs of shapes were presented in each block of trials. Each block produced 1 threshold value. A single trial is represented schematically in figure 7-3.

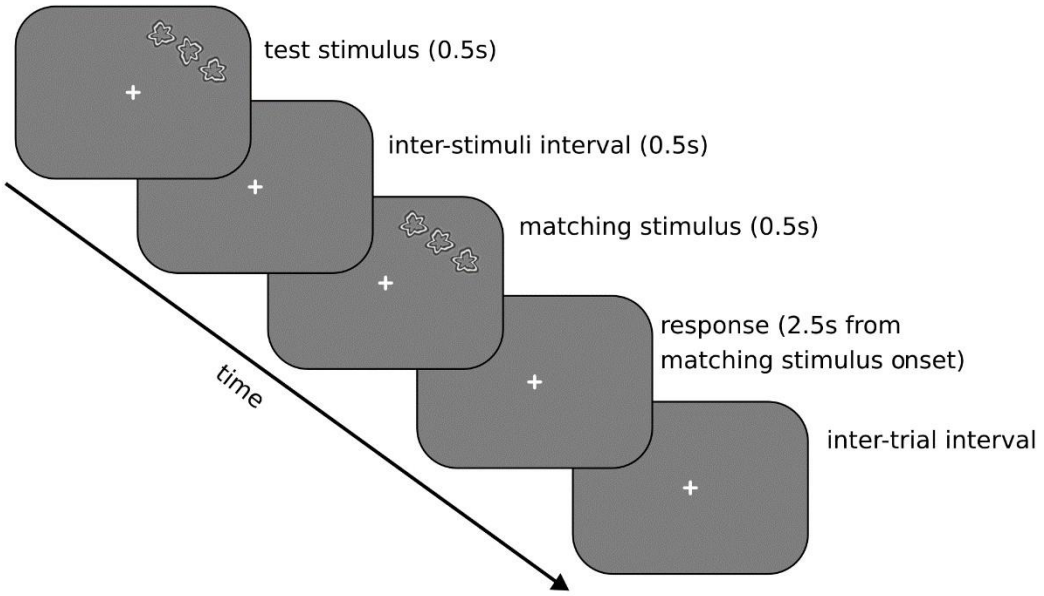

Figure 7-3 Crowding experimental paradigm: schematic representation of a single trial. A trial in the crowded condition (upper right visual field presentation condition) is shown. Control trials were identical but the matching stimulus was presented without flankers.

Participants were instructed to keep their eyes focused on the fixation cross throughout the trials. This instruction was repeated regularly throughout the testing session. Participants were informed that the second shape may be rotated in comparison to the first, but that the rotation should not be considered during the judgement of similarity. They were told that if the 2 shapes were identical except for the rotation, they should indicate that the 2 shapes were the same.

Each testing sessions began with a short practice phase. This usually consisted of 1 block of trials, but occasionally lasted for 3 blocks of trials for inexperienced subjects. In each testing session the grating was presented at 4 eccentricities. Each eccentricity was repeated 2 times with flankers and 2 times without flankers. Blocks with flankers (crowded condition) and blocks without flankers (control condition) were alternated. If a threshold was not achieved, the block was repeated. Failure to achieve a threshold was determined by inspecting the staircase output following each block of trails. In total there were 16 blocks of trials. The testing sessions took approximately 60 minutes, including a break of 10 minutes half way through the experiment. Subjects attended 4 testing sessions. 2 testing sessions included trials in only the left visual field and 2 sessions included trials in only the right visual field.

7.3.6 Crowding Experimental Design

This task was carried out at a range of eccentricities (0°, 3°, 6°, 9°) and in 2 quadrants of the visual field (upper left and upper right). The task was also carried out with 2 different crowding conditions (flankers at a distance of 2.4 degrees no flankers). Within each block of trials, the gratings were always at the same eccentricity, within the same quadrant of the visual field and of the same flanker condition. Eccentricity was changed between blocks in a semi- randomised fashion. Blocks of the same eccentricity were not performed consecutively. Within each block of 4 runs, each eccentricity was used once. Within each testing session, the shapes were always within the same quadrant of the visual field. Within a single testing session, crowded and non-crowded runs were alternated.

7.4 Results

Crowding correlated with pRF centre size of V1. Mirroring first and second order surround suppression, this link indicated that high levels of crowding are associated with large V1 pRF size. Crowding was unrelated to pRF surround size and pRF surround/centre ratio.

7.4.1 Psychophysical Measurement of Crowding

Each participant performed each condition (shape matching with flankers and shape matching without flankers) 8 times at each eccentricity. The task was performed in 4 times in the left visual field and 4 times in the right visual field. An average crowding ratio was computed from the 8 thresholds control condition blocks (CC). Similarly, an average crowding ratio was computed from crowded condition blocks (CS). The crowding ratio was computed by dividing the radial frequency of the matching stimulus by the radial frequency of the target stimulus. A high ratio indicates a high level of crowding. These ratios are displayed in figure 7-4.

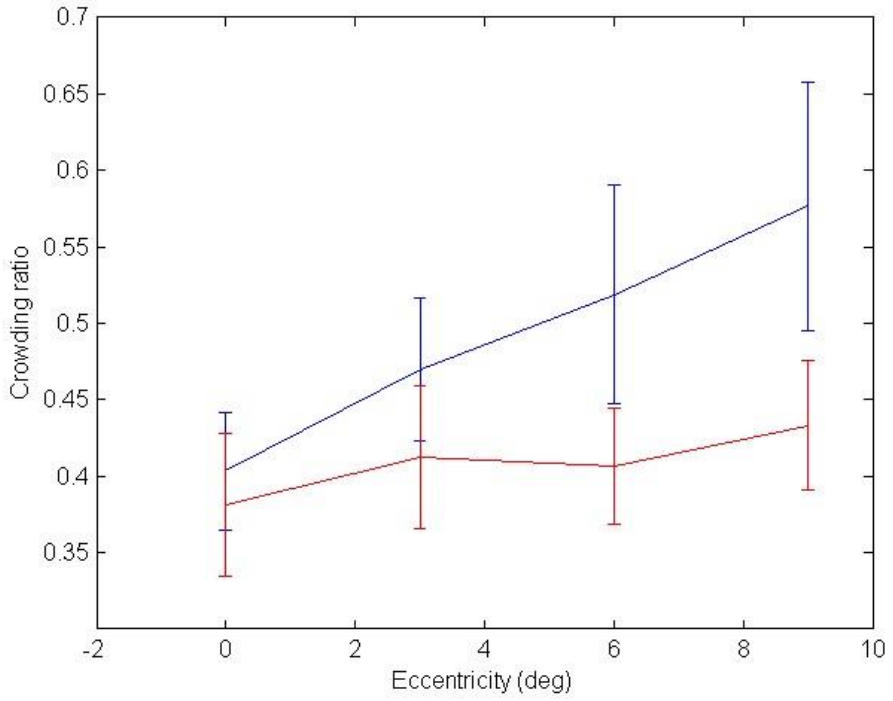

Figure 7-4 Average crowding ratio in a shape matching task (9 participants). Crowded condition (CS) in blue, control condition (no flankers; CC) in red. Standard errors shown.

A 2-way ANOVA was performed to examine interaction between the effects of eccentricity and the presence of flankers (e.g. CS vs. CC) on shape matching. There was not a main effect of eccentricity ($F(3, 64)= 1.53$, $p=.22$). There was a significant main effect of the presence of flankers ($F(1, 64)=4.98$, $p<.05$). The crowding ratio was high when the stimulus was presented alone ($M=0.41$, $SE=0.02$) than when it was presented with flankers ($M=0.49$, $SE=0.03$). There was no interaction between eccentricity and the presence of flankers ($F(3,64)=.53$, $p=.67$).

A crowding index (CI) was calculated for each participant at each eccentricity by dividing the crowding ratio in the crowded condition (CS) by the crowding ratio in the control condition (CC). This value represents the disruption to shape discrimination attributed to the presence of flankers. This value corrected for the eccentricity-specific effects of adaptation in shape matching. A value of less than 1 indicated no crowding. Values greater than 1 indicated crowding. A crowding index computed in this way is consistent with previous research (Levi & Carney, 2009). A one-way ANOVA demonstrated no difference between eccentricities ($F(1,32)=.07$, $p=.54$), although figure 7-5 indicates a trend for higher indices at higher eccentricities.

(1) $CI = \frac{cs}{cc}$

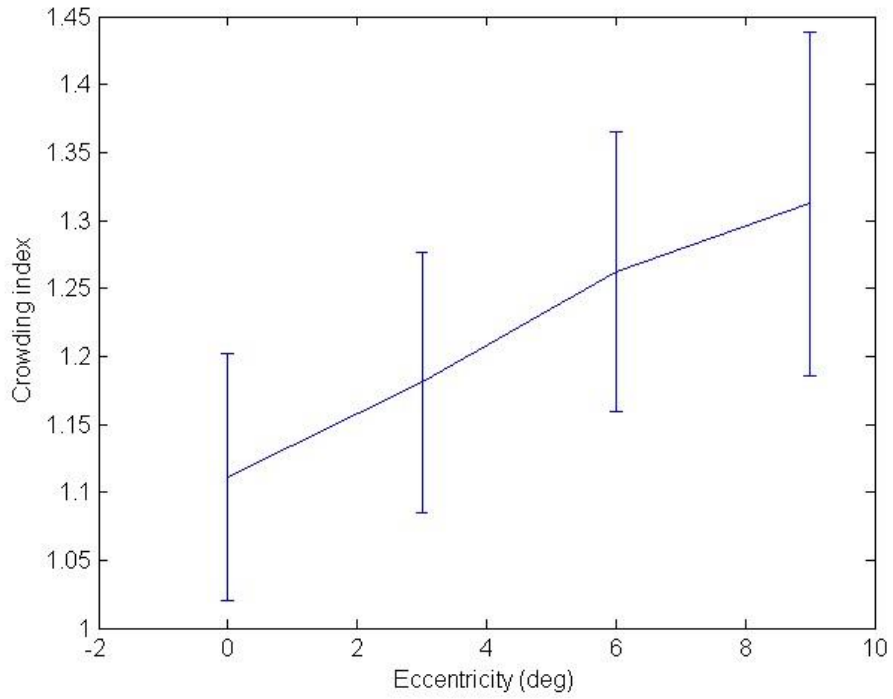

Figure 7-5 Average crowding indices (9 participants). Standard errors shown.

7.4.2 The Relationship between pRF Surround Size and Crowding

Measure of pRF surround size in V1, V2, V3 and V3A were submitted to a linear regression to predict the crowding index (table 7-1). Eccentricity squared and eccentricity were included as covariates to remove this source of variance. pRF surround size was a poor predictor of psychophysical estimates of crowding. No relationship was seen between the crowding index and pRF surround size of V1 (p=.21), V2 (p=.46), V3 (p=.27) or V3A (p=.27).

Table 7-1 Crowding index predicted from pRF surround size (deg). *p<.05 **p<.01 ***p<.001.

Model	B	SE	β
Constant	.724	.367	
Eccentricity	-.002	.058	-.027
Eccentricity²	-.001	.006	-.057
V1 Surround Size	.120	.094	.577
V2 Surround Size	-.077	.102	-.356
V3 Surround Size	.068	.061	.361
V3a Surround Size	-.035	.031	-.216

7.4.3 The Relationship between pRF Centre Size and Crowding

V1 pRF centre size correlated with the crowding index (T=2.58, p<.05; figure 7-6). This link was absent at all eccentricities (0° p=.74; 3° p=.39; 6° p=.61; 9° p=.93). Large V1 centre sizes were associated with high levels of crowding.

Table 7-2 Crowding index predicted from pRF centre size (deg) *p<.05 **p<.01 ***p<.001.

Model	B	SE	β
Constant	-.395	.487	
Eccentricity	-.001	.047	-.012
Eccentricity²	-.001	.005	-.057
V1 Centre Size	.654	.253	.606*
V2 Centre Size	.263	.228	.251
V3 Centre Size	-.197	.193	-.237
V3a Centre Size	-.017	.102	-.031

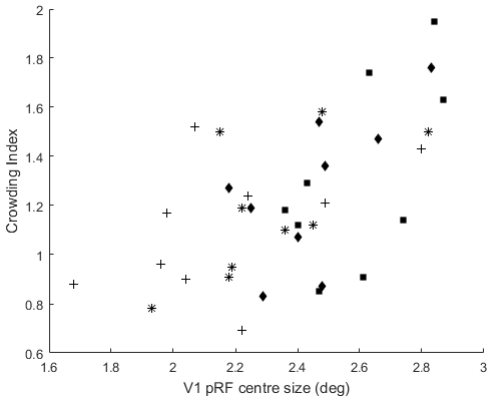

Figure 7-6 The relationship between crowding index (CI) and V1 pRF centre size (deg; p<.001). Each data point represents a single eccentricity patch for a single participant. Eccentricities are represented by different symbols (0°+; 3°*; 6°♦; 9°■).

7.4.4 The Relationship between pRF Surround/Centre Ratio and Crowding

Mirroring first and second order surround suppression (Chapters 5 & 6), pRF surround/centre ratio was a poor predictor of the crowding index (table 7-3). V1, V2, V3 and V3A showed no relationship with the psychophysical measure. Despite the links between V1 centre size and the crowding index, V1 surround/centre ratio was a poor predictor of crowding indices (T=1.18, p=.25).

Table 7-3 Crowding index predicted from pRF surround/centre ratio. *p<.05 **p<.01 ***p<.001.

Model	B	SE	β
Constant	1.061	.224	
Eccentricity	.022	.059	.244
Eccentricity²	-.001	.006	-.099
V1 Ratio	.456	.385	.406
V2 Ratio	.065	.419	.050
V3 Ratio	-.296	.245	-.309
V3a Ratio	-.028	.114	-.047

7.4.5 The Relationship between V3A pRF Centre Size and Shape Matching Ability

V3A pRF estimates were unrelated to susceptibility to crowding, as measured by the crowding index. V3A surround size (p=.27), centre size (p=.88) and ratio (p=.81) were poor predictors of the crowding index. However, performance in the simple shape matching task (in the absence of flankers) was correlated with V3A. A strong link was seen between performance in the control task and V3A centre size (R=.51, p<.01; figure 7-7). The link was present only at 0° (0° R=-.7037, p<.05; 3° p=.73, 6° p=.14, 9° p=.68). Participants with large V3A centre sizes performed poorly in the crowding control task (e.g. they obtained high shape matching thresholds).

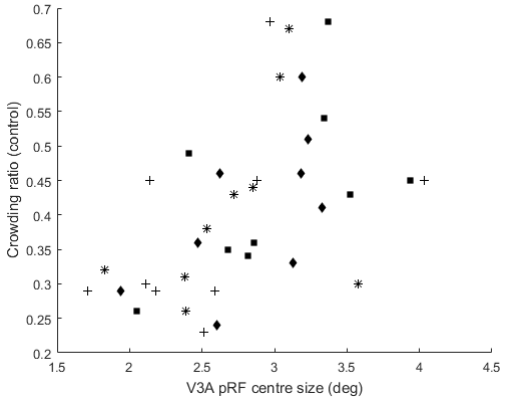

Figure 7-7 The relationship between control crowding ratio (CC) and V3A pRF centre size (deg, p<.01). Each data point represents a single eccentricity patch for a single participant. Eccentricities are represented by different symbols (0°+; 3°*; 6°♦; 9°■).

7.5 Discussion

The results from this study demonstrate that behavioural susceptibility to the disruptive influence of crowding is constrained by pRF estimates of centre size. This correlation was seen in V1 only. The presence of a pairing between receptive field measurements of V1 and psychophysical performance conflicts with the argument that crowding and surround suppression are distinct and separate processes (Petrov et al., 2007), but the absence of a correlation between crowding and V1 pRF surround size (as was seen for surround suppression; Chapters 5 & 6) suggests that the 2 processes may differ to some extent.

The psychophysical data shows a strong eccentricity effect (figures 7-4 & 7-5). At the fovea, there was little difference between performance in the shape matching task when the stimuli were presented alone and performance in the shape matching task in which crowding was elicited. The difference between these conditions increased with eccentricity, at the furthest peripheral location matching ability was greatly diminished by the presence of flankers. This eccentricity effect replicates previous studies (Levi et al., 2002a). Although the presence of an eccentricity effect in both the psychophysical data and the receptive field pattern of neurons suggests a retinotopic basis, it has been argued that this perceptual pattern is not evidence for a causal link between receptive fields and crowding (Levi, 2008).

Examination of the psychophysical data in relation to pRF parameters confirms that crowding does have a clear retinotopic basis, at least in V1. A predictive role was found for V1 pRF centre size in susceptibility to crowding. Participants with larger V1 centres showed greater levels of crowding in the shape matching task. Individual differences in perceptual crowding were correlated with individual differences in pRF centre size. Unlike first order surround suppression (Chapter 5), no correlation was seen between crowding and pRF estimates of surround size in V1.

The absence of a correlation between crowding and pRF surround size suggests that crowding is not mediated by cortical parameters in the same was as surround suppression (Chapters 5 & 6). Instead, I argue that the effects of crowding are mediated by the centre size rather than the surround size of receptive fields. Crowding is a result of spatial pooling. When participants have a large V1 centre size, both the flanker and the target appear in the centre of single receptive field (figure 7-9). Due to the pooling mechanism, features of the target and flanker are integrated, decreasing resolution and preventing accurate perception of the target. When participants have a small V1 centre size, the target is presented alone in a receptive field and this pooling does not occur (figure 7-8). It has previously been suggested that crowding may be the result of simultaneously presentation of a target and a flanker within a single receptive field (Levi, Hariharan, & Klein, 2002b).

This spatial pooling hypothesis is consistent with the size of V1 receptive fields and the size of the stimulus. The target stimulus and the flanker stimulus each measured 2 degrees, with the centre of the flanker positioned 2.4 degrees from the centre of the target. Whilst precise distance varied with the alternating radial frequency of the patterns, it can be estimated that there was a gap of approximately 0.4 degrees between the edge of the target and the edge of grating. V1 pRF centre sizes were between 1.68 and 2.88 (figure 5-10). This indicates that the flanker and the target would be presented simultaneously within a single large receptive field centre (e.g. when the centre size was larger than approximated 2.4 degrees), but would be presented in isolation when the centre was small. Conversely in areas V2, V3 and V3A the centre sizes are larger (figure 5-10) and so the target and the flanker would always be presented within a single receptive field centre, preventing identification of the effect of spatial pooling.

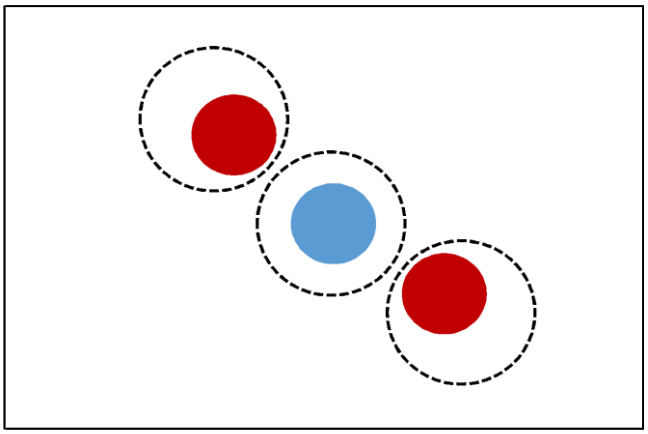

Figure 7-8 Representation of the stimulus on multiple small V1 receptive fields. Receptive field boundary shown by dotted black dotted line. Target stimulus in blue. Flankers in red.

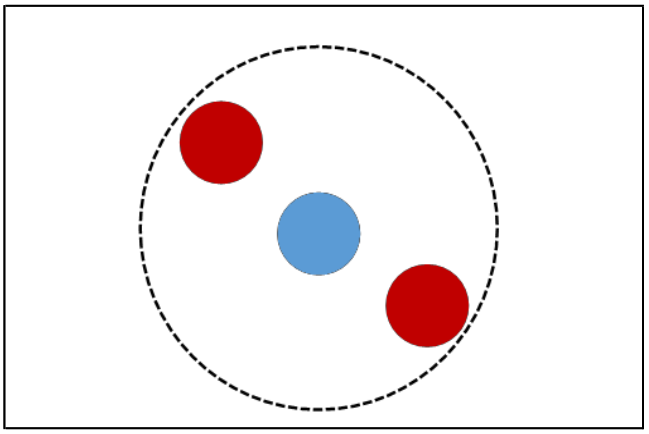

Figure 7-9 Representation of the stimulus on single large V1 receptive field. Receptive field boundary shown by dotted black dotted line. Target stimulus in blue. Flankers in red.

Spatial pooling has previously been proposed to underlie crowding (Levi et al., 2002b; Parkes et al., 2001). Levi et al. (2002b) argue that during observation of multiple stimuli in peripheral vision participants must perform a 2 stage process. Firstly, the features of the target stimulus and the flanker stimulus must be extracted. Secondly, the features of the target must be isolated from the features of the flanker. Crowding occurs at the second stage of this process. Levi et al. (2002b) present behavioural data demonstrating that peripheral crowding of Gabor stimuli is different to simple contrast matching and is a result of unwanted integration. Furthermore, it has been demonstrated that spatial pooling is vital in the perception of radial frequency patterns similar to the stimuli used in this chapter (Schmidtmann, Kennedy, Orbach, & Loffler, 2012), indicating that the

mechanism outlined by (Levi et al., 2002b) may be similarly applicable to the findings of this chapter.

Parkes et al. (2001) provide further evidence that crowding is a result of spatial integration, suggesting that crowding is a form of textual analysis. Following simultaneous presentation of multiple gratings of various orientations participants accurately estimated the average orientation of the gratings but were unable to provide an accurate estimate of a single grating within the cluster. It was suggested (Parkes et al., 2001) that the multiple orientations were pooled, stimuli features were integrated with one another. Importantly, this study demonstrated that the influence of crowding occurred at the second stage of the process outlined by Levi et al. (2002b). Participants had accurately extracted the features, as evidenced by the accurate estimation of the average orientation.

Whilst Parkes et al. (2001) argued that that the pooling had not occurred within a single receptive field, and instead relied on lateral interactions in the primary visual cortex (Usher, Bonneh, Sagi, & Herrmann, 1999) or via a higher level collector-unit model (Morgan & Baldassi, 1997), neurophysiological measures of single neurons suggest that pooling can occur at the level of a single receptive field. For example, it has been reported that the response of a single neuron in the macaque temporal cortex to a face stimulus was modulated by the simultaneous presentation of a second stimulus within the same receptive field (Rolls & Tovee, 1995). A similar interaction has also been seen in the inferior temporal cortex for simpler stimuli (Sato, 1989).

It is unexpected that no links were seen between pRF measures in V2, V3 and V3A and crowding. This finding conflicts with a recent fMRI study, investigating the neural correlates of crowding in the early visual cortex (Anderson, Dakin, Schwarzkopf, Rees, & Greenwood, 2012). The authors found crowding related activity in all early visual areas from V1 to V4 but with a parametric increase in terms of their involvement with crowding performance, with V1 being the least involved then increasing roughly linearly until V4. In contrast, the study reported here attributes the largest role in crowding to V1.

The findings of this chapter are particularly difficult to align with the work of Cai et al. (2014) who identified a positive relationship between crowding susceptibility and V2

receptive field size. It is thought unlikely that this discrepancy arises from the pRF mapping technique used by Cai et al. (2014). Although Cai et al. (2014) used the earlier methods of Dumoulin and Wandell (2008) obtaining only an estimate of centre size, these modelling differences are insufficient to explain the difference in findings. The analysis methods used in this chapter are suitable to identify any links between V2 centre size and crowding.

Instead, I argue that the conflicting findings between Cai et al. (2014) and the data reported in this chapter is a result of difference in the focus on individual differences. It is possible that Cai et al. (2014) are limited by a failure to acknowledge the presence of inter- and intra-individual variability, instead focusing on group differences only. As for surround suppression (Chapters 5 & 6), participants showed a high level of variability in crowding in the data presented in this chapter. Large differences were identified both between participants and within participants (e.g. performance changed with distance from the fovea). pRF estimates also varied in this way. This unacknowledged variance may have led to an exaggeration of the role for V2. Future work in this area should aim to account for the high level of variability in low level and intermediate level visual tasks.

However a failure to acknowledge intra- and inter-individual variability is likely to mask findings, rather than produce conflicting results. A more likely reason for the discrepancy between the data reported in this chapter and the findings of Cai et al. (2014) is the differences in analyses methods. Cai et al. (2014) did not measure psychophysical performance in a crowding task, instead using BOLD responses as an indication of crowding. I argue that the methods used in this chapter provide a more direct measure of the link between pRF size and perceptual susceptibility to crowding.

Visual area V3A has been suggested as a possible locus of crowding (Kastner et al., 1998). The data presented in this chapter does not support this proposal. None of the V3A pRF measures used here predicted susceptibility to crowding. However, pRF estimates of V3A predicted performance in the control condition. The centre size of this area correlated with shape matching ability in the absence of flankers. Previously collected data (Chapter 4) shows that performance in a shape discrimination task can be predicted from the surface area of this visual area.

It is likely that pRF centre size and surface area measures of cortical maps are correlated. Cortical magnification is correlated with surface area, larger visual areas generally have higher levels of cortical magnification (Dougherty et al., 2003). Cortical magnification is also correlated with pRF size, cortical magnification decreases at higher eccentricities whilst pRF size increases (Harvey & Dumoulin, 2011). Therefore, small pRF size would be expected to correlate with a large surface area. Generally, this pattern is seen across early visual regions, pRF size increases from V1 to V3 (Harvey & Dumoulin, 2011) whilst overall surface area decreases (Larsson & Heeger, 2006). Due to this correlation, the link reported in this chapter between V3A and the control condition is most likely a result of the correlation between V3A size and shape matching ability reported in Chapter 4. It is notable that whilst V3A underlies shape perception, it is not the locus of crowding for this stimulus. This mirrors the findings of Chapter 6, the cortical location of the perception of second order stimuli (Larsson et al., 2006) did not correlate with the suppression of second order stimuli.

There is much debate as to the locus of crowding (Whitney & Levi, 2011). The data presented in this chapter points towards the early visual areas, most likely V1, in agreement with Arman et al. (2006) and Freeman and Simoncelli (2011). Unlike Kastner et al. (1998) and Kastner et al. (2001), no evidence of crowding was identified in intermediate visual areas. The absence of a clear link between crowding and pRF surround size in visual areas V3 and V3A should not be interpreted as a definitive indication that crowding has no retinotopic basis in these regions. Firstly, the retinotopic methods used here are appropriate for V1, but may not suitable for mapping pRF properties of V3 and V3A. Additionally, the role of later visual areas cannot be deciphered using this data. fMRI data indicates that visual areas V4, TEO and MT (Kastner et al., 1998; Kastner et al., 2001) may be the locus of crowding, future research should aim to utilise the methods used here to investigate these regions. The predictive role of V4 would be of particular interest, a previous experiment (Chapter 4) indicates that this region plays a stronger role in the perception of the radial frequency pattern shapes used here than V3A. Furthermore, it should be noted that the data reported here examined only relationships between crowding and the pRF properties of visual maps. The absence of these relationships in V3 and V3A does not confirm that V3 and V3A are uninvolved in crowding. It is possible that these regions are involving in crowding but via a mechanism that is not associated with variability in pRF properties.

In conclusion, the experiment reported here demonstrates that crowding does not necessarily occur at in the cortical regions underlying perception of the stimulus. This has been clearly demonstrated by the involvement of V3A in the perception of the shape stimulus, but not the crowding of this stimulus. Instead, pRF estimates of V1 are linked to crowding. Unlike surround suppression, which is reliant on the surround size of V1 pRF estimates (Chapters 5 & 6), crowding is linked to the centre size of V1. It is suggested that crowding is facilitated through a spatial pooling mechanism rather than a suppressive mechanism.

Part III: A GABA Mediated Suppressive Mechanism

8 A Correlation between Visual Reasoning Ability and Surround Suppression

8.1 Introduction

8.1.1 Perceptual Abilities and IQ

A link between IQ and low level perceptual abilities has long been sought (Galton, 1883; Spearman, 1904). The search for this correlation has been driven by the belief that IQ measures some fundamental property of the brain. This general property should be expected to display itself in both the higher cognitive tasks traditionally associated with this measure, and in more basic sensory abilities. The presence of such a correlation would provide a more solid definition of the somewhat nebulous concept of general intelligence.

Delineation of a link between IQ and sensory abilities would also inform understanding of the basis of the high individual variation displayed in the tasks used in Chapters 2, 3, 4, 5, 6 and 7 of this thesis. Earlier chapters (3 & 4) have demonstrated that performance in psychophysical tasks cannot be fully accounted for by individual differences in retinotopic properties. Perception is not fully mediated by the amount and nature of the cortex dedicated to processing the stimulus. Instead, it may be top down processes that determine this variation.

Generally, correlations between IQ and low level sensory abilities have been weak. A variety of perceptual tasks in multiple modalities have been examined for correlations with measures of IQ. Tactile discrimination is related to general intelligence to some extent (Li et al., 1998). In the auditory modality, pitch discrimination has shown a modest correlation with measures of IQ taken from the Raven and Mill Hill intelligence tests in young adolescents (Deary, 1994) and loudness discrimination showed a similar relationship (Troche & Rammsayer, 2009b). Visual perception is correlated with

intelligence in tasks involving line length (Meyer et al., 2010) and duration judgement tasks (Haldemann, Stauffer, Troche, & Rammsayer, 2011, 2012).

Acton and Schroeder (2001) examined the sensory-IQ link in a large sample of adults. They compared general intelligence (*g*) to colour discrimination abilities and pitch discrimination abilities. Despite the large sample size of 899, only weak positive correlations were found for either ability. Pitch discrimination explained 21% of the variance in *g* and colour discrimination explained 31%. These relationships are much lower than results published by Spearman (1904), in which he claimed that measures of general discrimination and general intelligence were almost perfectly correlated.

The presence of a relationship between IQ and abilities in multiple sensory modalities indicates that there is a fundamental property that influences all perception. A failure to find a strong relationship between sensory discrimination and IQ indicates that the pairing may be more complicated that originally proposed. For example there may be a third factor influencing both measures. Cattell (1886a, 1886b) proposed that information processing speed may exert an influence on both IQ and perceptual abilities. It has been shown that information processing speed influences performance in a variety of intelligence measures (Sheppard & Verson, 2008). Although, when the full 1146 correlations were examined together the r value was only -0.24, indicating that processing speed is not the sole predictor of IQ (Sheppard & Verson, 2008). It is possible that a variety of other factors may play the intermediately role Cattell attributed to processing speed. For example, higher levels of test motivation would also explain why certain individuals perform well in both tests of IQ and measures of perceptual abilities.

An alternative explanation for the IQ-perception link is sensory deprivation during cognitive development. Patient studies suggest that the link between IQ and visual perception may be explained through developmental mechanisms. In a comparison of 43 cerebral palsied children with visual deficits to a matched group with normal vision, impaired vision correlated with lower intelligence (Schenk-Rootlieb, Van Nieuwenhuizen, Schiemanck, Van der Graaf, & Willemse, 1993). It is argued that, as for healthy children (Reynell, 1978), visual perception is vital for the normal development of higher cognitive functioning. In this way, the link between IQ and visual perception may be constrained by low level sensory abilities via a bottom-up mechanism.

The importance of sensory input to the maintenance of intelligence can also be demonstrated through consideration of ageing. The variance in IQ of a group of elderly people (mean age= 84.9) was accounted for by visual and auditory acuity abilities (Lindenberger & Baltes, 1994). One explanation for this link is the sensory deprivation hypothesis. Once the sensory input has been degraded through physiological degradation of perceptual processes, the higher level cognitive functions receive insufficient information to remain fully active. In the same way that children require perceptual input to develop higher cognition, the elderly require perceptual input to maintain higher cognition. Whether this bottom up mechanism is applicable to the healthy population is unknown. It is possible that there is a low ceiling effect to this link. Once perceptual input reaches a certain minimum, any additional information fails to influence IQ levels.

8.1.2 Surround Suppression and IQ

In recent years, interest in the link between IQ and low level sensory perception has been reignited. Through reconsideration of the intermediator driving factors of this pairing, a strong and interactive relationship between these 2 measures has been documented (Melnick et al., 2013). Instead of considering low level perceptual abilities in terms of discrimination thresholds, as previous studies have done (Li et al., 1998), Melnick et al. (2013) considered perceptual suppression.

In a simple psychophysical experiment, participants were better able to judge the direction of a grating's movement when the grating was smaller than when it was larger (Tadin, Lappin, Gilroy, & Blake, 2003). This finding was thought to reflect neural mechanisms that prevent motion sensitive neurons from responding to large stimuli. This inhibition is thought to ensure that background information, which is likely to be less relevant, is ignored (Churan, Khawaja, Tsui, & Pack, 2008). Melnick et al. (2013) utilised this phenomena to compute a suppression index for each participant. The time taken for each participant to identify the direction of a grating was measured. An analogous threshold was established for each participant for a small stimulus. The suppression index was calculated as the difference between these thresholds. A large index indicated that the time taken to judge the stimulus direction increased greatly as stimulus size increased.

The IQ of 67 participants was measured using the Wechsler Adult Intelligence Scale (WAIS-IV; Wechsler, 2008). The suppression index strongly correlated with measures of IQ, explaining 71% of variance in IQ (Melnick et al., 2013). Participants with high IQs were disproportionately impaired by the increase in size. The suppression index correlated more strongly with sensory IQ measures than performance IQ measures, with the strongest relationships seen for verbal comprehension, perceptual reasoning and processing speed. A measure of working memory was also correlated with surround suppression. It should be noted that perceptual ability differences between participants in neither the small stimulus nor the large stimulus were sufficient to explain IQ; it was the suppression index that carried the correlation. For this reason, it can be established that IQ was not driven by general factors such as motivation or acuity as these qualities would be equal for both small and large stimuli.

The positive correlation between IQ and the disruptive effects of an increased stimulus size were greatest in the periphery, decreasing towards the centre of the visual field. Surround suppression is greater in the periphery than the fovea (Flom et al., 1963). Therefore, this finding again confirms that the link between IQ and psychophysics is centred on the specifics of surround suppression rather than general visual abilities. Factors such as motivation would not be expected to be confined to particular eccentricities.

Melnick et al. (2013) argued that participants with high IQ scores have a general ability to suppress irrelevant information. This ability materialises as a high suppression index, they perform poorly for large stimulus trials because they supress information assumed to be background noise. How this individual variability in suppression acts to determine IQ is unclear. It may be utilised to facilitate the exclusion of irrelevant information, thereby improving the signal of the correct response. The experimental design utilised by Melnick et al. (2013) offers a novel route to re-examine Spearman's proposals.

The strong link between low level sensory abilities and IQ (Melnick et al.,2013) is of interest given the absence of such conclusive findings in the field (Sheppard & Verson, 2008), although the neural mechanisms mediating this link are uncertain. For this reason,

the links between higher level cognitive abilities and other forms of suppression, both within vision and other modalities, are difficult to predict.

The task used by Melnick et al (2011) is hypothesised to reflect the activity of receptive fields in visual area MT (Tadin et al., 2003). MT is considered to be the location of motion processing in the visual cortex (Kolster et al., 2010). Additionally, MT has much larger receptive field sizes than V1 (Gattass & Gross, 1981). The stimulus size at which surround suppression is seen matches the size of receptive fields in MT (Tadin et al., 2003), but is too large to indicate the involvement of V1. As surround suppression is known to occur in visual regions other than MT (see Chapters 5 & 6), examination of psychophysical thresholds obtained in tasks reliant of this region and the correlation with IQ will allow further specification of this relationship. For example, the effect of surround suppression on contrast discrimination is well established. The perceived contrast of a grating can be modulated by the introduction of a secondary grating surrounding the first (Xing & Heeger, 2000).

8.1.3 Neural Mechanisms of the Link between IQ and Perception

The mediating relationship between IQ and surround suppression is currently poorly defined. Melnick et al. (2013) attribute the relationship to a reflection of a canonical process across the whole brain. They identify normalization as a possible mechanism. Normalization is a computational process by which a ratio is produced between the response of an individual neuron and the summed activity of a pool of neurons. In this way, weaker responses from individual neuron are supressed. The process is clearly demonstrated in perceptual surround suppression. Alone, a low contrast grating elicits a response. However, when the same grating is presented alongside a high contrast grating, the low contrast grating will no longer produce a response (Cavanaugh et al., 2002; Kapadia, Westheimer, & Gilbert, 1999). The theory of normalization states that this occurs because the high contrast grating has decreased the sensitivity of the pool of neurons to a point at which the low contrast grating can no longer elicit a response. The process was first identified in early visual areas (Heeger, 1992) but has now been expanded to multiple elements of the visual system and other sensory cortices (Carandini & Heeger, 2013). Whilst the implication of low level normalization on perception is

clear, its role in IQ is less well defined. The proposal that high IQ reflects an ability to ignore extraneous background information is persuasive, but how this ties to the neural process of normalization is unknown.

Others have argued that the link between IQ and surround suppression is simply a result of individual differences in working memory. Troche, Wagner, Voelke, Roebers, and Rammsayer (2014) present modelling data that indicates that the link is completely mediated by working memory. This top-down hypothesis for the link is supported by findings that sensory discrimination tasks correlate with increases in BOLD response of brain regions thought to underlie working memory (Ferrandez et al., 2003; Livesey, Wall, & Smith, 2007; Nenadic et al., 2003).

The approach of Troche et al. (2014) raises some valuable points regarding consideration of multiple higher level processes when considering performance in psychometric studies. However, it arguably overstates the role of working memory in explaining the IQ-surround suppression link. Most importantly, the perceptual tasks used by Troche et al. (2014) do not elicit surround suppression. Four tasks were used; auditory duration discrimination, visual duration discrimination, pitch discrimination and line length discrimination. The neural processes implicated in the link between psychophysical performance and IQ specifically implicate surround suppression. For this reason, it is thought that the role ascribed to working memory by Troche et al. (2014) is not fully relevant to the findings of Melnick et al. (2013).

It is clearly necessary to establish a framework to explain the link between IQ and surround suppression. Melnick et al. (2013) suggest a bottom-up link, with neural processes underlying both measures. Conversely, Troche et al. (2014) favour a top-down approach, with psychophysical abilities constrained entirely by working memory. It is hypothesised that although working memory plays a role, both psychophysical performance and IQ are driven primarily by a bottom-up mechanism.

Whilst the results of Melnick et al. (2013) reflect only MT functioning and motion processing, the hypothesised mechanism implicates canonical processing. If, as has been argued, normalization underlies the link (Melnick et al., 2013) and normalization occurs across the whole brain (Carandini & Heeger, 2013) then the link between IQ and

perception should be evident for multiple tasks involving suppression. Before further speculation regarding the neural underpinnings of the IQ-perception link can be made, the specificity of the surround suppression task must be explored.

8.2 Methods

8.2.1 Participants

11 Participants (3 males) were used in this experiment. First order surround suppression and second order surround suppression thresholds were collected for the full participant group. Crowding data was collected for 9 of the participants. All participants were also used in the experiments reported in Chapters 2 and 4. 6 of the participants (3 males) were also used in the experiment reported in Chapter 3. Participants used had normal or corrected to normal vision and were aged between 21 and 35. Participants were post-graduate students or post-doctorate researchers at the Psychology department of Royal Holloway University. All participants were fluent English speakers. 7 participants spoke English as a first language. Written consent was obtained from all participants. The experimental procedure was in accordance with the Declaration of Helsinki and was approved by the appropriate local ethics committee.

8.2.2 Measurement of First Order Surround Suppression, Second Order Surround Suppression and Crowding

Psychophysical data for first order surround suppression, second order surround suppression and crowding were taken from Chapters 5, 6 and 7.

8.2.3 IQ Measurement

8.2.3.1 IQ Testing Materials

8.2.3.1.1 Matrix Reasoning from Weschler Abbreviated Scale of Intelligence

The Matrix Reasoning subtest of WASI (Weschler, 1999) was administered. This test required participants to examine a collection of visual images (4, 6, 8 or 9) and select the missing piece of the pattern from a selection of 5. There were 2 practice questions and 35 test questions. Patterns were coloured and presented on a white background. The task measured non-verbal abstract problem solving. This ability will be referred to as visual reasoning.

8.2.3.1.2 Shortened Raven's Advanced Progressive Matrices (APM)

A shortened form of APM was administered (Bors & Stokes, 1998). 12 items were presented. The 12 items used in the APM shortened form were items 1, 4, 8, 11, 15, 18, 21, 23, 25, 30, 31 and 35 from Set II of the full length APM. Each item consisted of 3x3 matrices, each missing a single item. The items in the matrices followed a pattern. Participants were required to select the missing piece of the puzzle from a selection of 8. The matrices were presented in black ink on a white background. The matrices became more difficult with progression through the sets. In addition to the shortened APM, items 1 and 2 from Raven's Standard Progressive Matrices (Raven, Styles, & Raven, 1998) were used as practice stimuli.

8.2.3.2 IQ Experimental Procedure

Testing took place in a quiet well lit room. Participants were tested alone and accompanied at all times by the experimenter. All psychometric testing occurred in a single session. Both Matrix Reasoning and APM were administered to all participants. Matrix Reasoning was administered before APM.

8.2.3.2.1 WASI Matrix Reasoning

Matrix Reasoning was administered in accordance with the standardised procedures outlined in the WASI user's manual (Weschler, 1999) Participants were given the following instructions verbally:

"I am going to show you some pictures. In each picture, there is a piece missing. Look carefully at all the pieces of each picture and choose the missing piece from the five choices at the bottom of the page. There is only one correct answer to each problem. If you believe that more than one answer is right, choose the best one."

Two practice items were first completed by the participant. All participants correctly answered the practice questions. Participants answered 29 of 35 test questions. Answers were given verbally and recorded by the author. No strict time limit was enforced, but if the participant spent more than approximated 30 seconds on a single item then the participant was encouraged to move on and the item was recorded as a failure. If a participant answered 4 successive questions incorrectly then testing was terminated. Participants were awarded 1 point for each correct answer; no points were deducted for incorrect answers.

8.2.3.2.2 APM

Raven's 12 item APM was administered in accordance with normal practice outlined in the manual, but modified to account for the lower number of test items (Raven, Raven, & Court, 2000). Participants were given the following instructions verbally prior to testing:

"Look at the matrices and try to understand the pattern. Choose a piece from the selection of 8 that best fits the pattern. You will have 15 minutes to complete the set. The problems become progressively harder so work through the matrices in the right order. You can return to questions if you have spare time at the end of the test."

Participants were given 2 practice stimuli and required to answer verbally. All participants correctly answered both practice stimuli. Following completion they were given the opportunity to ask questions. Participants were then given 15 minutes to complete the set of matrices. A stop watch was visible to participants at all times.

Participants recorded their decisions on a response sheet by circling the correct response. Although the author was present throughout, the participant worked independently. Participants were awarded 1 point for each correct answer; no points were deducted for incorrect answers.

8.2.3.3 IQ Data Analysis

Psychometric scores were analysed in their raw form. For Raven, this value was the number of correct answers given from a total of 12. For WASI, this value was the total number of correct responses given before termination of the test. Standard criteria for termination were used (see Appendix C). The highest possible WASI score is 35. IQ scores were not calculated for either test.

8.3 Results

The results of this experiment demonstrate a strong correlation between WAIS visual reasoning scores and first and second order surround suppression. Other psychophysical abilities did not correlate with performance in the IQ subtest.

8.3.1 IQ Measures

Measures of performance in the WASI Matrix Reasoning test were examined for correlations with measures of performance in the Raven's Matrices test. The 2 scores did not correlate (R=.17, p=.61).

8.3.2 First Order Surround Suppression

First order surround suppression values were obtained at eccentricities of 0°, 3°, 6° and 9°. Psychophysical measures of suppression (SS_1) for each trial were calculated by dividing the staircase output (the matching contrast; Cmatch) by the contrast of the first centre grating (the test contrast; Ctest). This was a ratio of the matching contrast and the

test contrast. A value of 1 indicated that no surround suppression had occurred within the trial, the participant perceived the second stimulus as equal to the first stimulus. Values lower than 1 indicate surround suppression. A suppression ratio was computed for surrounded trials (SS_1) and control trials (SC_1).

(1) $SS_1 = \frac{Cmatch}{Ctest}$

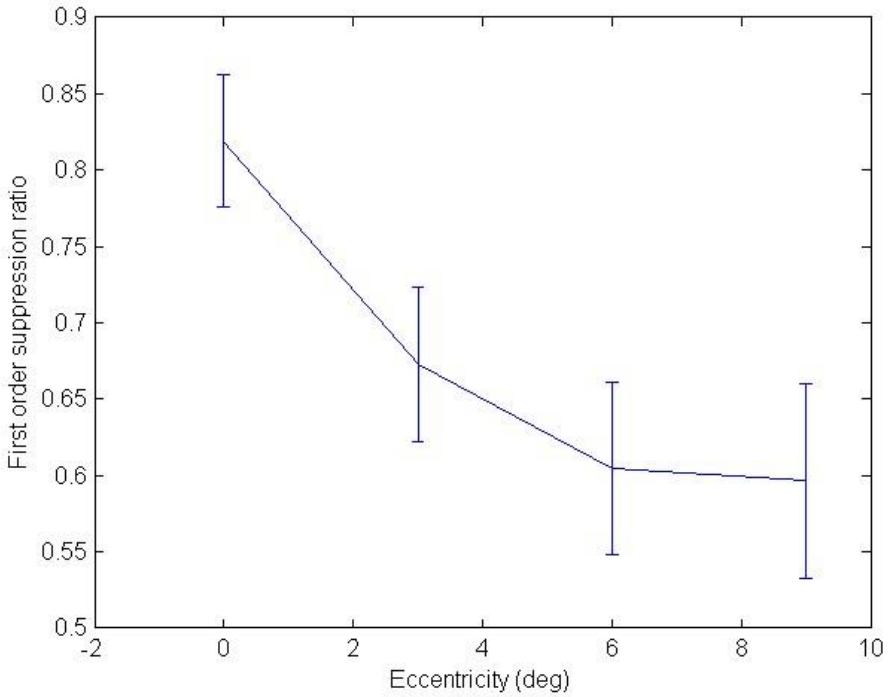

Figure 8-1 Average suppression ratio (11 participants; SS_1) in a first order contrast matching task (surrounded condition). Standard errors shown.

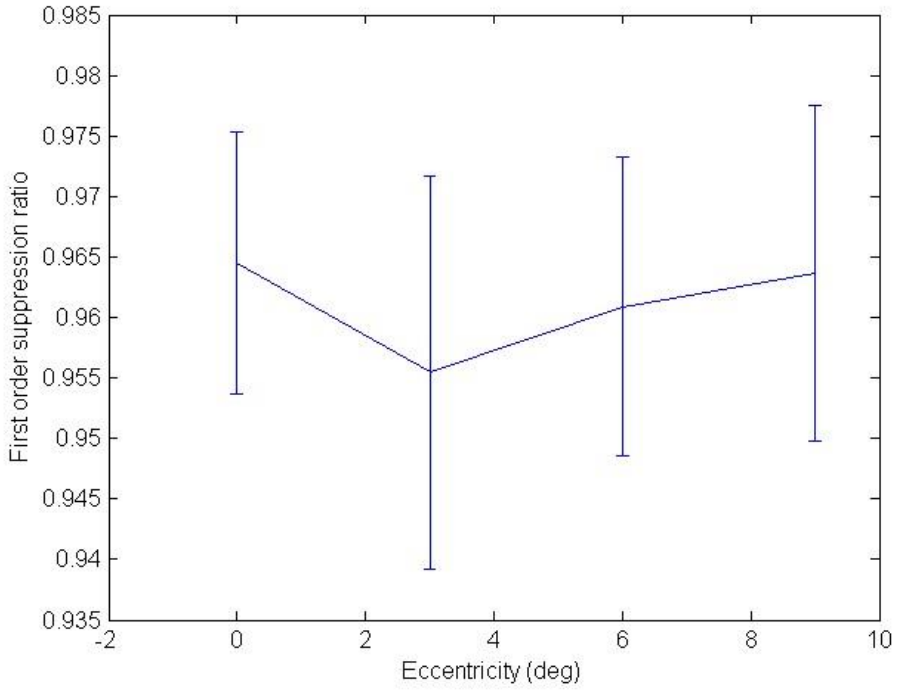

Figure 8-2 Average suppression ratio (11 participants; SC_1) in a first order contrast matching task (control condition). Standard errors shown.

A suppression index (SI_1) was calculated for each participant at each eccentricity by dividing the suppression ratio in the surrounded condition by the suppression ratio in the control condition at the equivalent eccentricity. This corrected for the eccentricity-specific effects of adaptation in contrast matching within trial adaptation. This value was then subtracted from 1. This number represents the increase in matching thresholds with the introduction of a surround stimulus. A high value indicates that the introduction of a surround has had a high impact on the perceived contrast (e.g. high suppression).

(2) $SI_1 = 1 - (\frac{SS_1}{SC_1})$

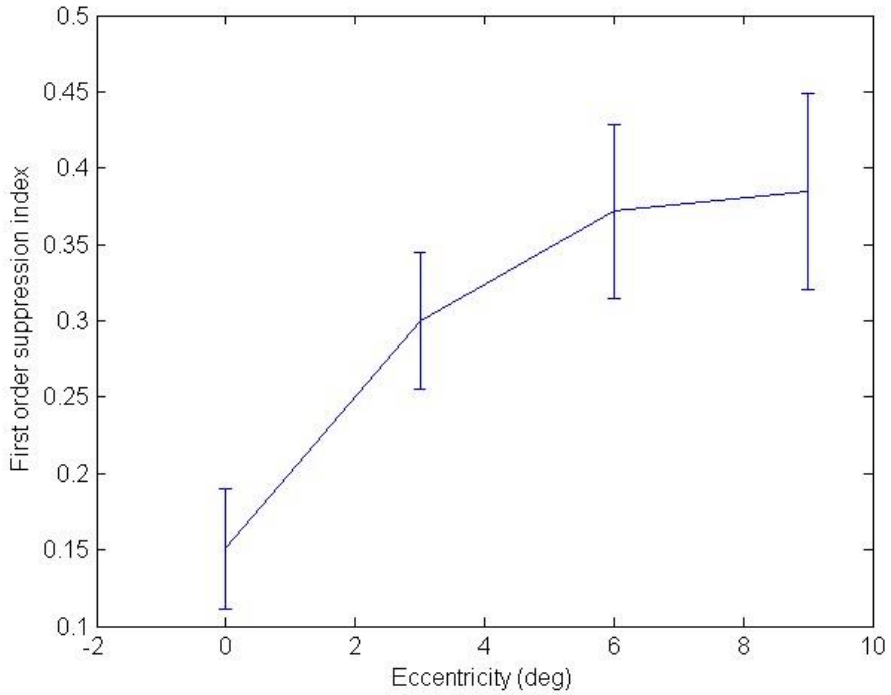

Figure 8-3 Average first order suppression index (11 participants; SI_1) across all participants. Standard errors shown.

The suppression index was compared to WASI scores at each eccentricity. No links were seen at lower eccentricities (0° p=.16; 3°, p=.1). A significant relationship was noted at 6° (figure 8-4; R=.72, p<.05) and 9 (figure 8-5; R=.78, p<.01), participants with high levels of perceptual suppression also had high measures of visual reasoning. False discovery rate was applied to these correlations to correct for multiple comparisons. The significant relationships survived this test (6° p<.05; 9° p<.05). False discovery rate was used in this analysis to correct for the increased likelihood of type 1 errors resulting from the high number of correlations performed. In previous chapters false discovery rate was not necessary as correlations were performed only as post hoc explorations following the main analysis.

A bivariate correlation between WASI visual reasoning scores and SS_1 supported the presence of this link solely at higher eccentricities (0° p=.11; 3° p=.16; 6° R=-.71, p<.05, figure 8-4; 9° R=-.77, p<.01, figure 8-5). These links were absent when visual reasoning was compared to SC_1 (0° p=.17; 3° p=.09; 6° p=.85; 9° p=.57).

Raven measures of IQ did not correlate with SI, SS_1 or SC_1. All p values were greater than .1.

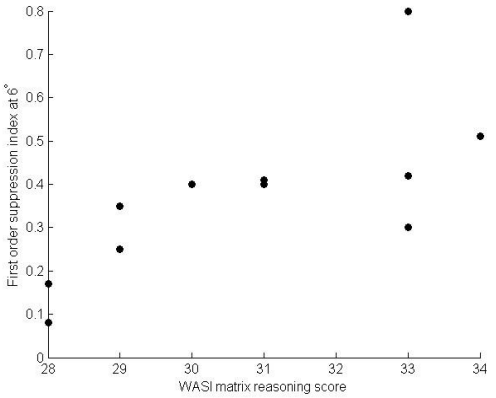

Figure 8-4 The relationship between visual reasoning (WASI) and first order suppression index (SI_1) at 6° ($p<.05$ following correction for multiple comparisons). Each data point represents a single participant.

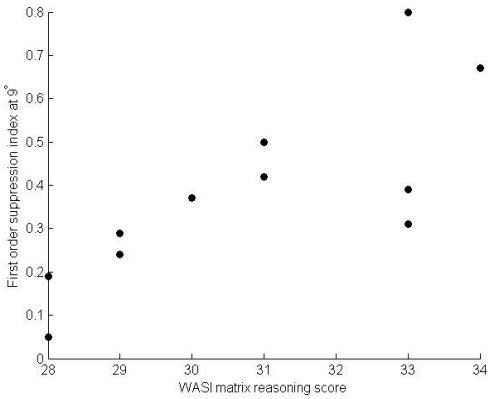

Figure 8-5 The relationship between visual reasoning (WASI) and first order suppression index (SI_1) at 9° ($p<.05$ following correction for multiple comparisons). Each data point represents a single participant.

8.3.3 Second Order Surround Suppression

Second order surround suppression values were obtained at eccentricities of 0°, 3°, 6° and 9°. Psychophysical measures of suppression (SS_2) for each trial were calculated by dividing the staircase output (the matching contrast; Cmatch) by the

contrast of the first centre grating (the test contrast; Ctest). This was a ratio of the matching contrast and the test contrast. A value of 1 indicated that no surround suppression had occurred within the trial, the participant perceived the second stimulus as equal to the first stimulus. Values lower than 1 indicate surround suppression. A suppression ratio was computed for surrounded trials (SS2) and control trials (SC2)

(3) $SS_2 = \frac{Cmatch}{Ctest}$

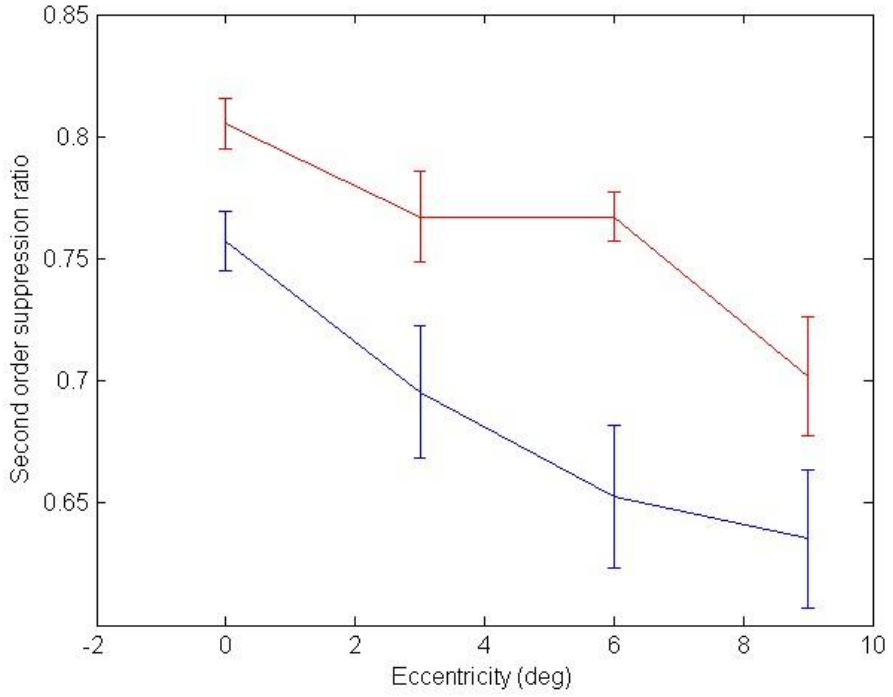

Figure 8-6 Average surround suppression ratios (11 participants). Control stimuli (SC_2) in red and suppressed stimuli (SS_2) in blue. Standard errors shown.

A suppression index (SI_2) was calculated for each participant at each eccentricity by dividing the suppression ratio in the surrounded condition by the suppression ratio in the control condition at the equivalent eccentricity. This corrected for the eccentricity-specific effects of adaptation in contrast matching within trial adaptation. This value was then subtracted from 1. This number represents the increase in matching thresholds with the introduction of a surround stimulus. A high value indicates that the introduction of a surround has had a high impact on the perceived contrast. This index is analogous to SI_1.

(4) $SI_2 = 1 - (\frac{SS_2}{SC_2})$

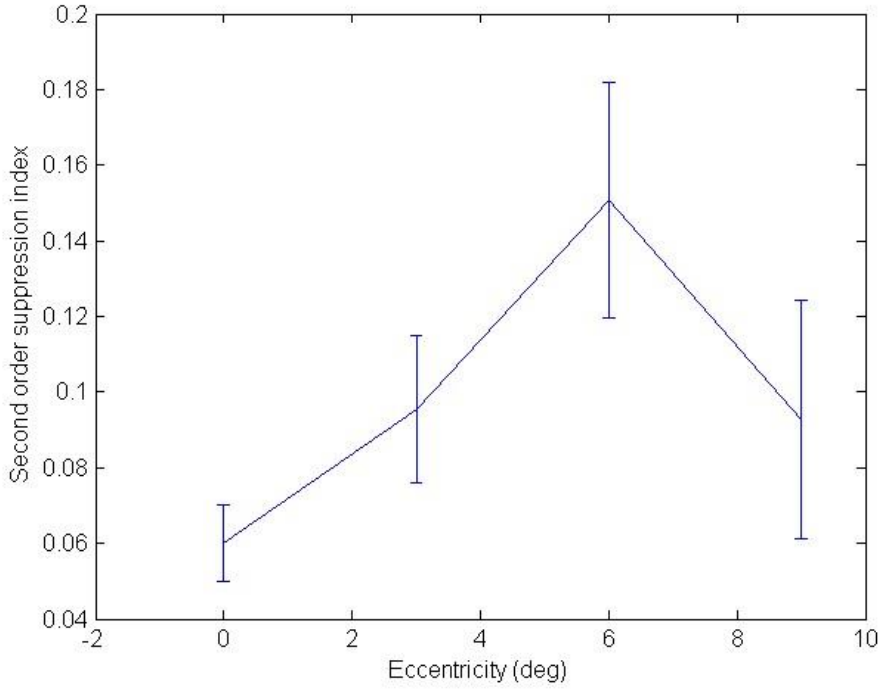

Figure 8-7 Average second order surround suppression index (11 participants; SI_2). Standard errors shown.

A bivariate correlation demonstrated that following correction for multiple comparisons, WASI visual reasoning measures correlated with second order surround suppression indices (0° R=.72, p<.05; 3° p=.19; 6° R=.71, p<.05; 9° R=.72, p<.05). Figures 8-8 and 8-9 demonstrate that these links were not driven by outliers.

The correlation between second order surround suppression and WASI visual reasoning was specific to surround suppression rather than general perception. Following correction for multiple comparisons, no links between surround suppression in the control condition (SC_2) and WASI visual reasoning remained (all p values were greater than .1).

IQ scores taken from the Raven test did not correlate with second order suppression index, SS_2 or SC_2. All p values were greater than .1.

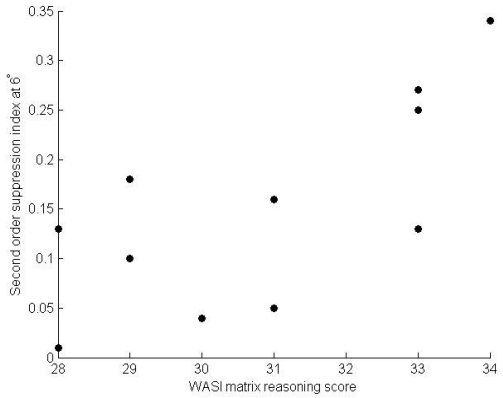

Figure 8-8 The relationship between WASI visual reasoning and second order suppression index (SI_2) at 6° ($p<.05$ following correction for multiple comparisons). Each data point represents a single participant.

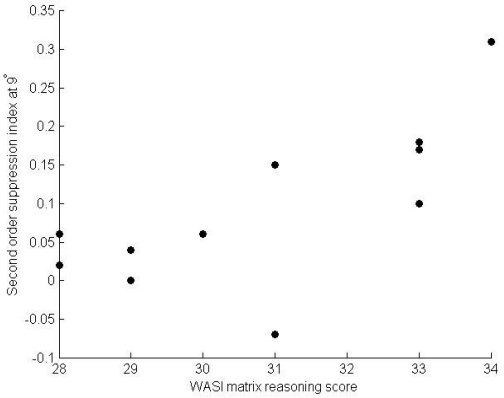

Figure 8-9 The relationship between WASI visual reasoning and second order suppression index (SI_2) at 9° ($p<.05$ following correction for multiple comparisons). Each data point represents a single participant.

8.3.4 Crowding

In the crowded condition, crowding ratios (CS) were obtained at eccentricities of 0°, 3°, 6° and 9°. Flankers were present. Crowding ratios for the control condition (CC) were obtained at eccentricities of 0°, 3°, 6° and 9°. Flankers were not present in the control condition, the target shape was presented alone. The crowding ratio was computed by dividing the radial frequency of the matching stimulus by the radial frequency of the target stimulus. A high ratio indicates a high level of crowding.

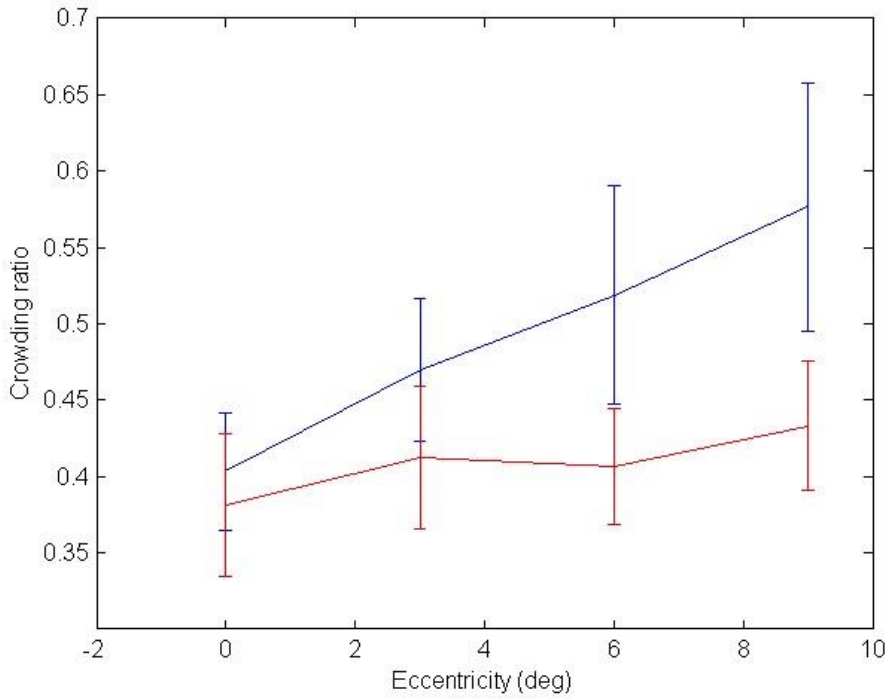

Figure 8-10 Average crowding ratios in a shape matching task. Crowded condition (9 participants; CS) in blue, control condition (CC) in red. Standard errors shown.

As for first and second order surround suppression, an index was calculated to show the influence exerted by the presence of non-target stimuli. A crowding index (CI) was calculated for each participant at each eccentricity by dividing the crowding ratio in the crowded condition (CS) by the crowding ratio in the control condition (CC). This value represents the disruption to shape discrimination attributed to the presence of flankers. This value corrected for the eccentricity-specific effects of within-trial adaptation. A value of less than 1 indicates no crowding. Values greater than 1 indicate crowding.

(5) $CI = \frac{CS}{CC}$

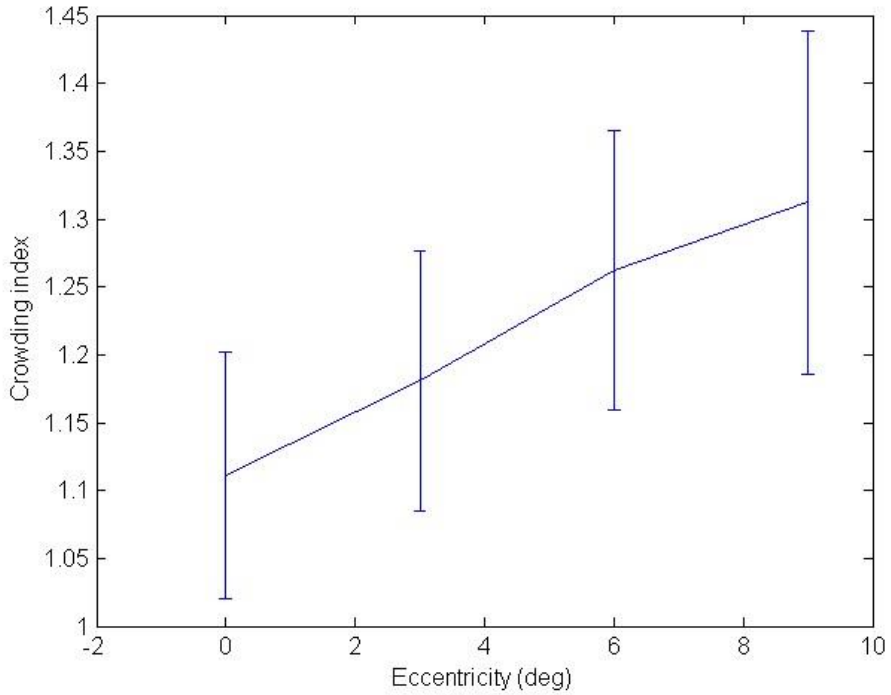

Figure 8-11 Average crowding index (9 participants; CI) in a shape matching task. Standard errors shown.

The crowding index showed no relation to either the WASI measure of visual reasoning (0° p=.99; 3° p=.58; 6° p=.78; 9° p=.94) or the raven measure (0° p=.14; 3° p=.68; 6° p=.38; 9° p=.6).

Similarly, WASI visual reasoning scores showed no correlation with CS (0° p=.26; 3° p=.51; 6° p=.71; 9° p=.81) or CC (0° p=.43; 3° p=.93; 6° p=.69; 9° p=.66).

As for all other psychophysical tasks, Raven IQ was unrelated to CS (0° p=.58; 3° p=.97; 6° p=.73; 9° p=.85) and CC (0° p=.69; 3° p=.61; 6° p=.8; 9° p=.92).

8.3.5 Additional Psychophysics

To confirm that the IQ-perception link was confined to psychophysical tasks which involved the suppression of irrelevant information, additional analysis was performed on previously collected psychophysical thresholds in other tasks.

8.3.5.1 IQ and Orientation Discrimination of Motion Defined Boundaries

This data was taken from Chapter 3. 3 participants were excluded as IQ data was unavailable. In total data from 7 participants was used. 7 participants performed in the task in the right visual field. Of these 7, only 5 also performed the task in the left visual field. Visual fields were treated as individual participants.

In the radial condition, no links between psychophysical performance and IQ were identified. This was seen for WASI (0° p=.61; 3° p=.05; 6° p=.63; 9° p=.99) and Raven (0° p=.19; 3° p=.92; 6° p=.79; 9° p=.32).

Similarly, in the tangential condition, IQ did not correlate with psychophysical thresholds. Again, this was seen for both WASI (0° p=.46; 3° p=.66; 6° p=.5; 9° p=.89) and Raven (0° p=.43; 3° p=.07; 6° p=.3; 9° p=.96).

8.3.5.2 IQ and Orientation Discrimination of Luminance Defined Boundaries

Measurements of accuracy in a luminance defined boundary orientation discrimination task were taken from Chapter 3. 3 participants were excluded as IQ measures were unavailable. In total 11 participants were used, measures from the left and right visual fields were summed.

For the IQ measures obtained through WASI, there were no links at any eccentricity (0° p=.32; 3° p=.7; 6° p=.57; 9° p=.39). No links were identified using the Raven measures of IQ (0° p=.3; 3° p=.06; 6° p=.11; 9° p=.08).

Again, no relationships were seen between tangential psychophysical thresholds an IQ for WASI (0° p=.47; 3° p=.82; 6° p=.85; 9° p=.54). Similarly, when IQ was measured using the Raven test, no links were seen (0° p=.38; 3° p=.69; 6° p=.94; 9° p=.14).

8.3.5.3 IQ and Performance in a Shape Matching Task

Using the data collected in Chapter 4, IQ measures were compared to accuracy in a shape matching task. Data from 11 participants was used in this experiment. All participants performed the task in both the left and right visual fields. The visual fields were summed to give a single measure for each participant at each eccentricity.

Using the WASI measures of IQ, no links between IQ and psychophysical thresholds were seen (0° p=.38; 3° p=.16; 6° p=.15; 9° p=.09). Similarly, no links were seen using the Raven measure of IQ (0° p=.55; 3° p=.78; 6° p=.17;
9° p=.29).

8.4 Discussion

A strong positive relationship was identified between surround suppression and visual reasoning ability. Participants who were more influenced by the presence of a background grating during a contrast matching task scored highly in a standardised test of visual reasoning. This relationship showed a clear eccentricity effect. The relationship was present at the higher eccentricities of 6° and 9°, but not significant at 0° and 3°. A relationship was also seen between visual reasoning and susceptibility to surround suppression in a second order discrimination task. No link was identified between visual reasoning and individual differences in measures of crowding. The data presented here replicates and extends the findings of Melnick et al. (2013).

8.4.1 Exclusion of Extraneous Information

The data presented here shows a clear link between individual differences in susceptibility to the suppressive influence of a surround and performance in an IQ subtest. Mirroring the findings of Melnick et al. (2013), the data presented here indicates

that the IQ of participants predicts the extent of surround suppression. Following the proposal of Melnick et al. (2013), it would be expected that high IQ scores would correlate with the ability to exclude extraneous information (e.g. high IQ participants would perform contrast matching equally as well when a surround was present). In fact, a strong relationship was identified in the opposite direction. Participants with high visual reasoning scores showed a greater difference in performance when contrast matching ability in the absence of a surround was compared to contrast matching ability when the target grating was surrounded.

Melnick et al. (2013) hypothesised that participants with high IQs suppressed the large stimulus because they assumed it to be irrelevant background noise. It is possible that high IQ participants also showed this ability in the experiment reported here, but in an unexpected manner. These participants may have treated the surrounded target not as an image consisting of a relevant target and irrelevant background, but as a single large stimulus. In this way, it would be consistent with the findings of Melnick et al. (2013) that the high IQ participants would suppress the large stimulus (consisting of a target and surround) and therefore perform poorly in the contrast matching task.

The link between IQ and the suppression of visual stimuli did not extend to crowding. No links were seen between performance in the WASI Matrix Reasoning task and measures of crowding. This dissociation between surround suppression and crowding supports the argument that these perceptual phenomenon are not two levels of the same phenomenon (Levi, 2008). In surround suppression, the target portion of the stimulus is clearly identifiable. Conversely, in a crowding task the target and flankers cannot be distinguished, instead appearing as undifferentiated elements of a cluster. For this reason, the hypothesised top down suppressive mechanism may exert influence on surround suppression in an alternative way to crowding.

8.4.2 IQ Tests

The IQ-suppression link was generally confined to one measure of IQ. Relationships between surround suppression and WASI IQ were strong and links between psychophysical performance and Raven IQ were absent. This

disparity is surprising as previous research has linked IQ measured with this test to perceptual abilities (Deary, 1994). Furthermore, no correlation was noted between the 2 measures of IQ, in contrast with earlier work (McLaurin & Farrar, 1973). It is thought that the shortened 12 question form of APM did not measure intelligence with a sufficient degree of sensitivity. Unlike the full test, which is widely used and has been demonstrated to show stability across time and cultures (Raven, 2000), the shortened form has received less thorough investigation.

The manner of administration may also explain the abnormal results of the Raven measure. Whilst WASI was administered verbally, participants were given 15 minutes to complete APM independently. The involvement of the experimenter may have increased motivation in WASI relative to APM. Similarly, the WASI was administered before APM, potentially leading to fatigue effects. Administration explanations seem unlikely. Firstly, the testing session was short, lasting no longer than 30 minutes. Secondly, the participants had demonstrated high levels of concentration and motivation throughout several hours of psychophysics.

Previous research has demonstrated that the link between IQ and perceptual abilities spans multiple forms of IQ (Melnick et al., 2013) included verbal comprehension, working memory and processing speed. Surround suppression is distinct from other tests of perception as it accounts for variance in verbal intelligence (Crawford, Deary, Allan, & Gustafsson, 1998). In the experiment presented here, only visual reasoning was measured. This is a key limitation of this study. Recognition of the breadth of the IQ link with psychophysical performance may inform understanding of underlying mechanisms. It should be noted that although the single correlating IQ measure here was highly dependent of visual abilities, the link cannot be understood through individual differences in low level visual abilities. Other measures of visual abilities did not correlate with IQ scores. In neither a luminance defined boundary orientation discrimination task (Chapter 3) nor a spatial frequency pattern shape discrimination task (Chapter 4) did participant performance show a correlation with IQ.

A major criticism of previous studies showing links between IQ and visual abilities was the failure to properly acknowledge the role of working memory (Troche et al., 2014). The data presented here cannot fully address this criticism. A minor limitation of this

study is the absence of a measure of working memory. This test was excluded as the aim of the study reported in this section of this thesis is to demonstrate that neuronal properties in early sensory regions influence intelligence. The role of working memory and other top-down influences is acknowledged, but it not the focus of this work.

In terms of the possible mechanism mediating the IQ-perception link, the data presented here supports the argument for a general, suppressive mechanism mediating both simple perceptual and complex cognitive individual differences. In addition to the intermediate visual area MT (Melnick et al., 2013), tasks reliant on V1 also correlate with IQ. This extension supports the hypothesis that the link reflects a canonical process of the brain.

9 Visual Reasoning and Surround Suppression in the Visual Cortex: A Retinotopic Link between IQ and Surround Suppression?

9.1 Introduction

In Chapter 8 a link was identified between psychophysical measures of surround suppression and IQ. Participants who showed high levels of surround suppression scored highly in a visual reasoning test. The link has been identified in multiple forms of surround suppression. Suppression of motion stimuli (Melnick et al., 2013), first order gratings and second order gratings (Chapter 8) have been linked to IQ.

The documentation of the variety of forms of surround suppression linked to IQ indicates possible neural loci of underlying mechanisms. The work of Melnick et al. (2013) implicates the involvement of MT (Melnick et al., 2013). The links between IQ and first and second order surround suppression suggest V1 (Chapters 5 & 6) may be involved in this relationship. There is also some suggestion that characteristics of LO1, VO1 and V3A/B underlie the link as these areas have been associated with second order contrast discrimination (Larsson et al., 2006).

Now that the breadth and possible loci of this correlation have been outlined, the mechanisms of the link must be considered. Previous attempts to explain why participants with high IQ show greater suppression in psychophysical tasks have been limited. Troche et al. (2014) attribute the link solely to working memory. Given the conflict with Melnick et al. (2013), and absence of a link with non-suppression psychophysical abilities, this explanation seems unlikely. Although it is acknowledged that top-down mechanisms influence task performance to some degree, it is argued that it is not the sole determinant. Melnick et al. (2013) and proposed a role for normalization as a canonical process that underlies both psychophysical abilities and IQ. This suggestion seems likely for low level abilities (Carandini & Heeger, 2013), but its application to intelligence is poorly specified.

Recent developments in retinotopic methodology offers an opportunity for exploration of this link (Zuiderbaan et al., 2012). Characteristics of the organisation of early sensory regions have been shown to constrain perceptual abilities (Duncan & Boynton, 2003, 2007). Parameters of visual retinotopic areas, particularly cortical magnification, correlate with performance in psychophysical measures of perceptual ability. This relationship is seen for low level visual abilities reliant on early visual areas (Duncan & Boynton, 2003), as well as for more complex perceptual tasks such as orientation discrimination of motion defined boundaries (Chapter 3). It is possible that in the same way that cortical parameters constrain perception, retinotopy also limits complex cognitive skills such as those measured in an IQ test.

Population Receptive Field (pRF) mapping provides information about the organisation of the receptive fields of neurons in the visual cortex. Recent work (Zuiderbaan et al., 2012) has further developed this technique, allowing measurement of the size of centres and surrounds. In this way, the underlying mechanisms of surround suppression can be directly linked with the behavioural performance. Considering the relationship between visual reasoning (a subtest of IQ measurement) and pRF mapping may develop understanding of the link between surround suppression and IQ. Furthermore, a link between cortical parameters and visual reasoning would strongly challenge the suggestion that the IQ-surround suppression link is fully mediated by top- down processes such as working memory (Troche et al., 2014) and motivation.

Speculation regarding the direction of possible links between pRF parameters and visual reasoning are informed by previous experiments (Chapters 5, 6 & 8). Good visual reasoning abilities are associated with high levels of psychophysical suppression (Melnick et al., 2013; Chapter 8). High psychophysical suppression is correlated with large pRF surround size in V1. The role for V1 is expected to expand to links with IQ, with high IQ associated with large V1 surround size.

pRF parameters in the early visual areas have been shown to correlate with ability to direct attention in a psychophysical task (Zhang, Zhaoping, Zhou, & Fang, 2012). A modified version of the Posner cueing paradigm was used to obtain measures of saliency strength of a foreground stimulus. Automatic redirection of attention in response to cues correlated with activity in V1 (Zhang et al., 2012). It was concluded that the saliency

map, e.g. the allocation of attention via a bottom up mechanism, is located in this region. Furthermore, the saliency strength of the foreground stimulus correlated negatively with V1 pRF size (Zhang & Fang, 2014). Participants with large V1 pRF sizes were less able to direct attention appropriately. Zhang and Fang (2014) used the pRF methods of Dumoulin and Wandell (2008). Unlike more recently developed pRF mapping techniques, the methods of Dumoulin and Wandell (2008) provide only an estimate of pRF centre size.

Theoretically, it would be expected that the ability to direct attention is correlated with IQ. Participants better able to direct attention away from irrelevant information in the visual reasoning matrix stimuli and towards relevant pattern features are more likely to obtain high scores. Although, the direction of this link suggested by Zhang and Fang (2014) is difficult to integrate with the direction indicated by previous chapters of this thesis. Participants with high IQ scores must suppression information (and therefore large pRF surround sizes are optimal) but they must also direct attention appropriately (for which small pRF surround sizes are optimal). It is possible that an inverse correlation between centre size and surround size existed within the data used by Zhang and Fang (2014). In this way, the reported correlation between large pRF centre size and good attentional direction may have occurred because participants with large pRF centre sizes also had small pRF surround sizes.

Visual areas V2, V3, V4 and IPS were also examined for correlations with psychophysical performance, but none were found (Zhang & Fang, 2014).
Zhang and Fang (2014) used the pRF methods of Dumoulin and Wandell (2008) which prevents description of the link between saliency and specific pRF parameters, such as the negative receptive field surround and the ratio between the centre and surround. It is possible that the improved methodology used in the experiment reported here will allow delineation of a role for later visual areas.

Whilst there appears to be sufficient grounds to expect a link between IQ and pRF parameters, previous studies have failed to identify a direct relationship. Schwarzkopf, Anderson, de Haas, White, and Rees (2014) report larger receptive field sizes in the extrastriate visual areas (particularly V3) of autistic patients. The size of receptive fields in this area correlated with individual differences in autistic traits. However, despite the

larger receptive field sizes, the autistic patients did not have higher levels of intelligence in comparison to a control group.

It is possible that the findings of Schwarzkopf et al. (2014) are not applicable to healthy participants. The use of participants on the autistic spectrum may have prevented identification of any IQ-pRF links. It is notable that Schwarzkopf et al. (2014) also failed to find a correlation between visual abilities in the autistic group and pRF parameters as this association has been demonstrated to exist in the healthy population (Chapters 5 & 6). However, Schwarzkopf et al. (2014) only collected measures of orientation and direction discrimination and susceptibility to an Ebbinghaus illusion. The failure to measure surround suppression and exert sufficient control on the psychophysical testing procedures prevents full comparison with the data of this thesis.

Melnick et al. (2013) suggested that IQ test performance is correlated with psychophysical surround suppression task performance because both abilities are reliant on the ability to suppress information. This direction of attention is associated with pRF parameters of V1 (Zhang & Fang, 2014). An investigation of the relationship between measures of IQ and the pRF parameters of early visual areas is expected to extend the constraining role for pRF from low level visual abilities to higher cognitive abilities.

9.2 Methods

9.2.1 Estimation of pRF Surround Size, Centre Size and Surround/Centre Ratio

pRF data was taken from Chapter 5. See Chapter 5 for full details. pRF surround size, pRF centre size and pRF surround/centre ratio was measured for visual areas V1, V2, V3 and V3A.

9.2.2 IQ Measurement

Weschler Abbreviated Scale of Intelligence (WASI) measures for 11 participants were used. This data was taken from Chapter 8. See Chapter 8 for full details of test administration and materials.

9.3 Results

The results present here will outline the absence of a correlation between pRF estimates and scores from the WASI IQ subtest. A series of linear regressions were performed across eccentricities to predict IQ (WASI visual reasoning score) from pRF surround size, centre size and ratio. As for Chapter 5, 6 and 7, eccentricity and eccentricity squared were included as additional covariates to remove the confounding, non-linear and linear effects of eccentricity.

9.3.1 The Relationship between IQ and pRF Surround Size

IQ was unrelated to pRF surround size of all visual areas (table 9-1; V1 p=.1, V2 p=.32, V3 p=.67, V3A p=.15).

Table 9-1 WASI visual reasoning score (IQ) predicted from pRF surround size (deg). *p<.05 **p<.01 ***p<.001.

Model	B	SE	β
Constant	30.019	2.539	
Eccentricity	-.118	.372	-.190
Eccentricity²	.000	.035	.000
V1 Surround Size	.923	.553	.664
V2 Surround Size	-.598	.599	-.384
V3 Surround Size	.154	.382	.121
V3a Surround Size	-.298	.201	-.272

9.3.2 The Relationship between IQ and pRF Centre Size

IQ did not correlate with pRF centre size of any visual area. V1 (p=.74) V2 (p=.71) V3 (p=.55) and V3A (p=.83) were unrelated to WASI visual reasoning scores.

Table 9-2 WASI visual reasoning score (IQ) predicted from pRF centre size (deg). *p<.05 **p<.01 ***p<.001.

Model	B	SE	β
Constant	29.264	4.045	
Eccentricity	-.056	.365	-.091
Eccentricity²	.000	.038	.000
V1 Surround Size	.598	1.807	.083
V2 Surround Size	-.653	1.735	-.085
V3 Surround Size	.920	1.542	.155
V3a Surround Size	-.175	.794	-.047

9.3.3 The Relationship between IQ and pRF Surround/Centre Ratio

Mirroring the results of surround size and centre size analyses, pRF surround/centre ratio was also uncorrelated with WASI visual reasoning scores. The linear regression (table 9-3) demonstrates that V1 (p=.24), V2 (p=.49), V3 (p=.26) and V3A (p=.95) were unrelated to WASI scores.

Table 9-3 WASI visual reasoning score (IQ) predicted from pRF surround/centre ratio. *p<.05 **p<.01 ***p<.001.

Model	B	SE	β
Constant	32.733	1.346	
Eccentricity	-.219	.353	-.354
Eccentricity²	.036	.039	.547
V1 Surround Size	-2.978	2.516	-.374
V2 Surround Size	1.876	2.687	.211
V3 Surround Size	-1.700	1.493	-.252
V3a Surround Size	.050	.742	.012

9.4 Discussion

The data presented here demonstrates that IQ is not correlated with pRF surround size, centre size or surround/centre ratio in early and intermediate visual areas. This experiment does not support a bottom-up mechanisms for the IQ-surround suppression link outlined in Chapter 8. This study expands the results of Schwarzkopf et al. (2014) to the normal population, receptive field properties measured using pRF techniques are not linked to IQ.

Based on previous research (Zhang & Fang, 2014), pRF measures made in V1 were expected to correlate with IQ. In fact, the data outlined here indicates no predictive role for V1 in visual reasoning. Both V1 surround size and centre size have previously been linked to psychophysical measures of perceptual suppression (Chapters 5 & 6). IQ was unrelated to both V1 surround size and V1 centre size.

The failure to find a significant relationship between visual reasoning and V1 pRF estimates does not exclude the possibility that V1 is linked to IQ via an alternative mechanism. In fact, the consistent link between V1 and first order surround suppression (Zenger-Landolt & Heeger, 2003) and the correlation between visual reasoning and first order surround suppression (Chapter 8) suggests a strong link between these measures. Performance in the visual reasoning task is complex and dispersed (in contrast with the simpler attentional modulation task used by Zhang & Fang, 2014), it is possible that any V1 pRF links are obscured by other relationships.

Good performance in the visual reasoning task requires multiple skills. Two important processes may be the direction of attention and the suppression of irrelevant information. To successfully identify the pattern in the puzzle, participants must ignore the irrelevant information and direct attention to the relevant aspects of the image. Based on the findings of Zhang and Fang (2014), good attentional modulation (and therefore high IQ) should correlate with small V1 pRF size. Conversely, based on the findings of Chapters 5, 6 and 8, efficient suppression of irrelevant information (and therefore high IQ) should correlate with large V1 pRF size. It is possible that these conflicting facilitatory roles for pRF have masked the presence of any relationship in the experiment reported in this chapter. Future research should aim to subdivide the complex process of visual reasoning performance in order to fully delineate the competing mechanisms.

The data in this chapter does not confirm the existence of a bottom-up mechanism linking IQ to perceptual abilities, the assertion of Troche et al. (2014) for a mainly top-down process cannot be dismissed. Whilst this study failed to identify a link between IQ and receptive field properties, it remains possible that IQ will correlate with other low level cortical properties of early visual areas.

10 Individual Differences in Levels of Visual Cortex GABA Mediates the Relationship between Visual Reasoning and Surround Suppression

10.1 Introduction

A correlation between IQ and perceptual surround suppression has been demonstrated (Melnick et al., 2013). In Chapter 8 it was shown that the correlation between visual reasoning (a subtype of IQ) and psychophysical performance is specific to surround suppression, it is absent in other psychophysical tasks. The specificity of the correlation between IQ and surround suppression suggests that it is mediated by a general ability to suppress information.

Analyses performed in previous chapters explored the possibility that the cortical basis of IQ and surround suppression are mediated by the same suppressive mechanisms. The population receptive field (pRF) surround size of V1, and to a lesser extent the centre size of V1, were related to psychophysical surround suppression in a contrast matching task (Chapters 5 & 6) but did not correlate with performance in a visual reasoning matrix IQ subtest (Chapter 9). It was concluded that the shared suppressed mechanism of IQ and perceptual surround suppression cannot be understood through pRF methodology.

Schizophrenia patients show abnormal performance in a psychophysical surround suppression task (Yoon et al., 2009) and higher levels of gamma- aminobutyric acid (GABA) in the visual cortex (Yoon et al., 2010). Furthermore, a correlation has been identified between the susceptibility to the suppressive influence of a surround and levels of visual cortex GABA (Yoon et al., 2010). This indicates that at the level of an individual participant, high levels of GABA predict high levels of surround suppression. Whether this link also exists in the normal population is unknown. Yoon et al. (2010) identified a trend towards a correlation in the normal population, but significance was not reached. Schizophrenia is linked to both unusual GABAergic activity (Wassef, Baker, &

Kochan, 2003) and visual perception (O'Donnell et al., 2006) which may complicate the application of the findings of Yoon et al. (2010) to the normal population.

The role of GABA in IQ is less well specified, largely due to the wide dispersion across the brain of perceptual processes underlying higher cognitive abilities. A complex task such as the visual reasoning matrix test requires a variety of skills in addition to visual abilities, including short term memory, logical reasoning and the suppression of irrelevant information. To confirm the role of GABA as the link between IQ and surround suppression, GABA levels must be directly compared to both IQ scores and surround suppression.

10.2 Methods

10.2.1 Participants

9 participants (2 males) took part in this experiment. All participants also took part in the experiments reported in Chapters 5, 6, 7, 8 and 9. All participants had normal or corrected to normal vision and were aged between 22 and 35. Participants were post-graduate students or post-doctorate researchers at the Psychology department of Royal Holloway University. Written consent was obtained from all participants. The experimental procedure was in accordance with the Declaration of Helsinki and was approved by the appropriate local ethics committee.

10.2.2 Measurement of IQ

Weschler Abbreviated Scale of Intelligence (WASI) Visual Reasoning Subtest measures for 9 participants were used. This data was taken from Chapter 8. See Chapter 8 for full details of test administration and materials.

10.2.3 Estimation of GABA

An estimate of GABA concentration in the visual cortex was obtained for 9 participants using the methods of Edden, Puts, Harris, Barker, and Evans (2014). Magnetic resonance spectroscopy (MRS) was performed using a 3T whole-body MR scanner (Magentrom Trio: Siemens, Erlagen, Germany) at Royal Holloway. Data collection for each participant took approximately 35 minutes and was completed in a single session. During collection of this data participants were instructed to lie as still as possible, no task was performed.

A short (approximately 10 minutes) T2 anatomical scan was performed to collect anatomical images in 3 planes. This was used to correctly place the voxel in the MRS scan. The anatomical volume had a voxel size of 1x1x1mm. Following visual inspection of this anatomical image the MRS voxel was placed over the primary visual cortex, defined according to the calcarine sulcus. The voxel was placed so as to exclude as much cerebrospinal fluid as possible. No control voxel was used. Multiple-voxel MRS techniques require much longer scans (Zhu & Barker, 2011). The use of a single voxel limits the power of this study to conclusively localize the relationship between GABA and IQ to the visual cortex.

The acquisition of MRS data was performed using the MEGA-PRESS sequence (Mescher, Merkle, Kirsch, Garwood, & Gruetter, 1998). The following parameters were used; voxel size= 30 x 35 x 25 mm, repetition time (TR)=2000 ms, echo time (TE)= 68. Voxel placement for a single participant is displayed in figure 10-1. MRS acquisition took approximated 15 minutes. An editing pulse was applied to the GABA signal at 1.9ppm to isolate GABA signals from the spectra. An editing pulse is a radiofrequency pulse that separates the GABA signal from the water signal in the MRS. A reference scan was also collected, no editing pulse was applied and water was unsuppressed. In total, 2 GABA scans and 2 reference scans were collected. GABA scans and reference scans were collected in alternating order, with a GABA scan always collected first.

MRS data was processed using Gannet (Edden et al., 2014), a Matlab based toolbox that estimates GABA concentration. This analysis techniques exploits the difference between the references scan and the scan in which the editing pulse was applied. In this way, the

GABA signal is separated from the underlying creatine signal at 3ppm. The final estimate of GABA concentration represents the peak of the GABA spectrum. The toolbox provides two estimates of GABA, one relative to water (GABA/H20) and one relative to creatine (GABA+/Cr). GABA/H20 was used due to the superior signal to noise ratio (Puts & Edden, 2012). The GABA spectrum is shown in figure 10-2.

2 estimates of visual cortex GABA concentration were obtained for each participants by comparing each of the 2 GABA scans with the reference scan immediately following it. These 2 estimates were compared. Consistency across the 2 estimates indicated high reliability. The final single GABA estimate from each participant was the mean average of these 2 estimates.

The methods used here are consistent with current practice within the field (Puts & Edden, 2012). MEGA-PRESS is the most widely used technique for MRS GABA measurement (Mullins et al., 2014). All MRS GABA collection techniques, including those used here, are limited to some extent by the spatial resolution of MRS. Due to the low concentration of GABA, the spatial resolution must be compromised to allow the available signal to be increased (Toga & Mazziotta, 2002). Additionally, all available MRS GABA methods do not provide true absolute values of GABA concentration in meaningful units (Mullins et al., 2014). The institutional units that are referred to within this thesis are appropriate for comparing participants measured using the same technique but comparison with other studies is limited.

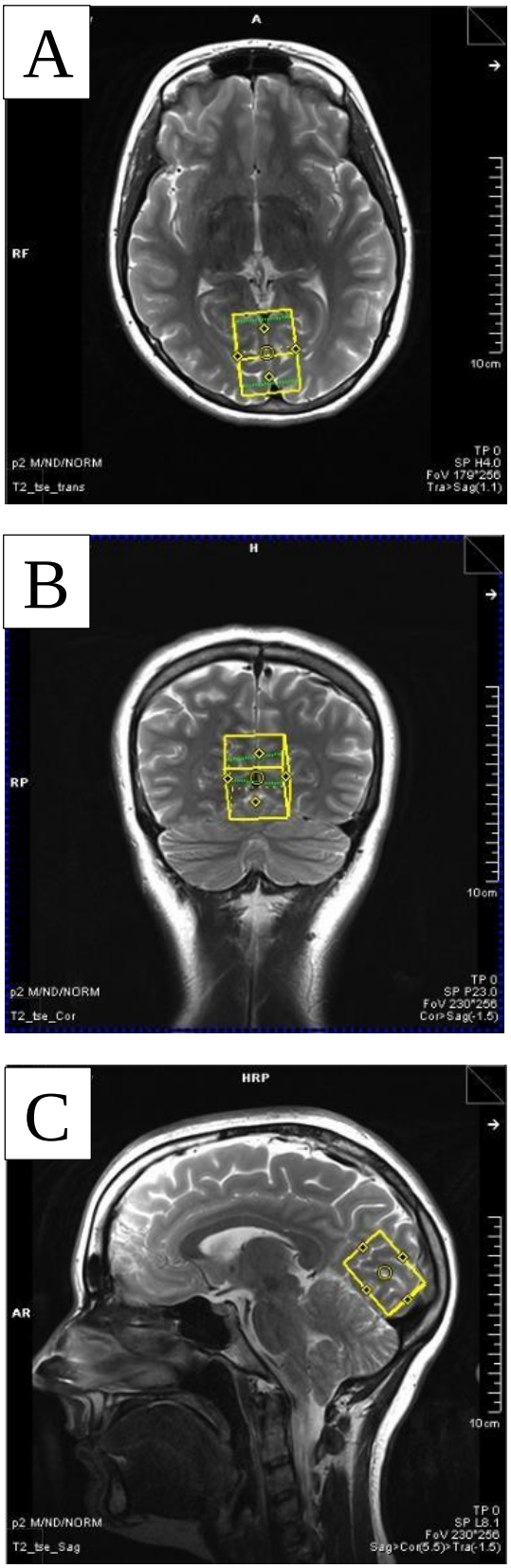

Figure 10-1 MPRAGE showing position of MRS Voxel (30x35x40ms) in single participant. A. axial section. B. coronal section. C. sagittal section.

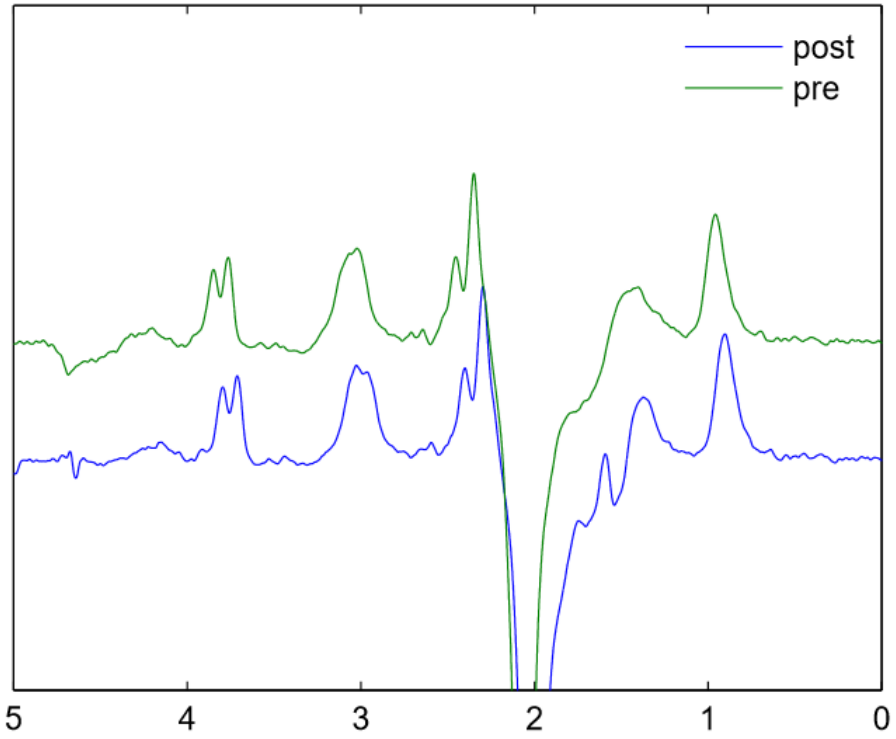

Figure 10-2 The GABA-edited difference spectrum taken from the Gannet toolbox output. The figure shows the GABA spectrum for a single participant before (green) and after (blue) frequency and phase correction (performed to reduce artefacts associated with frequency and phase instability). X axis displays ppm.

10.2.4 Psychophysical Surround Suppression Measurement

Psychophysical data for first order surround suppression and second order surround suppression were taken from Chapters 5 and 6. See Chapter 5 and 6 for full details of experimental methods. Participants performed the first order surround suppression task prior to second order data collection.

A first order surround suppression index (SI_1) was computed from the suppression measurement in the control trial (SC_1) and the suppression measurement in the surrounded condition (SS_1). This corrected for the eccentricity-specific effects of adaptation in contrast matching within trial adaptation. A value close to 1 indicates that the introduction of a surround reduces perceived contrast. An analogous second order suppression index (SI_2) was computed in the same way.

(1) $SI_1 = 1 - (\frac{SS_1}{SC_1})$

10.2.5 Psychophysical Crowding Measurement

Crowding data was taken from Chapter 7. Full details of data collection and analysis are provided in Chapter 7. First and second order surround suppression data was collected before crowding data. Crowding indices (CI) were computed in a similar way to suppression indices. CI was computed from measures of crowding in the control condition (CC) and measures of crowding in the surrounded condition (CS). As for surround suppression indices, a crowding index of 1 indicates that the presence of flankers reduces discrimination performance.

(2) $CI = \frac{CS}{CC}$

10.3 Results

In summary, this experiment demonstrates that IQ (WASI scores), first order surround suppression and second order surround suppression are correlated with GABA concentration in the visual cortex.

10.3.1 The Relationship between GABA and IQ (Visual Reasoning)

A correlation was performed between WASI scores and measures of GABA relative to water (GABA/H20). A strong positive correlation was identified (figure 10-3; R=.83, p<.01). Participants with good visual reasoning abilities had high levels of visual cortex GABA.

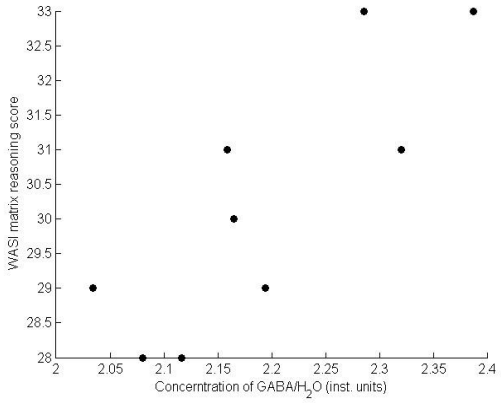

Figure 10-3 The relationship between GABA and visual reasoning (WASI; p<.01). Each data point represents a single participant.

10.3.2 The Relationship between GABA and First Order Surround Suppression

A correlation was performed between first order suppression indices (SI_1) and measures of GABA concentration. The GABA measure was obtained relative to water (GABA/H20). Across all eccentricities, SI_1 correlated with GABA (figure 10-4; R=.5, p<.01). There was some indication of a correlation between GABA and surround suppression at 6° (figure 10-5; R=.62, p=.08), but this link did not reach significance.

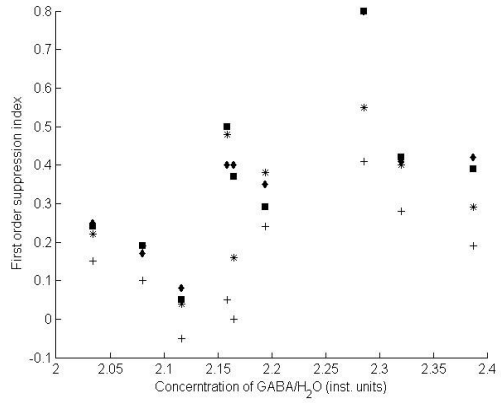

Figure 10-4 The relationship between GABA and first order surround suppression at eccentricities of 0° (+), 3° (*), 6° (♦) and 9° (■), (p<.01). Each data point represents a single participant at a single eccentricity patch.

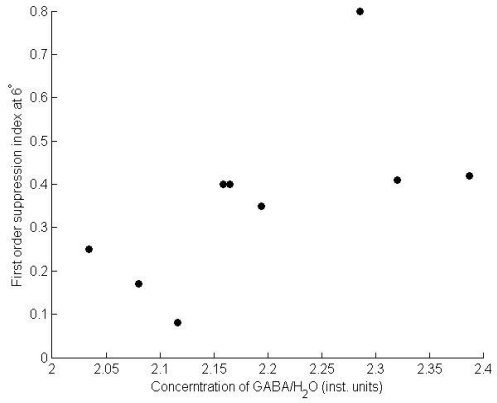

Figure 10-5 The relationship between GABA and first order surrounds suppression at 6° (p=.08). Each data point represents a single participant.

10.3.3 The Relationship between GABA and Second Order Surround Suppression

A correlation was performed between the second order suppression indices (SI_2) and measures of GABA concentration. The GABA measure was obtained relative to water (GABA/H20). A strong link between SI_2 and GABA was seen at eccentricities of 0° (figure 10-6; R=.78, p<.05), 6° (figure 10-7; R=.73, p<.05) and 9° (figure 10-8; R=.72, p<.05). This association was also seen when correlations were run across eccentricities (R=.58, p<.001). These links mirror the trend seen for first order suppression, high suppression is linked to high GABA.

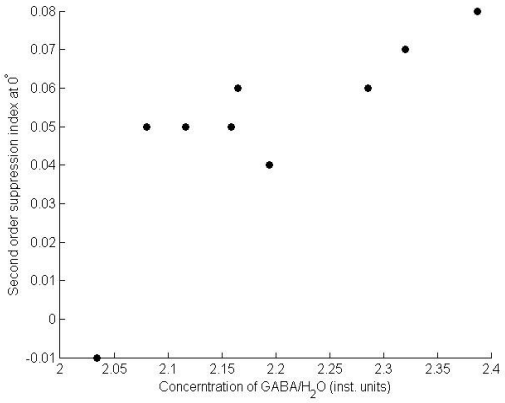

Figure 10-6 The relationship between GABA and second order surround suppression at 0° (p<.05). Each data point represents a single participant.

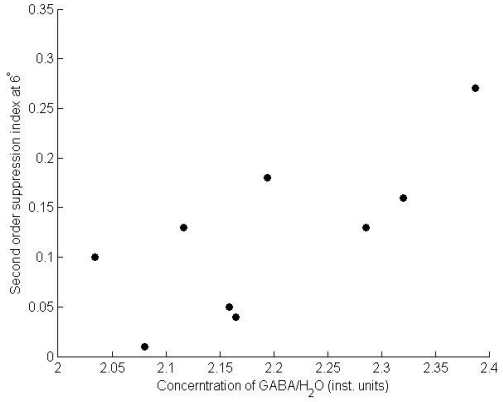

Figure 10-7 The relationship between GABA and second order surround suppression at 6° ($p<.05$). Each data point represents a single participant.

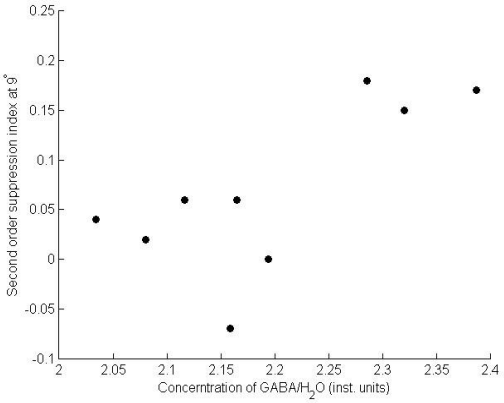

Figure 10-8 The relationship between GABA and second order surround suppression at 9° ($p<.05$). Each data point represents a single participant.

10.3.4 The Relationship between GABA and Crowding

The relationship between crowding indices (CI) and measures of GABA was investigated through a series of correlations. Analyses demonstrated that both across eccentricities ($R=-.03$, $p=.87$) and at specific eccentricities GABA was unrelated to crowding (0° $p=.72$; 3° $p=.99$; 6° $p=.85$; 9° $p=.86$).

10.4 Discussion

The data presented here indicates a positive relationship both between levels of visual cortex GABA and IQ and between GABA levels and surround suppression. Conversely, crowding correlated with neither IQ nor GABA. Taken together, this data extends the inhibitory role of GABA from low level visual abilities to complex cognitive tasks.

10.4.1 Surround Suppression and GABA

A correlation between susceptibility to surround suppression and GABA estimates is consistent with past studies. Yoon et al. (2010) found that, for schizophrenia patients, high susceptibility to first order surround suppression was correlated with levels of GABA in the visual cortex. Yoon et al. (2010) found a similar, but non-significant trend in a control group. The data presented here has expanded this link to the normal population and demonstrated that GABA also correlates with second order surround suppression. Taken together, these findings suggest that GABA plays a broad role in suppressive visual processing mechanisms.

It is notable that GABA was more closely linked to the suppressive effects in a second order task than the first order. The most likely reason for this discrepancy is the order of testing. For all participants, first order surround suppression conditions were run before second order surround suppression. It is likely that for this reason, the second order indices are a more accurate measure. After 4 hours of testing, participants were most likely highly trained to fixate at the appropriate screen location. The higher level of variance in first order than second order indices is consistent with this assertion.

An alternative explanation is that the voxel placement was insufficiently accurate and extended into the extrastriate cortex. GABA correlations with first order surround suppression would be expected in V1 (Yoon et al., 2010), with any second order relationships located at later visual areas (Larsson et al., 2006). This possibility is unlikely as despite the sub-optimal voxel placement methodology, all voxel were located substantially in the calcarine cortex and therefore primarily measured V1.

Despite this hypothesised general role for GABA, the suppressive role of GABA in perceptual suppression did not extend to measures of crowding. Crowding is not associated with IQ (Chapter 8), further supporting the argument that this form of perception is not involved in the general suppressive mechanism outlined here. This dissociation between surround suppression and crowding supports the argument that these perceptual phenomenon are not two levels of the same phenomenon (Levi, 2008). It is also possible that the voxel placement used here is unsuitable for investigating neural correlates of crowding, previously shown to occur in later regions of the visual cortex (Freeman & Simoncelli, 2011).

10.4.2 IQ and GABA

Estimates of GABA in the visual cortex were strongly associated with performance in a Weschler IQ subtest. The test used here measured visual reasoning, a task heavily reliant on pattern recognition. Participants with higher IQ scores had higher levels of visual cortex GABA. It is suggested that the inhibitory activity of GABA facilitates the suppression of irrelevant information, thereby revealing the aspects of the image necessary for pattern identification. This findings provides a mechanism for the link between perceptual surround suppression and IQ (Chapter 8; Melnick et al., 2013).

The full Weschler test was not administrated, thereby preventing comparison of the participant sample IQ scores with the general population. There is reason to consider the possibility that participant performance in the visual reasoning task differs from the general population. All participants were PhD students or post- graduate researchers, thereby having undertaken an undergraduate degree and 1-4 years of additional post-graduate study. This level of education and the technical occupations held by these participants has been linked to higher levels of IQ (Reynolds, Chastain, Kaufman, & McLean, 1988). The correlation between performance and education was present for measures of performance IQ, including the perceptual reasoning task used here.

It is suggested that the participants used here represent the higher end of both the GABA and perceptual reasoning spectrum. There is no evidence to indicate that the pairing should not be present in participants of a different demographic. Yoon et al. (2010) report

a link between surround suppression and GABA in alternative populations, indicating that the suppressive role of GABA is a general phenomenon. To confirm this hypothesis is it necessary to perform a wider investigation of the IQ-GABA link to demonstrate the presence across demographics. It would also be of interest to explore performance in other subtests of IQ, particularly those that do not depend as heavily on vision as the perceptual reasoning ability task used here.

10.4.3 A Global Suppressive Mechanism

Throughout Chapters 8, 9 and 10 multiple links have been explored between neurological parameters, complex cognitive abilities and low level perceptual abilities. Participants with high IQ scores also have high levels of surround suppression and high levels of GABA. Additionally, IQ is linked to surround suppression in a corresponding direction. It has been demonstrated that GABA acts to inhibit both low and high level psychological processes.

I argue that a global suppressive mechanism acts to determine abilities in a variety of tasks. WASI performance, surround suppression and GABA concentration are correlated with one another. The directions of these relationship cannot be determined by the data reported here although consideration of the strength of these links may inform speculation.

Some argue that the link between IQ and psychophysical surround suppression is mediated by top-down processes (Troche et al., 2014). The association between GABA and IQ measures is stronger than the link between GABA and first order surround suppression. This conflicts with the hypothesis of Troche et al. (2014). The data presented here heavily favours a bottom-up account of the IQ-psychophysical link (figure 10-9). GABA most likely determines both IQ and surround suppression susceptibility, with the identified relationship between the 2 behavioural measures secondary. The correlation between pRF surround size and psychometric performance has been explored (Chapter 9) but no relationships were identified.

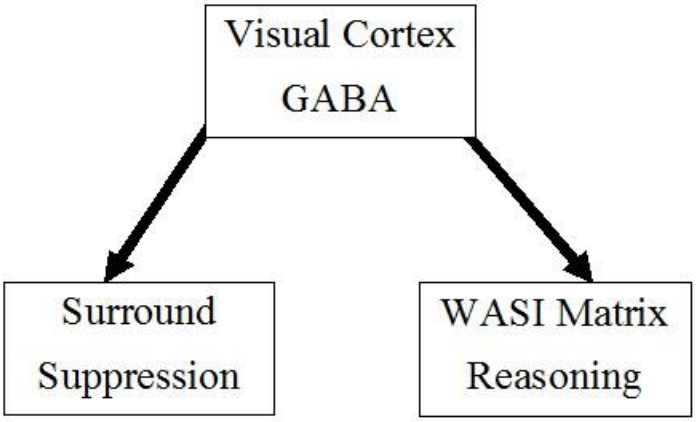

Figure 10-9 Illustration of the hypothesised direction of parameters involved in the global suppressive mechanism.

10.4.4 The Role of Alpha Oscillations

To date, the mechanisms of the correlation between IQ and surround suppression are poorly specified. The cognitive abilities required for an IQ test are complex, how they could be constrained by cortical parameters of the earliest visual area is unknown. Alpha oscillations have been proposed as a link between task performance and neural parameters. Alpha oscillations increase during both psychophysical suppression (Harvey et al., 2013) and cued ignoring (Payne, Guillory, & Sekuler, 2013). If, as is hypothesised, a high IQ score is reliant on the ability to ignore extraneous information, alpha oscillations should also mediate performance in the matrix task.

A recent study utilizing pRF techniques has specified the role of alpha in surround suppression (Harvey et al., 2013). Subdural electrocorticography and fMRI measures were made in V1 and IPS of a single participant. Oscillations in the alpha bandwidth (9-12 Hz) increased during stimulation to the region directly outside the receptive field. The change correlated with negative fMRI responses. Increases in alpha in V1 and IPS were thought to reflect surround suppression. The increase in V1 alpha was highly localized to the stimulation site, suggesting a role in local computations. The IPS alpha increase was broader and dispersed across a large area of cortex, indicating a secondary large-scale inhibition role for alpha oscillations.

Alpha oscillations have also been linked with higher cognitive processes (Klimesch, Sauseng, & Gerloff, 2003; Payne et al., 2013). EEG data demonstrated a spike in alpha activity during both cued attending, in which extraneous background information must be ignored, and cued ignoring, in which all information must be ignored. Payne et al. (2013) indicate that in addition to suppression at a neuronal level (Harvey et al., 2013), alpha oscillations also play some suppressive role in higher level abilities.

The increase in alpha oscillations during the suppression of information is thought to reflect changes in GABA levels (Angelucci & Bressloff, 2006; Schwabe, Obermayer, Angelucci, & Bressloff, 2006). This link is clearest in psychophysical surround suppression, both alpha oscillations (Marshall et al.,
2002) and GABAergic interneurons (Fitzpatrick, 2000) have been linked to this perceptual phenomenon.

10.4.5 Further Research Directions

Performance in the Wechsler perceptual reasoning subtest is not an abstract ability. Measures similar to this are a predictor of occupational success (Kuncel, Hezlett, & Ones, 2004). Many organizations use pattern recognition tasks as part of a recruitment process. For example, 50% of the top 10 UK graduate employers of 2014 (Birchall, 2014) publically advertised their use of a pattern recognition matrix reasoning task.

Understanding the cortical basis of performance in psychometric tests presents opportunities for future research to improve performance through manipulation of the cortical basis. The details of this mechanism remain unspecified, although the involvement of alpha oscillations is hypothesised. GABA can be modulated through the use of transcranial direct current stimulation (Stagg, Bachtiar, & Johansen-Berg, 2011). Changes to GABA influenced behavioural and cortical measures of motor learning (Stagg et al., 2011). It would be of interest to utilise this paradigm to explore further the links outlined in this chapter. This would serve both to confirm the role of GABA in between participant IQ variability and to demonstrate the possibility of influencing higher cognitive abilities.

11 Discussion

11.1 Summary of Thesis Aims and Findings

Past research has indicated a close link between retinotopic parameters and low level visual abilities (Duncan & Boynton, 2007). Information regarding the breadth of this bottle-neck role is sparse in the current literature. Research has generally focused on V1 (Duncan & Boynton, 2007; Schwarzkopf et al., 2011; Song et al., 2013). Additionally, the absence of understanding regarding the inter-areal correlations has prevented the localisation of the constraining role to a specific visual map. This thesis had three key aims. Firstly, to outline inter- areal correlations in cortical parameters. Secondly, to identify links between visual abilities and cortical parameters. Thirdly, to study the link between cortical parameters (such as the centre–surround configurations in early visual cortex and the concentration of specific neurotransmitters) and participant performance on modality-specific and modality-general tasks. Understanding this link was expected to allow the drawing of inferences about the cortical mechanisms underlying inter-participant variability in different testing conditions.

In this chapter I will summarise and review the key findings regarding these aims. I will discuss the implications of the data presented here on current debates within the literature. The general limitations and strengths of the methodology will be considered.

To fully document the characteristics of the participants used here, extensive measures were made of cortical parameters, visual abilities and higher cognitive functioning. To obtain cortical measures, retinotopic maps were defined using fMRI data. The surface area, cortical magnification (polar and radial) and population receptive field (pRF) characteristics (centre size, surround size and surround/centre ratio) of these maps were estimated. Additionally, early visual cortex gamma-aminobutyric acid (GABA) was estimated. To obtain visual ability data, psychophysical measures of visual discrimination and surround suppression were collected for a variety of stimuli. Psychometric data was

obtained using an IQ subtest to measure visual reasoning abilities. The participant group remained broadly consistent across experiments.

Briefly, the key findings of the 9 experimental chapters can be summarised as follows:

Part 1: Does cortical magnification constrains visual abilities?

- Chapter 2: Visual areas generally showed high levels of independence in measures of surface area and cortical magnification, inter-areal correlations were sparse and weak. Within retinotopic maps, variability was high. The dominant source or variance was the strong effect of eccentricity.
- Chapter 3: Cortical magnification in V3A constrained performance in a motion defined orientation discrimination task. The link was identified in the opposite direction to that expected, good performance was associated with low levels of cortical magnification and a smaller V3A surface area.
- Chapter 4: Shape matching ability did not strongly correlate with cortical magnification in intermediate visual areas. A weak link was identified for LO1 polar cortical magnification.

Part 2: Do pRF surround size, centre size and surround/centre ratio estimates constrain visual abilities?

- Chapter 5: Estimates of pRF surround size in V1 predicted performance in a first order surround suppression task. Large V1 surround size was associated with high perceptual suppression.
- Chapter 6: Performance in a second order surround suppression task was constrained by V1 surround size in an analogous way to first order surround suppression.
- Chapter 7: Crowding in a shape discrimination task was correlated with V1 pRF centre size. Unlike surround suppression, no link was identified between V1 surround size and crowding.

Part 3: A GABA mediated global suppressive mechanism

- Chapter 8: Performance in the visual reasoning IQ subtest correlated with performance in first- and second-order surround suppression tasks. Measures of crowding were unrelated to visual reasoning ability.
- Chapter 9: pRF estimates of surround size, centre size and surround/centre ratio in early visual areas were poor predictors of performance in the WASI IQ subtest.
- Chapter 10: GABA estimates in the early visual cortex predicted both IQ subtest scores and psychophysical surround suppression measures. Crowding was unrelated to GABA.

11.2 Do Retinotopic Parameters Constrain Visual Abilities?

The primary question that this thesis aimed to address was whether the cortical parameters of early and intermediate visual areas constrained visual abilities. A general and simple answer is that quantitative parameters of retinotopic visual areas do not strongly constrain or determine differences between participants in performance in the tasks measured here. Individual differences in low level and intermediate visual areas showed only a weak association with performance in visual abilities. In fact, higher cognitive abilities were a stronger determinant of basic visual processing than any of the cortical parameters investigated here.

Inter-individual variability was not strongly predicted by the characteristics of the cortical region thought to underlie the processing of the stimulus. All variables collected in the experiments addressing this issue showed a high level of variation, as expected from the literature. Between participants, variability in cortical magnification was high (Brewer et al., 2005; Larsson & Heeger, 2006). Although, whilst behavioural measured showed a similarly high level of variation, they did not correlate strongly with the cortical measures.

Intra-individual variability was the dominant feature throughout analyses. Within a single retinotopic map the changes in cortical magnification and receptive field parameters with movement away from the foveal representation was clear (Dumoulin & Wandell, 2008; Popovic & Sjöstrand, 2001). Perceptual performance in multiple tasks mirrored this

strong eccentricity effect. Discrimination thresholds were poorer in the periphery (Chapters 3 & 4) and the suppressive influence of surrounding stimuli was greater (Chapters 5, 6 &7). Unlike inter-individual variability, intra-individual variability in retinotopic measurements was consistently correlated with psychophysical performance.

11.2.1 Cortical Magnification and Visual Abilities

Duncan and Boynton (2003, 2007) proposed that cortical magnification acts as a bottle-neck to limit visual perception. Experiments reported in Chapters 3 and 4 directly tested the hypothesis that individual differences in cortical parameters constrain visual abilities. Measures of cortical magnification and size were used to predict performance in a variety of psychophysical tests of varying complexity. The dependency of these abilities on retinotopic cortical parameters is mixed, but generally stronger for the lower level visual tasks. Cortical magnification constrains performance in an orientation discrimination task using motion defined boundaries more strongly than the intermediary process of shape perception.

It has proved more difficult to pair intermediate visual abilities with a specific retinotopic map. For example, simple tasks such as discrimination of luminance defined orientation are closely linked to V1. This pairing has been well documented (Duncan & Boynton, 2003). Conversely, the cortical location of complex visual tasks such as shape perception remains debateable. It is likely that the cortical constraints limiting performance in complex psychophysical tasks are dispersed over multiple regions, most likely including non-retinotopic areas.

11.2.2 pRF and Visual Abilities

pRF estimates of surround size were better determinants of low level visual abilities than cortical magnification. Both pRF surround size and pRF centre size predicted performance. The third pRF estimate, surround/centre ratio, was a poor predictor of psychophysical suppression. Mirroring cortical magnification, the brain-behaviour associations were more easily understandable for simpler tasks than the more complex

phenomenon of crowding. Simple forms of suppression were linked to the visual areas previously shown to underlie perception (e.g. first order suppression was correlated with V1 pRF estimates). Conversely, complex forms of suppression were not linked to the visual areas previous shown to underlie perception (e.g. crowding of radial frequency shapes was linked to V1 pRF estimates only). As for the cortical magnification experiments, it was difficult to pair intermediate retinotopic maps to specific tasks.

It is possible that the pRF methods used here are not appropriate for mapping visual areas later than V1. The stimuli used in the collection of retinotopic data from which pRF estimates are made consists of luminance defined checker board stimuli. Processing of first order patterns, such as the checkboard stimuli, is thought to occur in V1 (Larsson et al., 2006). It has also been suggested that fMRI lacks the resolution necessary to accurately measure the receptive field centre surround configurations of later visual areas such as V3A (Zuiderbaan et al., 2012).

Zuiderbaan et al. (2012) report the normalized variance in the fMRI time series data explained by a 2 Gaussian pRF model (similar to the model used in this thesis). The model was most useful in explaining V1 variance and very poor in explaining V3A variance. The model was moderately successful in explaining V2 and V3 variance. Whilst the retinotopic stimuli used by Zuiderbaan et al. (2012) were not identical to the stimuli used in this thesis, Zuiderbaan et al. (2012) also used first-order checkboard patterns.

The investigation of the predictive role for pRF size informed speculation regarding a spatial pooling mechanism in the early visual system mediating crowding. Unlike perceptual surround suppression which was primarily associated with V1 pRF surround size, large V1 pRF centre size predicted crowding. This was attributed to a spatial pooling mechanism at the level of a single receptive field. To date, this is the first indication of similar but distinct roles for pRF centre size and pRF surround size in the mediation of surround suppression and crowding. This demonstrates that the methodology used here, of comparing retinotopic parameters to separately collected psychometric data, and may provide insight absent in other investigations into the cortical locus of visual processing. For example, Cai et al. (2014) used alternative methodology to address a similar hypothesis regarding the correlation between crowding and pRF size and identified no mediating role for spatial pooling in V1.

11.2.3 IQ

Recently it has been shown (Melnick et al., 2013) that IQ measured with the Weschler scale is strongly correlated with performance in a surround suppression task consisting of a moving stimuli of varying size. In this thesis I extended this finding and tested the link between IQ (measured via WASI) and first and second order surround suppression, identifying a strong correlations between the psychometric and psychophysical measures. Interestingly this relationship does not extend to crowding performance, corroborating the proposal that surround suppression and crowding are not 2 levels of the same process (Levi, 2008).

Whilst the original focus of this thesis was to consider low level constraints on psychophysical performance, it is clear that the best predictor of performance is IQ. This finding conflicts with the assertions of Duncan and Boynton (2003) that visual abilities are primarily determined by retinotopic properties of the early visual system. IQ was specifically involved in surround suppression psychophysical tasks. These findings suggest novel directions for future research. It would be of interest to uncover an analogous top-down mechanism involved in the mediation of other visual abilities.

I explored what mechanism might mediate the established relationship between IQ levels and surround suppression. The final experiment reported here addresses the role of GABA in mediating the link between visual abilities and a subtype of IQ. The finding opens multiple novel paths of enquiry to further specify this correlation. Only a single type of IQ was measured, performance in a matrix visual reasoning task. This test is heavily reliant on visual abilities. It is necessary to expand the breadth of cognitive tests mediated by GABA levels. The findings of Melnick et al. (2013) indicate non-visual measures of IQ have a similar link to psychophysical surround suppression. Furthermore, the hypothesised GABA mediated mechanism is expected to exist across the brain, there is no reason to assume it is constrained to a solely visual domain.

Multiple perceptual modalities have been linked to IQ (Li et al., 1998; Troche & Rammsayer, 2009b). Both the original hypothesis of Spearman (1904) and the presence of GABA throughout the CNS supports the prediction that the suppressive mechanism outlined in this thesis will extend to other perceptual abilities. The involvement of GABA

in the auditory cortex is well documented, it has been linked to processing frequency, intensity and temporal coding (Wang, McFadden, Caspary, & Salvi, 2002). Additionally IQ has been found to correlate with auditory abilities, including loudness discrimination (Troche & Rammsayer, 2009b) and pitch discrimination (Deary, 1994). For these reasons, the auditory cortex may be a suitable location in which to expand understanding of the scope of the suppressive mechanism linking IQ, GABA and perception.

There is also opportunities for improvement in the methodology of GABA collection. In the experiment reported in Chapter 10, a single estimate of GABA was taken using a large voxel. Whilst for the purposes of this exploratory study these methodologies were sufficient, future research should aim to more accurately localise GABA activity. For example, the voxel location and size could be selected based on a short localisation scan rather than visual approximation based on anatomical landmarks, thereby further minimising the inclusion of CSF in the voxel.

Improved localization would allow GABA levels to be compared in multiple retinotopic maps. Measures of perceptual surround suppression are constrained specifically by pRF estimates in V1 (Chapters 5, 6 & 7). This thesis has identified no cortical locus for surround suppression in visual areas later than V1. This implies that the link between GABA and surround suppression will be absent in V2, V3 and V3A. Whilst GABA estimates may not be as diverse as suggested here, given the high intra-areal variability reported throughout this thesis it is strongly predicted that GABA levels will differ to some extent across maps.

Similarly, the intra-areal variability in both cortical magnification (Chapter 2) and pRF surround size and centre size (Chapter 5) would suggest that GABA measures may differ within a single visual area. Surround suppression and pRF surround size are greater at higher eccentricities (Chapter 5; Harvey et al.,2011). Both psychophysical surround suppression (Yoon et al., 2010) and pRF size (Harvey et al., 2013) have been linked to GABA (although the relationship with pRF size is speculative and indirect). It is therefore expected that GABA may also increase at portions of the cortex representing peripheral vision.

More generally, as understanding of individual variations in GABA progresses there will be opportunities to improve the methodology of studies such as the one reported in Chapter 10. Understanding of individual variation in GABA levels remains in its infancy. This is partly due to a lack of research into the time frame of GABA metabolism, which limits the pairing of GABA changes to particular tasks. The influence of equivalent tasks on GABA levels is not consistent across studies (Mrsic-Flogel, Hofer, Ohki, Reid, Bonhoeffer & Hubener, 2007; Lunghi, Emir, Concetta, Bridge, 2015). There is evidence that 2.5 hours of monocular deprivation results in temporarily decreased levels of GABA in the visual cortex of the corresponding hemisphere (Lunghi et al., 2015). Although, there is no evidence that the converse effect occurs. An increase in visual stimulation does not result in increased levels of GABA (Lin, Xin, Napolitano & Morris, 2012; Schaller, Mekle, Xin, Kunz & Gruetter, 2013). Variations in the GABA-ergic system have also been linked to sleep deprivation (Scalise et al., 2006).

Due to this uncertainty, future studies investigating correlations between GABA and perceptual and cognitive tasks should aim to limit the time period between MRS and perceptual testing as much as possible. Additionally, MRS should be completed after perceptual testing. During scanning participants generally receive little or no visual stimulation. The GABA time frame indicated by Lunghi et al. (2015) suggests that ocular deprivation is unlikely to lower GABA levels during the scan, although it is possible that a decrease may occur in the hours following the scan. It is vital that perceptual testing does not occur in this post-deprivation period.

The findings reported in the final 3 experimental chapters of this thesis also inform understanding of the nature of intelligence more broadly. Spearman (1904) argued that intelligence should be considered as a single construct (*g*). This single factor was believed to underlie individual differences in performance in a variety of abilities including low level perceptual tasks (Li et al., 1998), working memory (Colom, Rebollo, Palacios, Juan-Espinosa, & Kyllonen, 2004) and reaction times (Deary, Der, & Ford, 2001). Furthermore, this general intelligence factor has also been shown to predict life success, indicating a high level of practical validity. Intelligence as a single construct has been linked to academic success (Colom & Flores-Mendoza, 2007) and job performance (Ree & Earles, 1992).

Although, there is debate within the literature regarding the importance of IQ in life success. For example, it has been demonstrated that working memory in 5 year old children is a better predictor of literacy and numeracy at age 11 than IQ, as measured with Weschler tests (Weschler, 1990, 1992) suitable for this age group (Alloway & Alloway, 2010). Similarly, it has been claimed that financial earnings are better correlated with factors such as peer support and aspirations than IQ (Zax & Rees, 2002). These findings indicate that rather than a single measure of *g*, there are diverse cognitive and social factors that determine success.

The theory of multiple intelligences is conceptual similar to the suggestion that life success to dependent on more than factor. In opposition to the proposal of Spearman (1904), it has been argued that intelligence should be considered as a multi-dimension construct (Gardner, 1983). Instead of a single measure of *g*, intelligence was proposed to be better described as a collection of cognitive aspects (linguistic, musical, spatial, bodily, interpersonal, intrapersonal, logico- mathematical). Later revisions also considered the inclusion of naturalist intelligence, describing the ability to recognize distinctions of the natural world and utilise this information productively (Gardner, 1995). These forms of intelligence are considered independent of one another, although overlap is expected (Gardner, 1993). The theory of multiple intelligences has not been supported by empirical behavioural data (Deary, Penke, & Johnson, 2010), generally all dimensions of intelligence correlate closely with one another indicating that they may all represent a single factor (Visser, Ashton, & Vernon, 2006).

However, support for the theory of multiple intelligences can be found in the fMRI literature. If intelligence is a single concept (*g*), then similar activation should be observed across tasks reliant on this cognitive measure (Hampshire, Highfield, Parkin, & Owen, 2012). Hampshire et al. (2012) report that different components of intelligence can be linked to disparate and separate cortical networks, conflicting with the concept of *g*. The authors demonstrated that different elements of psychometric tests (e.g. deductive reasoning, spatial rotations, digit span) are associated with different activation patterns in the frontal and parietal brain regions.

It should be noted that the investigation of Hampshire et al. (2012) have been extensively criticised (Haier, Karama, Colom, Jung, & Johnson, 2014). In particular, the principal

component analysis methodologies used by Hampshire et al. (2012) are argued to be inappropriate. Additionally, the analyses performed by Hampshire et al. (2012) do not include the early visual cortex so are not fully applicable to the global suppressive mechanism I outline in Chapter 10.

The data reported in this thesis strongly supports the existence of *g*. Mirroring previously documented correlations between low level perception and IQ (Li et al., 1998), a relationship was noted between multiple forms of surround suppression and performance in a visual reasoning IQ subtest. Furthermore, both these abilities were constrained by the concentration of GABA in the visual cortex. I propose that further research will reveal a broader role for GABA in mediating both intelligence and other perceptual abilities previously shown in the literature to correlate with IQ. In this way, I suggest that GABA is conceptually similar to *g*, constraining both intelligence and perception.

As described in Chapter 10, the participants used here were assumed to represent the higher end of the IQ spectrum due to their educational and occupational backgrounds (Reynolds et al., 1988). It can therefore be argued that the link between IQ and visual abilities may not be found in the general population and no correlation would be identified in a larger scale study. If the link was found to be constrained to high IQ participants than the findings reported in Chapters 8 and 10 would not offer support for *g*. Spearman (1904) defined *g* as a universal construct underlying performance in multiple tasks for all participants.

It is possible that IQ is determined by visual abilities in the high IQ sample used here because all other factors contributing to IQ are similar. For example, all participants in the sample may have displayed ceiling level problem solving and abstract thinking abilities in the IQ test. In addition to these critical markers of intelligence, some participants also had optimal eye sight. In this way, the high IQ participants were separated from one another solely on the basis of eye sight. Following this argument, in the general population performance in the IQ test may be less dependent on eye sight (as other critical markers of intelligence have higher levels of variability) and therefore the links between IQ and visual abilities would be weakened.

Despite the theoretical possibility that the correlation between IQ and surround suppression is constrained to high IQ participants, part research does not support this argument. The work of Melnick et al (2013) indicates that the correlation between surround suppression and IQ exists throughout the population. Melnick et al (2013) report a strong correlation within a much larger and more representative sample than was used in this chapter. Menick et al (2013) collected data from undergraduate students. The participants used in Melnick et al (2013) would be expected to have lower IQ scores than the participants used in this thesis (Reynolds et al., 1988). It can therefore be reasonably assumed that the correlations between IQ and visual abilities reported in this thesis are also present in the general population.

It is important to note that I have considered a relatively narrow aspect of intelligence, which may not necessarily be fully applicable to arguments of Gardner (1983). There is debate within the literature regarding the definition of intelligence. For example, Gardner (1983) heavily weighted practical expertise. Other tests of intelligence (such as the WASI subtest used in this thesis) measure abstract reasoning abilities. A broad consensus was produced by 52 prominent researches within this field (Gottfredson, 1997). They describe intelligence as a broad concept that is characterised by an ability to 'catch on' and 'make sense of things.' Whilst it can be measured using tests, intelligence is not merely the ability to perform well in tests. Instead it reflects a deeper comprehension of the surroundings. The 52 researchers listed reasoning, planning, problem solving and abstract thinking as critical markers of intelligence. Based on the findings I report in Chapters 8 and 10, I argue for an expansion of this definition to include the ability to suppress irrelevant information.

11.3 Theories of Cortical Development

There is debate within the literature regarding the characteristics of retinotopic inter-areal correlations (Dougherty et al., 2003). The multiple cortical parameters of retinotopic maps have generally been considered separately in the literature. The experiment reported in Chapter 2 expands on previous studies documenting the retinotopic parameters of visual areas (Dougherty et al., 2003; Larsson & Heeger, 2006) by focusing on inter-areal and intra-areal correlations throughout the visual system. Correlations between visual

areas were surprisingly sparse, particularly in terms of cortical magnification. In agreement with the literature (Dougherty et al., 2003; Polimeni et al., 2006), V1 and V2 were closely paired. V3 also showed some inheritance from V1 in both measures of size and cortical magnification. A second, distinct and separate cluster was seen at a later point in the visual hierarchy. LO1 and LO2 correlated in both cortical magnification and size measures.

These findings demonstrate that variance was inherited from earlier visual areas, but the strongest and most consistent determinant of cortical magnification was the effect of eccentricity. A combination of parametric and non-parametric statistical tests in addition to the use of three cortical magnification fitting functions were necessary to locate the small number of links reported here. The strongest effect throughout the analyses performed in Chapter 2 was the intra-area variability, the effect of eccentricity was the dominant source of shared variance between visual areas. The independence of retinotopic maps was conducive to the aims of this thesis. The relative absence of inter-areal correlations allowed links to be identified between visual abilities and specific maps.

This independence of visual areas can inform understanding of the developmental pattern of retinotopy in the visual cortex. The structure and function of visual areas changes in early childhood. For example, both visual acuity and V1 cortical magnification has been shown to increase in infancy (Stanley, 1991). Multiple models have been proposed to explain the underlying mechanisms of this refinement (Cang & Feldheim, 2013), broadly divided by the focus on the role of sensory experience.

Some argue that the retinotopic patterns are predetermined by molecular labels. Following surgical intervention, retinal ganglion cells show regrowth to their original position (Sperry, 1963). This indicates that there is some predetermination in cortical connections and therefore the global format of visual retinotopy. The molecular mechanisms are not fully understood, but most likely involve Eph-related receptors and ligands (Drescher, Bonhoeffer, & Müller, 1997). Understanding of the genetic underpinnings of this retinotopic development remains in its infancy (Rosa, 2002).

Other models focus on the description of a developmental trajectory driven by sensory experience. The importance of experience is more clearly illustrated in patients with significant visual anatomical abnormalities. For example Muckli, Naumer, and Singer (2009) report the retinotopic organisation of the visual cortex in a patient born with a single cerebral hemisphere. The remaining hemisphere developed maps of both the ipsilateral and contralateral visual fields. This patient demonstrates the high level of flexibility in retinotopic development, indicating that experience can override the predetermined molecular-driven connections.

Considered together, all mechanism point towards a developmental process in which genetically determined molecular labels provide a starting point and general format for retinotopy which is then modulated by sensory experience (the topographic-anchor model, Rosa, 2002). This explains the broad consistency across individuals, as well as the substantial individual differences.

An extension of this exploration is to understand how the developmental trajectory of individual maps differ from one another. Previous literature has focused on the early visual maps, particularly V1. This map shows very high consistency across primate species (Rosa, 2002), indicating that it may be more heavily reliant on pre-determined ligand direction than later areas. If this is the case then findings regarding the genetic component of V1 development may not be fully applicable to intermediate visual areas. Expanding understanding to later visual areas may inform the underlying causes for the lack of inter-areal correlations outlined in Chapter 2.

The data presented in Chapter 2 supports the suggestion that visual areas may have independent developmental trajectories. Despite reports of consistency within the literature (Rosa, 2002), I found little correlation between visual areas within the same participant. Specifically the data presented here points towards a topographic-anchor model of development (Rosa, 2002).

As described above, molecule gradients are thought to guide retinotopic development (Drescher et al., 1997). The activity of these gradients, specifically Ephrin-A5, have been shown to underlie the specification of maps in the somatosensory cortex (Vanderhaeghen et al., 2000). The higher level of complexity in the visual cortex renders this simple

molecular specification mechanism inappropriate (Rosa, 2002). The multiple second-order representations of areas higher than V1 could not be defined in this manner. Instead, molecular gradients may only define particular visual maps. The remaining maps would then use the limitations imposed by these areas to develop via activity dependent mechanisms (Rosa, 2002). For example, V2 would utilise the shared boundary with gradient-defined V1 to limit the range of possible configurations. In this way, V2 follows a similar pattern across all individuals despite an absence of molecular gradient definition.

Rosa (2002) argues that V1 and MT should be considered anchors due to their early maturation (Condé, Lund, & Lewis, 1996; Watson et al., 1993). The data presented in Chapter 2 supports the suggestion that V1 acts as a template for adjacent areas, and also indicates that LO1 may play a similar role. These visual areas were the earliest regions of the 2 discrete clusters identified in size and cortical magnification analyses. It is possible that the shared variance between LO1 and LO2 is a result of common inheritance from the MT anchor. This could not be explored due to the methodological limitations regarding the retinotopic mapping of MT.

The influence of the topographic-anchor mechanism on the constraint of visual abilities can be considered through examination of the experiments reported here. It would be expected that the secondary, non-anchor regions would show the strongest links with visual abilities. These regions are less constrained by predetermined molecule gradients and heavily dependent on sensory experience. This experience driven plasticity would allow the development of correspondence with visual abilities. In fact, the opposite pattern was seen. The strongest links between retinotopic parameters and visual abilities were seen in V1 (Chapters 5, 6 & 7). LO1 also played a weak role in the correlations between visual discrimination and cortical magnification outlined in Chapters 3 and 4.

11.4 Linking Disparate Psychological Phenomena

In addition to documenting links between psychophysical task performance and retinotopic measures, this thesis aimed to exploit these associations to better understand the relationships between disparate psychological abilities. It was proposed that evidence

of a shared cortical constraint would support the argument for a close pairing between seemingly dissimilar visual abilities.

pRF fitting allowed the separate and independent estimation of the excitatory centre and inhibitory surround of cortical locations pooling a large number of neurons. In this thesis I showed that performance in first and second order suppression tasks was correlated with large V1 pRF surround size. This finding suggests a close similarity in the cortical processing of first and second order stimuli, located primarily in V1. This view contrasts with psychophysical studies indicating separate processing streams for first and second order defined stimuli (Chubb & Sperling, 1988; Solomon & Sperling, 1994).

It is important to note that some modelling attempts to elaborate first order and second order stimuli did not imply a completely separate and independent cortical basis (Ellemberg et al., 2004). Instead the model proposed by Ellemberg et al. (2004) would allow, in principle, a later, non-linear, processing stage (possibly V2) to elaborate second order information that is then fed-back to a linear processing stage (possibly V1) for a further elaboration stage. This view can be compatible with our findings. First and second order stimulus may both be firstly processed by V1 (and therefore constrained by the pRF estimates of this area), but with second order stimuli undergoing a second stage of processing in V2 that is less dependent on the characteristics of receptive fields.

Conversely, the conclusions drawn regarding the hypothesis that crowding and surround suppression are different levels of same cortical process are less clear. Crowding is a phenomenon where the recognition of objects presented in the periphery of the visual field is impaired by the presence of flanking objects surrounding the target. Crucially, the distance between these flanking objects and the target stimuli strongly affects behavioural performance, with closer flankers resulting in a lower performance level than flankers placed away from the target. From a naïve perspective the phenomenon of crowding might be associated with the suppression of visual responses when the surround of a given receptive field in early visual cortex is stimulated (surround suppression).

Chapter 7 demonstrated that as for surround suppression, crowding was correlated with pRF estimates in V1. Mirroring first and second surround suppression, larger pRF estimates were associated with higher levels of perceptual suppression. This indicates the

2 psychophysical phenomena share a common cortical basis; receptive field characteristics of V1. However, the pRF centre size was the sole determinant of crowding, whereas the pRF surround size was the main predictor of surround suppression.

Additionally, Chapters 8 and 10 support the argument of Levi (2008) and indicate that crowding is a separate and distinct process to surround suppression. In Chapter 8 it was demonstrated that whilst surround suppression (both first and second order) and IQ are closely linked, crowding showed no correlation with IQ. Additionally, GABA was found to correlate with both first and second order surround suppression, but not crowding (Chapter 10). This GABA-mediated suppressive mechanism includes both low level perceptual abilities and complex visual reasoning skills, but excludes crowding.

A definitive conclusion cannot be drawn regarding the relationship between crowding and surround suppression but this thesis suggests future directions in delineating this relationship. The data presented in this thesis indicates that similarities between the 2 phenomena may not be based on suppressive mechanisms, as was suggested in Chapter 1. The broad suppressive mechanism outlined in Chapters 8, 9 and 10 does not include crowding. Instead, it appears that although constrained by receptive field properties of V1, crowding is not mediated by the surround-centre suppressive mechanism that mediates perceptual surround suppression. Crowding is hypothesised to result from spatial pooling. In this way, surround suppression is dependent on the size of the receptive field surround whilst crowding is related to the size of the receptive field centre.

11.5 Methodological Considerations

11.5.1 Sample Size

A substantial and important strength of this thesis is the consistency of the participant group used throughout all experiments (although there was some drop-out and re-recruitment following the experiments reported in Chapters 2, 3 & 4). This allowed a full and thorough documentation of a wide range of cortical parameters, visual abilities and

cognitive abilities. Due to the reuse of participants throughout, a wider range of correlations were possible and data was utilised in the most economical way. The retention of a core participant group over 3 years of testing is unusual in the literature and fills a significant gap.

The retention of participants throughout a 3 year period was achieved at the expense of other considerations. The sample size for all experiments was relatively small, ranging from 9 to 14 participants. This sample size was chosen in line with previous literature (Duncan & Boynton, 2003). Given the high inter-individual variability revealed by the analyses reported here, it may have been beneficial to use a larger sample size. It is argued that the failure to find a clearer link between cortical parameters and visual abilities cannot be attributed to this small sample size. Following the main analyses of Chapter 3, in which thresholds from radial and tangentially orientated stimuli conditions were considered separately, additional analyses were performed to explore the effect of power. Radial and tangential conditions were merged and this new psychophysical measure was investigated for correlations with cortical magnification. Despite the increase in the number of data points, the results remained generally consistent with the findings of the main analysis.

The small sample size is much more problematic in the experiments comparing psychological measures, such as the investigation into the association between surround suppression and IQ (Chapter 8). Previous literature in this area (Melnick et al., 2013) used a higher number of participants. Given the low financial and time demands of data collection of this type, future studies should aim to correct this issue. Despite this limitation, the small sample size did not prevent the identification of clear relationships between the two variables.

Global practice effects also influenced the data to some extent. This confound was unavoidable, due to the importance of using a consistent sample throughout. The confounding effect of practice was minimised as much as possible by ensuring participants performed experiments in an identical order. The key benefit obtained throughout the testing session may be improved fixation. The ability to fixate has been demonstrated to improve with practice (Di Russo, Pitzalis, & Spinelli, 2003). In the experiments presented here, the global practice effect is illustrated by comparing the

cleaner data of second order surround suppression (Chapter 6) to the earlier collected first order surround suppression (Chapter 5).

11.5.2 Sample Characteristics

All participants used here were final year undergraduate student, PhD students or postgraduate students at Royal Holloway Psychology department. This occupational and educational status may have influenced the nature of the data reported here. The participant group was selected for 2 reasons. Firstly, recruitment and maintenance of the sample was easier when participants worked at the testing site. Secondly psychophysical testing required a high level of motivation. Students and staff of the Psychology department have experience of participating in experiments of this type and were fully aware of the importance of concentration and adherence to instructions.

Despite the high level of motivation across the sample, it is accepted that there was most likely some variability within the participant group that influenced some findings of this thesis. In particular, Chapter 8 is thought to have been affected by variability in levels of motivation. The role of motivation in intelligence testing is well documented (Duckworth, Quinn, Lynam, Loeber & Stouthamer-Loeber, 2010). A meta-analysis indicated that IQ scores were higher when motivation was increased via the presence of material incentives. Additionally, after adjusting for the effect of motivation, the predictive power of IQ tests to determine later life success was decreased (Duckworth et al., 2010). Similarly, visual perception is influenced by motivation. When viewing an ambiguous image that could be seen as either the number 13 or the letter B, participants were more likely to judge the image to be the outcome they favoured (Balcetis & Dunning, 2006). Implicit measures of perception confirmed that the effect of motivation influenced the preconscious visual processing. As both IQ and visual perception are influenced by motivation, it must be considered that the strong correlation seen in Chapter 8 may have been partially driven by variability in levels of motivation.

The impact of the high educational status of the participant group on psychometric data (Chapters 8, 9 & 10) has been discussed previously and will not be described here. An alternative issue is the impact of the occupational status on the measurement of low level

abilities and corresponding retinotopic parameters. Evidence exists to indicate that the visual abilities of the participant group used may differ from the general population.

Training on a visual task leads to an improvement in performance. The ability to discriminate between subtle differences in the orientation of a grating (Fahle, 1997) and the spatial frequency of a grating (Fiorentini & Berardi, 1980) improves following training. These training improvements can be long lasting in both normal participants (Fahle, 2005) and amblyopic participants (Huang, Zhou, & Lu, 2008; Polat, Ma-Naim, Belkin, & Sagi, 2004).

Improved performance is linked to brain plasticity (Fahle & Poggio, 2002) and changes in abilities are reflected in cortical parameters (Buonomano & Merzenich, 1998). This has been suggested for both low level tasks and more complex visual abilities. Karni and Sagi (1991) trained participants on a simple texture discrimination task. Training effects were orientation specific. It was proposed that changes were occurring at an early visual region in which different orientations were processed separately, most likely V1. Auditory learning has been more closely tied to cortical consequences (Menning, Roberts, & Pantev, 2000). Learning to read, a complex visual function, has also been linked to changes in cortical parameters (Ben-Shachar, Dougherty, Deutsch, & Wandell, 2011).

In addition to training obtained within an experimental paradigm, experience gained in an occupational setting is also thought to lead to changes in visual abilities. For example, there is some indication that radiographers have contrast discrimination skills that are superior to the general population (Sowden, Davies, & Roling, 2000). This difference is hypothesised to result from the high level of sensory training obtained by studying small contrast differences in X- ray data.

It is possible that an effect analogous to the radiographers described by Sowden et al. (2000) is present in the sample used throughout this thesis. The majority of the participants worked within the field of visual neuroscience. For this reason, they spent a much greater amount of time studying psychophysical stimuli than the general population. It is possible that this sensory training resulted in heightened visual abilities. Unfortunately the small size of the sample prevented further investigation of this

limitation. There were insufficient participants to perform a statistical comparison of participants working with psychophysical stimuli and those working in alternative fields.

11.6 Final Remarks

The experiments reported throughout this thesis have outlined the high levels of variability present within both measures of cortical parameters and psychophysical perceptual abilities. The use of a consistent participant group has allowed a full exploration of the interactions between these retinotopic measurements and multiple psychophysical tasks. The key finding throughout these experiments is that whilst variability in cortical parameters did not predict differences between participants in perceptual abilities, retinotopic intra- individual variability (e.g. the strong effect of eccentricity) did correlate with psychophysical performance.

Instead, the top down influence of IQ was found to be a much stronger predictor of inter-individual differences than either cortical magnification or pRF size. By approaching the investigation of intelligence from a psychophysical standpoint, developments have occurred in understanding of psychological functioning at multiple levels. Primarily, the neurophysiology of a complex cognitive task have been outlined. This provides a biological framework to the field of intelligence research and supports the hypothesis that IQ measures a fundamental property of the brain (Galton, 1883; Spearman, 1904). Secondly, this work also highlights the importance of considering top-down influences in psychophysical measures of perception. This thesis indicates that the higher cognitive processes account for a significant amount of variance in low level abilities and should be acknowledged in models of perception.

References

Acton, G. S., & Schroeder, D. H. (2001). Sensory discrimination as related to general intelligence. *Intelligence, 29*(3), 263-271. doi:10.1016/S0160-2896(01)00066-6

Adams, D. L., & Horton, J. C. (2003a). Capricious expression of cortical columns in the primate brain. *Nature Neuroscience, 6*(2), 113-114. doi:10.1038/nn1004

Adams, D. L., & Horton, J. C. (2003b). A precise retinotopic map of primate striate cortex generated from the representation of angioscotomas. *The Journal of Neuroscience, 23*(9), 3771-3789.

Aghdaee, S.M. & Cavanagh, P. (2007). Temporal limits of long-range phase discrimination across the visual field. *Vision Research, 47,* 2156—2163.

Alloway, T. P., & Alloway, R. G. (2010). Investigating the predictive roles of working memory and IQ in academic attainment. *Journal of Experimental Child Psychology, 106*(1), 20-29. doi:10.1016/j.jecp.2009.11.003

Anderson, E. J., Dakin, S. C., Schwarzkopf, D. S., Rees, G., & Greenwood, J. A. (2012). The neural correlates of crowding-induced changes in appearance. *Current Biology, 22*(13), 1199-1206. doi:10.1016/j.cub.2012.04.063

Andrews, T. J., Halpern, S. D., & Purves, D. (1997). Correlated size variations in human visual cortex, lateral geniculate nucleus, and optic tract. *The Journal of Neuroscience, 17*(8), 2859-2868.

Andriessen, J., & Bouma, H. (1976). Eccentric vision: Adverse interactions between line segments. *Vision Research, 16*(1), 71-78. doi:10.1016/0042-6989(76)90078-X

Angelucci, A., & Bressloff, P. C. (2006). Contribution of feedforward, lateral and feedback connections to the classical receptive field center and extra-classical receptive field surround of primate V1 neurons. *Progress in Brain Research, 154,* 93-120. doi:10.1016/S0079-6123(06)54005-1

Appelle, S. (1972). Perception and discrimination as a function of stimulus orientation: the" oblique effect" in man and animals. *Psychological Bulletin, 78*(4), 266-278.

Arcaro, M. J., McMains, S. A., Singer, B. D., & Kastner, S. (2009). Retinotopic organization of human ventral visual cortex. *The Journal of Neuroscience, 29*(34), 10638-10652. doi: 10.1523/JNEUROSCI.2807-09.2009

Arman, A. C., Chung, S. T., & Tjan, B. S. (2006). Neural correlates of letter crowding in the periphery. *Journal of Vision, 6*(6), 804-804. doi: 10.1167/6.6.804

Attkinson, J. (1991). Review of human visual development: Crowding and dyslexia. In J. Cronly-Dillon & J. Stein (Eds.), *Vision and Visual Dyslexia* (pp. 44-57). London: MacMillian Press.

Bair, W., Cavanaugh, J. R., & Movshon, J. A. (2003). Time course and time- distance relationships for surround suppression in macaque V1 neurons. *The Journal of Neuroscience, 23*(20), 7690-7701.

Baker, C. L., & Mareschal, I. (2001). Processing of second-order stimuli in the visual cortex. *Progress in Brain Research, 134*, 171-191. doi:10.1016/S0079-6123(01)34013-X

Balasubramanian, M., Polimeni, J., & Schwartz, E. L. (2002). The V1–V2–V3 complex: quasiconformal dipole maps in primate striate and extra-striate cortex. *Neural Networks, 15*(10), 1157-1163. doi:10.1016/S0893-6080(02)00094-1

Balcetis, E. & Dunning, D. (2006). See what you want to see: Motivational influences on visual perception. *Journal of Personality and Social Psychology, 91*(4), 612-625.

Bartels, A., & Zeki, S. (2000). The architecture of the colour centre in the human visual brain: new results and a review. *European Journal of Neuroscience, 12*(1), 172-193. doi: 10.1046/j.1460-9568.2000.00905.x

Ben-Shachar, M., Dougherty, R. F., Deutsch, G. K., & Wandell, B. A. (2011). The development of cortical sensitivity to visual word forms. *Journal of Cognitive Neuroscience, 23*(9), 2387-2399. doi:10.1162/jocn.2011.21615

Berkley, M. A., Kitterle, F., & Watkins, D. W. (1975). Grating visibility as a function of orientation and retinal eccentricity. *Vision Research, 15*(2), 239-244. doi:10.1016/0042-6989(75)90213-8

Birchall, M. (2014). *The Times Top 100 Graduate Employers 2014-2015* (16th ed.). London: High Fliers Publications Ltd.

Blasdel, G., & Campbell, D. (2001). Functional retinotopy of monkey visual cortex. *The Journal of Neuroscience, 21*(20), 8286-8301.

Boekel, W., Wagenmakers, E.-J., Belay, L., Verhagen, J., Brown, S., & Forstmann, B. U. (2015). A purely confirmatory replication study of structural brain-behavior correlations. *Cortex, 66*, 115-133. doi:10.1016/j.cortex.2014.11.019

Born, R. T., & Bradley, D. C. (2005). Structure and function of visual area MT.

Annual Review of Neuroscience, 28, 157-189. doi: 10.1146/annurev.neuro.26.041002.131052

Bors, D. A., & Stokes, T. L. (1998). Raven's Advanced Progressive Matrices: Norms for First-Year University Students and the Development of a Short Form. *Educational and Psychological Measurement, 58*(3), 382-398. doi: 10.1177/0013164498058003002

Bouma, H. (1970). Interaction effects in parafoveal letter recognition. *Nature, 226*, 177-178. doi: 10.1038/226177a0

Bouma, H. (1973). Visual interference in the parafoveal recognition of initial and final letters of words. *Vision Research, 13*(4), 767-782. doi:10.1016/0042-6989(73)90041-2

Braddick, O. J., O'Brien, J. M., Wattam-Bell, J., Atkinson, J., Hartley, T., & Turner, R. (2001). Brain areas sensitive to coherent visual motion. *Perception, 30*(1), 61-72. doi:10.1068/p3048

Brewer, A. A., & Barton, B. (2012). Visual field map organization in human visual cortex. S. Moltochnikoff, S., & Rouat, J. (Ed.), *Visual Cortex- Current Status and Perspectives* (pp. 29-60). New York, NY: InTech.

Brewer, A. A., Liu, J., Wade, A. R., & Wandell, B. A. (2005). Visual field maps and stimulus selectivity in human ventral occipital cortex. *Nature Neuroscience, 8*(8), 1102-1109. doi:10.1038/nn1507

Brewer, A. A., Press, W. A., Logothetis, N. K., & Wandell, B. A. (2002). Visual areas in macaque cortex measured using functional magnetic resonance imaging. *The Journal of Neuroscience, 22*(23), 10416-10426.

Britten, K. H., & Heuer, H. W. (1999). Spatial summation in the receptive fields of MT neurons. *The Journal of Neuroscience, 19*(12), 5074-5084.

Brodmann, K. (1918). Individuelle Variationen der Sehsphäre und ihre Bedeutung für die klink der Hinterphauptschüsse. *Allgz Psychiat (Berlin), 74*, 564-568.

Bruce, N. D., & Tsotsos, J. K. (2006). A statistical basis for visual field anisotropies. *Neurocomputing, 69*(10), 1301-1304. doi:10.1016/j.neucom.2005.12.096

Bruce, V., Green, P. R., & Georgeson, M. A. (2003). *Visual Perception: Physiology, Psychology & Ecology* (4th ed.). Hove, UK: Psychology Press. Buonomano, D. V., & Merzenich, M. M. (1998). Cortical plasticity: from synapses to maps. *Annual review of neuroscience, 21*(1), 149-186.

Burkhalter, A., Felleman, D., Newsome, W., & Van Essen, D. (1986). Anatomical and physiological asymmetries related to visual areas V3 and VP in macaque extrastriate cortex. *Vision Research, 26*(1), 63-80. doi:10.1016/0042-6989(86)90071-4

Burkhalter, A., & Van Essen, D. C. (1986). Processing of color, form and disparity information in visual areas VP and V2 of ventral extrastriate cortex in the macaque monkey. *The Journal of Neuroscience, 6*(8), 2327-2351.

Cai, P., He, D., & Fang, F. (2014). The size of population receptive field in V2 and crowding effect. *Journal of Vision, 14*(10), 769-769. doi:10.1167/14.10.769

Campbell, F., Kulikowski, J., & Levinson, J. (1966). The effect of orientation on the visual resolution of gratings. *The Journal of Physiology, 187*(2), 427-436. doi: 10.1113/jphysiol.1966.sp008100

Cang, J., & Feldheim, D. A. (2013). Developmental mechanisms of topographic map formation and alignment. *Annual Review of Neuroscience, 36*, 51-77. doi: 10.1146/annurev-neuro-062012-170341

Cannon, M. W., & Fullenkamp, S. C. (1991). Spatial interactions in apparent contrast: inhibitory effects among grating patterns of different spatial frequencies, spatial positions and orientations. *Vision Research, 31*(11), 1985-1998. doi:10.1016/0042-6989(91)90193-9

Cannon, M. W., & Fullenkamp, S. C. (1993). Spatial interactions in apparent contrast: Individual differences in enhancement and suppression effects. *Vision Research, 33*(12), 1685-1695. doi:10.1016/0042-6989(93)90034-T

Carandini, M., & Heeger, D. J. (2013). Normalization as a canonical neural computation. *Nature Reviews Neuroscience, 13*(1), 51-62. doi:10.1038/nrn3424

Cattell, J. M. (1886a). The time it takes to see and name objects. *Mind, 11*(41), 63-65.

Cattell, J. M. (1886b). The time taken up by cerebral operations. *Mind*(42), 220-242.

Cavanaugh, J. R., Bair, W., & Movshon, J. A. (2002). Nature and interaction of signals from the receptive field center and surround in macaque V1 neurons. *Journal of Neurophysiology, 88*(5), 2530-2546. doi: 10.1152/jn.00692.2001

Chen, A. C., & Herrmann, C. S. (2001). Perception of pain coincides with the spatial expansion of electroencephalographic dynamics in human subjects. *Neuroscience Letters, 297*(3), 183-186. doi:10.1016/S0304-3940(00)01696-7

Chubb, C., & Sperling, G. (1988). Drift-balanced random stimuli: a general basis for studying non-Fourier motion perception. *Journal of the Optical Society of America A, 5*(11), 1986-2007. doi: 10.1364/JOSAA.5.001986

Chubb, C., Sperling, G., & Solomon, J. A. (1989). Texture interactions determine perceived contrast. *Proceedings of the National Academy of Sciences, 86*(23), 9631-9635.

Chung, S. T., Levi, D. M., & Legge, G. E. (2001). Spatial-frequency and contrast properties of crowding. *Vision Research, 41*(14), 1833-1850. doi:10.1016/S0042-6989(01)00071-2

Chung, S. T., Li, R. W., & Levi, D. M. (2007). Crowding between first-and second-order letter stimuli in normal foveal and peripheral vision. *Journal of Vision, 7*(2), 1-13. doi:10.1167/7.2.10

Churan, J., Khawaja, F. A., Tsui, J. M., & Pack, C. C. (2008). Brief motion stimuli preferentially activate surround-suppressed neurons in macaque visual area MT. *Current Biology, 18*(22), R1051-R1052. doi:10.1016/j.cub.2008.10.003

Colom, R., & Flores-Mendoza, C. E. (2007). Intelligence predicts scholastic achievement irrespective of SES factors: Evidence from Brazil. *Intelligence, 35*(3), 243-251. doi:10.1016/j.intell.2006.07.008

Colom, R., Rebollo, I., Palacios, A., Juan-Espinosa, M., & Kyllonen, P. C. (2004). Working memory is (almost) perfectly predicted by g. *Intelligence, 32*(3), 277-296. doi:10.1016/j.intell.2003.12.002

Condé, F., Lund, J. S., & Lewis, D. A. (1996). The hierarchical development of monkey visual cortical regions as revealed by the maturation of parvalbumin- immunoreactive neurons. *Developmental Brain Research, 96*(1), 261-276. doi:10.1016/0165-3806(96)00126-5

Crawford, J., Deary, I. J., Allan, K. M., & Gustafsson, J.-E. (1998). Evaluating competing models of the relationship between inspection time and psychometric intelligence. *Intelligence, 26*(1), 27-42. doi:10.1016/S0160-2896(99)80050-6

Dakin, S., & Watt, R. (1997). The computation of orientation statistics from visual texture. *Vision Research, 37*(22), 3181-3192. doi:10.1016/S0042-6989(97)00133-8

Damasio, A. R., Damasio, H., & Van Hoesen, G. W. (1982). Prosopagnosia Anatomic basis and behavioral mechanisms. *Neurology, 32*(4), 331-331. doi: http://dx.doi.org/10.1212/WNL.32.4.331

Daniel, P. M., & Whitteridge, D. (1961). The representation of the visual field on the cerbral cortex in monkeys. *Journal of Physiology, 159.* 203-221.

De Valois, R. L., Yund, E. W., & Hepler, N. (1982). The orientation and direction selectivity of cells in macaque visual cortex. *Vision Research, 22*(5), 531-544. doi:10.1016/0042-6989(82)90112-2

DeAngelis, G. C., Freeman, R. D., & Ohzawa, I. (1994). Length and width tuning of neurons in the cat's primary visual cortex. *Journal of Neurophysiology, 71*(1), 347-374.

Deary, I. J. (1994). Intelligence and auditory discrimination: Separating processing speed and fidelity of stimulus representation. *Intelligence, 18*(2), 189-213. doi:10.1016/0160-2896(94)90027-2

Deary, I. J., Der, G., & Ford, G. (2001). Reaction times and intelligence differences: A population-based cohort study. *Intelligence, 29*(5), 389-399. doi:10.1016/S0160-2896(01)00062-9

Deary, I. J., Penke, L., & Johnson, W. (2010). The neuroscience of human intelligence differences. *Nature Reviews Neuroscience, 11*(3), 201-211. doi:10.1038/nrn2793

Deichmann, R. (2006). Fast structural brain imaging using an MDEFT sequence with a FLASH–EPI hybrid readout. *Neuroimage, 33*(4), 1066-1071. doi:10.1016/j.neuroimage.2006.08.005

Di Russo, F., Pitzalis, S., & Spinelli, D. (2003). Fixation stability and saccadic latency in elite shooters. *Vision Research, 43*(17), 1837-1845. doi:10.1016/S0042-6989(03)00299-2

Dougherty, R. F., Koch, V. M., Brewer, A. A., Fischer, B., Modersitzki, J., & Wandell, B. A. (2003). Visual field representations and locations of visual areas V1/2/3 in human visual cortex. *Journal of Vision, 3*(10), 586-598. doi:10.1167/3.10.1

Dow, B.M., Snyder, A.Z., Vautin, R.G. & Bauer, R. (1981). Magnification factor and receptive field size in foveal striate cortex of the monkey. *Experimental Brain Research, 44,* 213-228.

Drescher, U., Bonhoeffer, F., & Müller, B. K. (1997). The Eph family in retinal axon guidance. *Current opinion in neurobiology, 7*(1), 75-80. doi:10.1016/S0959-4388(97)80123-7

Duckworth, A.L., Quinn, P.D., Lynam, D.R., Loeber, R. & Stouthamer-Loeber, M. (2010). Role of test motivation in intelligence testing. *Proceedings of the National Academy of Sciences, 108*(19), 7716-7720,

Dumoulin, S. O., Baker, C. L., Hess, R. F., & Evans, A. C. (2003). Cortical specialization for processing first-and second-order motion. *Cerebral Cortex, 13*(12), 1375-1385. doi: 10.1093/cercor/bhg085

Dumoulin, S. O., & Wandell, B. A. (2008). Population receptive field estimates in human visual cortex. *Neuroimage, 39*(2), 647-660. doi:10.1016/j.neuroimage.2007.09.034

Duncan, R. O., & Boynton, G. M. (2003). Cortical magnification within human primary visual cortex correlates with acuity thresholds. *Neuron, 38*(4), 659-671. doi:10.1016/S0896-6273(03)00265-4

Duncan, R. O., & Boynton, G. M. (2007). Tactile hyperacuity thresholds correlate with finger maps in primary somatosensory cortex (S1). *Cerebral Cortex, 17*(12), 2878-2891. doi: 10.1093/cercor/bhm015

Dupont, P., De Bruyn, B., Vandenberghe, R., Rosier, A.-M., Michiels, J., Marchal, G., Mortelmans, L., & Orban, G. (1997). The kinetic occipital region in human visual cortex. *Cerebral Cortex, 7*(3), 283-292. doi: 10.1093/cercor/7.3.283

Dupont, P., Sáry, G., Peuskens, H., & Orban, G. (2003). Cerebral regions processing first- and higher-order motion in an opposed-direction discrimination task. *European Journal of Neuroscience, 17*(7), 1509-1517. doi: 10.1046/j.1460-9568.2003.02571.x

Duvernoy, H. (1991). *The Human Brain: Surface, Blood Supply, and Three- Dimensional Anatomy*. New York: Springer-Verlag.

Dykmans, N. & Anstis, S. (2015). Dmax: Motion seen better in the periphery than in the fovea [Abstract]. *Journal of Vision, 15,* 1175.

Ebbinghaus, H. (1902). *The Principles of Psychology*. Leipzig: Veit.

Edden, R. A., Puts, N. A., Harris, A. D., Barker, P. B., & Evans, C. J. (2014). Gannet: A batch-processing tool for the quantitative analysis of gamma-aminobutyric acid–edited MR spectroscopy spectra. *Journal of Magnetic Resonance Imaging, 40*(6), 1445-1452. doi: 10.1002/jmri.24478

Eeckman, F. H., & Freeman, W. J. (1990). Correlations between unit firing and EEG in the rat olfactory system. *Brain research, 528*(2), 238-244. doi:10.1016/0006-8993(90)91663-2

Elder, J. H., & Sachs, A. J. (2004). Psychophysical receptive fields of edge detection mechanisms. *Vision Research, 44*(8), 795-813. doi:10.1016/j.visres.2003.11.021

Ellemberg, D., Allen, H. A., & Hess, R. F. (2004). Investigating local network interactions underlying first-and second-order processing. *Vision Research, 44*(15), 1787-1797. doi:10.1016/j.visres.2004.02.012

Engel, S. A., Glover, G. H., & Wandell, B. A. (1997). Retinotopic organization in human visual cortex and the spatial precision of functional MRI. *Cerebral Cortex, 7*(2), 181-192. doi: 10.1093/cercor/7.2.181

Fahle, M. (1997). Specificity of learning curvature, orientation, and vernier discriminations. *Vision Research, 37*(14), 1885-1895. doi:10.1016/S0042-6989(96)00308-2

Fahle, M. (2005). Learning to tell apples from oranges. *Trends in cognitive sciences, 9*(10), 455-457. doi:10.1016/j.tics.2005.07.005

Fahle, M., & Poggio, T. (2002). *Perceptual Learning*. Cambridge: MIT Press. Felleman, D. J., Lim, H., Xiao, Y., Wang, Y., Eriksson, A., & Parajuli, A. (2015). The Representation of Orientation in Macaque V2: Four Stripes Not Three. *Cerebral Cortex, 25*, 2354-2369.

Felleman, D. J., & Van Essen, D. C. (1987). Receptive field properties of neurons in area V3 of macaque monkey extrastriate cortex. *Journal of Neurophysiology, 57*(4), 889-920.

Felleman, D. J., & Van Essen, D. C. (1991). Distributed hierarchical processing in the primate cerebral cortex. *Cerebral Cortex, 1*(1), 1-47. doi: 10.1093/cercor/1.1.1

Ferrandez, A.-M., Hugueville, L., Lehéricy, S., Poline, J.-B., Marsault, C., & Pouthas, V. (2003). Basal ganglia and supplementary motor area subtend duration perception: an fMRI study. *Neuroimage, 19*(4), 1532-1544. doi:10.1016/S1053-8119(03)00159-9

Fiorentini, A., & Berardi, N. (1980). Perceptual learning specific for orientation and spatial frequency. *Matire. 287,* 43-44. doi:10.1038/287043a0

Fishman, R. S. (1997). Gordon Holmes, the cortical retina, and the wounds of war. The seventh Charles B. Snyder Lecture. *Documenta Ophthalmologica, 93*(1-2), 9-28.

Fitzpatrick, D. (2000). Seeing beyond the receptive field in primary visual cortex. *Current Opinion in Neurobiology, 10*(4), 438-443. doi:10.1016/S0959-4388(00)00113-6

Flom, M. C., Weymouth, F. W., & Kahneman, D. (1963). Visual resolution and contour interaction. *Journal of the Optical Society of America, 53*(9), 1026-1032. doi: 10.1364/JOSA.53.001026

Forstmann, B. U., Anwander, A., Schäfer, A., Neumann, J., Brown, S., Wagenmakers, E.-J., Bogacz, R., & Turner, R. (2010). Cortico-striatal connections predict control over speed and accuracy in perceptual decision making. *Proceedings of the National Academy of Sciences, 107*(36), 15916-15920.

Freeman, J., Brouwer, G. J., Heeger, D. J., & Merriam, E. P. (2011). Orientation decoding depends on maps, not columns. *The Journal of Neuroscience, 31*(13), 4792-4804. doi: 10.1523/JNEUROSCI.5160-10.2011

Freeman, J., & Simoncelli, E. P. (2011). Metamers of the ventral stream. *Nature Neuroscience, 14*(9), 1195-1201. doi:10.1038/nn.2889

Furmanski, C. S., & Engel, S. A. (2000). Perceptual learning in object recognition: Object specificity and size invariance. *Vision Research, 40*(5), 473-484. doi:10.1016/S0042-6989(99)00134-0

Galletti, C., Battaglini, P., & Fattori, P. (1990). 'Real-motion'cells in area V3A of macaque visual cortex. *Experimental Brain Research, 82*(1), 67-76.

Galton, F. (1883). *Inquiries into Human Faculties*. New York: EP Dutton and Company.

Gardner, H. (1983). *Frames of Mind: The Idea of Multiple Intelligence*. New York: Basic Books.

Gardner, H. (1993). Intelligence and intelligences: Universal principles and individual differences. *Archives de psychologie, 61*(238), 169-172.

Gardner, H. (1995). Reflections on multiple intelligences: Myths and messages. *Phi Delta Kappan, 77*, 200-200.

Gaska, J. P., Jacobson, L. D., & Pollen, D. A. (1988). Spatial and temporal frequency selectivity of neurons in visual cortical area V3A of the macaque monkey. *Vision Research, 28*(11), 1179-1191. doi:10.1016/0042-6989(88)90035-1

Gattass, R., Gross, C., & Sandell, J. (1981). Visual topography of V2 in the macaque. *Journal of Comparative Neurology, 201*(4), 519-539. doi: 10.1002/cne.902010405

Gattass, R., & Gross, C. G. (1981). Visual topography of striate projection zone (MT) in posterior superior temporal sulcus of the macaque. *Journal of Neurophysiology, 46*(3), 621-638.

Gattass, R., Sousa, A., & Gross, C. (1988). Visuotopic organization and extent of V3 and V4 of the macaque. *The Journal of Neuroscience, 8*(6), 1831-1845. Gattass, R., Sousa, A. P., & Rosa, M. G. (1987). Visual topography of V1 in the Cebus monkey. *Journal of Comparative Neurology, 259*(4), 529-548. doi: 10.1002/cne.902590404

Gilbert, C. D., Das, A., Ito, M., Kapadia, M., & Westheimer, G. (1996). Spatial integration and cortical dynamics. *Proceedings of the National Academy of Sciences, 93*(2), 615-622.

Godde, B., Leonhardt, R., Cords, S. M., & Dinse, H. R. (2002). Plasticity of orientation preference maps in the visual cortex of adult cats. *Proceedings of the National Academy of Sciences, 99*(9), 6352-6357.

Goebel, R., Khorram-Sefat, D., Muckli, L., Hacker, H., & Singer, W. (1998). The constructive nature of vision: direct evidence from functional magnetic resonance imaging studies of apparent motion and motion imagery. European Journal of Neuroscience, 10(5), 1563-1573.

Gottfredson, L. S. (1997). Mainstream science on intelligence: An editorial with 52 signatories, history, and bibliography. *Intelligence, 24*(1), 13-23.

Gottfredson, L.S. (1997). Why g matters: The complexity of everyday life. *Intelligence, 24*(1), 79-132.

Greene, C. A., Dumoulin, S. O., Harvey, B. M., & Ress, D. (2014). Measurement of population receptive fields in human early visual cortex using back-projection tomography. *Journal of Vision, 14,* 1-17. doi:10.1167/14.1.17

Grill-Spector, K. (2003). The neural basis of object perception. *Current Opinion in Neurobiology, 13*(2), 159-166. doi:10.1016/S0959-4388(03)00040-0

Grill-Spector, K., Kushnir, T., Edelman, S., Avidan, G., Itzchak, Y., & Malach, R. (1999). Differential processing of objects under various viewing conditions in the human lateral occipital complex. *Neuron, 24*(1), 187-203. doi:10.1016/S0896-6273(00)80832-6

Grill-Spector, K., Kushnir, T., Hendler, T., Edelman, S., Itzchak, Y., & Malach, R. (1998). A sequence of object-processing stages revealed by fMRI in the human occipital lobe. *Human brain mapping, 6*(4), 316-328.

Haier, R. J., Karama, S., Colom, R., Jung, R., & Johnson, W. (2014). A comment on "Fractionating Intelligence" and the peer review process. *Intelligence, 46*, 323-332. doi:10.1016/j.intell.2014.02.007

Haldemann, J., Stauffer, C., Troche, S., & Rammsayer, T. (2011). Processing visual temporal information and its relationship to psychometric intelligence. *Journal of Individual Differences, 32*(4), 181-188. doi: http://dx.doi.org/10.1027/1614-0001/a000050

Haldemann, J., Stauffer, C., Troche, S., & Rammsayer, T. (2012). Performance on auditory and visual temporal information processing is related to psychometric intelligence. *Personality and Individual Differences, 52*(1), 9-14. doi:10.1016/j.paid.2011.08.032

Halgren, E., Dale, A. M., Sereno, M. I., Tootell, R. B., Marinkovic, K., & Rosen, B. R. (1999). Location of human face-selective cortex with respect to retinotopic areas. *Human Brain Mapping, 7*(1), 29-37.

Hampshire, A., Highfield, R. R., Parkin, B. L., & Owen, A. M. (2012). Fractionating human intelligence. *Neuron, 76*(6), 1225-1237. doi:10.1016/j.neuron.2012.06.022

Harvey, B. M., & Dumoulin, S. O. (2011). The relationship between cortical magnification factor and population receptive field size in human visual cortex: constancies in cortical architecture. *The Journal of Neuroscience, 31*(38), 13604-13612. doi: 10.1523/JNEUROSCI.2572-11.2011

Harvey, B. M., Vansteensel, M. J., Ferrier, C. H., Petridou, N., Zuiderbaan, W., Aarnoutse, E. J., Bleichner, M.G., Dijkerman, H.C., van Zandvoort, M.J.E., Leijten, F., Ramsey, N.F., & Dumoulin, S.O. (2013). Frequency specific spatial interactions in human electrocorticography: V1 alpha oscillations reflect surround suppression. *Neuroimage, 65*, 424-432. doi:10.1016/j.neuroimage.2012.10.020

He, S., Cavanagh, P., & Intriligator, J. (1996). Attentional resolution and the locus of visual awareness. *Nature, 383*(6598), 334-337. doi:10.1038/383334a0

Heeger, D. J. (1992). Normalization of cell responses in cat striate cortex. *Visual Neuroscience, 9*(2), 181-197.

Heeley, D., & Timney, B. (1988). Meridional anisotropies of orientation discrimination for sine wave gratings. *Vision Research, 28*(2), 337-344. doi:10.1016/0042-6989(88)90162-9

Henriksson, L., Karvonen, J., Salminen-Vaparanta, N., Railo, H., & Vanni, S. (2012). Retinotopic maps, spatial tuning, and locations of human visual areas in surface coordinates characterized with multifocal and blocked fMRI designs. *PLoS ONE, 7*(5), e36859. doi: 10.1371/journal.pone.0036859

Herrmann, C. S., Fründ, I., & Lenz, D. (2010). Human gamma-band activity: a review on cognitive and behavioral correlates and network models. *Neuroscience & Biobehavioral Reviews, 34*(7), 981-992. doi:10.1016/j.neubiorev.2009.09.001

Hoogenboom, N., Schoffelen, J.-M., Oostenveld, R., Parkes, L. M., & Fries, P. (2006). Localizing human visual gamma-band activity in frequency, time and space. *Neuroimage, 29*(3), 764-773. doi:10.1016/j.neuroimage.2005.08.043

Horton, J., & Hoyt, W. (1991a). Quadrantic visual field defects. A hallmark of lesions in extrastriate (V2/V3) cortex. *Brain: A Journal of Neurology, 114*, 1703-1718. doi: http://dx.doi.org/10.1093/brain/114.4.1703

Horton, J., & Hoyt, W. (1991b). The Representation of the Visual Field in Human Striate Cortex: A Revision of the Classic Holmes Map. *Journal of the American Medical Association Ophthalmology, 109*(6), 816-824. doi:10.1001/archopht.1991.01080060080030

Huang, C.-B., Zhou, Y., & Lu, Z.-L. (2008). Broad bandwidth of perceptual learning in the visual system of adults with anisometropic amblyopia. *Proceedings of the National Academy of Sciences, 105*(10), 4068-4073. doi:10.1073/pnas.0800824105

Hubel, D. H., Wensveen, J., & Wick, B. (1995). *Eye, Brain, and Vision*. New York: Scientific American Library.

Hubel, D. H., & Wiesel, T. N. (1962). Receptive fields, binocular interaction and functional architecture in the cat's visual cortex. *The Journal of Physiology, 160*(1), 106-154.

Hubel, D. H., & Wiesel, T. N. (1965). Receptive fields and functional architecture in two nonstriate visual areas (18 and 19) of the cat. *Journal of Neurophysiology, 28*(2), 229-289.

Hubel, D. H., & Wiesel, T. N. (1974). Uniformity of monkey striate cortex: a parallel relationship between field size, scatter, and magnification factor. *Journal of Comparative Neurology, 158*(3), 295-305.

Inouye, T. (1909). *Die Sehstörungen bei Schussverletzungen der kortikalen Sehsphäre: nach Beobachtungen an Verwundeten der letzten japanischen Kriege*. Leipzig: Wilhelm Engelmann.

James, T. W., Culham, J., Humphrey, G. K., Milner, A. D., & Goodale, M. A. (2003). Ventral occipital lesions impair object recognition but not object-directed grasping: an fMRI study. *Brain, 126*(11), 2463-2475. doi: http://dx.doi.org/10.1093/brain/awg248

Johnston, A., & Wright, M. (1985). Lower thresholds of motion for gratings as a function of eccentricity and contrast. *Vision Research, 25*(2), 179-185. doi:10.1016/0042-6989(85)90111-7

Jones, H., Grieve, K., Wang, W., & Sillito, A. (2001). Surround suppression in primate V1. *Journal of Neurophysiology, 86*(4), 2011-2028.

Kaas, J. H. (1997). Topographic maps are fundamental to sensory processing. *Brain Research Bulletin, 44*(2), 107-112. doi:10.1016/S0361-9230(97)00094-4

Kaas, J. H. (2000). Why is brain size so important: Design problems and solutions as neocortex gets biggeror smaller. *Brain and Mind, 1*(1), 7-23.

Kanai, R., Bahrami, B., & Rees, G. (2010). Human parietal cortex structure predicts individual differences in perceptual rivalry. *Current Biology, 20*(18), 1626-1630. doi:10.1016/j.cub.2010.07.027

Kanai, R., Bahrami, B., Roylance, R., & Rees, G. (2012). Online social network size is reflected in human brain structure. *Proceedings of the Royal Society B: Biological Sciences, 279,* 1327-1334. doi: 10.1098/rspb.2011.1959

Kanai, R., Carmel, D., Bahrami, B., & Rees, G. (2011). Structural and functional fractionation of right superior parietal cortex in bistable perception. *Current Biology, 21*(3), R106-R107. doi:10.1016/j.cub.2010.12.009

Kanai, R., Dong, M. Y., Bahrami, B., & Rees, G. (2011). Distractibility in daily life is reflected in the structure and function of human parietal cortex. *The Journal of Neuroscience, 31*(18), 6620-6626. doi: 10.1523/JNEUROSCI.5864-10.2011

Kanai, R., & Rees, G. (2011). The structural basis of inter-individual differences in human behaviour and cognition. *Nature Reviews Neuroscience, 12*(4), 231-242. doi:10.1038/nrn3000

Kapadia, M. K., Westheimer, G., & Gilbert, C. D. (1999). Dynamics of spatial summation in primary visual cortex of alert monkeys. *Proceedings of the National Academy of Sciences, 96*(21), 12073-12078. doi: 10.1073/pnas.96.21.12073

Karni, A., & Sagi, D. (1991). Where practice makes perfect in texture discrimination: evidence for primary visual cortex plasticity. *Proceedings of the National Academy of Sciences, 88*(11), 4966-4970.

Kass, J. (2000). Why is brain size so important: design problems and solutions as neocortex gets bigger or smaller. *Brain and Mind, 1,* 7-22.

Kastner, S., De Weerd, P., Desimone, R., & Ungerleider, L. G. (1998). Mechanisms of directed attention in the human extrastriate cortex as revealed by functional MRI. *Science, 282*(5386), 108-111. doi: 10.1126/science.282.5386.108

Kastner, S., De Weerd, P., Pinsk, M. A., Elizondo, M. I., Desimone, R., & Ungerleider, L. G. (2001). Modulation of sensory suppression: implications for receptive field sizes in the human visual cortex. *Journal of Neurophysiology, 86*(3), 1398-1411.

Kastner, S., De Weerd, P., & Ungerleider, L. G. (2000). Texture segregation in the human visual cortex: a functional MRI study. *Journal of Neurophysiology, 83*(4), 2453-2457.

Klein, R., Berry, G., Briand, K., D'Entremont, B., & Farmer, M. (1990). Letter identification declines with increasing retinal eccentricity at the same rate for normal and dyslexic readers. *Perception and Psychophysics, 47*(6), 601-606.

Kleinschmidt, A., Büchel, C., Zeki, S., & Frackowiak, R. (1998). Human brain activity during spontaneously reversing perception of ambiguous figures. *Proceedings of the Royal Society of London. Series B: Biological Sciences, 265*(1413), 2427-2433. doi: 10.1098/rspb.1998.0594

Klekamp, J., Riedel, A., Harper, C., & Kretschmann, H.J. (1991). Quantitative changes during the postnatal maturation of the human visual cortex. *Journal of the Neurological Sciences, 103*(2), 136-143. doi:10.1016/0022-510X(91)90156-2

Klimesch, W., Sauseng, P., & Gerloff, C. (2003). Enhancing cognitive performance with repetitive transcranial magnetic stimulation at human individual alpha frequency. *European Journal of Neuroscience, 17*(5), 1129-1133.

Knierim, J. J., & Van Essen, D. C. (1992). Neuronal responses to static texture patterns in area V1 of the alert macaque monkey. *Journal of Neurophysiology, 67*(4), 961-980.

Kolster, H., Peeters, R., & Orban, G. A. (2010). The retinotopic organization of the human middle temporal area MT/V5 and its cortical neighbors. *The Journal of Neuroscience, 30*(29), 9801-9820. doi: 10.1523/JNEUROSCI.2069-10.2010

Koyama, S., Sasaki, Y., Andersen, G. J., Tootell, R. B., Matsuura, M., & Watanabe, T. (2005). Separate processing of different global-motion structures in visual cortex is revealed by FMRI. *Current Biology, 15*(22), 2027-2032. doi:10.1016/j.cub.2005.10.069

Kuncel, N. R., Hezlett, S. A., & Ones, D. S. (2004). Academic performance, career potential, creativity, and job performance: Can one construct predict them all? *Journal of Personality and Social Psychology, 86*(1), 148-161.

Kushnir, T., Grill-Spector, K., Mukamel, R., Malach, R., & Itzchakl, Y. (1999, May). *Linear Aspects of the BOLD Response in Object Related Visual Areas: An MRI study*. Paper presented at the Proceedings of ISMRM 7th Scientific Meeting, Philadelphia, PA.

Larsson, J. (2001). *Imaging vision: functional mapping of intermediate visual processes in man* (PhD thesis). Karolinska Institutet, Stockholm, Sweden. Larsson, J., & Heeger, D. J. (2006). Two retinotopic visual areas in human lateral occipital cortex. *The Journal of Neuroscience, 26*(51), 13128-13142. doi: 10.1523/JNEUROSCI.1657-06.2006

Larsson, J., Heeger, D. J., & Landy, M. S. (2010). Orientation selectivity of motion-boundary responses in human visual cortex. *Journal of Neurophysiology, 104*(6), 2940-2950. doi: 10.1152/jn.00400.2010

Larsson, J., Landy, M. S., & Heeger, D. J. (2006). Orientation-selective adaptation to first-and second-order patterns in human visual cortex. *Journal of Neurophysiology, 95*(2), 862-881. doi: 10.1152/jn.00668.2005

Leingärtner, A., Thuret, S., Kroll, T. T., Chou, S.-J., Leasure, J. L., Gage, F. H., & O'Leary, D. D. (2007). Cortical area size dictates performance at modality-specific behaviors. *Proceedings of the National Academy of Sciences, 104*(10), 4153-4158. doi: 10.1073/pnas.0611723104

Leuba, G. & Garey, L. (1987). Evolution of neuronal numerical density in the developing and aging human visual cortex. *Human Neurobiology, 6*, 11-18.

Leuba, G., & Kraftsik, R. (1994). Changes in volume, surface estimate, three-dimensional shape and total number of neurons of the human primary visual cortex from midgestation until old age. *Anatomy and Embryology, 190*(4), 351-366.

LeVay, S., Hubel, D. H., & Wiesel, T. N. (1975). The pattern of ocular dominance columns in macaque visual cortex revealed by a reduced silver stain. *Journal of Comparative Neurology, 159*(4), 559-575. doi: 10.1002/cne.901590408

Leventhal, A. G. (1983). Relationship between preferred orientation and receptive field position of neurons in cat striate cortex. *Journal of Comparative Neurology, 220*(4), 476-483. doi: 10.1002/cne.902200409

Levi, D. M. (2008). Crowding- An essential bottleneck for object recognition: A mini-review. *Vision Research, 48*(5), 635-654. doi:10.1016/j.visres.2007.12.009

Levi, D. M., Hariharan, S., & Klein, S. A. (2002b). Suppressive and facilitatory spatial interactions in peripheral vision: Peripheral crowding is neither size invariant nor simple contrast masking. *Journal of Vision, 2*, 167-177. doi:10.1167/2.2.3

Levi, D. M., Klein, S. A., & Aitsebaomo, A. (1985). Vernier acuity, crowding and cortical magnification. *Vision Research, 25*(7), 963-977. doi:10.1016/0042-6989(85)90207-X

Levi, D. M., Klein, S. A., & Hariharan, S. (2002a). Suppressive and facilitatory spatial interactions in foveal vision: Foveal crowding is simple contrast masking. *Journal of Vision, 2*, 140-166. doi:10.1167/2.2.2

Levi, D.M., Song, S. & Pelli, D.G. (2007). Amblyopic reading is crowded. *Journal of Vision, 7*(2): 21.

Levitt, J. B., Kiper, D. C., & Movshon, J. A. (1994). Receptive fields and functional architecture of macaque V2. *Journal of Neurophysiology, 71*(6), 2517-2542.

Levitt, J. B., & Lund, J. S. (1997). Contrast dependence of contextual effects in primate visual cortex. *Nature, 387*(6628), 73-76.

Levy, I., Hasson, U., Avidan, G., Hendler, T., & Malach, R. (2001). Center–periphery organization of human object areas. *Nature Neuroscience, 4*(5), 533-539. doi:10.1038/87490

Li, B., Peterson, M. R., & Freeman, R. D. (2003). Oblique effect: a neural basis in the visual cortex. *Journal of Neurophysiology, 90*(1), 204-217. doi:10.1152/jn.00954.2002

Li, S.-C., Jordanova, M., & Lindenberger, U. (1998). From good senses to good sense: A link between tactile information processing and intelligence. *Intelligence, 26*(2), 99-122. doi:10.1016/S0160-2896(99)80057-9

Lin, Y., Stephenson, M.C., Xin, L., Napolitano, A. & Morris, P.G. (2012). Investigating the metabolic change due to visual stimulation using functional proton magnetic resonance spectroscopy at 7cT. *Journal of Cerebral Blood Flow & Metabolism, 32,* 1484-1495.

Lindenberger, U., & Baltes, P. B. (1994). Sensory functioning and intelligence in old age: a strong connection. *Psychology and Aging, 9*(3), 339-355.

Livesey, A. C., Wall, M. B., & Smith, A. T. (2007). Time perception: manipulation of task difficulty dissociates clock functions from other cognitive demands. *Neuropsychologia, 45*(2), 321-331. doi:10.1016/j.neuropsychologia.2006.06.033

Livne, T., & Sagi, D. (2007). Configuration influence on crowding. *Journal of Vision, 7*(2): 4, 1-12. doi:10.1167/7.2.4

Louie, E. G., Bressler, D. W., & Whitney, D. (2007). Holistic crowding: Selective interference between configural representations of faces in crowded scenes. *Journal of Vision, 7*(2), 1-11. doi:10.1167/7.2.24

Lueck, C., Zeki, S., Friston, K., Deiber, M.-P., Cope, P., Cunningham, V. J., Lammertsma, C.K., Kennard, C., & Frackowiak, R. (1989). The colour centre in the cerebral cortex of man. *Nature, 340,* 386-389. doi:10.1038/340386a0

Lumer, E. D., Friston, K. J., & Rees, G. (1998). Neural correlates of perceptual rivalry in the human brain. *Science, 280*(5371), 1930-1934. doi:10.1126/science.280.5371.1930

Lunghi, C., Emir, U.E., Morrone, M.C. & Bridge, H. (2015). Short-term monocular deprivation alters GABA in the adult human visual cortex. *Current Biology, 25*(11), 1496-1501.

Malach, R., Levy, I., & Hasson, U. (2002). The topography of high-order human object areas. *Trends in Cognitive Sciences, 6*(4), 176-184. doi:10.1016/S1364-6613(02)01870-3

Malach, R., Reppas, J., Benson, R., Kwong, K., Jiang, H., Kennedy, W., Ledden, P.J., Rosen, B.R., & Tootell, R. (1995). Object-related activity revealed by functional magnetic resonance imaging in human occipital cortex. *Proceedings of the National Academy of Sciences, 92*(18), 8135-8139.

Mannion, D. J., McDonald, J. S., & Clifford, C. W. (2010). Orientation anisotropies in human visual cortex. *Journal of Neurophysiology, 103*(6), 3465-3471. doi: 10.1152/jn.00190.2010

Mansfield, R. (1974). Neural basis of orientation perception in primate vision. *Science, 186*(4169), 1133-1135. doi: 10.1126/science.186.4169.1133

Marshall, L., Henze, D. A., Hirase, H., Leinekugel, X., Dragoi, G., & Buzsáki, G. (2002). Hippocampal pyramidal cell-interneuron spike transmission is frequency dependent and responsible for place modulation of interneuron discharge. *The Journal of Neuroscience, 22*, RC197.

Maunsell, J., & Van Essen, D. C. (1983). The connections of the middle temporal visual area (MT) and their relationship to a cortical hierarchy in the macaque monkey. *The Journal of Neuroscience, 3*(12), 2563-2586.

Maunsell, J. H., & Newsome, W. T. (1987). Visual processing in monkey extrastriate cortex. *Annual Review of Neuroscience, 10*(1), 363-401.

Mazer, J. A., Vinje, W. E., McDermott, J., Schiller, P. H., & Gallant, J. L. (2002). Spatial frequency and orientation tuning dynamics in area V1. *Proceedings of the National Academy of Sciences, 99*(3), 1645-1650. doi: 10.1073/pnas.022638499

McKeefry, D., & Zeki, S. (1997). The position and topography of the human colour centre as revealed by functional magnetic resonance imaging. *Brain, 120*(12), 2229-2242.

McLaurin, W. A., & Farrar, W. E. (1973). Validities of the Progressive Matrices tests against IQ and grade point average. *Psychological Reports, 32*(3), 803-806. Meadows, J. (1974). Disturbed perception of colours associated with localized cerebral lesions. *Brain, 97*(4), 615-632.

Melnick, M. D., Harrison, B. R., Park, S., Bennetto, L., & Tadin, D. (2013). A strong interactive link between sensory discriminations and intelligence. *Current Biology, 23*(11), 1013-1017. doi:10.1016/j.cub.2013.04.053

Menning, H., Roberts, L. E., & Pantev, C. (2000). Plastic changes in the auditory cortex induced by intensive frequency discrimination training. *Neuroreport,11*(4), 817-822.

Mescher, M., Merkle, H., Kirsch, J., Garwood, M., & Gruetter, R. (1998). Simultaneous in vivo spectral editing and water suppression. *NMR in Biomedicine, 11*(EPFL-ARTICLE-177509), 266-272. doi:10.1002/(SICI)1099-1492(199810)11:6<266::AID-NBM530>3.0.CO;2-J

Meyer, C. S., Hagmann-von Arx, P., Lemola, S., & Grob, A. (2010). Correspondence between the general ability to discriminate sensory stimuli and general intelligence. *Journal of Individual Differences, 31*(1), 46-56. doi: http://dx.doi.org/10.1027/1614-0001/a000006

Michael, G. A., & Desmedt, S. (2004). The human pulvinar and attentional processing of visual distractors. *Neuroscience Letters, 362*(3), 176-181. doi:10.1016/j.neulet.2004.01.062

Miller, S. M., Hansell, N. K., Ngo, T. T., Liu, G. B., Pettigrew, J. D., Martin, N. G., & Wright, M. J. (2010). Genetic contribution to individual variation in binocular rivalry rate. *Proceedings of the National Academy of Sciences, 107*(6), 2664-2668. doi: 10.1073/pnas.0912149107

Morgan, M., & Baldassi, S. (1997). How the human visual system encodes the orientation of a texture, and why it makes mistakes. *Current Biology, 7*(12), 999-1002. doi:10.1016/S0960-9822(06)00421-0

Morgan, M., Mason, A., & Baldassi, S. (2000). Are there separate first-order and second-order mechanisms for orientation discrimination? *Vision Research, 40*(13), 1751-1763. doi:10.1016/S0042-6989(00)00015-8

Mrsic-Flogel, T.D., Hofer, S.B., Ohki, K., Reid, R.C., Bonhoeffer, R.T. & Hubener, M. (2007). Homeostatic regulation of eye-specific responses in visual cortex during ocular dominance plasticity. *Neuron, 54,* 961-972.

Muckli, L., Naumer, M. J., & Singer, W. (2009). Bilateral visual field maps in a patient with only one hemisphere. *Proceedings of the National Academy of Sciences, 106*(31), 13034-13039. doi: 10.1073/pnas.0809688106

Mullins, P.G., McGonigle, D.J., O'Gorman, R.L., Puts, N.A.J., Vidyasagar, R., Evans, C.J. & Edden, R.A. (2014). Current practice in the use of MEGA-PRESS spectroscopy for the detection of GABA. *NeuroImage, 86,* 43-52.

Munk, H. (1960). On the functions of the cortex. In Von Bonin, G. (Eds., & Trans.) *Some Papers on the Cerebral Cortex. Springfield, IL: Thomas.* (Original work published 1881).

Murphy, G. M. (1985). Volumetic asymmetry in the human striate cortex. *Experimental Neurology, 88*(2), 288-302. doi:10.1016/0014-4886(85)90192-X Mysore, S. G., Vogels,

R., Raiguel, S. E., & Orban, G. A. (2006). Processing of kinetic boundaries in macaque V4. *Journal of Neurophysiology, 95*(3), 1864-1880. doi: 10.1152/jn.00627.2005

Nefs, H. T., O'Hare, L., & Harris, J. M. (2010). Two independent mechanisms for motion-in-depth perception: Evidence from individual differences. *Frontiers in Psychology, 1*(155), 1-8.

Nenadic, I., Gaser, C., Volz, H.-P., Rammsayer, T., Häger, F., & Sauer, H. (2003). Processing of temporal information and the basal ganglia: new evidence from fMRI. *Experimental Brain Research, 148*(2), 238-246.

Nestares, O., & Heeger, D. J. (2000). Robust multiresolution alignment of MRI brain volumes. *Magnetic Resonance in Medicine, 43*(5), 705-715.

Nicholls, J. D., Martin, A. R., Fuchs, P. A., Brown, D. A., Diamond, M. E., & D., W. (2001). *From Neuron to Brain* (4th ed.). Sunderland, MA: Sinauer Associates, Inc.

Nishida, S. Y., Sasaki, Y., Murakami, I., Watanabe, T., & Tootell, R. B. (2003). Neuroimaging of direction-selective mechanisms for second-order motion. *Journal of Neurophysiology, 90*(5), 3242-3254. doi: 10.1152/jn.00693.2003

O'Donnell, B. F., Bismark, A., Hetrick, W. P., Bodkins, M., Vohs, J. L., & Shekhar, A. (2006). Early stage vision in schizophrenia and schizotypal personality disorder. *Schizophrenia Research, 86*(1), 89-98. doi:10.1016/j.schres.2006.05.016

O'Keefe, L. P., & Movshon, J. A. (1998). Processing of first-and second-order motion signals by neurons in area MT of the macaque monkey. *Visual Neuroscience, 15*(02), 305-317. doi: http://dx.doi.org/

Olzak, L. A., & Laurinen, P. I. (1999). Multiple gain control processes in contrast–contrast phenomena. *Vision Research, 39*(24), 3983-3987. doi:10.1016/S0042-6989(99)00131-5

Orban, G. A. (1997). Visual processing in macaque area MT/V5 and its satellites (MSTd and MSTv). In K.S. Rockland, J.F. Kaas & A. Peters (Ed.) *Extrastriate Cortex in Primates* (pp. 359-434). New York, NY: Plenum.

Orban, G. A., Vandenbussche, E., & Vogels, R. (1984). Human orientation discrimination tested with long stimuli. *Vision Research, 24*(2), 121-128. doi:10.1016/0042-6989(84)90097-X

Pantev, C. (1995). Evoked and induced gamma-band activity of the human cortex. *Brain Topography, 7*(4), 321-330.

Parkes, L., Lund, J., Angelucci, A., Solomon, J. A., & Morgan, M. (2001). Compulsory averaging of crowded orientation signals in human vision. *Nature Neuroscience, 4*(7), 739-744. doi:10.1038/89532

Payne, L., Guillory, S., & Sekuler, R. (2013). Attention-modulated alpha-band oscillations protect against intrusion of irrelevant information. *Journal of Cognitive Neuroscience, 25*(9), 1463-1476. doi:10.1162/jocn_a_00395

Pearce, E., & Bridge, H. (2013). Is orbital volume associated with eyeball and visual cortex volume in humans? *Annals of Human Biology, 40*(6), 531-540. doi:10.3109/03014460.2013.815272

Pearce, E., & Dunbar, R. (2012). Latitudinal variation in light levels drives human visual system size. *Biology Letters, 8*(1), 90-93. doi: 10.1098/rsbl.2011.0570

Pelli, D. G., Palomares, M., & Majaj, N. J. (2004). Crowding is unlike ordinary masking: Distinguishing feature integration from detection. *Journal of Vision, 4*(12), 1136-1169. doi:10.1167/4.12.12

Pelli, D.G, Tillman, K.A., Freeman, J., Su, M., Berger, T. & Majaj, N.J. (2007). Crowding and eccentricity determine reading rate. *Journal of Vision, 20,* 1-36.

Petrov, Y., Carandini, M., & McKee, S. (2005). Two distinct mechanisms of suppression in human vision. *The Journal of Neuroscience, 25*(38), 8704-8707. doi: 10.1523/JNEUROSCI.2871-05.2005

Petrov, Y., Carandini, M., & McKee, S. P. (2006). The time course of contrast masking reveals two distinct mechanisms of human surround suppression. *Journal of Vision, 6*(6), 808-808. doi:10.1167/9.1.21

Petrov, Y., & McKee, S. P. (2006). The effect of spatial configuration on surround suppression of contrast sensitivity. *Journal of Vision, 6*(3), 224-238. doi:10.1167/6.3.4

Petrov, Y., Popple, A. V., & McKee, S. P. (2007). Crowding and surround suppression: Not to be confused. *Journal of Vision, 7*(2), 1-9. doi:10.1167/7.2.12

Pettigrew, J. D., & Miller, S. M. (1998). A 'sticky'interhemispheric switch in bipolar disorder? *Proceedings of the Royal Society of London. Series B: Biological Sciences, 265*(1411), 2141-2148. doi: 10.1098/rspb.1998.0551

Pinon, M., Gattass, R., & Sousa, A. (1998). Area V4 in Cebus monkey: extent and visuotopic organization. *Cerebral Cortex, 8*(8), 685-701. doi:10.1093/cercor/8.8.685

Pinsk, M. A., Doniger, G. M., & Kastner, S. (2004). Push-pull mechanism of selective attention in human extrastriate cortex. *Journal of Neurophysiology, 92*(1), 622-629. doi: 10.1152/jn.00974.2003

Pizzorni-Ferrares, F., & Larsson, J. (2014, February/March). *A data-driven model- free population receptive field estimation framework*. Poster presented at the Proceedings of Computational and System Neuroscience, Salt Lake City, UT. Poirier, F.J.A.M., & Wilson, H. R. (2006). A biologically plausible model of human radial frequency perception. *Vision Research, 46*(15), 2443-2455. doi:10.1016/j.visres.2006.01.026

Polat, U., Ma-Naim, T., Belkin, M., & Sagi, D. (2004). Improving vision in adult amblyopia by perceptual learning. *Proceedings of the National Academy of Sciences of the United States of America, 101*(17), 6692-6697. doi:10.1073/pnas.0401200101

Polimeni, J. R., Balasubramanian, M., & Schwartz, E. L. (2006). Multi-area visuotopic map complexes in macaque striate and extra-striate cortex. *Vision Research, 46*(20), 3336-3359. doi:10.1016/j.visres.2006.03.006

Ponzo, M. (1911). Intorno ad alcune illusioni nel campo delle sensazioni tattili sull'illusione di Aristotele e fenomeni analoghi [On some tactile illusions, Aristotle's illusion, and similar phenomena]. *Archive für die Gesamte Psychologie, 16*, 307-345.

Popovic, Z., & Sjöstrand, J. (2001). Resolution, separation of retinal ganglion cells, and cortical magnification in humans. *Vision Research, 41*(10), 1313-1319. doi:10.1016/S0042-6989(00)00290-X

Press, W. A., Brewer, A. A., Dougherty, R. F., Wade, A. R., & Wandell, B. A. (2001). Visual areas and spatial summation in human visual cortex. *Vision Research, 41*(10), 1321-1332. doi:10.1016/S0042-6989(01)00074-8

Puts, N. A., & Edden, R. A. (2012). In vivo magnetic resonance spectroscopy of GABA: a methodological review. *Progress in Nuclear Magnetic Resonance Spectroscopy, 60*, 29-41. doi:10.1016/j.pnmrs.2011.06.001

Raemaekers, M., Lankheet, M. J., Moorman, S., Kourtzi, Z., & Van Wezel, R. J. (2009). Directional anisotropy of motion responses in retinotopic cortex. *Human Brain Mapping, 30*(12), 3970-3980. doi: 10.1002/hbm.20822

Raven, J. (2000). The Raven's progressive matrices: change and stability over culture and time. *Cognitive Psychology, 41*(1), 1-48. doi:10.1006/cogp.1999.0735

Raven, J., Raven, J., & Court, J. (2000). *Manual for Standard Progressive Matrices*. San Antonio, TX: Harcourt Assessment.

Raven, J., Styles, I., & Raven, M. A. (1998). *Raven's Progressive Matrices: SPM plus test booklet*. Oxford UK, Oxford Psychologists Press.

Ree, M. J., & Earles, J. A. (1992). Intelligence is the best predictor of job performance. *Current Directions in Psychological Science, 1*(3), 86-89.

Rees, G., Kreiman, G., & Koch, C. (2002). Neural correlates of consciousness in humans. *Nature Reviews Neuroscience, 3*(4), 261-270. doi:10.1038/nrn783

Reynell, J. (1978). Developmental patterns of visually handicapped children. *Child: Care, health and development, 4*(5), 291-303. doi: 10.1111/j.1365-2214.1978.tb00088.x

Reynolds, C. R., Chastain, R. L., Kaufman, A. S., & McLean, J. E. (1988). Demographic characteristics and IQ among adults: Analysis of the WAIS-R standardization sample as a function of the stratification variables. *Journal of School Psychology, 25*(4), 323-342. doi:10.1016/0022-4405(87)90035-5

Ringo, J. L. (1991). Neuronal interconnection as a function of brain size. *Brain, Behavior and Evolution, 38*(1), 1-6. doi:10.1159/000114375

Roe, A., & Ts'o, D. (1995). Visual topography in primate V2: multiple representation across functional stripes. *The Journal of Neuroscience, 15*(5), 3689-3715.

Rolls, E. T., & Tovee, M. J. (1995). The responses of single neurons in the temporal visual cortical areas of the macaque when more than one stimulus is present in the receptive field. *Experimental Brain Research, 103*(3), 409-420.

Rosa, M. (2002). Visual maps in the adult primate cerebral cortex: some implications for brain development and evolution. *Brazilian Journal of Medical and Biological Research, 35*(12), 1485-1498.

Rossi, A. F., Desimone, R., & Ungerleider, L. G. (2001). Contextual modulation in primary visual cortex of macaques. *The Journal of Neuroscience, 21*(5), 1698-1709.

Rothkopf, C., Weisswange, T., & Triesch, J. (2009). A walk through the woods explains the space variant oblique effect. *Journal of Vision, 9*(8), 1049-1049. doi:10.1167/9.8.1049

Rovamo, J. & Raninen, A. (1984). Critical flicker frequency and M-scaling of stimulus size and retinal illuminance. *Vision Reason, 24*, 1127-1131.

Rovamo, J., Virsu, V., Laurinen, P., & Hyvärinen, L. (1982). Resolution of gratings oriented along and across meridians in peripheral vision. *Investigative Ophthalmology & Visual Science, 23*(5), 666-670.

Salzman, C. D., Britten, K. H., & Newsome, W. T. (1990). Cortical microstimulation influences perceptual judgements of motion direction. *Nature, 346*(6280), 174-177.

Sary, G., Vogels, R., Kovacs, G., & Orban, G. (1995). Responses of monkey inferior temporal neurons to luminance-, motion-, and texture-defined gratings. *Journal of Neurophysiology, 73*(4), 1341-1354.

Sasaki, Y., Rajimehr, R., Kim, B. W., Ekstrom, L. B., Vanduffel, W., & Tootell, R. B. (2006). The radial bias: a different slant on visual orientation sensitivity in human and nonhuman primates. *Neuron, 51*(5), 661-670. doi:10.1016/j.neuron.2006.07.021

Sato, T. (1989). Interactions of visual stimuli in the receptive fields of inferior temporal neurons in awake macaques. *Experimental Brain Research, 77*(1), 23-30.

Sawamura, H., Georgieva, S., Vogels, R., Vanduffel, W., & Orban, G. A. (2005). Using functional magnetic resonance imaging to assess adaptation and size invariance of shape processing by humans and monkeys. *The Journal of Neuroscience, 25*(17), 4294-4306. doi: 10.1523/JNEUROSCI.0377-05.2005

Sayim, B., Greenwood, J. A., & Cavanagh, P. (2014). Foveal target repetitions reduce crowding. *Journal of Vision, 14*(6): 4, 1-12. doi:10.1167/14.6.4

Scalise A., Desiato, M.T., Gigli, G.L., Romigi, A., Tombini, M., Marciani, M.G.,…Placidi, F. (2006). Increasing cortical excitability: A possible explanation for the proconvulsant role of sleep deprivation. *Sleep, 29*(12), 1595-1598.

Schaller, B.., Mekle, R., Xin, L., Kunz, N. & Gruetter, R. (2013). Net increase of lactate and glutamate concerntration in activated human visual cortex detected with magnetic resonance spectroscopy at 7 tesla. *Journal of Neuroscience Research, 91, 1076-1083.*

Schein, S. J., & Desimone, R. (1990). Spectral properties of V4 neurons in the macaque. *The Journal of Neuroscience, 10*, 3369-3389.

Schenk-Rootlieb, A. J., Van Nieuwenhuizen, O., Schiemanck, N., Van der Graaf, Y., & Willemse, J. (1993). Impact of cerebral visual impairment on the everyday life of cerebral palsied children. *Child: Care, Health & Development, 19*(6), 411-423. doi: 10.1111/j.1365-2214.1993.tb00745.x

Schira, M. M., Tyler, C. W., Breakspear, M., & Spehar, B. (2009). The foveal confluence in human visual cortex. *The Journal of Neuroscience, 29*(28), 9050-9058. doi: 10.1523/JNEUROSCI.1760-09.2009

Schmid, M. C., Schmiedt, J. T., Peters, A. J., Saunders, R. C., Maier, A., & Leopold, D. A. (2013). Motion-sensitive responses in visual area V4 in the absence of primary visual cortex. The *Journal of Neuroscience, 33*(48), 18740-18745. doi: 10.1523/JNEUROSCI.3923-13.2013

Schmidtmann, G., Kennedy, G. J., Orbach, H. S., & Loffler, G. (2012). Non-linear global pooling in the discrimination of circular and non-circular shapes. *Vision Research, 62*, 44-56. doi:10.1016/j.visres.2012.03.001

Schwabe, L., Obermayer, K., Angelucci, A., & Bressloff, P. C. (2006). The role of feedback in shaping the extra-classical receptive field of cortical neurons: a recurrent network model. *The Journal of Neuroscience, 26*(36), 9117-9129. doi: 10.1523/JNEUROSCI.1253-06.2006

Schwartz, E. L. (1994). Computational Studies of the Spatial Architexture of Primate Visual Cortex: Columns, Maps, and Protomaps. In A. P. K. S. Rockland (Ed.), *Primary Visual Cortex in Primates* (Vol. 10, pp. 359-411). New York, NY: Kluwer Academic/ Plenum Publishers.

Schwarzkopf, D. S., Anderson, E. J., de Haas, B., White, S. J., & Rees, G. (2014). Larger extrastriate population receptive fields in autism spectrum disorders. *The Journal of Neuroscience, 34*(7), 2713-2724. doi: 10.1523/JNEUROSCI.4416-13.2014

Schwarzkopf, D. S., & Rees, G. (2013). Subjective size perception depends on central visual cortical magnification in human V1. *PLoS ONE, 8*(3), e60550. doi: 10.1371/journal.pone.0060550

Schwarzkopf, D. S., Robertson, D. J., Song, C., Barnes, G. R., & Rees, G. (2012). The frequency of visually induced gamma-band oscillations depends on the size of early human visual cortex. *The Journal of Neuroscience, 32*(4), 1507-1512. doi: 10.1523/JNEUROSCI.4771-11.2012

Schwarzkopf, D. S., Song, C., & Rees, G. (2011). The surface area of human V1 predicts the subjective experience of object size. *Nature Neuroscience, 14*(1), 28-30. doi:10.1038/nn.2706

Seiffert, A. E., Somers, D. C., Dale, A. M., & Tootell, R. B. (2003). Functional MRI studies of human visual motion perception: texture, luminance, attention and after-effects. *Cerebral Cortex, 13*(4), 340-349. doi: 10.1093/cercor/13.4.340

Sereno, M. I., Dale, A. M., Reppas, J. B., Kwong, K. K., Belliveau, J. W., Brady, T. J., Rosen, B. R., Tootell, R. B. (1995). Borders of multiple visual areas in humans revealed by functional magnetic resonance imaging. *Science, 268*(5212), 889-893. doi: 10.1126/science.7754376

Shaywitz, S. E., Escobar, M. D., Shaywitz, B. A., Fletcher, J. M., & Makuch, R. (1992). Evidence that dyslexia may represent the lower tail of a normal distribution of reading ability. *The New England Journal of Medicine, 326*(3), 145-150.

Sheppard, L. D., & Verson, P. A. (2008). Intelligence and speed of information-processing: A review of 50 years of research. *Personality and Individual Differences, 44*(3), 535-551.

Shipp, S., & Zeki, S. (1989). The organization of connections between areas V5 and V1 in macaque monkey visual cortex. *European Journal of Neuroscience, 1*(4), 309-332.

Silson, E. H., McKeefry, D. J., Rodgers, J., Gouws, A. D., Hymers, M., & Morland, A. B. (2013). Specialized and independent processing of orientation and shape in visual field maps LO1 and LO2. *Nature Neuroscience, 16*(3), 267-269. doi:10.1038/nn.3327

Sincich, L. C., & Horton, J. C. (2002). Pale cytochrome oxidase stripes in V2 receive the richest projection from macaque striate cortex. *The Journal of Comparative Neurology, 447*(1), 18-33. doi: 10.1002/cne.10174

Smith, A. T., Greenlee, M. W., Singh, K. D., Kraemer, F. M., & Hennig, J. (1998). The processing of first- and second-order motion in human visual cortex assessed by functional magnetic resonance imaging (fMRI). *The Journal of Neuroscience, 18*(10), 3816-3830.

Smith, A. T., Singh, K. D., Williams, A. L., & Greenlee, M. W. (2001). Estimating receptive field size from fMRI data in human striate and extrastriate visual cortex. *Cerebral Cortex, 11*(12), 1182-1190. doi:10.1093/cercor/11.12.1182

Snowden, R. J., & Hammett, S. T. (1998). The effects of surround contrast on contrast thresholds, perceived contrast and contrast discrimination. *Vision Research, 38*(13), 1935-1945. doi:10.1016/S0042-6989(97)00379-9

Solomon, J. A., & Sperling, G. (1994). Full-wave and half-wave rectification in second-order motion perception. *Vision Research, 34*(17), 2239-2257.

Solomon, J. A., Sperling, G., & Chubb, C. (1993). The lateral inhibition of perceived contrast is indifferent to on-center/off-center segregation, but specific to orientation. *Vision Research, 33*(18), 2671-2683. doi:10.1016/0042-6989(93)90227-N

Song, C., Schwarzkopf, D. S., & Rees, G. (2013). Variability in visual cortex size reflects tradeoff between local orientation sensitivity and global orientation modulation. *Nature Communications, 4*, 2201. doi:10.1038/ncomms3201

Sowden, P. T., Davies, I. R., & Roling, P. (2000). Perceptual learning of the detection of features in X-ray images: a functional role for improvements in adults' visual sensitivity?

Journal of Experimental Psychology: Human Perception and Performance, 26(1), 379-390.

Spearman, C. (1904). “General Intelligence” objectively determined and measured. *The American Journal of Psychology, 15*(2), 201-292.

Sperry, R. W. (1963). Chemoaffinity in the orderly growth of nerve fiber patterns and connections. *Proceedings of the National Academy of Sciences of the United States of America, 50*(4), 703-710.

Stagg, C. J., Bachtiar, V., & Johansen-Berg, H. (2011). The role of GABA in human motor learning. *Current Biology, 21*(6), 480-484. doi:10.1016/j.cub.2011.01.069

Stanley, D. A., & Rubin, N. (2005). Functionally distinct sub-regions in the lateral occipital complex revealed by fMRI responses to abstract 2-dimensional shapes and familiar objects [Abstract]. *Journal of Vision, 5*(8), 911a. doi:10.1167/5.8.911

Stanley, O. H. (1991). Cortical development and visual function. *Eye, 5*, 27-30.

Stensaas, S. S., Eddington, D. K., & Dobelle, W. H. (1974). The topography and variability of the primary visual cortex in man. *Journal of Neurosurgery, 40*(6), 747-755. doi: 10.3171/jns.1974.40.6.0747

Sterzer, P., & Kleinschmidt, A. (2007). A neural basis for inference in perceptual ambiguity. *Proceedings of the National Academy of Sciences, 104*(1), 323-328. doi: 10.1073/pnas.0609006104

Stevens, C. F. (2001). An evolutionary scaling law for the primate visual system and its basis in cortical function. *Nature, 411*(6834), 193-195. doi:10.1038/35075572

Swisher, J. D., Halko, M. A., Merabet, L. B., McMains, S. A., & Somers, D. C. (2007). Visual topography of human intraparietal sulcus. *The Journal of Neuroscience, 27*(20), 5326-5337. doi: 10.1523/JNEUROSCI.0991-07.2007

Tadin, D., Lappin, J. S., Gilroy, L. A., & Blake, R. (2003). Perceptual consequences of centre-surround antagonism in visual motion processing. *Nature, 424*(6946), 312-315. doi:10.1038/nature01800

Toet, A., & Levi, D. M. (1992). The two-dimensional shape of spatial interaction zones in the parafovea. *Vision Research, 32*(7), 1349-1357. doi:10.1016/0042-6989(92)90227-A

Toga, A.W. & Mazziotta, J.C. (2002) *Brain Mapping: The Methods (2nd ed.).* New York: Academic Press.

Tootell, R. B., & Hadjikhani, N. (2001). Where is 'dorsal V4' in human visual cortex? Retinotopic, topographic and functional evidence. *Cerebral Cortex, 11*(4), 298-311. doi: 10.1093/cercor/11.4.298

Tootell, R. B., Mendola, J. D., Hadjikhani, N. K., Ledden, P. J., Liu, A. K., Reppas, J. B., Sereno, M.I., & Dale, A. M. (1997). Functional analysis of V3A and related areas in human visual cortex. *The Journal of Neuroscience, 17*(18), 7060-7078.

Tootell, R. B., Reppas, J. B., Dale, A. M., Look, R. B., Sereno, M. I., Malach, R., Brady, T.J., & Rosen, B. R. (1995). Visual motion aftereffect in human cortical area MT revealed by functional magnetic resonance imaging. *Nature, 375*(6527), 139-141. doi: 10.1038/375139a0

Tootell, R. B., Switkes, E., Silverman, M. S., & Hamilton, S. L. (1988). Functional anatomy of macaque striate cortex. II. Retinotopic organization. *The Journal of Neuroscience, 8*(5), 1531-1568.

Tootell, R. B., & Taylor, J. B. (1995). Anatomical evidence for MT and additional cortical visual areas in humans. *Cerebral Cortex, 5*(1), 39-55. doi:10.1093/cercor/5.1.39

Tripathy, S. P., & Cavanagh, P. (2002). The extent of crowding in peripheral vision does not scale with target size. *Vision Research, 42*, 2357-2369. doi:10.1016/S0042-6989(02)00197-9

Tripathy, S. P., & Levi, D. M. (1994). Long-range dichoptic interactions in the human visual cortex in the region corresponding to the blind spot. *Vision Research, 34*(9), 1127-1138. doi:10.1016/0042-6989(94)90295-X

Troche, S., & Rammsayer, T. (2009a). The influence of temporal resolution power and working memory capacity on psychometric intelligence. *Intelligence, 37*(5), 479-486. doi:10.1016/j.intell.2009.06.001

Troche, S., & Rammsayer, T. (2009b). Temporal and non-temporal sensory discrimination and their predictions of capacity-and speed-related aspects of psychometric intelligence. *Personality and Individual Differences, 47*(1), 52-57. doi:10.1016/j.paid.2009.02.001

Troche, S., Wagner, F. L., Voelke, A. E., Roebers, C. M., & Rammsayer, T. (2014). Individual differences in working memory capacity explain the relationship between general discrimination ability and psychometric intelligence. *Intelligence, 44*, 40-50. doi:10.1016/j.intell.2014.02.009

Tyler, C. W., Likova, L. T., Chen, C. C., Knotsevich, L. L., Schira, M. M., & Wade, A. R. (2005). Extended concepts of occipital retinotopy. *Current Medical Imaging Reviews, 3*, 319-329.

Tynan, P. D., & Sekuler, R. (1982). Motion processing in peripheral vision: Reaction time and perceived velocity. *Vision Research, 22*(1), 61-68. doi:10.1016/0042-6989(82)90167-5

Usher, M., Bonneh, Y., Sagi, D., & Herrmann, M. (1999). Mechanisms for spatial integration in visual detection: a model based on lateral interactions. *Spatial Vision, 12*(2), 187-209. doi: 10.1163/156856899X00111

Van Essen, D. C. (2004). Organization of Visual Areas in Macaque and Human Cerebral Cortex. In L. M. Chalupa & J. S. Werner (Ed.), *The Visual Neurosciences* (Vol. 1, pp. 522-541). Cambridge, MA: The MIT Press.

Van Essen, D. C., Anderson, C. H., & Felleman, D. J. (1992). Information processing in the primate visual system: an integrated systems perspective. *Science, 255*(5043), 419-423. doi: 10.1126/science.1734518

Van Essen, D. C., Felleman, D. J., DeYoe, E. A., & Knierim, J. J. (1991). Probing the primate visual cortex: pathways and perspectives. In A. Valberg & B.B. Lee (Ed.). *From Pigments to Perception* (pp. 227-237). New York: Plenum.

Van Essen, D. C., Newsome, W. T., & Maunsell, J. H. (1984). The visual field representation in striate cortex of the macaque monkey: asymmetries, anisotropies, and individual variability. *Vision Research, 24*(5), 429-448. doi:10.1016/0042-6989(84)90041-5

Zhu, H. & Barker, P.B. MR Spectroscopy and Spectroscopic Imaging of the Brain. *Methods in Molecular Biology, 711,* 203-226.

Van Essen, D. C., & Zeki, S. (1978). The topographic organization of rhesus monkey prestriate cortex. *The Journal of Physiology, 277*(1), 193-226. doi: 10.1113/jphysiol.1978.sp012269

Van Gaal, S., Scholte, H. S., Lamme, V. A., Fahrenfort, J. J., & Ridderinkhof, K. R. (2011). Pre-SMA graymatter density predicts individual differences in action selection in the face of conscious and unconscious response conflict. *Journal of Cognitive Neuroscience, 23*(2), 382-390. doi:10.1162/jocn.2010.21444

Van Oostende, S., Sunaert, S., Van Hecke, P., Marchal, G., & Orban, G. (1997). The kinetic occipital (KO) region in man: an fMRI study. *Cerebral Cortex, 7*(7), 690-701. doi: 10.1093/cercor/7.7.690

Vanderhaeghen, P., Lu, Q., Prakash, N., Frisen, J., Walsh, C. A., Frostig, R. D., & Flanagan, J. G. (2000). A mapping label required for normal scale of body representation in the cortex. *Nature Neuroscience, 3*(4), 358-365. doi:10.1038/73929

Victor, J. D., Purpura, K., Katz, E., & Mao, B. (1994). Population encoding of spatial frequency, orientation, and color in macaque V1. *Journal of Neurophysiology, 72*(5), 2151-2166.

Visser, B. A., Ashton, M. C., & Vernon, P. A. (2006). Beyond g: Putting multiple intelligences theory to the test. *Intelligence, 34*(5), 487-502. doi:10.1016/j.intell.2006.02.004

Wandell, B., & Winawer, J. (2011). Imaging retinotopic maps in the human brain. *Vision Research, 51*(7), 718-737. doi:10.1016/j.visres.2010.08.004

Wandell, B. A. (1999). Computational neuroimaging of human visual cortex. *Annual Review of Neuroscience, 22*, 145-173. doi: 10.1146/annurev.neuro.22.1.145

Wandell, B. A., Brewer, A. A., & Dougherty, R. F. (2005). Visual field map clusters in human cortex. *Philosophical Transactions of the Royal Society of London B: Biological Sciences, 360*(1456), 693-707. doi: 10.1098/rstb.2005.1628

Wandell, B. A., Dumoulin, S. O., & Brewer, A. A. (2007). Visual field maps in human cortex. *Neuron, 56*(2), 366-383. doi:10.1016/j.neuron.2007.10.012

Wang, H. X., Heeger, D. J., & Landy, M. S. (2012). Responses to second-order texture modulations undergo surround suppression. *Vision Research, 62*, 192-200. doi:10.1016/j.visres.2012.03.008

Wang, J., McFadden, S. L., Caspary, D., & Salvi, R. (2002). Gamma- aminobutyric acid circuits shape response properties of auditory cortex neurons. *Brain Research, 944*(1), 219-231. doi:10.1016/S0006-8993(02)02926-8

Wassef, A., Baker, J., & Kochan, L. D. (2003). GABA and schizophrenia: a review of basic science and clinical studies. *Journal of Clinical Psychopharmacology, 23*(6), 601-640.

Watamaniuk, S. N., & Sekuler, R. (1992). Temporal and spatial integration in dynamic random-dot stimuli. *Vision Research, 32*(12), 2341-2347. doi:10.1016/0042-6989(92)90097-3

Watamaniuk, S. N., Sekuler, R., & Williams, D. W. (1989). Direction perception in complex dynamic displays: the integration of direction information. *Vision Research, 29*(1), 47-59.

Watson, J. D., Myers, R., Frackowiak, R. S., Hajnal, J. V., Woods, R. P., Mazziotta, J. C., Shipp, S., & Zeki, S. (1993). Area V5 of the human brain: evidence from a combined study using positron emission tomography and magnetic resonance imaging. *Cerebral Cortex, 3*(2), 79-94. doi: 10.1093/cercor/3.2.79

Wechsler, D. (2008). *Wechsler Adult Intelligence Scale- IV*. San Antonio, TX: NCS Pearson.

Wenderoth, P., Watson, J., Egan, G., Tochon-Danguy, H., & O'keefe, G. (1999). Second order components of moving plaids activate extrastriate cortex: a positron emission tomography study. *Neuroimage, 9*(2), 227-234. doi:10.1006/nimg.1998.0398

Weschler, D. (1990). *Wechsler Pre-school and Primary Scale of Intelligence –Revised.* London: Pearson Assessment.

Weschler, D. (1992). *Wechsler Intelligence Scale for Children –III*. London: Pearson Assessment.

Weschler, D. (1999). *Wechsler Abbreviated Scale of Intelligence*. San Antonio, TX: Psychological Corporation.

Westheimer, G. (2005). Anisotropies in peripheral vernier acuity. *Spatial Vision, 18*(2), 159-167. doi: 10.1163/1568568053320611

Westlye, L. T., Grydeland, H., Walhovd, K. B., & Fjell, A. M. (2011). Associations between regional cortical thickness and attentional networks as measured by the attention network test. *Cerebral Cortex, 21*(2), 345-356. doi: 10.1093/cercor/bhq101

Whitney, D., & Levi, D. M. (2011). Visual crowding: a fundamental limit on conscious perception and object recognition. *Trends in Cognitive Science, 15*(4), 160-168. doi:10.1016/j.tics.2011.02.005

Wilkinson, F., Wilson, H. R., & Habak, C. (1998). Detection and recognition of radial frequency patterns. *Vision Research, 38*(22), 3555-3568. doi:10.1016/S0042-6989(98)00039-X

Xing, J., & Heeger, D. J. (2000). Center-surround interactions in foveal and peripheral vision. *Vision Research, 40*(22), 3065-3072. doi:10.1016/S0042-6989(00)00152-8

Xing, J., & Heeger, D. J. (2001). Measurement and modelling of centre-surround suppression and enhancement. *Vision Research, 41*(5), 571-583. doi:10.1016/S0042-6989(00)00270-4

Xu, J., Kober, H., Carroll, K. M., Rounsaville, B. J., Pearson, G. D., & Potenza, M. N. (2012). White matter integrity and behavioural activation in healthy subjects. *Human Brain Mapping, 33*(4), 994-1002. doi: 10.1002/hbm.21275

Yoon, J. H., Maddock, R. J., Rokem, A., Silver, M. A., Minzenberg, M. J., Ragland, J. D., & Carter, C. S. (2010). GABA concentration is reduced in visual cortex in schizophrenia and correlates with orientation-specific surround suppression. *The Journal of Neuroscience, 30*(10), 3777-3781. doi: 10.1523/JNEUROSCI.6158-09.2010

Yoon, J. H., Rokem, A. S., Silver, M. A., Minzenberg, M. J., Ursu, S., Ragland, J. D., & Carter, C. S. (2009). Diminished orientation-specific surround suppression of visual processing in schizophrenia. *Schizophrenia Bulletin, 35*(6), 1078-1084. doi: 10.1093/schbul/sbp064

Yoshor, D., Bosking, W. H., Ghose, G. M., & Maunsell, J. H. (2007). Receptive fields in human visual cortex mapped with surface electrodes. *Cerebral Cortex, 17*(10), 2293-2302. doi: 10.1093/cercor/bhl138

Zax, J. S., & Rees, D. I. (2002). IQ, academic performance, environment, and earnings. *Review of Economics and Statistics, 84*(4), 600-616. doi:10.1162/003465302760556440

Zeki, S., Perry, R., & Bartels, A. (2003). The processing of kinetic contours in the brain. *Cerebral Cortex, 13*(2), 189-202. doi: 10.1093/cercor/13.2.189

Zeki, S. M. (1969). Representation of central visual fields in prestriate cortex of monkey. *Brain Research, 14*(2), 271-291. doi:10.1016/0006-8993(69)90110-3

Zeki, S. M. (1978). Functional specialisation in the visual cortex of the rhesus monkey. *Nature, 274*(5670), 423-428. doi: 10.1038/274423a0

Zenger-Landolt, B., & Heeger, D. J. (2003). Response suppression in v1 agrees with psychophysics of surround masking. *The Journal of Neuroscience, 23*(17), 6884-6893.

Zhang, X., & Fang, F. (2014). Cortical magnification factor and population receptive field size in human V1 predict the bottom-up saliency map. *Journal of Vision, 14*(10), 537-537. doi:10.1167/14.10.537

Zhang, X., Zhaoping, L., Zhou, T., & Fang, F. (2012). Neural activities in V1 create a bottom-up saliency map. *Neuron, 73*(1), 183-192. doi:10.1016/j.neuron.2011.10.035

Zuiderbaan, W., Harvey, B. M., & Dumoulin, S. O. (2012). Modeling center- surround configurations in population receptive fields using fMRI. *Journal of Vision 12*(3), 10. doi:10.1167/12.3.10

Appendices

Appendix A: Psychophysical Orientation Discrimination Pilot Data (Chapter 3)

Pilot data was collected for a single participant (the author) to explore the influence of longer inter-stimulus temporal gaps. Instead of an inter-stimulus temporal gap of 0.5s, a break of 2s occurred between the presentation of the first and second grating. All other experimental parameters were identical to the methods reported in Chapter 3.

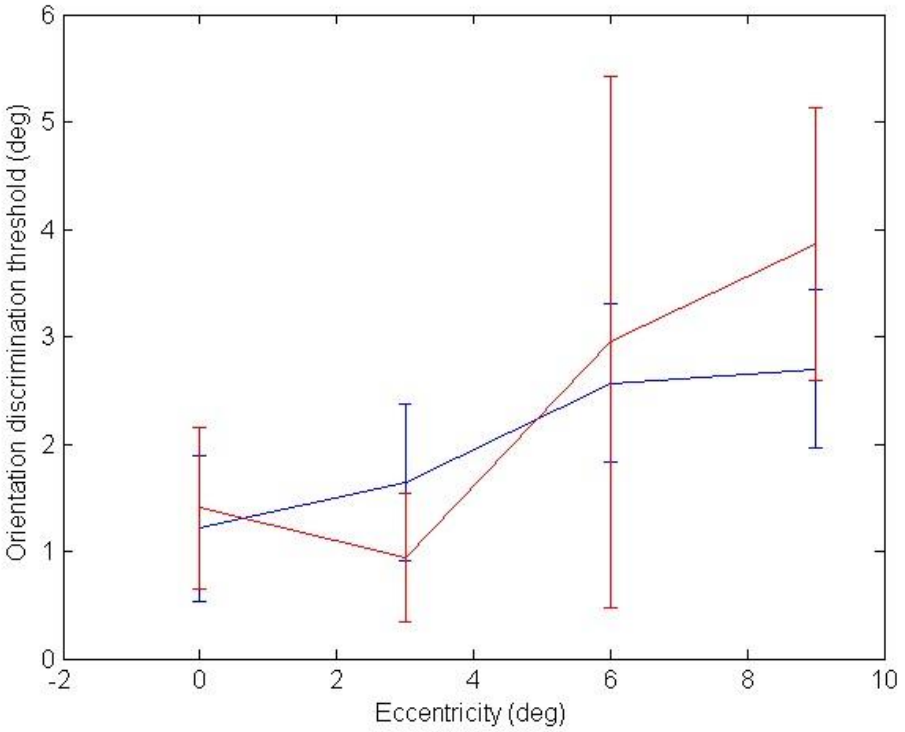

Figure 0-1 Average thresholds (3 blocks at each eccentricity for a single participant) in an orientation discrimination task with luminance defined boundaries Tangential in red and radial in blue. Standard deviations shown.

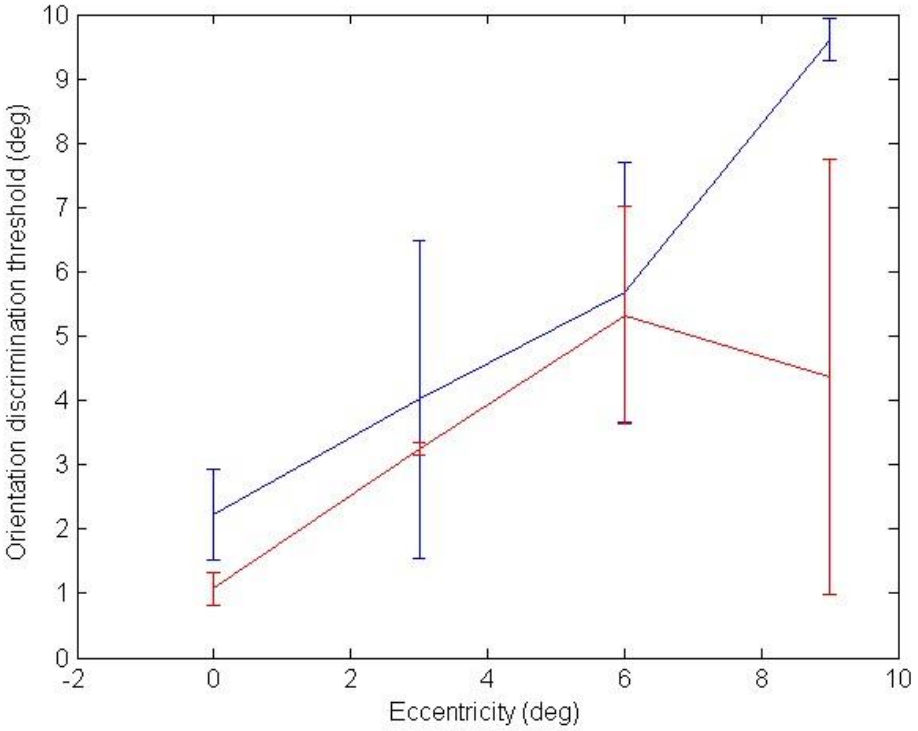

Figure 0-2 Average thresholds (3 blocks at each eccentricity for a single participant) in an orientation discrimination task with luminance defined boundaries Tangential in red and radial in blue. Standard deviations shown.

Appendix B: Psychometric Testing Response Sheets and Scoring Keys (Chapter 8)

Raven Advanced Progressive Matrix Short Form Response Sheet

Test Date:

Name:

Date of Birth:

Problem number								
1.	1	2	3	4	5	6	7	8
2.	1	2	3	4	5	6	7	8
3.	1	2	3	4	5	6	7	8
4.	1	2	3	4	5	6	7	8
5.	1	2	3	4	5	6	7	8
6.	1	2	3	4	5	6	7	8
7.	1	2	3	4	5	6	7	8
8.	1	2	3	4	5	6	7	8
9.	1	2	3	4	5	6	7	8
10.	1	2	3	4	5	6	7	8
11.	1	2	3	4	5	6	7	8
12.	1	2	3	4	5	6	7	8

Raven Advanced Progressive Matrix Short Form Scoring Key

Problem number								
1.	1	2	3	4	**5**	6	7	8
2.	1	2	3	**4**	5	6	7	8
3.	**1**	2	3	4	5	6	7	8
4.	1	2	3	4	**5**	6	7	8
5.	1	**2**	3	4	5	6	7	8
6.	1	2	3	4	5	6	**7**	8
7.	1	2	3	4	5	6	7	**8**
8.	1	2	3	4	5	**6**	7	8
9.	1	2	3	4	5	6	**7**	8
10.	1	2	3	4	**5**	6	7	8
11.	1	2	3	**4**	5	6	7	8
12.	1	2	**3**	4	5	6	7	8

WASI Matrix Reasoning Response Sheet[1]

item	Response options	Score (1 or 0)
A	1 **2** 3 4 5	
B	1 2 3 4 **5**	
1	1 **2** 3 4 5	
2	1 2 3 **4** 5	
3	1 **2** 3 4 5	
4	1 2 3 **4** 5	
5	1 2 **3** 4 5	
6	**1** 2 3 4 5	
7	**1** 2 3 4 5	
8	1 2 **3** 4 5	
9	1 2 3 4 **5**	
10	1 2 3 4 **5**	
11	1 2 3 4 **5**	
12	1 **2** 3 4 5	
13	1 2 **3** 4 5	
14	**1** 2 3 4 5	
15	1 **2** 3 4 5	
16	1 2 3 **4** 5	
17	1 2 **3** 4 5	
18	**1** 2 3 4 5	

[1] The material was reproduced from Wescher Abbreviated Scale of Intelligence testing materials (Pearsons, 1999)

19	**1** 2 3 4 5	
20	1 2 3 **4** 5	
21	1 2 3 4 **5**	
22	1 2 3 4 **5**	
23	1 **2** 3 4 5	
24	1 **2** 3 4 5	
25	**1** 2 3 4 5	
26	1 2 3 4 **5**	
27	1 2 3 **4** 5	
28	1 2 **3** 4 5	
29	1 2 **3** 4 5	
30	1 2 3 **4** 5	
31	**1** 2 3 4 5	
32	1 2 3 **4** 5	
33	1 **2** 3 4 5	
34	1 2 **3** 4 5	
35	1 2 3 4 **5**	

Appendix C: WASI Matrix Reasoning Administration Notes

Discontinuation and Reversal

Testing starts with Items A and B and then Item 7. If the examinee obtains perfect scores (1 point) on Items 7 and 8, give full credit for Items 1-6.
If the examinee fails Item 7 or Item 8, administer Items 1-6 in reverse sequence until the examinee obtains perfect scores on two consecutive items. If the examinee obtained a perfect score on item 7, count it in the reverse sequence. When this criterion is met, give full credit for any reversal items that were not administered. Then proceed with the subtest until the discontinue criterion is met or the stop point is reached. Discontinue after four consecutive scores of 0 or four scores of 0 on five consecutive items.

General Directions

Administer the sample items first. Sample Items A and B are teaching items intended to help the examinee understand the instructions of the test. Administer the two sample items to all examinees. If the examinee responds incorrectly to either sample item, illustrate the correct way to solve the problem. There are no rigid time limits for this subtest. Most examinees will finish an item within 30 seconds. If after 30 seconds, the examinee has not provided a response, say, “Let’s try the next one.” Count the item as a failure and proceed to the next item.

In the interest of maintaining rapport, do not abruptly stop the examinee if there is an indication that he or she is about to give a response, even if 30 seconds has elapsed. Allow the examinee to respond, give credit if the response is correct,

and proceed to the next item. Remember, 30 seconds is a guideline for consistent administration, not a strict time limit.

Scoring

Responses to Items 1-35 are scored 1 or 0 points. Correct responses are printed in boldfaced type on the Record Form. Award full credit for any unadministered reversal items.